Pontifícia Universidade Católica
do Rio de Janeiro

Arash Azadeh

Heat influence on Physical and Mechanical Properties of *Dendrocalamus Giganteus* Bamboo

Tese de Doutorado

Thesis presented to the Programa de Pós-graduação em Engenharia Civil of PUC-Rio in partial fulfillment of the requirements for the degree of Doutor em Engenharia Civil.

Advisor: Prof. Khosrow Ghavami

Rio de Janeiro

April 2018

Pontifícia Universidade Católica
do Rio de Janeiro

Arash Azadeh

Heat influence on Physical and Mechanical Properties of *Dendrocalamus Giganteus Bamboo*

Thesis presented to the Programa de Pós-graduação em Engenharia Civil of PUC-Rio in partial fulfillment of the requirements for the degree of Doutor em Engenharia Civil. Approved by the undersigned Examination Committee.

Prof. Khosrow Ghavami
Advisor
Departamento da Engenharia Civil – PUC-Rio

Prof. Normando Perazzo Barbosa
UFPB

Prof. Holmer Savastano Junior
FZEA-USP

Prof. Romildo Dias Toledo Filho
COPPE-UFRJ

Prof. Conrado de Souza Rodrigues
CEFET-MG

Prof. Daniel Cardoso
PUC-Rio

Prof. Márcio da Silveira Carvalho
Coordinator of the Centro Técnico Científico da PUC-Rio

Rio de Janeiro, April 27th, 2018

Arash Azadeh

Graduated in Civil Engineering at the Ferdowsi University of Mashhad (FUM) in 1994 and obtained his M.Sc. Degree in structural Engineering at the same university in 1999.

Bibliographic data

Azadeh, Arash

Heat influence on physical and mechanical properties of *Dendrocalamus giganteus* bamboo / Arash Azadeh ; advisor: Khosrow Ghavami. – 2018.

224 f. : il. color. ; 30 cm

Tese (Doutorado)–Pontifícia Universidade Católica do Rio de Janeiro, Departamento de Engenharia Civil, 2018.

Inclui bibliografia

1. Engenharia Civil – Teses. 2. Bambu *Dendrocalamus giganteus*. 3. Efeito de calor. 4. Propriedades mecânicas. 5. Absorção de água. 6. Processamento de imagem. I. Ghavami, K. II. Pontifícia Universidade Católica do Rio de Janeiro. Departamento de Engenharia Civil. III. Título.

CDD: 624

Dedicated to:
My dear daughter Khorshid
And also my parents,
The brilliant stars of my life

Acknowledgment

Special thanks to my dedicated advisor, Professor Khosrow Ghavami for competent supervision in all steps including editing patiently my research program. The first investigation about bamboo in Brazil and in the world started in 1979 by Prof. Ghavami at PUC-Rio. After that many well-known research centers and universities around the world started their investigation about this magic plant. Thanks to Prof. Holmer Savastano Jr. from FZEA-USP for the preparation and sending the bamboo culms from Pirassununga campus. Most of the experiments were carried out at the ITUC laboratory of PUC-Rio. My thanks are to Ms. Lucia Queiroz, Adrian Giassone, Roberta Madeira, Ubiratan Moreira and Luiz Paulo Jr. for their collaboration and patience to help in realizing the tests. Thanks also to the technicians of the structure and material laboratory (LEM-DEC) José Nilson de Melo, Euclides Moura Neto, Rogério Ross Daniel, Carlos Alexandre for their assistance in workshop operations and mechanical tests. Thanks to Prof. Sidnei Paciornik, Dr. Marcos Henrique and Asafe Bittencourt from the department of the materials, for their cooperation to prepare the meso scale and the X-ray microtomography images. Thanks to Prof. Maria Isabel, Henrique Meira and Gisele Barbosa made available the heat treatment equipments, also to Elaine Cabral for the TGA tests, from the department of chemistry. Special thanks to Tehran University which contributed through Prof. Kambiz Pourtahmasi, Prof. Ghanbar Ebrahimi and their students from the wood and paper department for the execution of the chemical analysis of bamboo and to Mr. Hashemi from engineering workshop for helping to fabricate the set up used in compression and transversal tensile tests of. Thanks to Rita de Cássia do Nascimento Leite, the secretary of the post-graduate course. I would like to thank to my good friends Dr. Henrique Alves, Dr. Alexandr Zhemchuzhnikov, Dr. João Queiroz Krause, Dr. Wellington Tatagiba de Carvalho and Monique Nascimento dos Santos for their assisting in one way or another in the development of my research work. Also, the financial support given by Brazilian financing agency of CNPq is well appreciated.

Abstract

Azadeh, Arash; Ghavami, Khosrow (Advisor). **Heat influence on physical and mechanical properties of *Dendrocalamus giganteus* bamboo.** Rio de Janeiro, 2018. 224p. Tese de Doutorado. Departamento de Engenharia Civil, Pontifícia Universidade Católica do Rio de Janeiro.

The principal objective of the present thesis is to investigate the effect of heat on physical and mechanical properties of *Dendrocalamus giganteus* bamboo. The chemical analysis carried out to study and compare chemical components among different species and the internal and external parts of *Dendrocalamus giganteus* bamboo. To establish the heating range and its intervals the thermogravimetric analysis test (TGA) carried out to study the degradation of different bamboo genera and species at macro, meso, and micro and nano level. Based on preliminary heat exposure tests and the results of TGA, the tests executed at initial temperatures 25°C considered as ambient temperature, 100°C, 125°C, 150°C, 175°C, 200°C and 225°C for 3 hours duration as short term, and 24 hours duration as long term heat exposure. Image processing carried out to investigate the meso structure of bamboo as a functionally graded material (FGM) and the fiber distribution alongside the radial direction from internal to external bamboo wall thickness. The volume fraction of fibers, matrix and voids for internal and external part of bamboo section established and used in the investigation of water absorption of each component of the bamboo. The scanning electronic microscope (SEM) and X-ray microtomography used to study the effects of different heat exposures on micro structure of fiber and matrix. The micro cracks initiate and propagate after 175°C. The influence of heat on hygroscopicity, water absorption, shrinkage and swelling of bamboo specimens in longitudinal, radial and tangential directions at different temperatures and time exposures investigated. The non-uniform shrinkage and water absorption of bamboo test specimens, measured in tangential direction at internal and external sides which permitted to establish the hygroscopic property of each component. The results show by heat exposure higher than 175°C the water absorption capacity reduces significantly. The tensile, compression, and shear resistance established along the fibers and only tensile experiments realized transversal to the fibers. In addition, the dynamic bending modulus of elasticity using impulse excitation technique applied to considered specimens. The result of mechanical

tests shows a close relation between transversal tensile and shear strength with matrix strength. The tangible variation in mechanical properties occurred after heat exposure-time at 175°C-3h or 150°C-24h. The modulus of elasticity and compression strength are not reduced significantly and nearly remain the same for samples treated at 225°C-3h or 200°C-24h while for the tensile, shear and transversal tensile samples, the mechanical strength decreases about 70% to 90% at these temperature-time.

Keywords

Bamboo *Dendrocalamus giganteus*; Heat effect; Mechanical properties; Water absorption; Image processing.

Resumo

Azadeh, Arash; Ghavami, Khosrow (Orientador). **Influencia do calor nas propriedades físicas e mecânicas do *Dendrocalamus giganteus* bambu.** Rio de Janeiro, 2018. 224p. Tese de Doutorado. Departamento de Engenharia Civil, Pontifícia Universidade Católica do Rio de Janeiro.

O principal objetivo da presente tese é investigar o efeito do calor nas propriedades físicas e mecânicas do bambu Dendrocalamus giganteus. A análise química foi realizada para estudar e comparar componentes químicos de diferentes espécies e partes internas e externas do bambu *Dendrocalamus giganteus*. Para estabelecer a faixa de aquecimento e seus intervalos, foi realizado o teste de análise termogravimétrica (TGA) para estudar a degradação de diferentes gêneros e espécies de bambu nos níveis macro, meso, micro e nano. Baseado em ensaios preliminares de exposição ao calor e nos resultados da TGA, ensaios executados a temperaturas iniciais de 25°C (considerado como temperatura ambiente), 100°C, 125°C, 150°C, 175°C, 200°C e 225°C foram expostos por um período de 3 horas, considerado como curto prazo, e 24 horas, considerado como um longo prazo de exposição ao calor. Processamento de imagem foi realizado para investigar a meso estrutura do bambu, como *functionally graded material* (FGM), e a distribuição das fibras da parte interna à parte externa da parede de espessura do bambu, ao longo da direção radial. A fração volumétrica das fibras e da matriz para a parte interna e externa da seção do bambu foi estabelecida e utilizada na investigação da absorção de água por cada componente do bambu. O microscópio eletrônico de varredura (MEV) e a microtomografia de raios X foram usados para estudar os efeitos de diferentes exposições ao calor na microestrutura da fibra e da matriz. As microfissuras iniciam e propagam após 175°C. Também foram investigados a influência do calor na higroscopicidade, a absorção de água, o encolhimento e o inchamento das amostras do bambu nas direções longitudinal, radial e tangencial sob diferentes temperaturas e exposições de tempo. O encolhimento não uniforme e a absorção da água de amostras do teste com o bambu, medido na direcção tangencial nos lados internos e externos, permitiram estabelecer a propriedade higroscópica de cada componente. Os resultados mostram que, com a exposição ao calor superior a 175°C, a capacidade de absorção de água reduz significativamente. Resistência à tração, compressão e cisalhamento estabelecida ao longo das fibras e somente

experimento de tração transversal realizado transversalmente às fibras. Além disso, o módulo dinâmico de elasticidade em flexão, usando a técnica de excitação por impulso aplicada a espécimes considerados. A variação tangível nas propriedades mecânicas ocorreu após a exposição do calor a 175°C durante 3h ou a 150°C por 24h. Os módulos de elasticidade e resistência à compressão não são reduzidos significativamente e, quase, permanecem os mesmos para amostras tratadas a 225°C durante 3h e 200°C por 24h mas para as amostras de tração, cisalhamento e tração transversal, a resistência mecânica diminui cerca de 70% - 90% a esta temperatura-tempo.

Palavras-chave

Bambu *Dendrocalamus giganteus*; Efeito de calor; Propriedades mecânicas; Absorção de água; Processamento de imagem.

Table of Contents

List of Figures

List of Tables

List of symbols and abbreviations

A	Cross section area
AFD	Average fiber distribution
AHS	Ambient humidity stabilized
$ANOVA$	Analysis of Variance
b	Width of specimen in tangential direction,
BV	Bambusa vulgaris
$DBMOE$	Dynamic Bending Modulus of Elasticity
DG	Dendrocalamus giganteus
DTG	Derivative Thermogravimetric
E	Modulus of elasticity
E_c	Compression modulus of elasticity
E_f	Modulus of elasticity of fiber
E_m	Modulus of elasticity of matrix
EMC	Equilibrium moisture content
E_t	Tensile modulus of elasticity
f_0	Fundamental resonant frequency of bar in flexure, Hz
FEM	Finite element method
FVF	Fiber volume fraction
G_m	Shear modulus of matrix
HST	Humidity stabilization time
I	Moment of inertia
k	for the case of fix ends ($\theta = 0$) with free horizontal movement (guided support) is equal to one; For the same case but without movement is equal to 0.5
L	Total length of specimen
L_e	Effective length
LOI	Limiting oxygen index
LSC	Longitudinal Shear test by applying Compression load
LS	Longitudinal Shear sample
LST	Longitudinal Shear test by applying tensile load
m	Mass

MC	Moisture content
MOE	Modulus of Elasticity
MOR	Modulus of Rupture
NUTS	Normalized Ultimate Tensile Strength
r	Gyration radius
SBMOE	Static Bending Modulus Of Elasticity
SEM	Scanning Electronic Microscope
t	Wall Thickness Of Bamboo (Thickness In Radial Direction),
T_c	Correction factor for fundamental flexural mode
TFA	Total Fiber Area
TG	Thermogravimetric
TGA	Thermogravimetric Analysis
TT	Transversal Tensile sample
UTS	Ultimate Tensile Strength
V_F	Fiber volume fraction (%)
V_{Fn}	Normalized fiber volume fraction (%)
V_m	Matrix volume fraction (%)
V_v	Vein volume fraction (%)
VSC	Volumetric Swelling Coefficient
w	Width
WA	Water absorption
σ_t	Hoop stress
r	Density
w	Angular Frequency

1. Introduction

Due to the actual energy crisis in the world, which has been started in the seventies of the twentieth century, some researchers started to investigate the physical, chemical and mechanical properties of nonconventional materials such as bamboo and vegetal fibers at macro, meso, micro and nano levels [1]. Bamboo as an herbaceous material is an all-purpose, non-timber forest product. Some of the advantages of bamboo as a construction and building material are rapid growth, being renewable, affordability, workability and high mechanical resistance especially in tensile strength comparable with steel.

Bamboo is a general term for woody grasses from Poaceae or Gramineae family and Bambusoideae subfamily [2]. This plant increases via seeds and rhizomes [3]. Roughly, bamboo species are divided into herbaceous and woody types [4]. Only some of the woody types of bamboo have remarkably mechanical resistance and can be used for industrial and structural purposes as a non-timber forest product [5]. Bamboo as an optimized and ready tubular element can be used as scaffolding, bridge construction, trusses, beams, columns and many other types of building components.

Beside those advantages there are some disadvantages which can limit the usage of bamboo as a conventional construction material. Shrinkage and swelling due to drying and water absorption is one the important destructive characteristic of the bamboo as a woody material especially when the bamboo used as reinforcement in concrete and cement mortars. The interaction between bamboo strips and concrete or mortars become an important factor due to water absorption of the bamboo. During the curing period of the concrete, bamboo starts to swell due to water absorption which may cause cracks in the concrete [6][7]. After the concrete has been cured the bamboo starts to lose its absorbed water, leaving a gap between bamboo and concrete. To control the cracks and create more cohesion between materials, the large dimensional changes should be reduced to minimum. For this purpose, any type of treatment which can help to minimizing the dimensional changes might be useful. In general for woody materials which are used in construction as structural or non-structural elements, any type of treatment which gives the material more immutability and consistency, by

improving the mechanical properties or at least without changing them, is more acceptable. One of the low-cost and feasible ways to improve some properties such as stabilizing the dimension of the woody materials is exposing them to a specific temperature during a specific time. Hitherto, few researches have been done the investigation the effect of heat on the bamboo properties, despite the fact that bamboo is a heat sensible material. Even though bamboo can be considered as an excellent alternative engineering material, but lack of knowledge about its behavior in elevated temperature may become a barrier for its mass use in engineering.

The objective of the present thesis is to investigate the effect of heat on physical and mechanical properties of *Dendrocalamus giganteus* bamboo when subjected to heat up to 225°C for 3 and 24 hours. Not only the temperature but also different exposure time for the same temperature is an effective parameter. The Thermogravimetric analysis (TGA) is the first step to know the behavior of a material and the degradation of material components due to elevating the temperature. TGA is carried out to measure the changes in mass due to heat increment [8]. By implementation of this test the heating range and proper intervals is obtained. The heating range is started from 100°C up to 225°C with increment equal to 25°C. 3 hours and 24 hours as short and long term heat exposure times respectively are considered for the tests.

The effect of heat on humidity absorption as well as shrinkage and swelling of bamboo specimens in Longitudinal, radial and tangential directions at different temperatures and times are investigated. To establish the difference between fiber and matrix hygroscopicity, the non-uniform shrinkage and water absorption test in tangential direction for internal and external sides is carried out and the hygroscopic property of each component measured separately. The longitudinal tensile test, transversal tensile test (hoop tensile), longitudinal compression test, longitudinal shear test, four point flexural test to obtain static bending modulus of elasticity and neuter axis, and excitation method to find the dynamic bending modulus of elasticity for the specimens heated at different temperatures and time programmed to do in this thesis as mechanical tests.

One section deals with bamboo image processing as a functionally graded material (FGM) and shows the difference of external and internal sides of wall thickness. In a functionally graded material (FGM) the properties changes

gradually with position [9] and for bamboo, the fiber density increases alongside the radial direction from internal to external side. This non uniform distribution of fibers makes differences for bamboo specimens which made from internal and external regions in terms of physical and mechanical behavior. Due to uneven distribution of fibers in radial direction the moment of inertia of a bamboo cross section should be estimated and corrected based on the fiber distribution in this direction. The results of this observation will be used to achieve the modulus of elasticity in static and dynamic flexural tests. By using image process also the distribution of fibers in radial, tangential and longitudinal directions is calculated.

In order to compare the effects of different heat exposures on micro structure of bamboo, by using a scanning electronic microscope (SEM) some images in different temperatures prepared and the effect of high temperature on fibers and matrix in micro scale studied. The material considered for the tests in this work is *Dendrocalamus giganteus* bamboo (*DG* bamboo). This bamboo considered because of its remarkable length, diameter and wall thickness. *Dendrocalamus giganteus* which is also famous as Giant Bamboo or Dragon Bamboo is a tropical and subtropical species native to Southeast Asia. Due to the same climate conditions, this bamboo grows in South America. The height of this bamboo can reach up to 35 m with the maximum diameter about 30 cm [10]. Also the geometrical dimensions of a typical *DG* bamboo culm measured to understand better the relation between the height to the node distances and thickness. The chemical tests have been done in Tehran university to find the percentage of bamboo components for three different species. Some of related tables, calculations, procedures are mentioned in appendix.

Based on physical, mechanical and chemical variations of a woody material such as bamboo, the heating range can be divided to different phases. The first is drying phase which can be started usually from freezing point up to water boiling point as can be seen in Figure 1.1. The freeze-drying at the temperatures close to 0°C normally used in food industry to preserve the perishable ingredients such as some special enzymes and vitamins. The process of drying removes the physical water of a material. The hot drying range is started usually from temperatures more than ambient temperatures to about the boiling water point [11]. Hot drying methods such as kiln method normally are used for wood and bamboo industry [12]. The second phase is the heat treatment which starts from the water boiling

point up to torrefaction temperature. By starting the torrefaction phase, the mechanical property of the bamboo reduces dramatically. The present study only deals with the drying and heat treatment phases as can be seen in Figure 1.1.

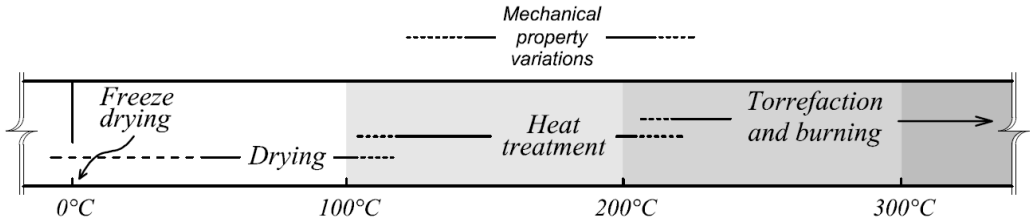

Figure 1.1 Different phases of heating a wood material

2. Literature review

The main aspects for literature review which are related to the effect on heat are:

- To compare the chemical components of different bamboos.
- To find out the proper range and intervals between heat treatments.
- The effect of heat and time duration on physical and mechanical property such as bamboo shrinkage, water absorption, tensile, compression and modulus of elasticity; and comparing with the researches carried out for another types of bamboo or hard and soft woods.

The mechanical and physical behavior as well as appearance of softwoods are comparable with bamboo then has been tried to study and adopt the experiments and codes carried out for wood to present investigation.

2.1. Bamboo structure as a natural composite

The cross section of a bamboo culm is shown in Figure 2.1a and b. Bamboo is a natural composite with two principal components, sclerenchyma which is considered as fibers and parenchyma assumed as matrix presented in Figure 2.1c [13][14][15]. Sclerenchyma with high resistance parallel fibers along the entire length of the bamboo surrounded by parenchyma is the matrix of this composite. Figure 2.1c shows the parenchyma as spongiform and porous structure, sclerenchyma as solid areas and veins as hollow tubes. The shape of the wall cells and porosity of parenchyma is magnified and presented in Figure 2.1d. the fiber and matrix cells can be seen in image prepared by Tomography in Figure 2.2.

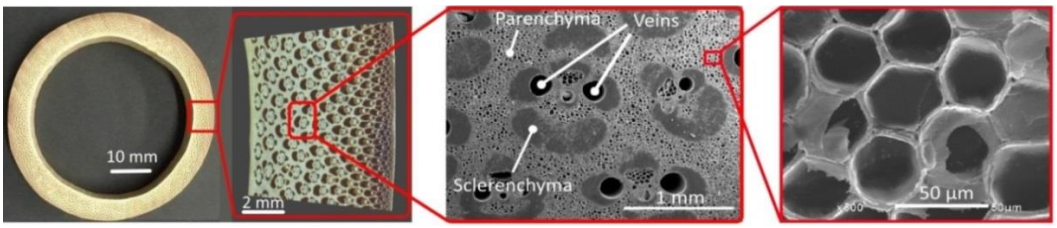

(a) bamboo culm section | (b) bamboo segment | (c) bamboo cross section components | (d) porosity of parenchyma

Figure 2.1 Bamboo macro and meso structure

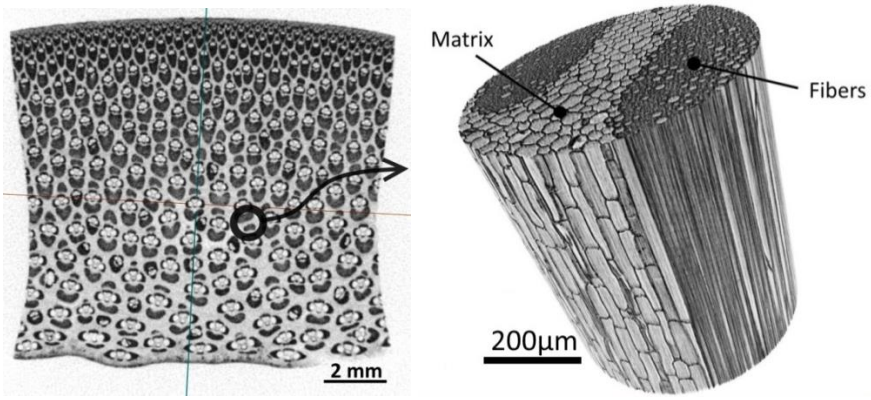

Figure 2.2 X-ray microtomography of *DG* bamboo fiber and matrix cells

Bamboo is Functionally Graded Material (FGM) [16][17]. A functionally graded composite material is an inhomogeneous material, consisting of two (or more) different materials which the properties changes gradually with position [18][19] as can be seen in Figure 2.3. For a bamboo as a FGM material, the fibers distribution on transversal cross section, in radial direction, gradually increases from the inside to the outside surface as can be seen in Figure 2.4.

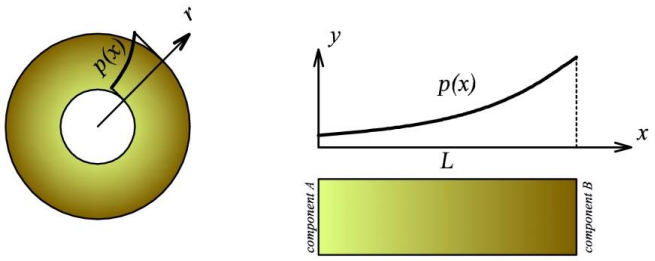

Figure 2.3 A functionally graded material

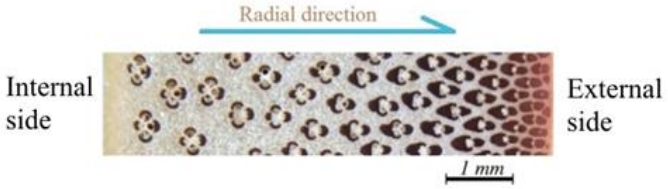

Figure 2.4 Bamboo as a FGM material

2.2. Chemical components of bamboo

The main chemical composition of bamboo material constitutes of cellulose, hemicellulose, lignin and extractives [20][2]. **Cellulose** is the main structural fiber in the plant kingdom and has remarkable mechanical properties. cellulose is the component which is responsible of bamboo fiber resistance and its stability is more than hemicellulose [21]. **Hemicellulose** consists of shorter chains (500–3,000 sugar units) as opposed to (7,000–15,000) glucose molecules per polymer

seen in cellulose [22][23]. Cellulose Young's modulus is cerca 130 GPa, and its tensile strength is close to 1 GPa. Hemicellulose is similar to cellulose but is less complex. The molecular weights are usually lower than that of cellulose and presents in almost all cell walls along with cellulose. The resistance of hemicellulose is much less than cellulose. The young's modulus of hemicellulose varies from 0.01 G Pa in nearly saturated hemicellulose to about 8 GPa in nearly dry hemicellulose compared with 120-140 GPa for cellulose [24]. Hemicellulose can be extracted from oat, barley, rice bran, corn bran and applicable as gels, films, coatings, adhesives, and gelling, stabilizing and viscosity-enhancing additives in food and pharmacy industry [25].

Lignin is the second most abundant organic compound on earth after cellulose. It has a complex chemical compound and makes up about one-quarter to one third of the dry mass of wood and can be find as interfaces or cell walls [26].

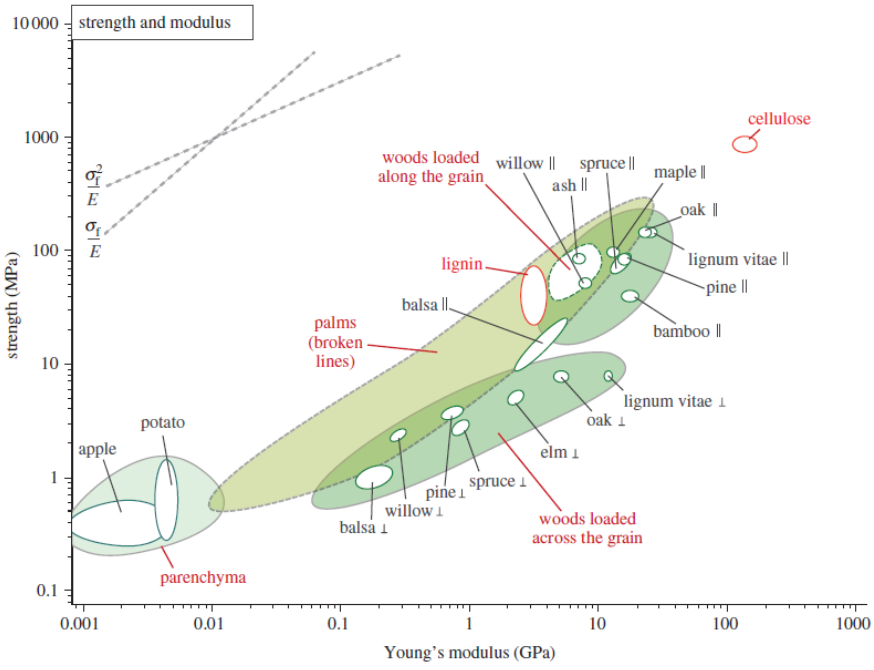

Figure 2.5 Strength against Young's modulus for some plant materials, cellulose and lignin [22]

Table 2.1 Typical property ranges for cellulose and lignin [27]

Material	Density ($kg.m^{-3}$)	Young's modulus (GPa)	Tensile strength (MPa)	Elongation (%)	Thermal conductivity (W/m.K)
Cellulose	1450-1590	120-140	750-1080	20-40	0.5-0.65
Lignin	1200-1250	2.5-3.7	25-75	3-4	0.13-0.18

lignin is comparable with cement in reinforced concrete and its role as filler impregnating the matrix of cellulose fibrils in the cell wall [28]. It has a large macromolecule with a molecular mass in excess of 10000 atomic mass units and the most hydrophobic (water-repelling) component of the cell and often considered nature's adhesive [29]. Table 2.1 shows some typical property ranges for cellulose and lignin [27].

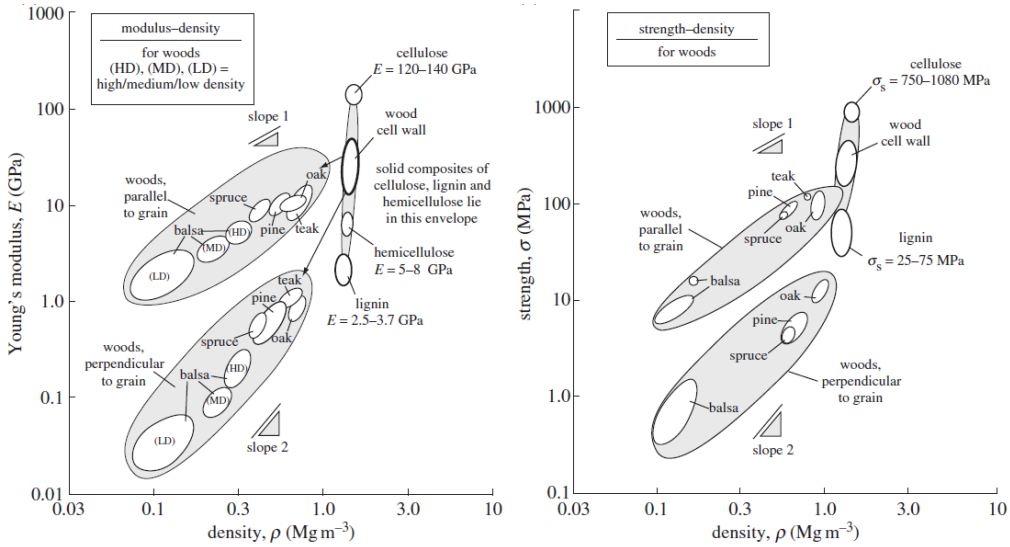

Figure 2.6 Density against Young's modulus and strength for some plant materials [22]

Figure 2.5 illustrates the relation between strength and young's modulus of some different plant materials as well as lignin and cellulose. The cellulose remarkably has more strength and modulus of elasticity than the lignin. The mechanical property of Cellulose and lignin have been mentioned in Gibson and Ashby [22][27]. The proportion of chemical compositions in various bamboos' species is different. The proportion of cellulose, hemicellulose, holocellulose and lignin for some different types of bamboo, have been shown in Table 2.2.

The minimum and maximum values of holocellulose in Table 2.2 are 51.8 to 76.8 respectively which shows the high range of holocellulose value. The average and coefficient of variation (CV%) of holocellulose and lignin at different types of bamboo mentioned in Table 2.2 are (68.8, 9.9%) and (23.6, 16.9%) respectively. The results presented in Table 2.2 shows the proportion of cellulose, hemicellulose and lignin for the *Pyllostachys pubescens* and *Pyllostachys makinoi hay bamboo* are close to each other. The amount of cellulose in *Bambusa sinospinosa bamboo* is significantly higher but the amount of lignin is less than the three other types.

Table 2.2 Chemical composition of some *different bamboos*

Bamboo species	Holocellulose (%)	Lignin (%)	Cellulose (%)	Hemicellulose (%)
Bambusa sinospinosa [30]	76.8	13.0	62.3	14.4
Dendrocalamus giganteus munro [31]	62.9	26.3	47.5	15.4
Phyllostachys makinoi hay [32]	69.6	25.5	45.3	24.3
Phyllostachys pubescens [33]	67.1	22.1	41.5	25.5
Dendrocalamus asper [34]	74.0	28.5	-	-
Phyllostachys heterocycle [35]	76.8	26.1	-	-
Phyllostachy nigra [35]	66.4	23.8	-	-
Phyllostachy reticulate[35]	51.8	25.3	-	-
Phyllostachy pubescens [36]	71.7	23.6	-	-
Gigantochloa scortechinii [37]	67.4	26.4	-	-
Bambusa clumeana [37]	69.2	21.6	-	-
Schizostachyum zollingeri [37]	71.6	21.4	-	-

Li (2004) [38] has been studied the *Moso* bamboo chemical analysis and compared the amounts of holocellulose, cellulose and lignin for different ages; different parts from top, middle and bottom; and four different sections in radial direction from epidermis to inner part with low fiber volume fraction as can be seen in Figure 2.7. It shows that the outer part with more fibers has relatively more amount of holocellulose and alfa-cellulose. Alfa cellulose is responsible of bamboo fiber resistance then and the higher amounts of alfa-cellulose at the middle and top of the culm represents the higher resistance relative to the bottom.

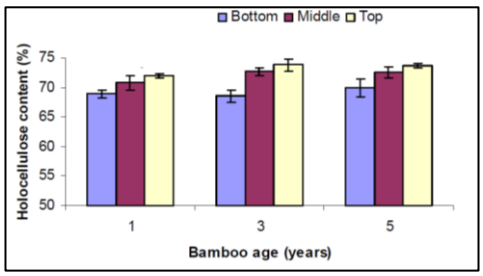

(a) Holocellulose content of bamboo at different ages and heights

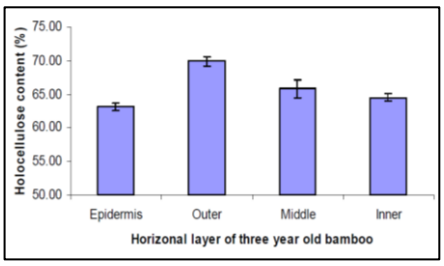

(b) Holocellulose content of three years old bamboo of different horizontal layers

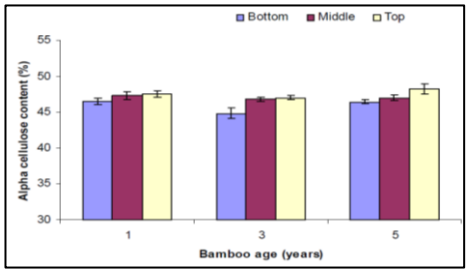

(c) Alpha-cellulose content of bamboo at different age and height location

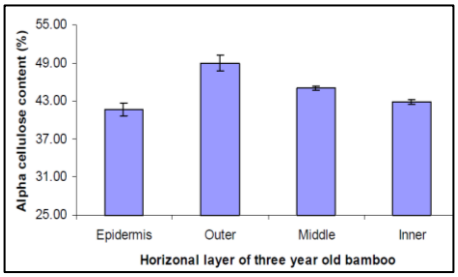

(d) Alpha-cellulose content of three years old bamboo of different horizontal layers

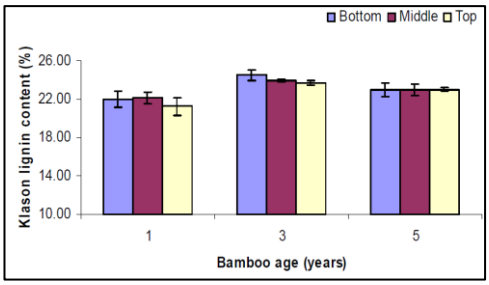

(e) Lignin content of bamboo at different age and height locations

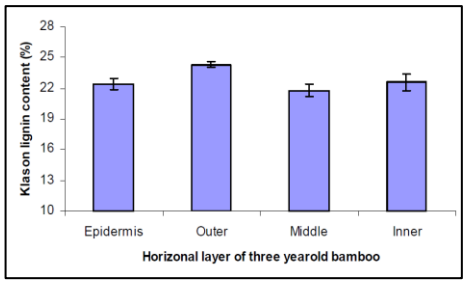

(f) lignin content of three years old bamboo of different horizontal layers

Figure 2.7 Bamboo chemical analysis for *Moso* bamboo comparing the bamboo ages, locations and different sections in radial direction [38]

Before comparing wood and bamboo, the differences between hardwood and softwood compositions should be mentioned. Softwood is a term which is used for evergreen trees such as cedar, pine, redwood and spruce. Alder, balsa, beech, mahogany, maple, oak, walnut and eucalyptus are considered as hardwood. In the hardwoods, the cellulose content varies from 40% to 50% and the lignin content is comprised between 15% and 25%, and the hemicelluloses varies from 15% to 25%. Softwoods have about 5% to 10% greater concentrations of lignin and about the same amount of cellulose 40% – 50%. Less hemicelluloses may be found in softwoods than hardwoods [39].

Comparing the bamboo with softwood and hardwood shows the values of bamboo components are nearly close to both softwood and hardwoods and there is not any significant difference between the amounts of similar components. In fact, the difference between the similar component values in different species of bamboo mentioned in Table 2.2 is more than the difference between wood and bamboo. Comparing the results presented for fiber components in Figure 2.8 with the values shown in Table 2.2 for whole bamboo reveals that the structure of fibers or sclerenchyma has more cellulose and the structure of parenchyma more constituted by lignin and hemicellulose.

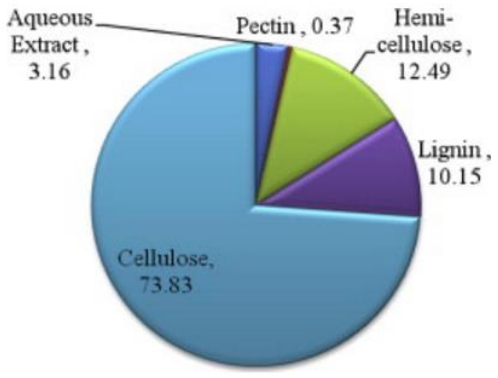

Figure 2.8 Bamboo fiber components for *Neosinocalamus affinis* bamboo [40] [41]

Based on Liese (1998) [13] and Amada (1996) [42] The proportion of elements (in terms of sclerenchyma and parenchyma) present in the anatomical stem of bamboo are: 52% of parenchymal cells, 40% fiber and 8% of vascular tissue.

2.3. Thermogravimetric analysis (TGA)

Thermal Gravimetric Analysis (TGA) is a common method to study material degradation due to elevating the temperature. By gradual temperature increment with special rate, the mass of the material decreased. By using the (TGA) in a controlled temperature and controlled atmosphere, any mass changes of a material is registered as a function of temperature (with constant heating rate) [43]. This injective function as a curve with its derivation can show some key points of material components degradation. The measurement is normally carried out in an inert atmosphere, such as Helium, Argon or nitrogen to prevent ignition the material by rising the temperature. Heating rates can vary between 1^{o}C/min to 100^{o}C/min. This test can be done for the whole material or each components of it. Bamboo as an organic material with different types and species has different proportion of cellulose, hemicellulose, lignin and extractives as mentioned in chapter 2.2. Before knowing the degradation of bamboo as a whole, the degradation of the chemical components of bamboo is studied.

The TGA test has been done by Wenjia *et al.* (2013) [44] shows the results for cellulose, lignin and xylan for wood in Figure 2.9. The left graph is the mass residual (x) and the right one is the derivation graph $\frac{dx}{dt}$ that shows maximum changes in weight loss for cellulose and lignin happens about 340°C but for xylan about 200°C. Song-lin *et al.* (2003) [45] shows that heat treatment of bamboo up to 200°C degrades hemicellulose, and free water is generated due to the chemical breakdown. Xylan is a group of hemicelluloses which are found in plant cell walls [46]. It means the degradation of the bamboo structure starts from cell walls at about 150°C and the pick of loss weight or maximum rate of degradation happens in 200°C.

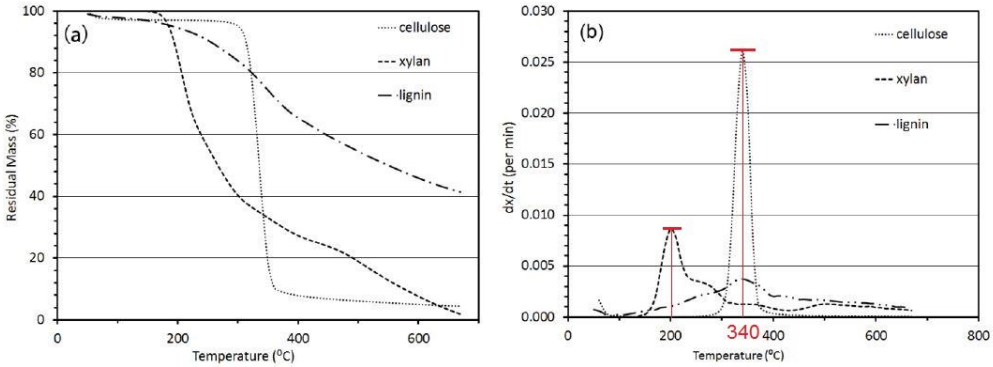

Figure 2.9 TGA curves (left) and related derivations (right) for cellulose, lignin and xylan [44]

The result of mass derivation for TGA test for cellulose, hemicellulose and lignin presented in Figure 2.10 done by Gašparovič *et al.* (2009) [47] shows the decomposition of hemicellulose and cellulose takes place in the temperature range of 200–380°C and 250–380°C respectively, while lignin decomposition seems to be ranging from 180°C up to 900°C. Also the TGA results for four different types of biomasses has been done by Chen *et al.* (2010) [48] shows wood (*Ficus benjamina*) and bamboo have the same behavior in losing mass at the first stage with temperature less than 200°C but in the second stage between 200°C to 500°C bamboo shows more sensibility than the other materials.

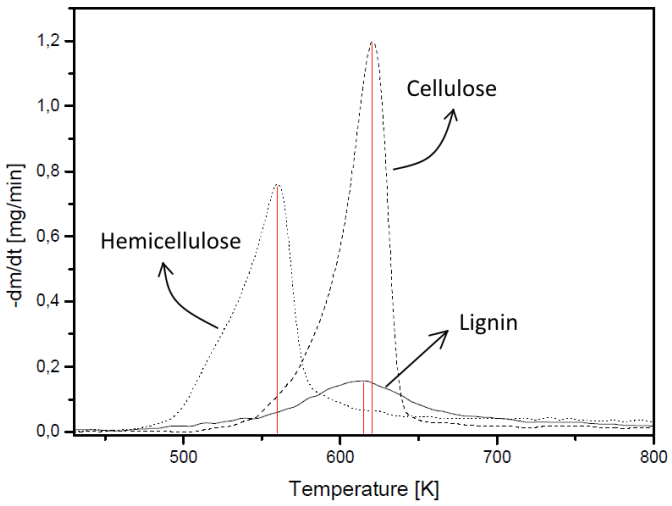

Figure 2.10 Mass derivation for hemicellulose, cellulose and lignin [47]

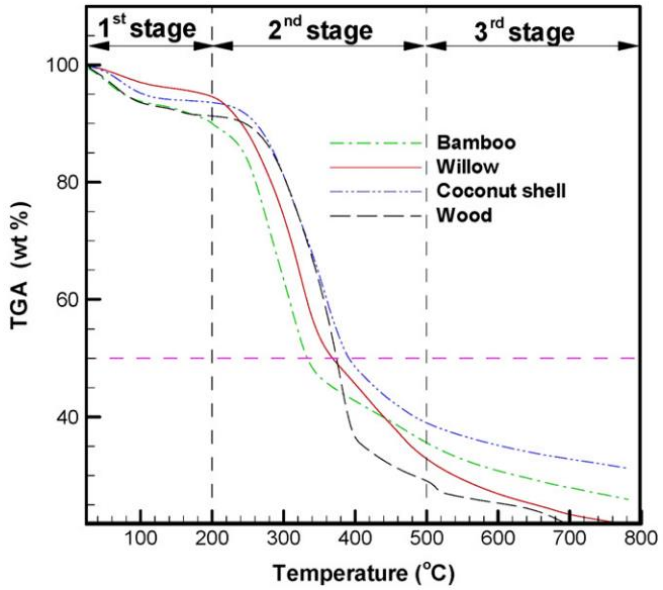

Figure 2.11 Distributions of TGA of four tested biomass [48]

Dorez *et al.* (2013) [49] implemented some tests for comparing the thermal degradation and fire reaction of different natural fibers and their corresponding biocomposites. The TGA result for different natural fibers is demonstrated in Figure 2.12. The effect of heating rate has been investigated by Chen *et al.* (2014) [50] for Moso bamboo. The experiments were performed up to 700°C with heating rates of 5, 10, 20, and 30°C/min using TGA.

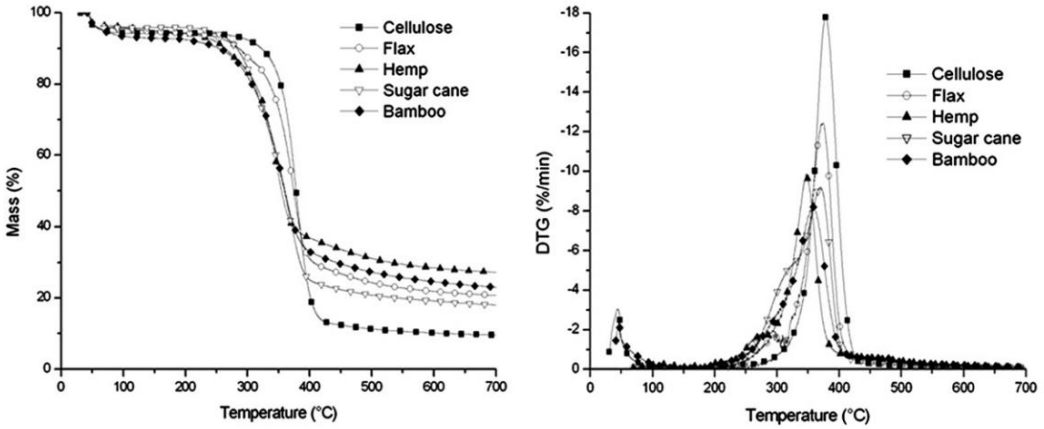

Figure 2.12 TG curves (left) and related DTG (right) for different natural fibers [49]

The results show that by increasing the heating rate, the curves shift to right side or higher temperature range as can be seen in Figure 2.13. The same result by using heating rates of 5, 20, and 100°C/min has been obtained by Skreiberg et al. (2011) [51].

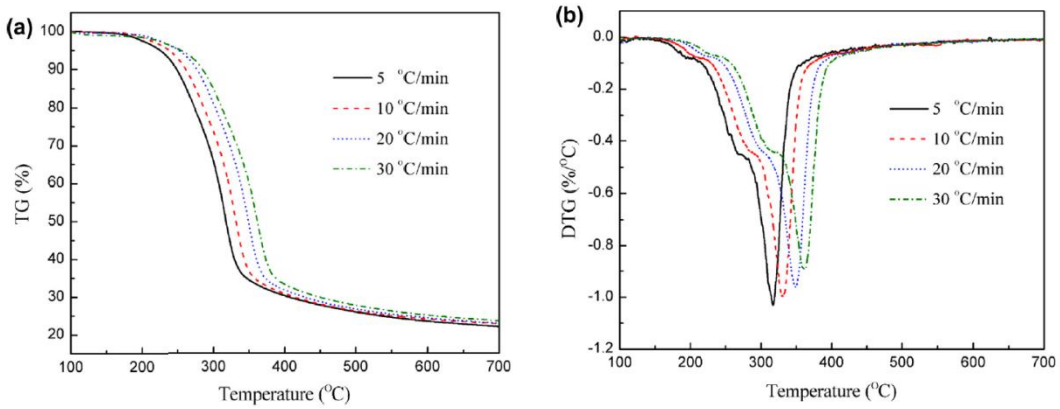

Figure 2.13 TGA curves (left) and related derivations (right) for four different heating rates [50]

A research done by Li *et al.* (2013) [52] shows the effect of heat treatment on fiber decomposition of Moso bamboo (*Phyllostachys edulis*), by exposing in 100°C, 150°C and 180°C for two hours. The thermal decomposition mechanism for three types of heat treatment had similar trends as can be seen in Figure 2.14. This study shows that the degradation of bamboo fibers heated at 180°C is the same as fibers heated at 100°C.

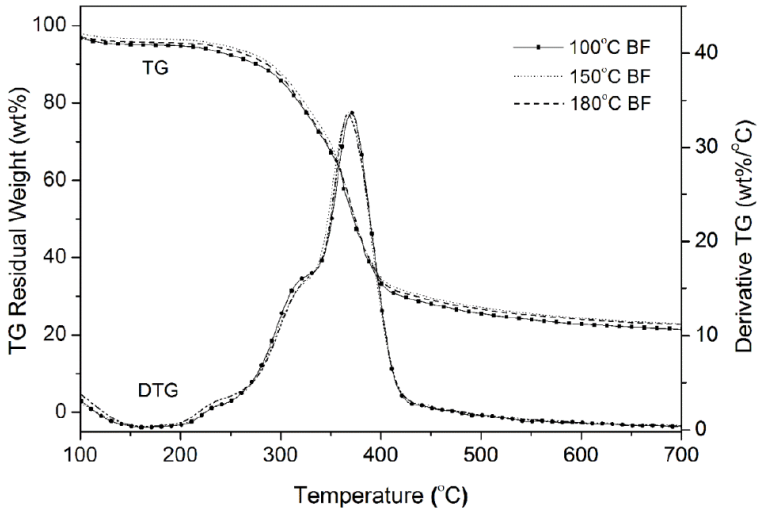

Figure 2.14 Thermal gravimetric decomposition process of heat treated *Moso* bamboo fibers for two hours [52]

2.4.The effect of temperature and time exposure on bamboo

The temperature and time exposure are two main factors in heating process. There are various investigations about heat and time exposure effect on mechanical property and physical behavior of different types of hard and soft woods. The result of studies shows exposing the wood at defined temperature-

time can improve the dimensional stability [53] and resistance to biological deterioration for different types of woods and bamboo makes them more hydrophobic [54][55]. The effect of high temperature on mechanical properties, dimensional stability and color of spruce has been investigated by Bekhta and Niemz [56]. Their research shows that after heat treatment at 200°C the color changes were drastic. The moisture content is lower for heated wood compared with non-heated wood when exposed to the same climate. Also wood samples heated at 200°C become more dimensionally stable than the non-heated samples. For the same temperature, 24h treatment duration gives more dimensionally stable wood than treatment duration of 2h at the same temperature. By increasing the treatment duration, the swelling both in tangential and radial directions decreased.

In most cases for hard and soft woods there is a nearly direct relation between elevating the heat treatment and reducing the water absorption capacity. The tests has been done by O. Unsal *et al.* [57] on Eucalyptus shows the swelling reduction for 180°C-10hrs exposure about 14% and 21.5% in radial and tangential directions respectively regarding to non-treated samples. The test has been done by D. S. Korkut and S. Hiziroglu [58] on oak and pine specimens shows 39.8% and 28.7% lower tangential swelling values, as a result of exposure to a temperature-time of 200°C-8hrs regarding to control samples.

The test results presented for pine sapwood[59] shows the water absorption actually increases by heat treatment from 170°C up to 230°C in contrary with the other results achieved by other types of wood and wood part. W. Scheiding *et al.* [60] also mentioned the water uptake difference between heat treated heartwood and sapwood of *Pinus sylvestris*. These results which some of them are contrary, proves the necessity of doing the water absorption tests on heat treated *DG* bamboo. The same as wood, by exposing the bamboo in specific temperatures and defined time exposure, not only the appearance and mechanical property but also the physical and hygroscopic property of bamboo such as capacity of water absorption and swelling is changed [61][55].

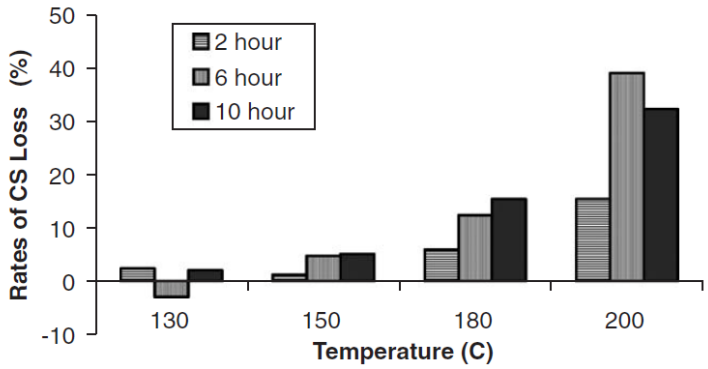

Figure 2.15 The rate of compression loss regarding to time and temperature on spruce wood [62]

Yildiz *et al.* [62] investigated the effect of heat treatment on spruce wood (*Picea orientalis*) at four different temperatures (130, 150, 180 and 200°C) and three different durations (2, 6 and 10 h) under atmospheric pressure. The rate of compression strength (CS) loss regarding to time and temperature has been presented in Figure 2.15. A dramatic diminution was observed above temperatures of about 150 °C.

A research carried out for *phyllostachys pubescens* bamboo has been done by Zhang *et al.* (2013) [63] shows the effect of heat treatment in 100°C up to 220°C with 20°C increment during 1,2,3 and 4 hours. The significant mass loss started about 180°C for all exposure times. As can be seen in Figure 2.16, MOR increased first up to 140°C and then decreased. the effect of heat exposure time up to 140°C is negligible for MOR test but after at about 160°C can be seen the difference between samples treated at different time exposure. Their study show not significant changes for the modulus of elasticity (MOE) by increasing the treatment temperature up to 180°C. It can be observed a significant decrease in MOE when samples treated above 200°C. The tested samples are the beams with 80^{mm} x 10^{mm} x 3^{mm} which tested in a three point bending device.

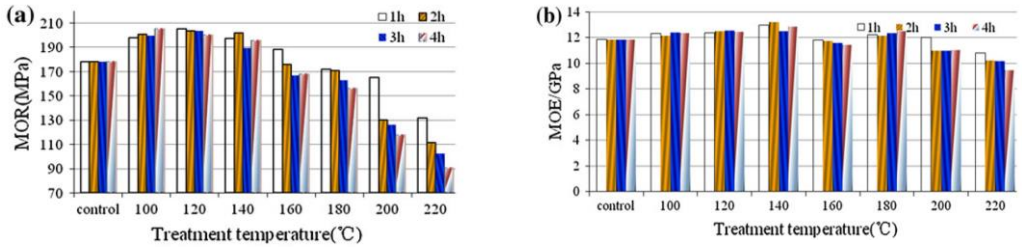

(a) Modulus of rupture (b) Modulus of elasticity

Figure 2.16 The effect of heat treatment on MOR and MOE [63]

Bamboo due to lack of radial or tangential fibers, uneven shrinkage and longitudinal shear loads is susceptible to splitting or cracking during the natural seasoning or kiln drying. Wu (1994) [64] shows when the bamboo culms dried under elevated temperatures (from 70°C up to 120 °C) no splits occurred on the culm surface.

Comprehensive research about physical and mechanical properties of *Moso* bamboo done by Yang *et al.* (2016) [65] presents the effect of heat treatment in different heating media; air, nitrogen and linseed oil. The heat treatments were conducted at 150, 170, 190 and 210°C for 1, 2, and 4 h. Mass loss due to heat treatment up to 150°C in air is mainly induced by evaporation of the integrated water and some extractives of bamboo. The mass loss (%) for heat treatment at different time and temperature in air and N_2 is presented in Table 2.3.

Table 2.3 The mass loss (%) of *Moso* bamboo heat treatment in air and N_2 media [65]

Temperature / Time	150°C		170°C		190°C		210°C	
	Air	N_2	Air	N_2	Air	N_2	Air	N_2
1 hr	0.91	0.2	1.48	0.66	2.09	1.20	4.97	4.31
2 hr	0.95	0.27	2.02	0.76	4.14	2.37	8.69	4.47
4 hr	1.14	0.62	2.04	1.03	4.21	4.01	8.56	7.39

As can be seen in Table 2.3 the mass loss due to heat treatments in air and N_2 increased with elevated treatment temperature and duration. For specimens treated in air, the mass loss was moderately low at 150°C and was mainly induced by evaporation of the integrated water and some extractives of bamboo. By treatment in 170°C a considerable loss of mass was observed however, no significant mass loss was observed for groups treated in N_2 at the same temperature conditions, since N_2 may isolate the bamboo from reacting with oxygen and mitigates inner thermal degradation.

The effect of heat treatment on EMC (Equilibrium Moisture Content) [66] of bamboo is presented in Figure 2.17. It shows the ability of bamboo moisture absorption reduces up to 50% for the samples treated in 210°C for 2 hours versus untreated specimens.

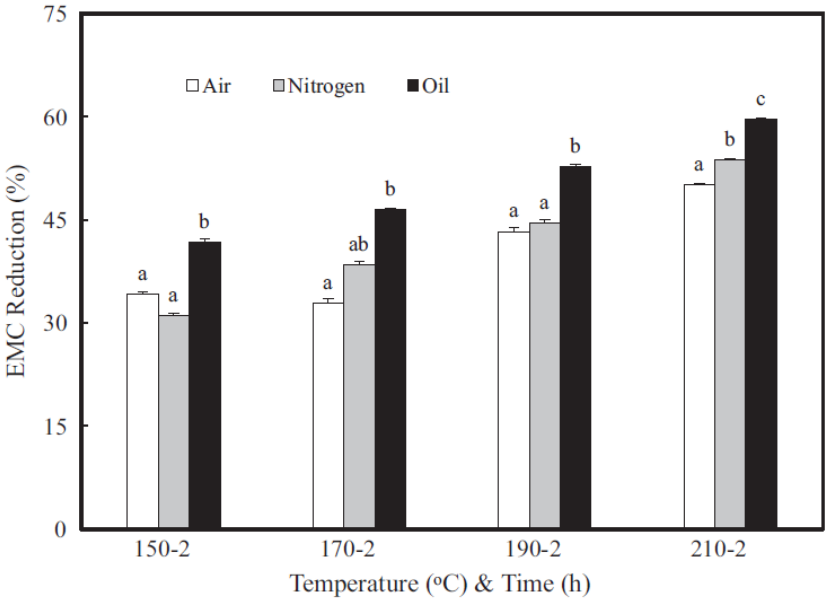

Figure 2.17 EMC reduction of heat treated versus untreated bamboo specimens [65]

The water absorption reduction investigated for different heat treatment and time exposure presented in Figure 2.18. the untreated bamboo samples were taken as the benchmarks and the reduction is compared with them. Significant changes happens at 170°C, the higher the treatment temperature results the higher the water absorption reduction. Figure 2.19 depicts the moisture content changes due to different heat treatment temperatures and times. By increment the heat treatment temperature and time, the ability of water absorption is reduced.

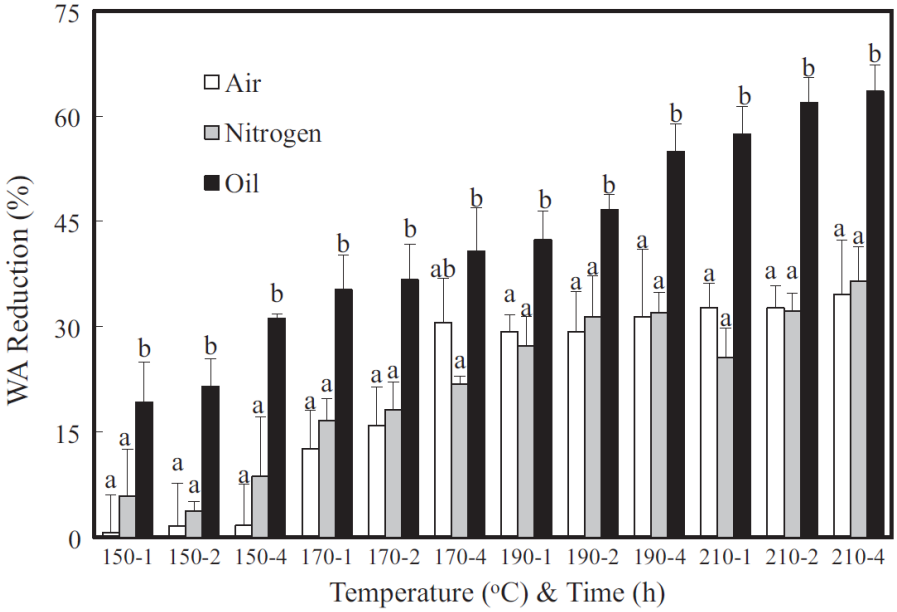

Figure 2.18 Water absorption reduction of heat treated versus untreated bamboo specimens [65]

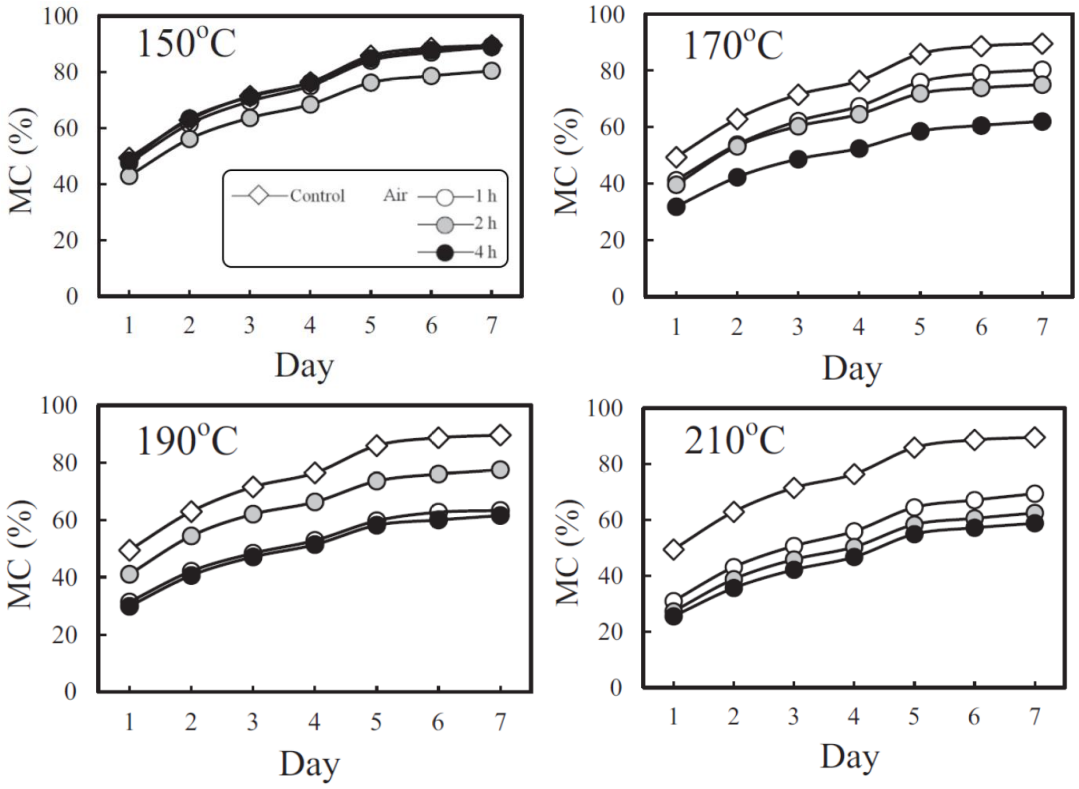

Figure 2.19 Water absorption curves of heat treated versus untreated bamboo specimens [65]

The comparison of volumetric swelling coefficient (VSC) of heat-treated bamboo shows quite similar swelling performances in the tangential and thickness (radial, R) directions, but no considerable swelling in the length (longitudinal, L) direction. This may be explained by the micro fibril angle in the bamboo cell wall structure tending to align with the longitudinal axis; however, there are no such reinforcing micro fibrils in the transverse directions [67].

The results of the mechanical tests has been done by Yang *et al.* [65] for the heat-treated Moso bamboo shows that the MOE (modulus of elasticity) tended to decrease after heat treatment. A similar tendency was observed with the MOR (modulus of rupture), indicating that the temperature was more significant in affecting the mechanical properties of the bamboo than the treatment duration. For heat treated samples, improved mechanical properties were observed at temperatures about 150°C.

The research has been done by Shangguan *et al.* (2016) [55] about heat treatment of *Neosinocalamus affinis* bamboo (a type of Chinese bamboo) composite shows the compressive strength increases by elevating the heat

treatment temperature for 2 hours up to 180°C and after decreases as can be seen in Figure 2.20.

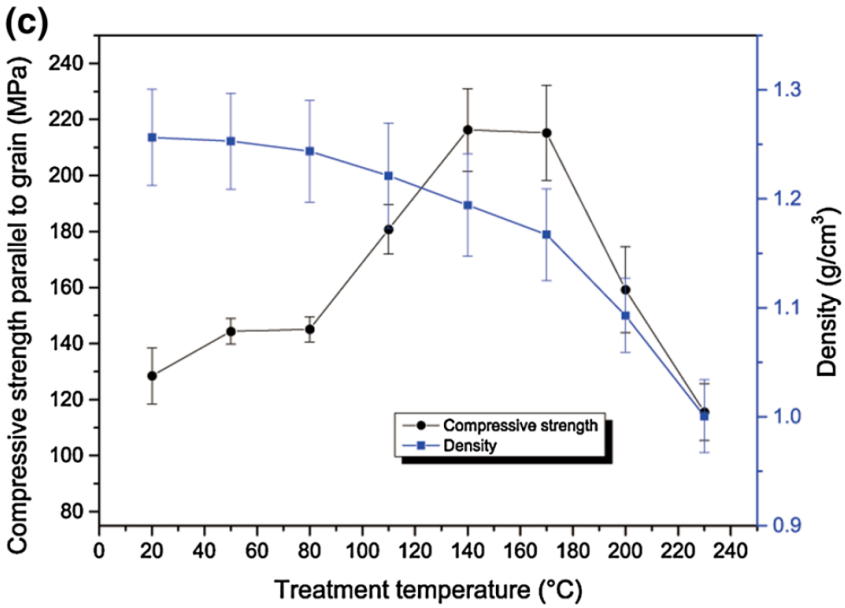

Figure 2.20 Compressive strength of heat treated bamboo composite at different temperature [55]

The test has been done by Ochi *et al.* (2002) [68] about Tensile properties of heat-treated hemp and bamboo fibers shows that the average tensile test of bamboo fibers is 516 MPa. After treatment in 200°C for 2 hours both fibers show a 60 percent decrease in tensile strength.

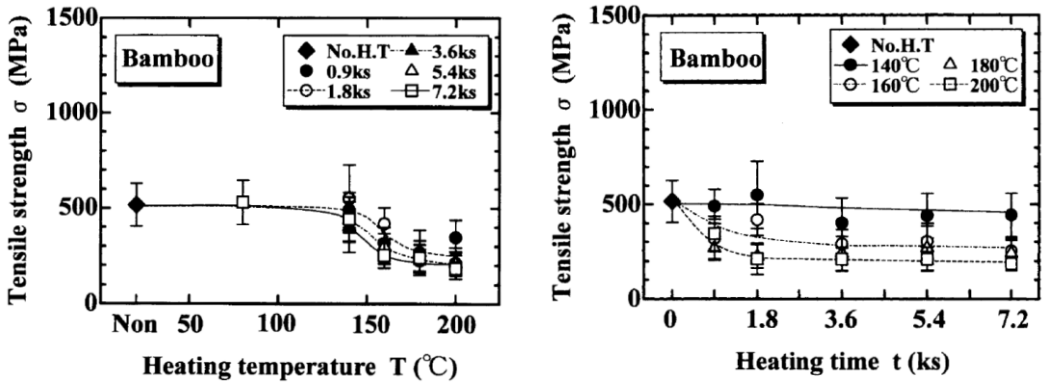

Figure 2.21 The effect of heating time and heating temperature on tensile strength of bamboo fiber [68]

Based on this report the degradation of the bamboo fiber starts from 140°C but in this range has not been observed any changes in young's modulus almost constant and independent of the heat treatment condition. In the other research about tensile properties of bamboo fiber reinforced biodegradable plastics by the same author Ochi (2012) [69] shows that the tensile strength of both bamboo fiber and bamboo fiber reinforced plastics decreased at 160°C.

2.5. The effect of moisture content on mechanical property of bamboo

The same as wood, moisture content of bamboo affects on mechanical properties. There are various investigations about effect of humidity on mechanical properties for different types of hard and soft woods [70]. Gerhards,2007 [71] has been gathered the results of four other researchers which presented in Figure 2.22. If the moisture content and modulus of elasticity normalized in 12% and 100% respectively, the samples with moisture content less than 12% show more values of modulus of elasticity and vice versa. By drying the different types of woods, the modulus of elasticity increases about 5% to 15%. Also by increasing the MC% up to 25% the MOE can be reduced up to 20% as can be seen in Figure 2.22. The effect of moisture content changes in mechanical properties normalized in 12% for *clear* wood is presented in Table 2.4.

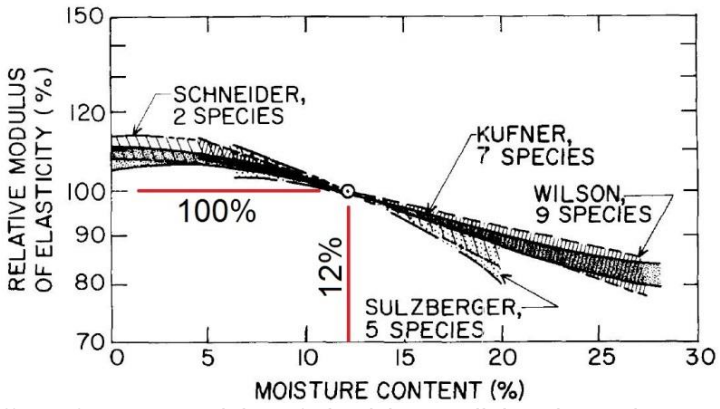

Figure 2.22 Effect of MC on modulus of elasticity parallel-to-the-grain normalized at 12% MC [71]

Table 2.4 The effect of moisture content on mechanical properties of clear wood [71]

Property	Relative changes In property from 12% MC	
	At 6% MC	At 20% MC
Modulus of elasticity parallel-to-the-grain	+9%	-13%
Modulus of elasticity perpendicular-to-the-grain	+20%	-23%
Shear modulus	+20%	-20%
Bending strength	+30%	-25%
Tensile strength parallel-to-the-grain	+8%	-15%
Compressive strength parallel-to-the-grain	+35%	-35%
Shear strength parallel-to-the-grain	+18%	-18%
Tensile strength perpendicular-to-the-grain	+12%	-20%
Compressive strength perpendicular-to-the-grain	+30%	-30%

The effect of moisture content on compression test of not treated bamboo (*Bambusa vulagaris*) for the moisture contents less than 30% is remarkable. The

compression resistance of bamboo samples with MC% less than 5% approximately is two times of the samples with MC more than 10% as can be seen in Figure 2.23 [72].

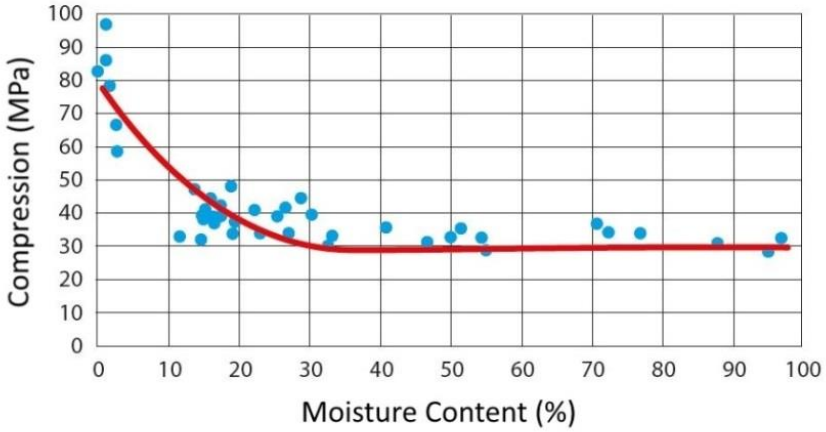

Figure 2.23 The effect of moisture content on compression resistance for *Bambusa vulgaris* [72]

The investigations have been done by researchers show that the tensile resistance as well as modulus of elasticity of bamboo by increasing the moisture content will be decreased [61]. Based on the experiments have been done by Achá [73] as can be seen in Figure 2.24 the bamboo specimens showing linear stress-strain behavior from the beginning of loading to the breaking point for the moisture content lower than 5%. For the moisture contents within 5% to 15% the behaviour of bamboo becomes elastic - plastic and for more than 15% up to 85% becomes elastic - extremely plastic.

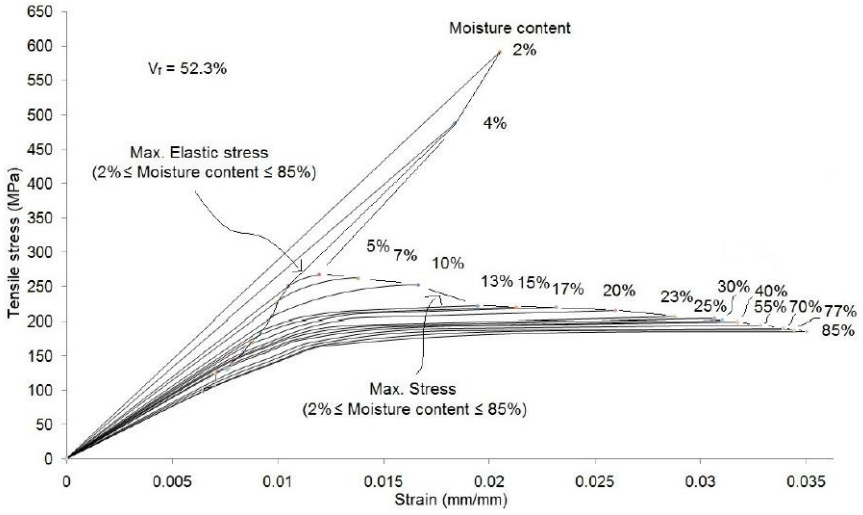

Figure 2.24 Tensile stress-strain curves for samples containing 52.3% fiber volume fraction at moisture content between 2% and 85% [73]

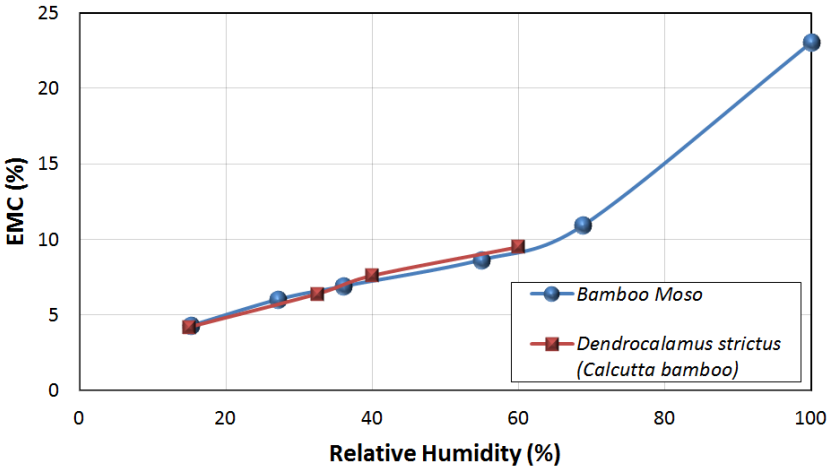

Figure 2.25 Relation between relative humidity and equilibrium moisture content for two different *Moso* [74] and *Dendrocalamus strictus* [75]

In general, by increasing the moisture contents after 5% the stress–strain curves become flatter. The tests in present thesis have been done in relative humidity about 60% up to 80%. At this relative humidity by considering the relation between relative humidity and moisture content presented in Figure 2.25, the moisture content of the all of test specimens are about 10% to 12%. Wang *et al.* (2013) [74] shows the relation between equilibrium moisture content (%) and relative humidity (%) of non-heat treated *Moso bamboo* between 22°C to 24°C. The result of Ahmad and Kamke (2005) [75] for *Calcutta bamboo* (*Dendrocalamus strictus*) without heat treatment shows the values close to the Moso bamboo as can be seen in Figure 2.25. Heat treatment can effect on the equilibrium moisture content. A study carried out by Gündüz *et al.* (2008) [76] shows that heat treatment at different temperatures and time exposures can reduce the equilibrium moisture content of wood at different RH% as presented in Figure 2.26 and Figure 2.27.

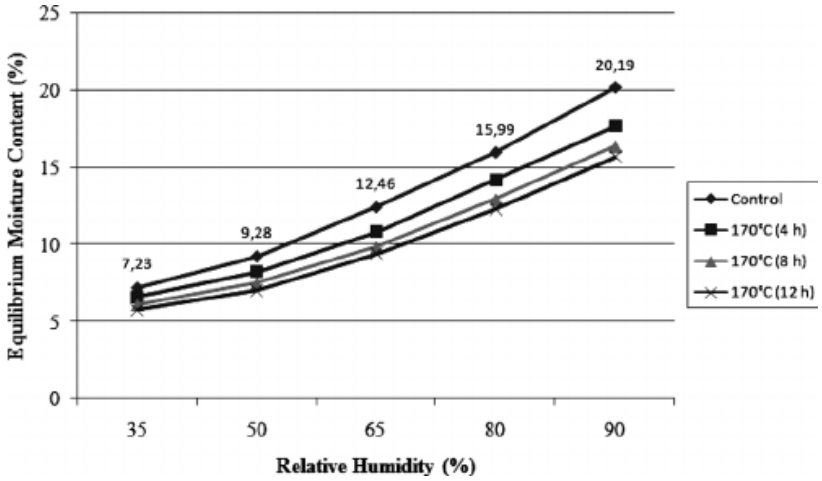

Figure 2.26 The effect of heat treatment on Fir wood at 170°C for 4,8 and 12 hours [76]

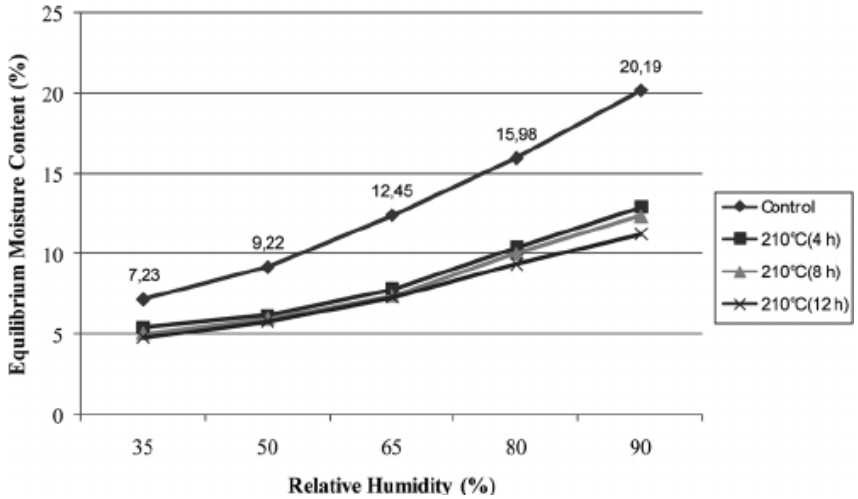

Figure 2.27 The effect of heat treatment on Fir wood at 210°C for 4,8 and 12 hours [76]

An study carried out by Yang *et al.* (2016) [65] presented in Figure 2.28 shows the moisture sorption curves of the heat treated bamboo specimens. The EMC values of the untreated bamboo specimens for 50, 65 and 90% RH were 9.49, 10.42 and 15.95% respectively. The heat treatment reduces the bamboo hygroscopicity and capacity of moisture absorption. Is not observed significant variations between the samples which treated for 1,2 and 4 hours in this test.

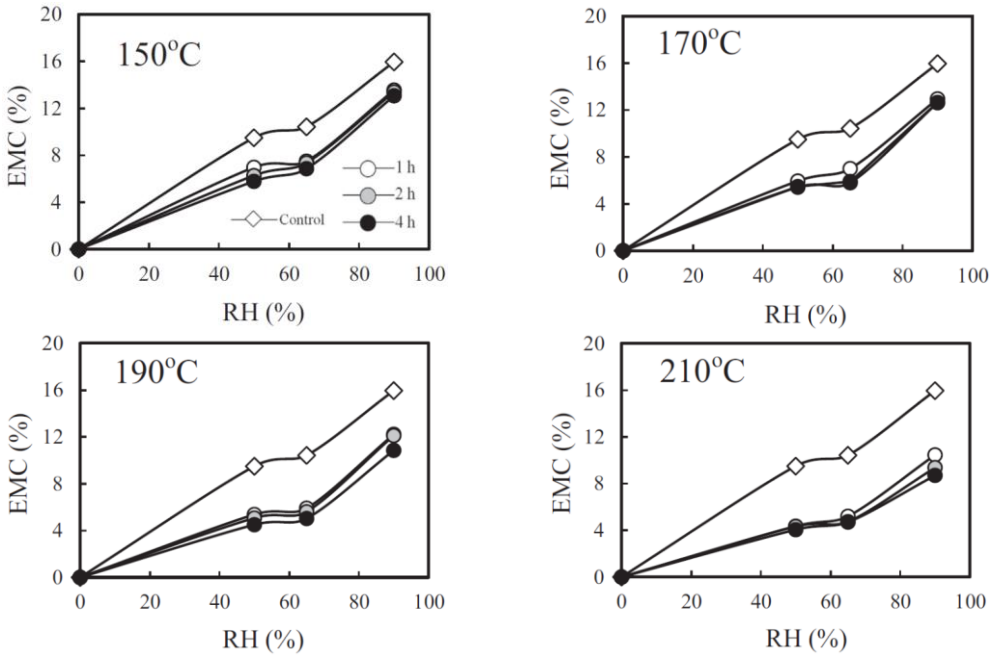

Figure 2.28 Moisture sorption curves of different heat treatment temperatures and times [65]

2.6. Bamboo Fire resistance

An investigation about the fire reaction and fire resistance of *Angustifolia Kunth* bamboo has been done by Mena et al. (2012) [77]. This study focused on

two aspects of material behavior: (1) fire reaction and (2) fire resistance. Fire reaction deals with how a material can be ignited and fire spread under specific conditions [78] and Fire resistance involves structural elements and describes how an element is able to maintain its sealing and isolation capacity and/or structural resistance under fire conditions [79]. The research has been done for round and glue laminated bamboo. Four different tests (ignition, flame spread, charring rate and bending stress) has been done for round and laminated as well as plywood. Observed that round *Guadua a.k.* and GLG (glued laminated *Guadua*) achieved the same value for ignition critical flux of 14 kW/m^2, which is higher than the value of 11 kW/m^2 registered by plywood. This means that *Guadua a.k.* requires higher energy per exposed surface to initiate the chemical decomposition processes. At the same time, *Guadua* a.k. achieves a higher value of ignition critical flux than the typical value of 12 kW/m^2 for most wood materials previously proposed [80], which has been adopted by several countries as critical ignition flux value for design purposes. Also this test proves that cortex provides an enhanced protection against fire, possibly due to its silica content [13], delaying the ignition process.

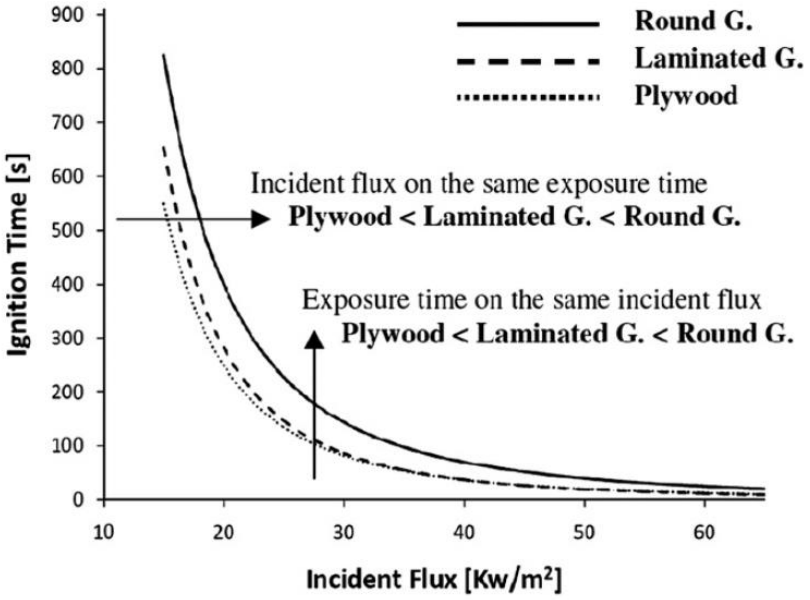

Figure 2.29 Heat flux vs. ignition time comparison between round G., laminated G. and plywood [77]

Unlike the ignition phenomena, the values of critical flux from flame spread test conducted on round *Guadua a.k.* (5.1 kW/m^2), GLG (10.4 kW/m^2) and plywood (3.5 kW/m^2) shows the plywood is the one that needs less energy and takes less time to fire propagation. Then, it can be considered as a weak point for

using plywood as a construction material. On the other hand the GLG by possessing the maximum value of critical flux is safer than the round Guadua and plywood.

The results for the charring rate obtained for the three materials under study shows the round Guadua a.k. has the lowest charring rate among the three materials under study by a large margin (Values obtained for round Guadua a.k. were approximately 40% of those obtained for GLG and plywood).

Finally, all three materials under study show a clear decrease in flexural strength as temperature increases. First all the flexural strength results in 15°C normalized to one. The variation of the flexural strength with temperature for each material is shown in Figure 2.30.

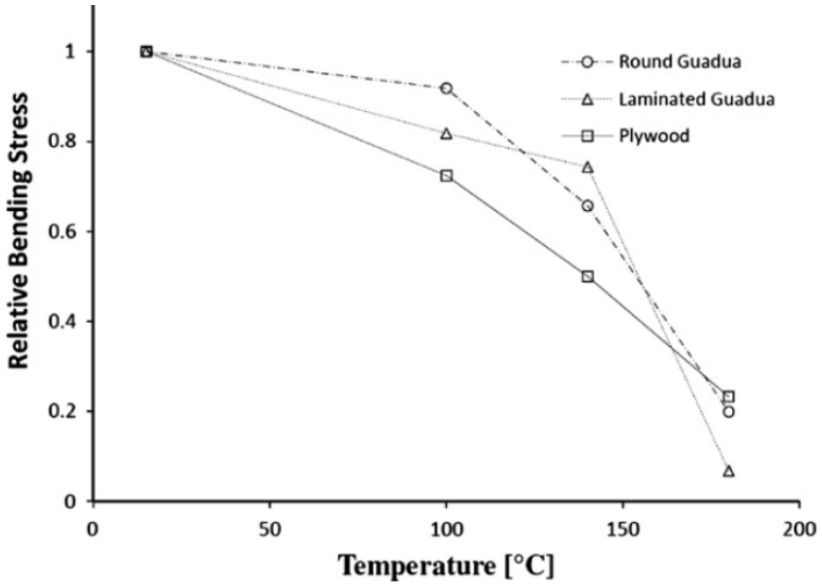

Figure 2.30 Relative flexure strength vs. temperature [77].

Sharma *et al* (2014) [81] used some chemical treatments as fire retardant for improving the behavior of *Dendrocalamus Strictus* bamboo against fire. They used 5 different types of treatments. The LOI (Limiting Oxygen Index [82]) test showed the LOI% for untreated bamboo was the minimum (18.2%) and for bamboo treated with borax and boric acid (generally used as bamboo treatment against pests) was (21.5%) and for treatment with melamine phosphate showed the max value for LOI (31.4%).

3. Experimental program

The experimental program divided into chemical, physical, mechanical and image process for meso structure. The result of study about geometrical properties of a *DG* bamboo is presented in section 3.2. TGA is the first chemical experiment carried out in the present thesis to study the bamboo behavior subjected to different temperature.

Mechanical tests are consist of tensile experiments along the fibers and to the fibers, compression along the fibres, longitudinal shear and bending tests for the specimens subjected to heat in dry oven (without pressure or vapor) at different times and temperatures. The static and dynamic tests carried out but for the present investigation the results of dynamic test used for the bending modulus of elasticity. The dynamic non-destructive tests have been done using Sonelastic equipment. Several preliminary tests have been carried out in order to establish the testing program.

Bamboo shrinkage and water absorption treated at different temperatures and time exposures are two important chemical-physical aspects of the material which is discussed in related sections. The effect of different fiber volume fraction at external and internal wall thickness of bamboo in radial direction, on shrinkage and water absorption investigated. Stabilization test realized in order to establish the required time to reach a specific humidity for the different geometrical shapes of the samples considered in this investigation.

Images with different scales from macro to micro have been taken from bamboo section. The images in meso scale taken by an iPad-Air with a magnifier and stereomicroscope (Discovery V.8 Zeiss). These images used to investigate the fiber distribution in radial direction at different elevations and directions of a whole culm of *DG* bamboo which is discussed in detail in chapter 3.4.4. Scanning electronic microscope (SEM) and X-ray tomography used to provide images in micro scale to study the effect of heat treatment on deformation of the parenchyma and sclerenchyma cells.

Chemical analysis of bamboo carried out based on TAPPI standard to understand about the quantity of bamboo chemical components. TGA test has been realized to find the rate of weight loss related to the temperature increment.

The results have been demonstrated with details in section 3.4.The residuals of holocellulose and lignin which had been done from *DG bamboo, Bambusa Vulgaris* and Iranian bamboo named *kiakalayeh* are used for TGA.

The test conditions in terms of ambient temperature and humidity for bamboo and wood is different. For wood sample tests, the standard temperature and humidity is considered to be 20°C ±2°C with about 65%± 5% but for the bamboo the temperature and humidity should be considered 27±2°C and 70± 5% respectively [83][84][85]. Oven drying is accomplished based on D4442-07 "*Standard Test Methods for Direct Moisture Content Measurement of Wood and Wood-Base Materials*" at the temperature of 103°C ± 2°C. This temperature is considered both as drying and heat treatment temperature. For the mechanical tests all of the heated samples stabilized at room temperature and humidity and are compared with the unheated samples. For water absorption tests, all of the results are compared with those dried at 100°C. Agreement about surfaces, Load and tension directions of bamboo sections are defined as Figure 3.1.

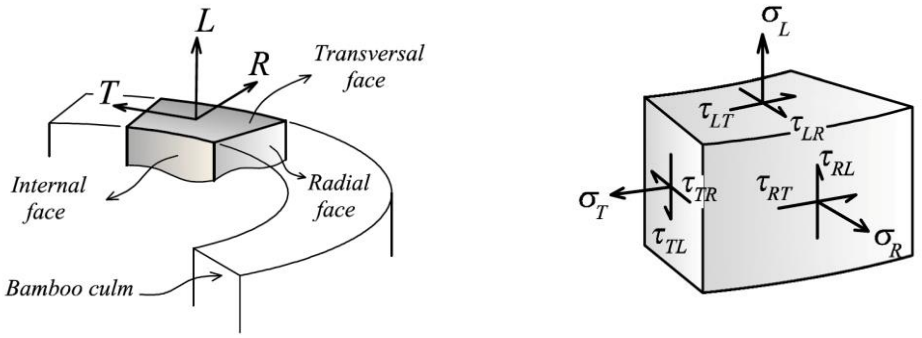

Figure 3.1 Conventional directions

The test samples shall be weighed to an accuracy of $\pm 0.1\%$. The moisture content (MC) of each test piece is calculated by using the Eq. 3.1 [86]:

$$MC\ \% = \frac{m - m_0}{m_0} \times 100 \qquad 3.1$$

where:

m is the mass of the test piece before drying;

m_o is the mass of the test piece after drying;

3.1. Norms and standards

For bamboo as an industrial and structural element, some special and independent standards and norms has been established, but in general, as a

herbaceous and composite material, the norms and standards provided for wood and composite are applicable for the test also. The norms and standards which are used in present thesis are listed in Table 3.1. The ISO standard has three codes related to the bamboo.

Table 3.1 The norms and standards related to bamboo, wood and composites

Name	Title
ISO 22156-1	Bamboo - Structural Design
ISO 22157-1	Bamboo - Determination of physical and mechanical properties Part 1:Requirements
ISO 22157-2	Bamboo - Determination of physical and mechanical properties Part 2: Laboratory manual
ASTM D9-12	Standard Terminology Relating to Wood and Wood-Based Products
ASTM D 198	Standard Test Methods of Static Tests of Lumber in Structural Sizes
ASTM D1037	Standard Test Methods for Evaluating the Properties of Wood-Based Fiber and Particleboard Material
ASTM D3039	Standard Test Methods for Tensile Properties of Polymer Matrix Composite Materials
ASTM D3410−03	Standard Test Method for Compressive Properties of Polymer Matrix Composite Materials with Unsupported Gage Section by Shear Loading
ASTM D4255−15	Standard Test Method for In-Plane Shear Properties of Polymer Matrix Composite Materials by the Rail Shear Method
ASTM D4442–07	Standard Test Methods for Direct Moisture Content Measurement of Wood and Wood- Base Materials
ASTM D4761-05	Standard Test Methods for Mechanical Properties of Lumber and Wood-Base Structural Material
ASTM D4762 –11	Standard Guide for Testing Polymer Matrix Composite Materials
ASTM D4933-99	Guide for Moisture Conditioning of Wood and Wood-Based Materials
ASTM D6874-03	Standard Test Methods for Nondestructive Evaluation of Wood-Based Flexural Members Using Transverse Vibration
ASTM D7031-04	Guide for Evaluating Mechanical and Physical Properties of Wood-Plastic Composite Products

3.2. Geometrical property of *DG* bamboo

The *DG* bamboo samples used for this thesis prepared from two different locations; PUC-Rio as can be seen in Figure 3.2 and USP- Pirassununga. The 4 to 5 years old culms used for making the samples. Before cutting, the north direction is marked on the culm, then the bamboo cut into 5 pieces for easier transportation. The end of pieces marked properly in order to not losing the cardinal directions. The height measurement (elevation points) is done from the ground. The internodes located above the node have the same number as shown in Figure 3.3.

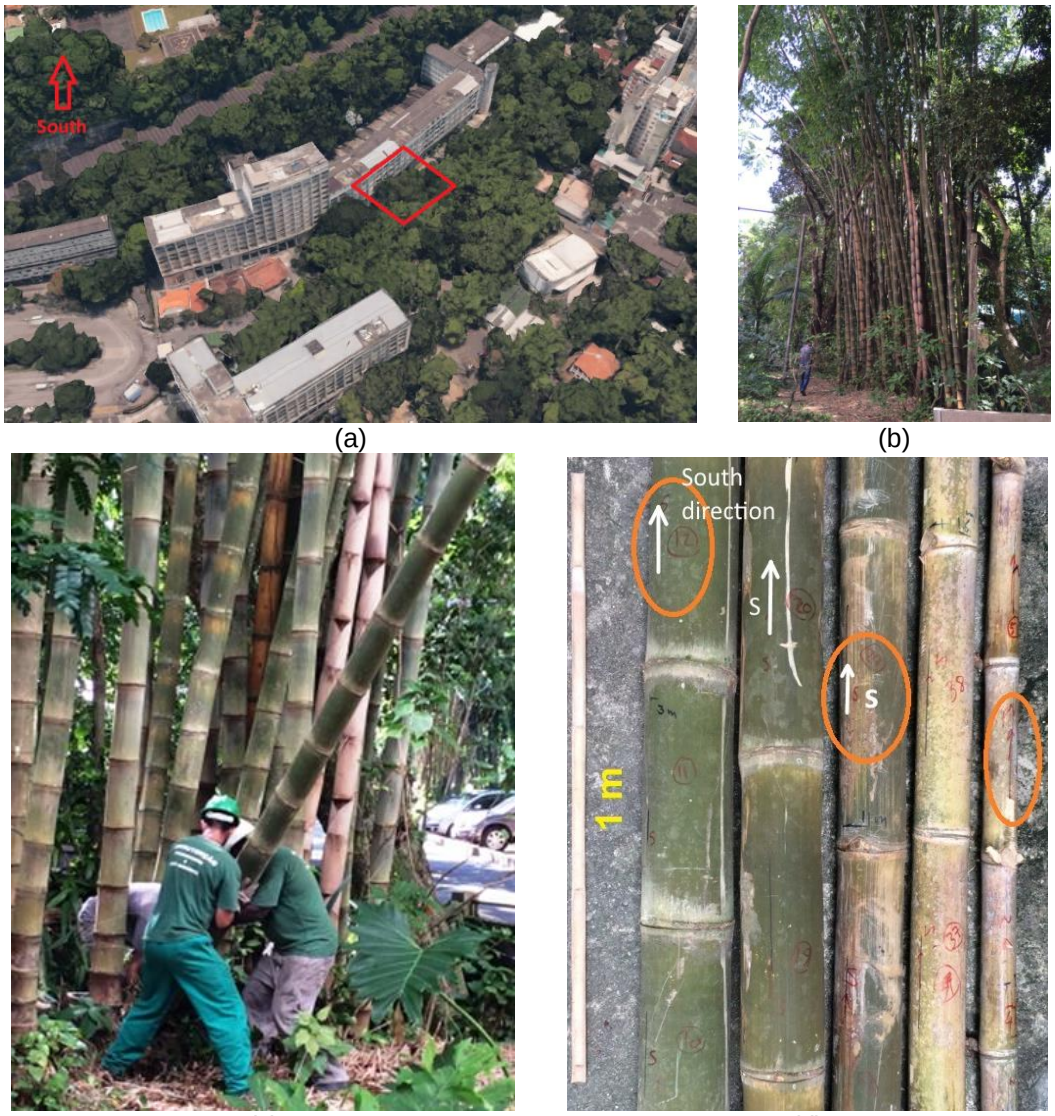

(a) (b)

(c) (d)

Figure 3.2 General views of the bamboo at the campus of PUC-Rio (a) Location of bambuzal inside the PUC-Rio campus; (b) bamboo culms at the bambuzal; (c) bamboo cutting (d) marking the internode numbers and cardinal direction

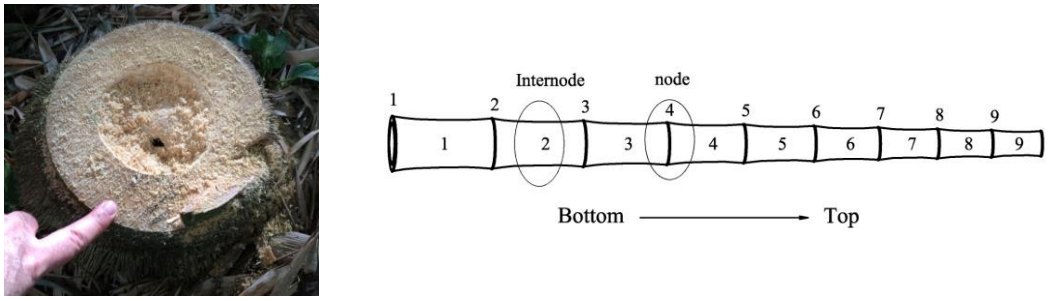

(a) (b)

Figure 3.3 (a) Cutting point about 15cm above ground level; (b) numbering the nodes and internodes

Before cutting the culm to smaller parts the geometrical parameters of entire bamboo culm, the elevation, diameter, node number, wall thickness and internode

length are recorded. The related diagrams for the mentioned parameters are shown in Figure 3.4 to Figure 3.6.

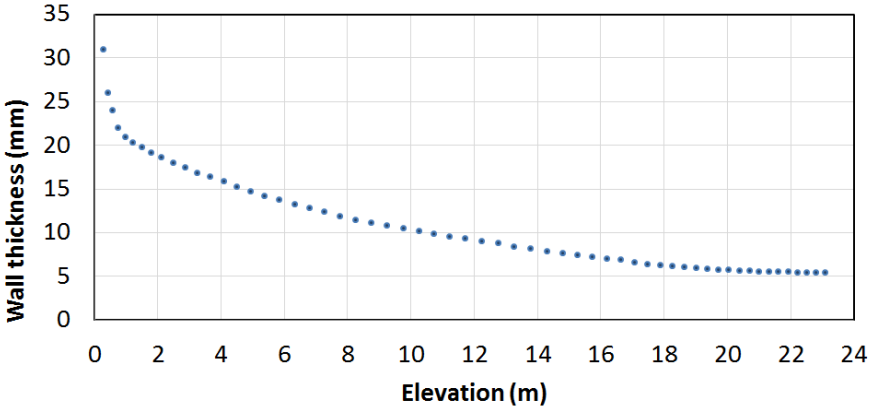

Figure 3.4 Wall thickness vs elevation for a *DG* bamboo culm

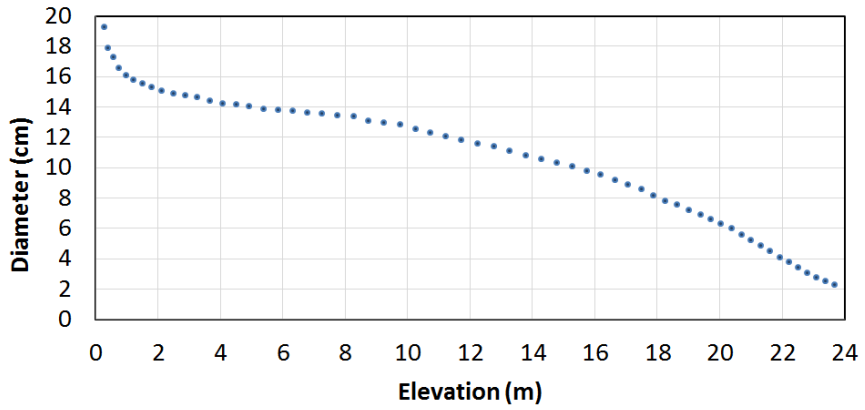

Figure 3.5 Diameter vs elevation for a *DG* bamboo culm

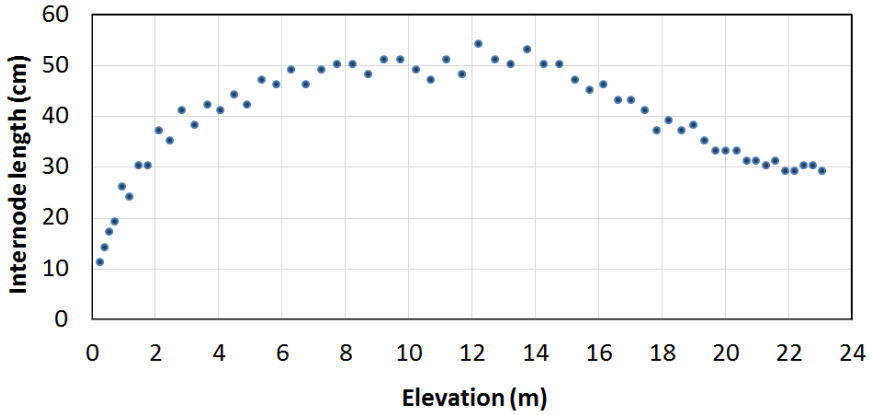

Figure 3.6 Internode length vs elevation for a *DG* bamboo culm

(a) (b)

Figure 3.7 a) The bamboo package sent from USP- Pirassununga; b) average diameter of bamboo about 16cm with thickness between 12mm to 18mm

The wall thickness of culms which have been sent from Pirassununga varies from 12 mm to 16 mm and the diameter varies from 17 cm to 14 cm. also the distance between nodes for all of them were more than 40 cm. The culm cut from elevation 4 m up to 8m.

3.3. Bamboo chemical analysis

The bamboo chemical analysis is accomplished in order to find the main bamboo components (holocellulose, lignin and extractives). Three different species, *Dendrocalamus giganteus, Bambusa vulgaris* and Iranian species close to *Phyllostachys pubescence* have been considered to compare the results. *DG* bamboo was divided into internal and external parts from the middle of section with less and more fibers respectively. The abbreviations are presented in Table 3.2.

Table 3.2 bamboo name and abbreviations

name	location	Abb. name
Dendrocalamus giganteus	inside	DGI
	outside	DGO
Bambusa vulgaris	Whole section	BV
Kiakalayeh (Phyllostachys pubescence!)	Whole section	IR

The process is started by grinding the material. Bamboo cut to small pieces prepare for grinding (Figure 3.8-a). The bamboo powder passed from sieve no. 60

is not used and the material passed from sieve no. 30 and remained on the sieve no. 60 is used for material analysis (Figure 3.8-b).

(a) Small pieces of bamboo before grinding

(b) bamboo particles after grinding and remained on sieve no. 60

Figure 3.8 bamboo preparation for the tests

3.3.1. Moisture content

Moisture content has been measured based on TAPPI test method - T264 om-88 [120] . To obtain the moisture content of bamboo, 2 gr of each sample put in the oven with 103±2°C for 24h (the ambient temperature and humidity at the time of experiment were equal to 25°C and 35% respectively). The results of the moisture content for the four mentioned samples presented in Table 3.3. Then, 8 gr of sieved material from each type was taken for doing the analysis.

Table 3.3 MC% of bamboo samples

Name	Initial weight (gr)	Dry weight (gr)	MC (%)
DGI	2	1.87	6.95
DGO	2	1.91	4.71
BV	2	1.89	5.82
IR	2	1.91	4.71

3.3.2. Extractive components

At the first step of chemical analysis the extractive components such as aromas, resin, starch and pectin are removed from the sample base on TAPPI - T204 cm-97 [120]. Acetone is used as solvent to remove the extractives from the sample. By putting the sample inside the cartouche (Figure 3.9a) and putting it inside a soxhlet this procedure will be accomplished (Figure 3.9b). Four to five hours boiling is enough to remove all the extractives. The results for the samples are mentioned in Table 3.4.

(a) the sample powder in cartouche

(b) boiling process

Figure 3.9 the process of removing the extractives

Table 3.4 The extractive percentage of three different bamboos

Name	Initial dry weight (gr)	Dry weight after process (gr)	Extract (%)
DGI	8	7.51	6.5
DGO	8	7.65	4.6
BV	8	7.58	5.5
IR	8	7.81	2.4

The results presented in Table 3.4 shows that the amount of extractives at internal part is more than the external part in *Dendrocalamus giganteus bamboo*. Also it shows the Iranian bamboo has the minimum extractives among the two other bamboos. By removing the extractives, the samples are ready to do the Lignin and cellulose tests.

3.3.3. Extraction the lignin component percentage

This test follows TAPPI - T222 om-02 [120] to obtain the lignin percentage of the component. This test needs 1 gr of dried bamboo powder. At first, the material should remain in 15 ml sulfuric acid 72% for two hours and during this time and every 10 mins it should be agitated. The samples before adding the sulfuric acid and after two hours have been shown in Figure 3.10a and Figure 3.10b.

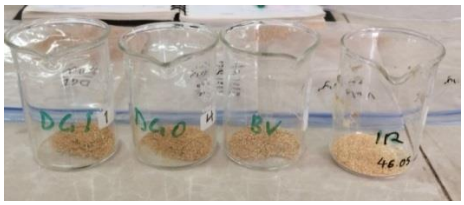

(a) Samples before adding the sulfuric acid

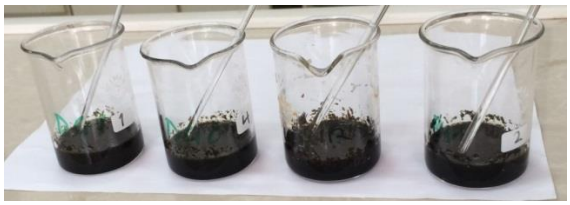

(b) samples after two hours in sulfuric acid

(c) boiling the samples about 4 hours

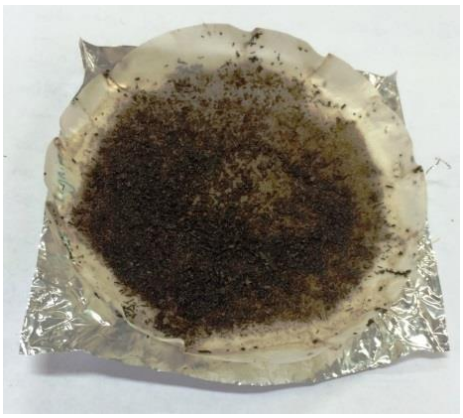

(d) samples in the filter paper after boiling and before drying

(e) the size of dried lignin particles

Figure 3.10 the process of lignin extraction

Then the mixture is moved to a balloon with 560 ml distilled water and after boiling about 4 to 6 hours (see Figure 3.10c) by using a filter paper the water content is removed (see Figure 3.10d). Finally the sample with filter paper should be located in oven with about 50°C for 24 hours to dry as can be seen in Figure 3.10e. The percentage of Lignin is calculated by Eq. 3.2. The lignin component of each type of bamboo is presented in Table 3.5.

$$Lignin\% = \frac{dried\ processed\ weight}{dried\ initial\ sample\ weight} \times 100 \qquad 3.2$$

Table 3.5 The lignin percentage of three different bamboos

Name	Dried initial weight (gr)	Filtration paper (gr)	total weight after process (gr)	Dried weight after process (gr)	Lignin (%)
DGI	0.94	2.25	2.52	0.27	28.7%
DGO	0.95	2.22	2.48	0.26	27.4%
BV	0.95	2.24	2.52	0.28	29.5%
IR	0.94	1.03	1.27	0.24	25.5%

3.3.4. Holocellulose component percentage

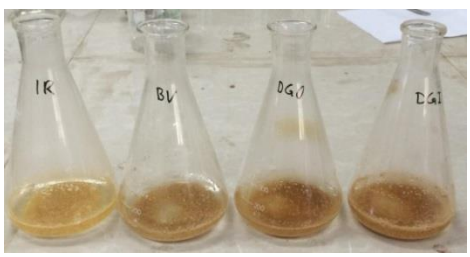

(a) Materials at the start of process

(b) Materials at the end of process

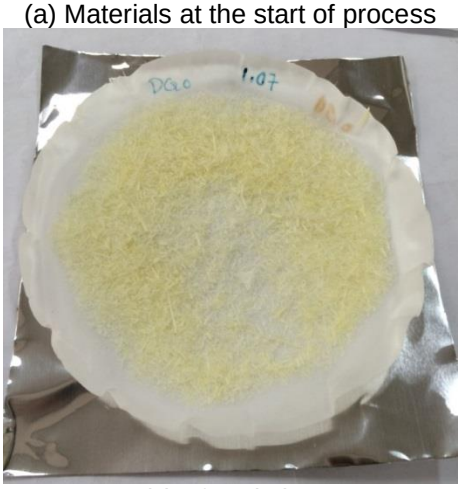

(c) After drying

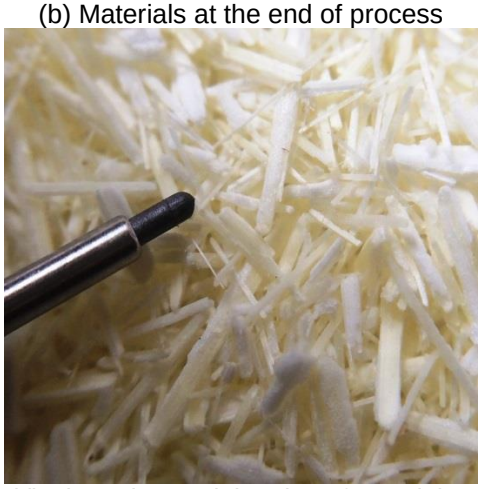

(d) The color and the size of remaining fibers

Figure 3.11 the process of holocellulose extraction

To measure the holocellulose, 2.5 gr of dry sample is mixed with 80 ml distilled water with temperature about 70°C, 0.5 ml of acetic acid and 1 gr of sodium chlorate and is mixed in an Erlenmeyer as presented in Figure 3.11a. Then the mixture put in Bain-marie with 70°C and every one hour 0.5 ml of acetic acid and 1 gr of sodium chlorate are added to the mixture for 6 hours. The lignin is solved in the solvent and the holocellulose is remained as can be seen in Figure 3.11b. Then the mixture is washed with distilled water and filtered the same as Lignin procedure. The remained holocellulose is presented in Figure 3.11c and d. The percentage of holocellulose is obtained by Eq. 3.3.

$$Holocellulose\% = \frac{dried\ processed\ weight}{dried\ initial\ sample\ weight} \times 100 \qquad 3.3$$

The holocellulose component of each type of bamboo is presented in Table 3.6. The extractive, holocellulose and lignin from Table 3.4 to Table 3.6 are presented in Table 3.7.

Table 3.6 The holocellulose percentage of three different bamboos

Name	Dried initial weight (gr)	Filtration paper (gr)	total weight after process (gr)	Dried weight after process (gr)	Holocellulose (%)
DGI	2.5	1.11	2.72	1.61	64.2%
DGO	2.5	1.07	2.76	1.69	68.5%
BV	2.5	1.05	2.68	1.63	65.3%
IR	2.5	1.11	2.90	1.79	72.3%

Table 3.7 The chemical component percentage of three different bamboos

Name	Holocellulose (%)	Lignin (%)	Extractive (%)
DGI	64.2	28.7	6.5
DGO	68.5	27.4	4.6
BV	65.3	29.5	5.5
IR	72.3	25.5	2.4

Based on Table 3.7 the internal part of *DG* bamboo has more extractive and lignin than the external part. Comparing the results of Table 3.7 with the chemical components presented in literature review Table 2.2 shows the chemical components of Iranian bamboo (*IR*) is close to *phyllostachys pubescens.*

3.4. TGA test study

The first experiment in this section shows the effect of different heating rate on the results of TGA. The second experiment shows the results of TGA test for *Moso* bamboo and *DG* bamboo at five different parts from external skin to internal cover. The third experiment shows the results of TGA for the powder of three different bamboo types after removing the extractives as well as comparing the TGA of holocellulose and lignin. The external and internal parts of the *DG* bamboo are considered separately. Based on the results of section 2.3, The heating range in the tests is started from ambient temperature to 900^{o}C.

3.4.1. The effect of heating rate on the results of TGA test

The effect of heating rate studied by using the powder of *Bambusa vulgaris* for three different heating rates, 5, 10 and 25^{o}C/min. The results are presented in

Figure 3.12 and Figure 3.13. As can be seen in Figure 3.12 by increasing the heating rate the result for 25°C/min always shows more remained weight for the sample at the same temperature. For example at 400°C the remained weight for the heating rates 5 and 10 °C/min is about 40% but for the sample with 25°C/min is about 60% and difference is about 20%. The result of weight derivation verifies that elevating the heating rate can move the pick of derivation to higher temperatures as can be observed in Figure 3.13.

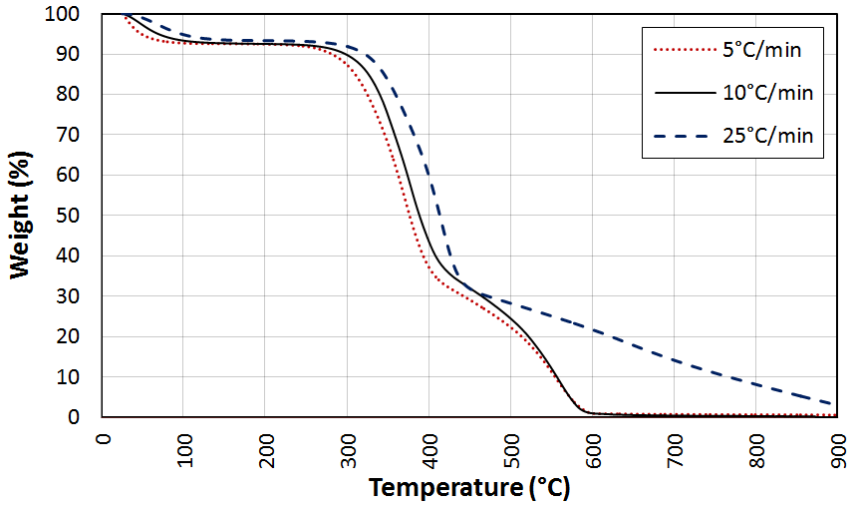

Figure 3.12 TG for Bambusa Vulgaris at three different heating rates

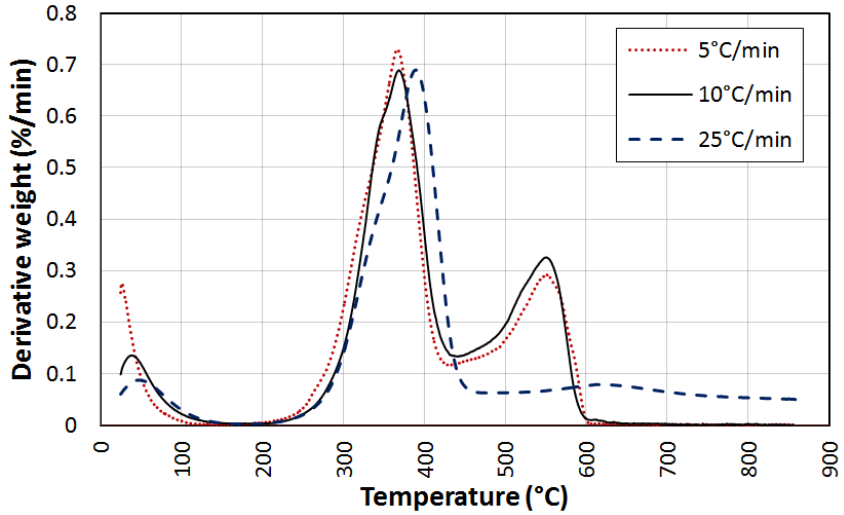

Figure 3.13 DTG for Bambusa Vulgaris at three different heating rates

At the higher heating rates the sample has not enough time to become isotherm with the equipment temperature due to the heat conductivity in the material and has a delay with regards to the temperature registered by equipment. This test shows the rate of 10°C/min is an optimized rate for implementing the TGA tests.

3.4.2. TGA test for different parts of *DG* and *Moso* bamboos

This test was implemented to compare the results of *Moso bamboo* and *DG* bamboo. As can be seen in Figure 3.14 five different parts of *DG* and *Moso* bamboo have been considered for TGA test. These parts from inside to outside are respectively: a) internal skin without fiber; b) low fiber density area; c) middle fiber density area; d) high fiber density area and e) external skin. The results of the tests for DG and Moso bamboo presented in Figure 3.15 to Figure 3.24.

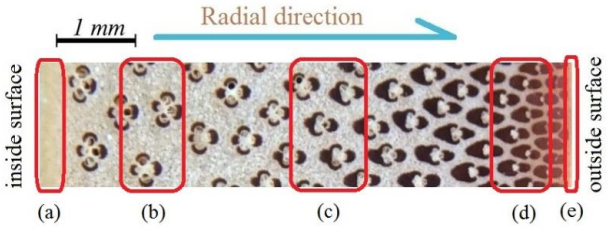

Figure 3.14 Different areas of bamboo section in terms of fiber volume fraction

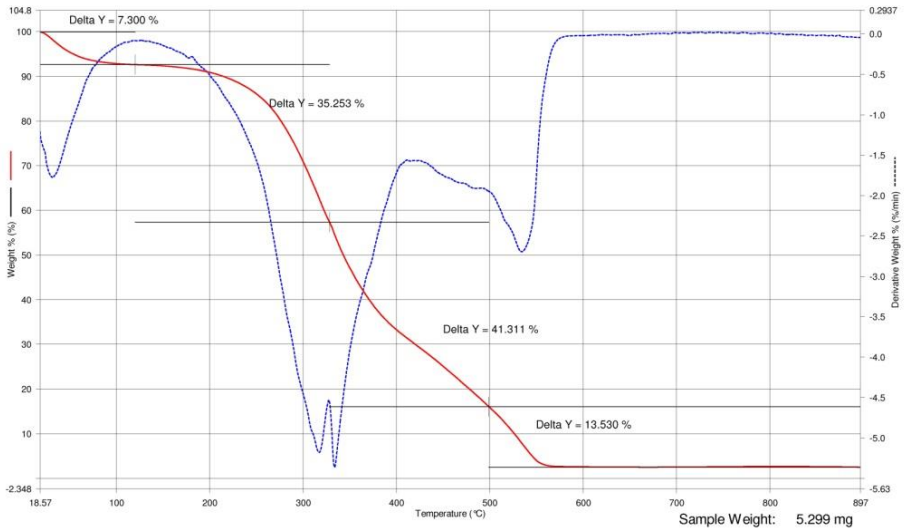

Figure 3.15 Internal skin without fiber for *DG* bamboo

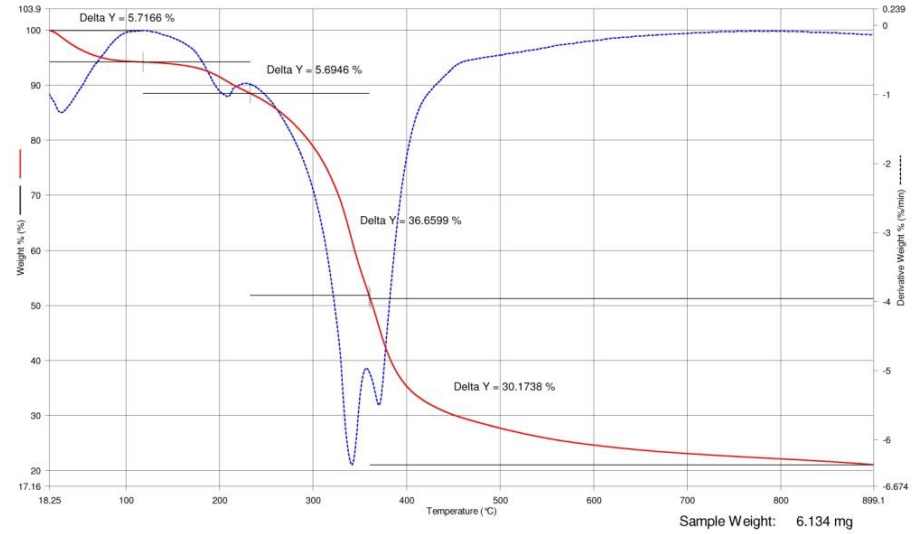

Figure 3.16 Low fiber density area for *DG* bamboo

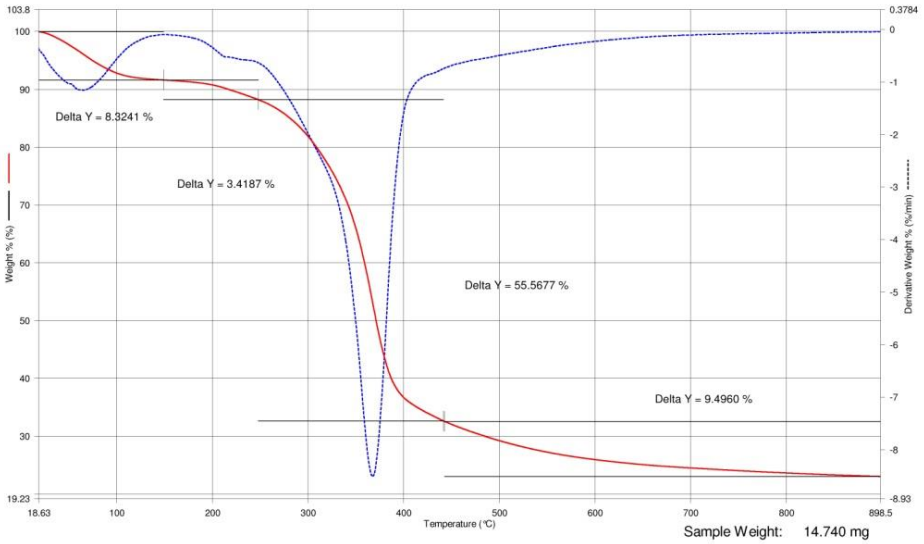

Figure 3.17 Middle fiber density area for *DG* bamboo

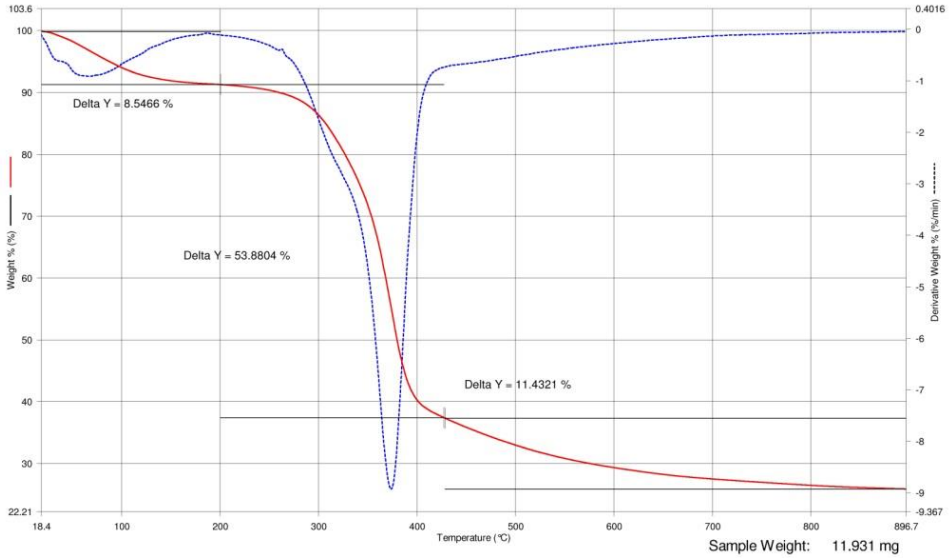

Figure 3.18 High fiber density area for *DG* bamboo

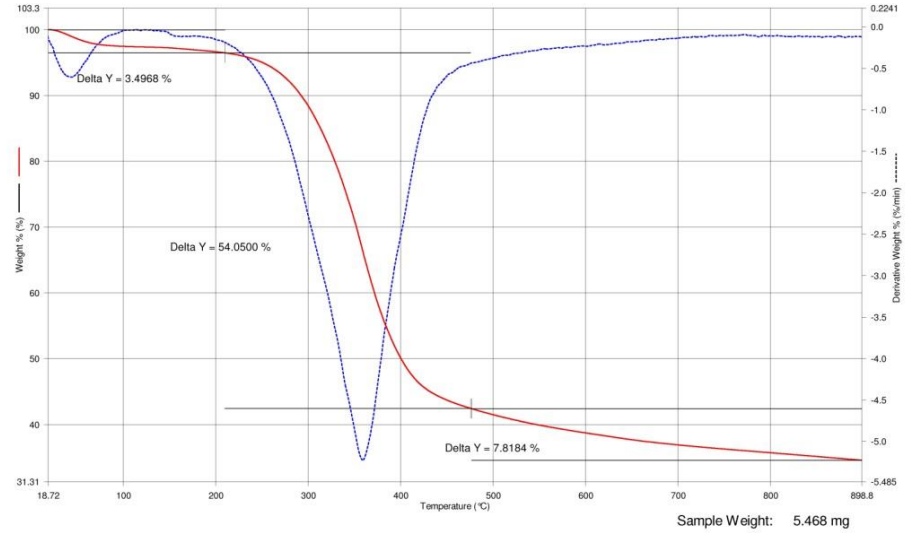

Figure 3.19 External skin for *DG* bamboo

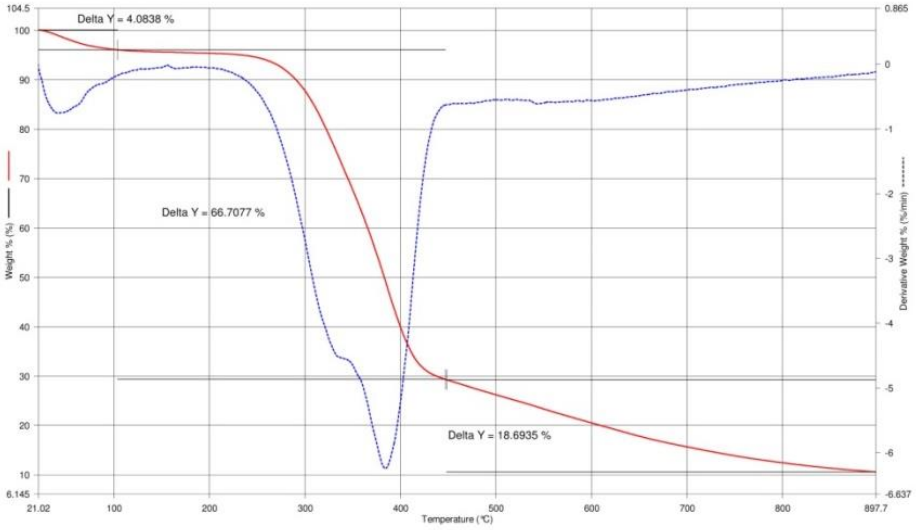

Figure 3.20 Internal skin without fiber for *Moso* bamboo

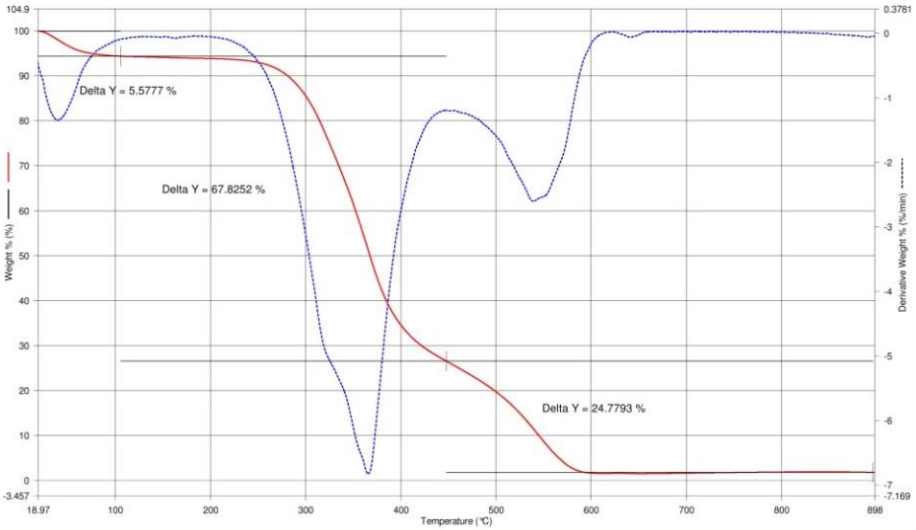

Figure 3.21 Low fiber density area for *Moso* bamboo

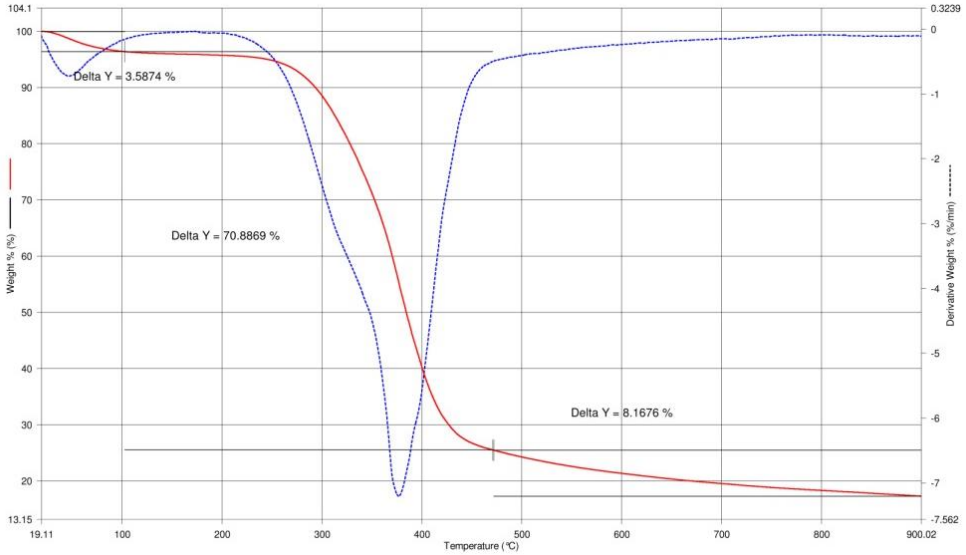

Figure 3.22 Middle fiber density area for Moso bamboo

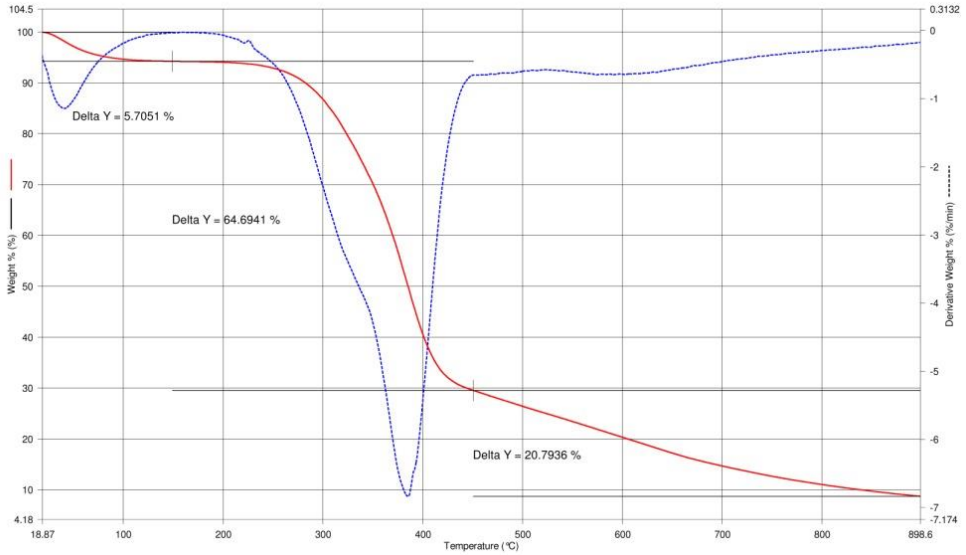

Figure 3.23 High fiber density area for Moso bamboo

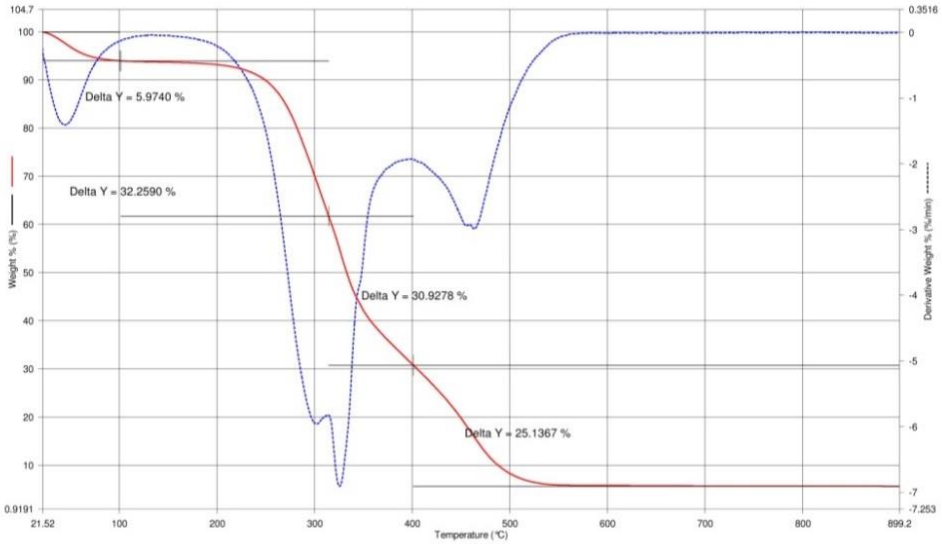

Figure 3.24 External skin layer for Moso bamboo

Interpretation of graphs: the red curve shows the loss weight percentage of specimen and the blow dotted curve shows the derivation of the red curve and shows the losing weight rate regarding to heat increment. As is observed among the graphs presented from Figure 3.15 to Figure 3.24, for the external part with more fiber the maximum speed of losing weight happens about 380^{o}C but by reducing the fibers at the internal part without fiber it happens about 320^{o}C. It can show that the amount of cellulose in segments with more fiber is more.

3.4.3. TGA test for bamboo components

After doing the chemical analysis for three types of bamboo; *Dendrocalamus giganteus* bamboo *(DG)*, *Bambusa vulgaris (BV)* and *Kiakalayeh*(IR) (a type of Iranian bamboo close to phyllostachys species cultivated in north of Iran used mainly for the sake of handicrafts), the TGA test is implemented for two main residual components; holocellulose and lignin of each bamboo as well as bamboo powder after removing extractives by acetone. Only the *DG* bamboo is divided to two internal and external halves and measuring has been done for each half. Figure 3.25 illustrates the prepared samples. Each group has the powder of bamboo after removing extractives, holocellulose and lignin.

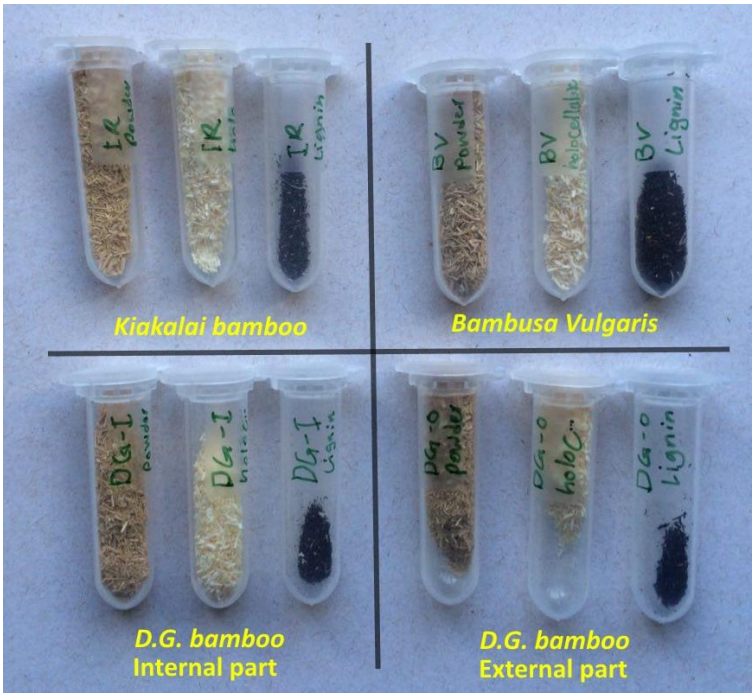

Figure 3.25 prepared samples for TGA test

The TGA results for comparison between the powders of these three species presented in Figure 3.26 and Figure 3.27. As can be seen in these graphs, the behaviour of all of the three species at the range of heat treatment (between 100°C to 225°C) are the same but a little after this range, the Iranian species shows higher weight loss regarding to the *BV* and *DG* bamboo. The external and internal parts of *DG* bamboo show the same behaviour or the same amount of weight loss.

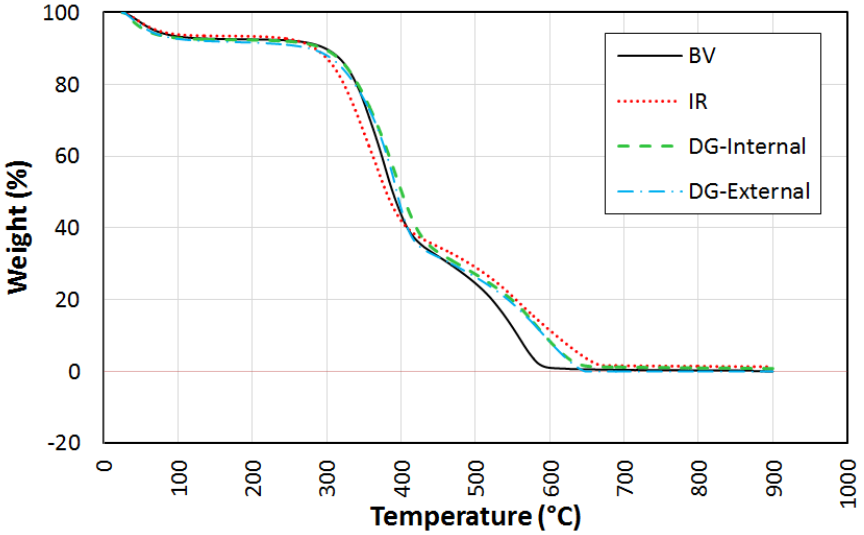

Figure 3.26 TG result for weight loss of *Bambusa vulgaris (BV), Kiakalayeh* bamboo (IR) and Dendrocalamus giganteus (*DG)* internal and external parts

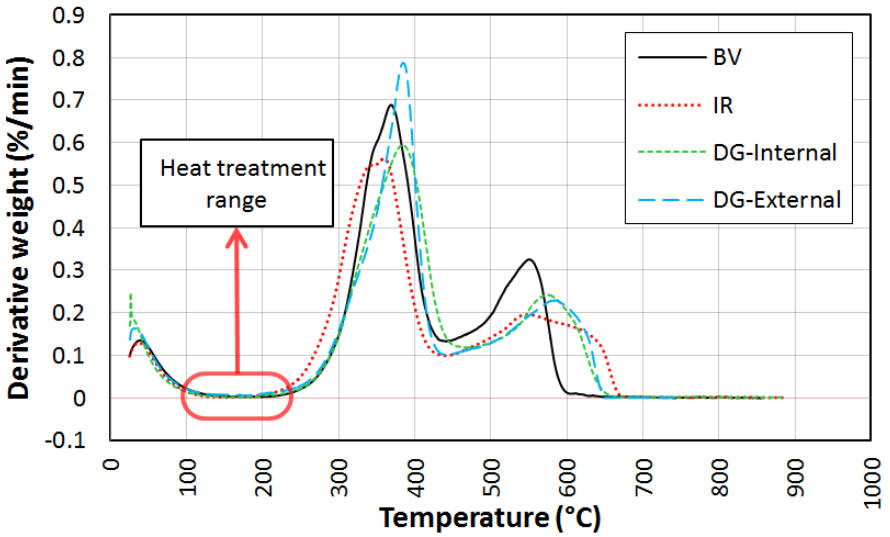

Figure 3.27 DTG result for Derivation of weight loss for *Bambusa vulgaris (BV), Kiakalayeh* bamboo (IR) and *Dendrocalamus giganteus* (*DG*) internal and external parts

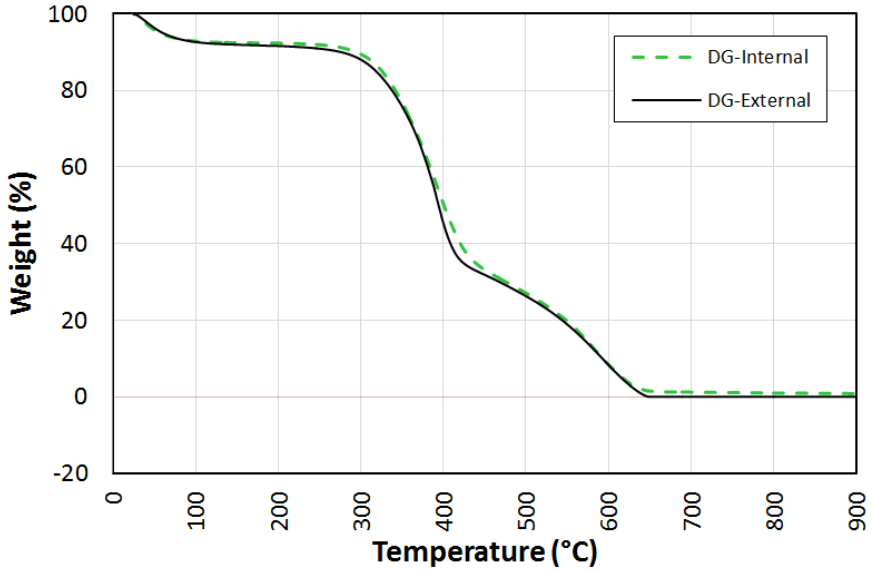

Figure 3.28 TG result for weight loss of internal and external parts *DG bamboo*

Comparing the results of internal and external part of *DG* bamboo does not show significant difference between these two parts as can be seen in Figure 3.28 and Figure 3.29. The results of TG and DTG for holocellulose and lignin for DG, BV and IR types of bamboo presented in Figure 3.30 to Figure 3.33. The DTG result for holocellulose shows in the range of heat treatment (up to 225^{o}C) the degradation rate of extractive holocellulose for all three species are the same and the maximum occurred at about 365^{o}C. For the extracted lignin the DTG graph in Figure 3.33 more variation at this range is observed.

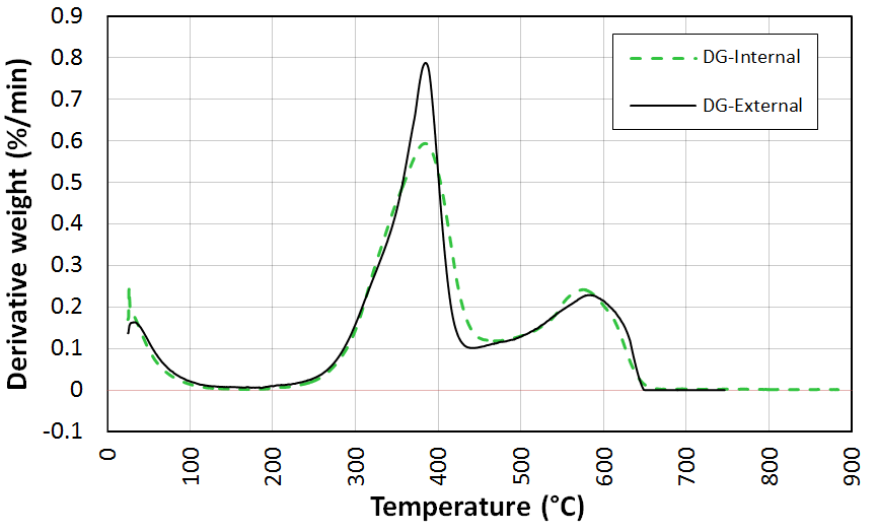

Figure 3.29 DTG result for Derivation of internal and external parts *DG bamboo*

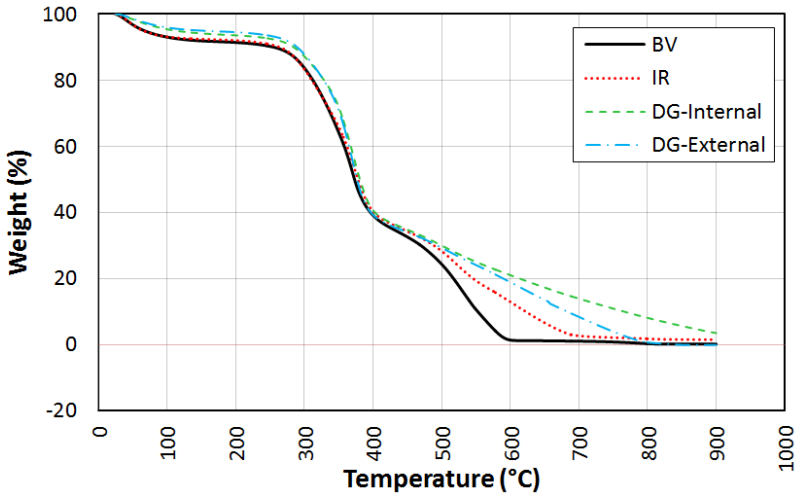

Figure 3.30 TG result for extracted holocellulose from three types of bamboo

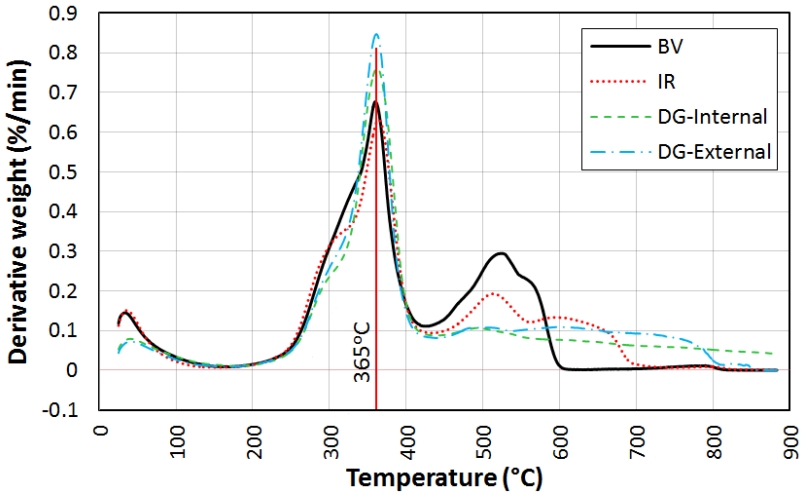

Figure 3.31 DTG result for extracted holocellulose from three types of bamboo

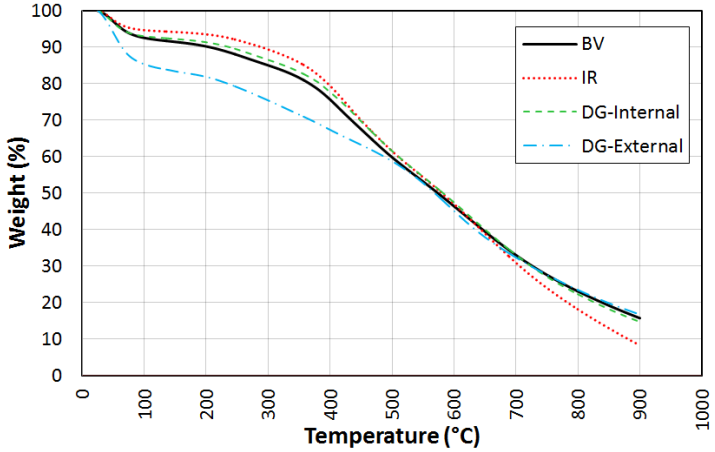

Figure 3.32 TG result for extracted lignin from three types of bamboo

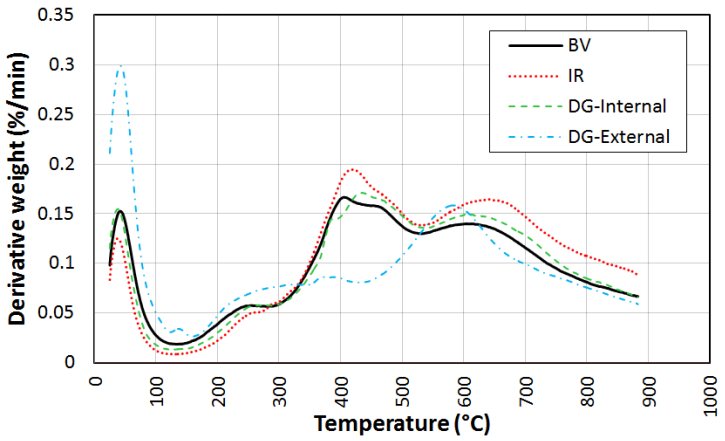

Figure 3.33 DTG result for extracted lignin from three types of bamboo

3.4.4. Determination of heating range by TGA results

The TGA result for the middle segment of *DG* bamboo shows that the weight change and degradation of bamboo starts at about 150°C as can be seen in Figure 3.34. The continuous curve is the weight loss percentage regarding temperature and the dotted curve shows the derivative weight loss (percentage per min). Up to 150°C, the humidity and some of the volatile extractives of bamboo are evaporated and it reaches to the most stable situation at about 150°C based on the derivative weight loss curve. Increasing the derivative weight loss after this temperature shows the starting of the material degradation. The selected heating range starts from the ambient temperature up to the torrefaction temperature. The phenomenon which can change the mechanical property of materials significantly is torrefaction. Torrefaction is a thermal process that involves heating the biomass to temperatures between about 200°C up to 300°C in an inert atmosphere [87][88][89]. Actually after temperatures more than 200°C the mechanical property of bamboo decreases significantly and the bamboo transfers into charcoal which is not the interest of present research. Based on wood species the minimum temperature for wood degradation begins at 100°C for pine as a softwood and at 130-150°C for oak as a hard wood [54].

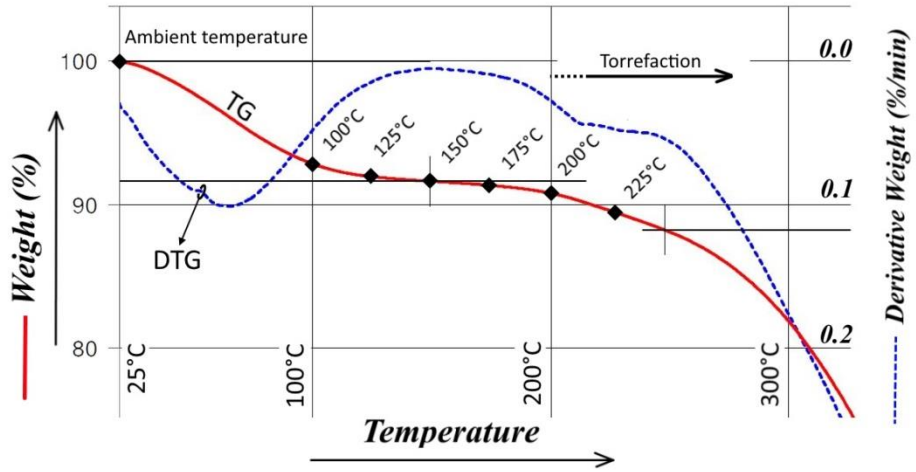

Figure 3.34 A part of TGA graph for the middle segment of *DG* bamboo from ambient temperature to about 300°C

The maximum temperature based on the initial tests on bamboo samples and TGA results in this study considered 225°C which is 25°C more than the limit of the bamboo torrefaction for sample subjected to heat during three hours. The interval between the selected temperatures was considered 25°C starting from 100°C. Then, the tests executed at initial temperatures 25°C considered as ambient temperature, 100°C, 125°C, 150°C, 175°C, 200°C and 225°C as can be seen in Figure 3.34.

3.5. Bamboo image processing

3.5.1. Bamboo section and image preparation

Before providing images, the cross section of bamboo segment polished by using a disc polishing machine and water, starting with coarse sandpaper No. 150 and increasing gradually to superfine No. 1200. In this process, the veins become clean from sap due to the water pressure produced between sandpaper and the segment surface. Two different methods have been used for taking photos. As a rapid but exact method, an iPad Air with a magnifier (f=5 cm) and the daylight with a desk lamp is used to provide the images. In this method by smearing white toothpaste on the polished surface, the veins are filled and separated from fibers instead of removing digitally after [119]. This method is useful when only the fiber volume fraction is important. When the exact volume fractions of all of the fiber, matrix and vein are required, a stereomicroscope with two different light

exposures should be used to distinguish all these three components from each other.

The cross section of bamboo in general is not a perfect circular shape with a constant diameter a . In most cases they are oval with wall thickness variation along the circumferential direction as can be seen in Figure 3.35. Then a segment prepared from a part of this ring is a quadrilateral with unequal sides as presented in Figure 3.35b.

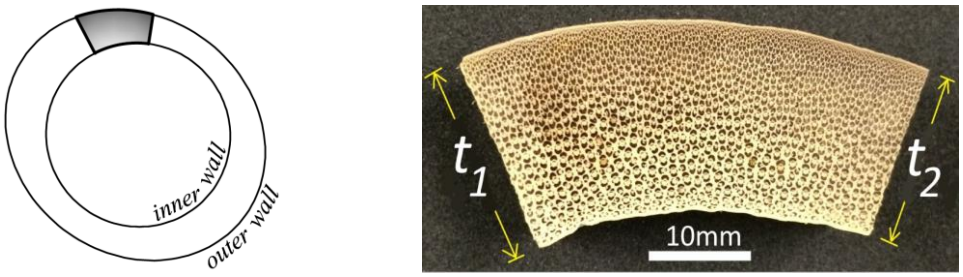

(a) Whole cross section (b) Thickness variation of a bamboo segment (t1>t2)

Figure 3.35 Cross section of bamboo segment

The first modification after preparing the images, is transfer them to a rectangular shape by a specific process which has been done in a proper image software program as can be seen in Figure 3.36. The "***ImageJ***" software has been used to process the registered RGB color raw images. Image processing is started by converting bamboo segment in quadrilateral shape with curved sides into pre-defined size of a rectangular shape as presented in Figure 3.37. This process is necessary because after converting to a rectangular shape, it should be transferred to a numerical matrix. The prepared normalized images are now subjected to the filtration process. Proper filtration can remove uneven light exposure, and the contrast between fibers and matrix are intensified. Then the RGB color image is converted to binary.

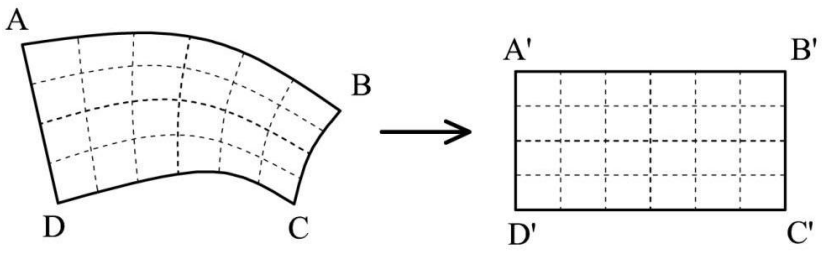

(a) (b)

Figure 3.36 Image modification from a (a) Quadrilateral section with curved sides transferred into a (b) rectangular section

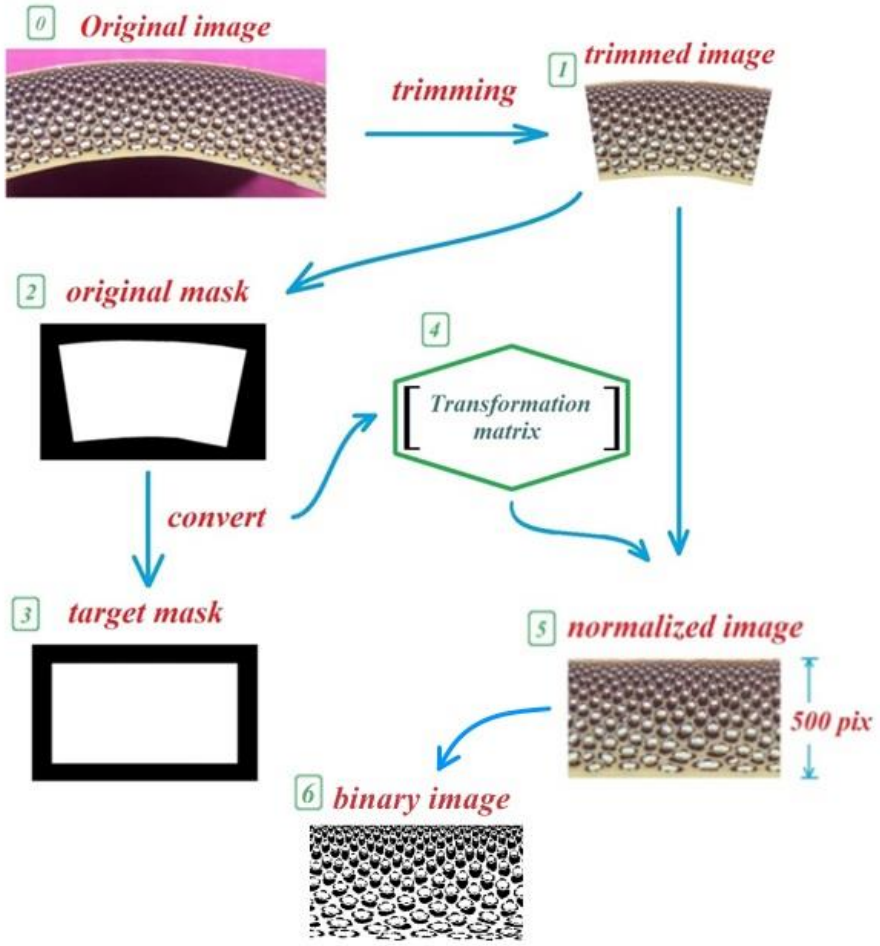

Figure 3.37 Converting process to make a rectangular section

In this process an original image segment, Figure 3.37-0, is trimmed into image, Figure 3.37-1 which is transformed into an original mask considering only the perimeter of the image, Figure 3.37-2. The mask is changed into the target mask Figure 3.37-3 which is a rectangular with the dimensions close to the original mask, Figure 3.37-2. This procedure of converting creates a Transformation Matrix (TM), shown in Figure 3.37-4. Then by using the trimmed image Figure 3.37-1 and transformation matrix (TM), the image is converted to a rectangular shape, denominated normalized image Figure 3.37-5. The image thickness should be normalized to 500 pixels. Finally, the normalized rectangular image is converted to binary image as can be seen in Figure 3.37-6 prepared for the next step of image processing.

3.5.2. Fiber distribution along the radial direction

To find the Fiber Volume Fraction (FVF) along the radial direction, at first the prepared binary image, is converted to a matrix with $m \times n$ pixels. These pixels can be transformed to number values and as a matrix is saved in an excel sheet. Each image consists of 500 rows or 500 pixels alongside the thickness (*y* axis) and could have n pixels in width (*x* axis). The pixel value in row *i* and column *j* considered as v_{ij} which can have only two values, "0" for black and "255" for white, as shown in Figure 3.38a. The fiber distribution alongside the radial direction or wall thickness is presented in Figure 3.38b.

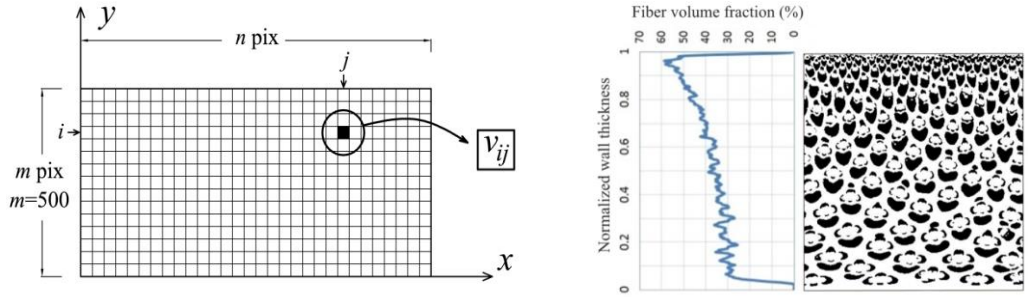

(a) (b)

Figure 3.38 a) Converted image to a matrix, b) FVF at normalized wall thickness

At the next step, fiber density is calculated row by row. The average value of each row after normalization can be considered as percentage of fibers in one row. By having this graph (Figure 3.38b) the exact value of FVF along the radial direction from internal to external side is obtained.

As an example the FVF (Fiber Volume Fraction) for two different types of *Moso* and *DG* bamboo is presented. Visually, the FVF for *Moso bamboo* at internal wall is less than the same value for the *DG* bamboo as it can be observed visually in Figure 3.39. The result of FVF in Figure 3.40 and Figure 3.41 verifies this visual observation.

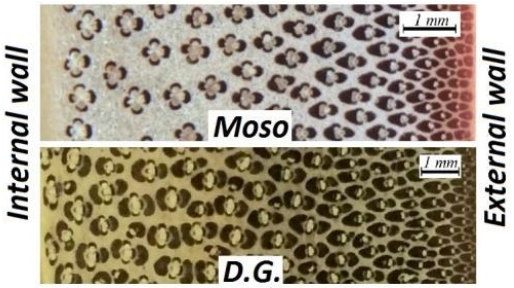

Figure 3.39 visual appearance of Moso and *DG* bamboo

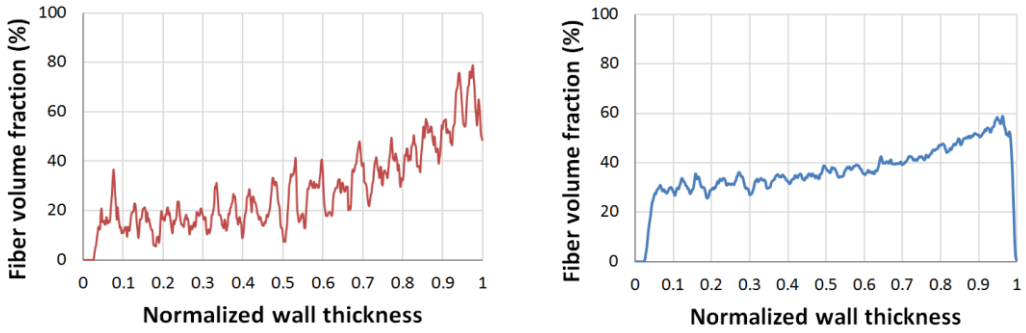

(a) Moso bamboo (b) *DG* bamboo

Figure 3.40 Fiber distribution in radial direction for *Moso* bamboo and *DG* bamboo

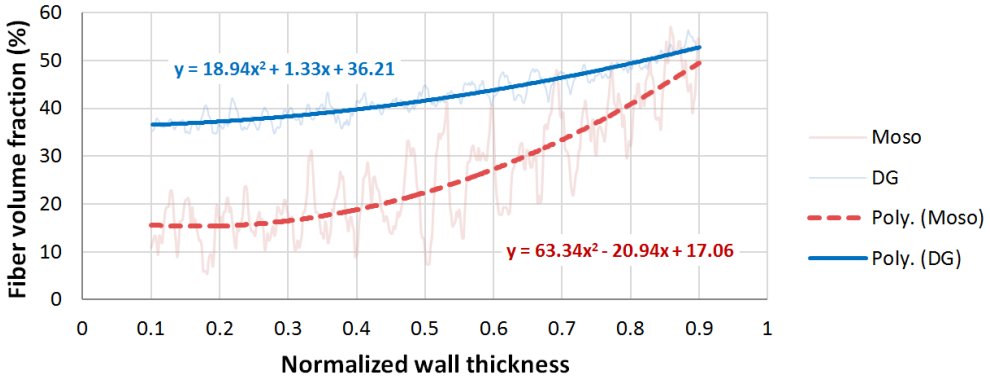

Figure 3.41 curve fitting along the wall thickness for *DG* and *Moso* bamboo

By doing the image process, the fiber distribution for a *Moso* and *DG bamboo* is shown in Figure 3.40. The second order normalized curve fitting with related equations are presented in Figure 3.41.

3.5.3. Image processing for showing the fiber, matrix and vain

This method is used when the volume fraction of each fiber, matrix and vein separately is required. By using a stereomicroscope with two different light exposures two types of images are provided. By using the light sources located at the top and perpendicular to the surface, the color of matrix and fibers appear light gray but the veins remain dark (Figure 3.42-a). This type of light exposure is proper to show the hollow veins. By using the two inclined light sources to the same cross section the fibers and veins are appeared as dark areas in a bright background (matrix) as shown in Figure 3.42-c.

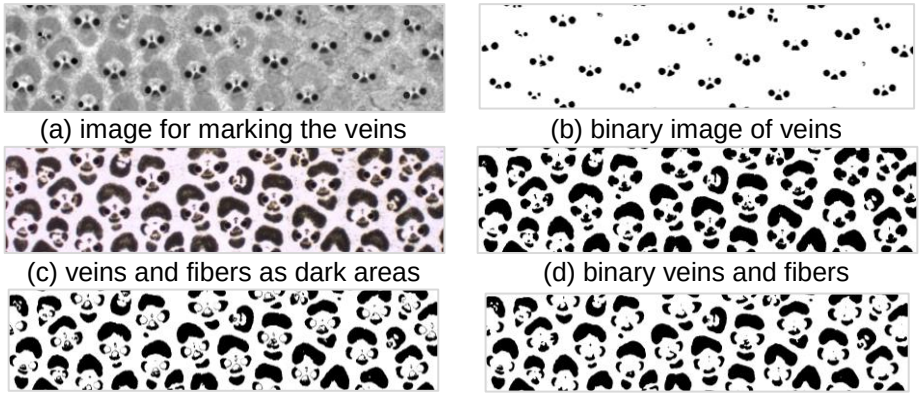

(a) image for marking the veins (b) binary image of veins

(c) veins and fibers as dark areas (d) binary veins and fibers

(e) subtraction of veins from fibers (f) pure fibers after median filtration

Figure 3.42 cross section of internal part

The next step is image processing which is done by "***ImageJ"*** software. By using this software, after filtration and removing the uneven light exposure and converting to binary image the veins appear as black points in a white background (Figure 3.42-b). The same procedure is carried out for Figure 3.42-c and is converted to a binary image. The fibers and veins are black and matrix is white as shown in Figure 3.42-d. By subtracting the veins presented in Figure 3.42-b from the Figure 3.42-d, the fiber area can be determined (Figure 3.42-e). By using the median filter the black remaining annular shadows from subtraction can be removed as shown in Figure 3.42-f.

The procedure is summarized as the following steps:

1- In Figure 3.42-b by using the Histogram for a binary image the volume fraction or percentage of veins is obtained by considering the black points.
2- In Figure 3.42-d by using the Histogram the white area percentage represents the matrix but the black area shows the fibers and veins. To find the percentage of fibers, the volume fraction of veins achieved from the first step should be subtracted in this step.

This procedure is explained with details for internal part.

1- Vein percentage resulted from Figure 3.42-b:

Total black area (vein) =36462 pix

Total white area (fiber + matrix) =538890 pix

Total image area (vein + fiber + matrix) = 538890+36462 =575352

Then:

Vein volume percentage = $\frac{36462}{575352} \times 100 = 6.34\%$

2- Matrix volume percentage from Figure 3.42-d:

Total black area (vein + fiber) =210279 pix

Total white area (matrix) =357077 pix

Total image area (vein + fiber + matrix) = 567356 pix

Matrix volume percentage= $\frac{357077}{567356} \times 100 = 62.94\%$

Fiber + vein volume percentage = $\frac{210279}{567356} \times 100 = 37.06\%$

Fiber volume percentage = 37.06% - 6.34% = 30.72%

Then, for the internal part of bamboo the values of volume fraction of fiber, matrix and vein are 30.72%, 62.94% and 6.34% respectively. By doing the same procedure for external part the values of volume fraction of fiber, matrix and vein are 56.12%, 42.22% and 1.66% respectively.

3.5.4. Variation of FVF at different heights and directions of a bamboo culm

Bamboo as a natural organic material has bigger coefficient of variation (CV%) in physical, structural, geometrical and mechanical properties regarding to synthetic materials. As the sclerenchyma, more than the parenchyma represents the mechanical property of bamboo then knowing about the quantity and quality of fiber distribution in vertical and radial orientations is essential.

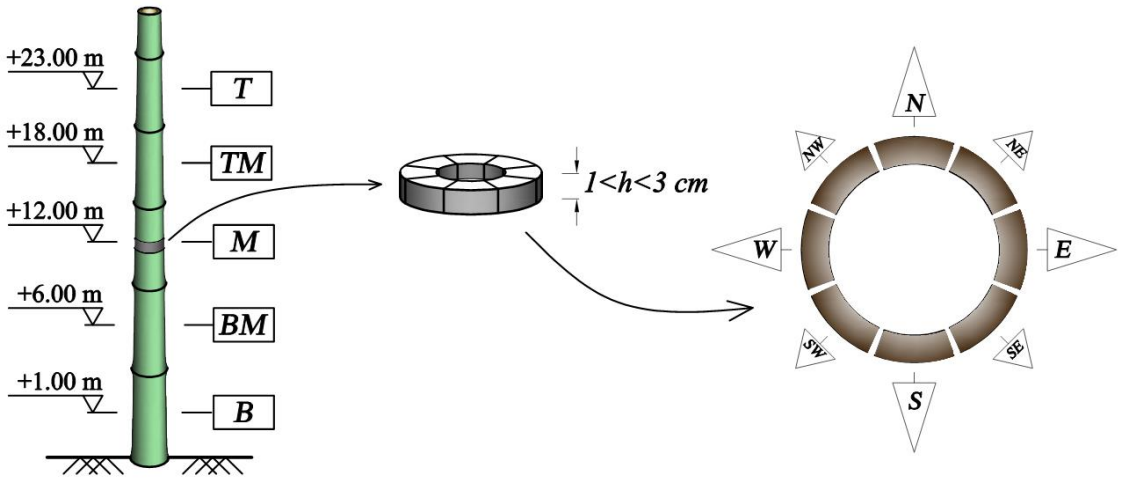

Figure 3.43 elevations and orientations

This section presents the results of a study establishing the bamboo fiber distribution in three directions; radial, tangential and longitudinal. Five years old *DG* bamboo with about 24*m* high and 19*cm* base diameter was cut at PUC-Rio (see 3.2). At first, the annular sections are prepared from five different elevations, 1, 6, 12, 18 and 23*m* from bottom to top of the culm and the elevations are

abbreviated as ***B***, ***BM***, ***M***, ***TM*** and ***T*** respectively as bottom, bottom middle, middle, top middle and top of culm as shown in Figure 3.43. From each annular section and for each cardinal (***N-E-S-W***) and ordinal directions (***NE-NW-SE-SW***) a sample is prepared as shown in Figure 3.43.

For each segment, FVF regarding normalized thickness is obtained and shown in a chart. Total fiber area for the 8 segments in each elevation and for 5 segments in the same direction from each elevation by doing statistical analysis (ANOVA) is compared and the relation between direction and changing in fiber area is investigated. Finally, the variation of fiber volume fraction in radial and longitudinal directions will be presented in equations and graphs.

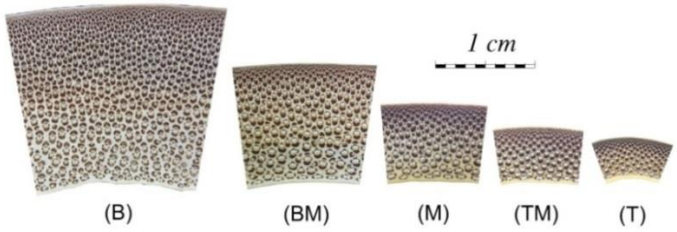

Figure 3.44 segment from different elevations

Figure 3.44 shows the relative size of the sections. Based on bamboo image processing chapter 3.4.4, all the forty cross sections are prepared and converted to numerical table to get the results.

3.5.4.1. Total Fiber Area (TFA) for each segment

The purpose is finding the variation of total fiber area alongside the tangential direction to realize meaningful difference between them in special direction. There are 5 elevations and each of them has 8 segments. Then the TFA for 40 samples at different elevation and direction has been presented in Table 3.8 and in Figure 3.45. Based on Table 3.8, the average for TFA is 38.3% with standard deviation equal to 3.33, and the maximum and minimum values are 33.1% and 47.3% respectively. The result of averaging the total fiber area of 5 segments located in each direction is presented in Figure 3.46.

Table 3.8 Fiber total area for each segment

Location	N	NE	E	SE	S	SW	W	NW
T	34.2	36.2	36.1	35.6	36.2	35.9	35.4	33.1
TM	43.9	43.9	37.5	38.3	39.8	36.3	37.5	37.0
M	39.0	38.2	36.8	36.5	34.9	35.4	34.2	35.3

BM	37.9	41.6	39.4	34.6	34.8	37.3	37.8	39.6
B	42.2	47.3	42.4	41.5	44.1	41.4	40.8	42.6

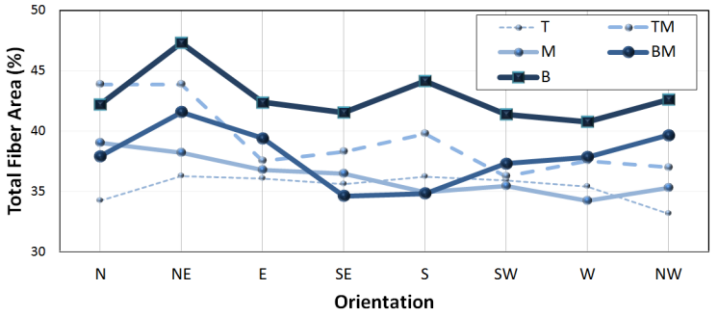

Figure 3.45 TFA for all 40 samples

It seems in ***NE*** direction the fiber volume fraction with 41.4% is more than the other directions and in the approximately opposite side for ***W*** there is minimum fiber density (37.1%) that should be taken in to account. By statistical analyze of variation (ANOVA) proves that the difference can be meaningful or not. To find dependency between variables (fiber volume fraction and tangential direction) the ANOVA test is used. Based on first hypothesis, at least should be exist one difference among the means of each group. In this case obviously all of means for 8 groups are different which can satisfy the first hypothesis.

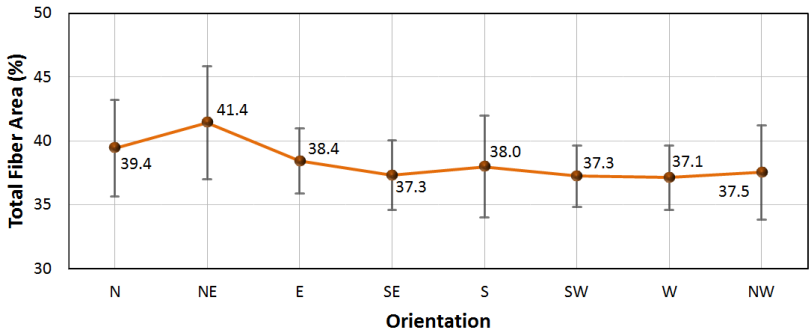

Figure 3.46 TFA for 5 samples in each direction

Second step is to find the degrees of freedom between groups and within groups in order to determine the critical F value. Degrees of freedom between groups (df_b): there are 8 groups then g=8 and the value of df_b is equal to:

$$df_b = g - 1 = 7$$

Degree of freedom within is equal to the number of all of data's (*n=40*) subtracted by the number of groups:

$$df_w = n - g = 32$$

Then the total degree of freedom is equal to:

$df_t = df_w + df_b = 39$

By having the df_w and df_b the value of $F_{critical}$ can be obtained from related tables which is equal to 2.31 for the value of $\alpha = 0.05$.

$F_{critical} = 2.31$

The total mean for all 40 samples is equal to:

$\bar{x}_t = 38.31$

Then the total sum of squares is calculated for all 40 values and named SS_t which ***g*** is subscript for showing the group (8 groups) and ***i*** the members of each group (5 members).

$$SS_t = \sum_{g=1}^{8}\sum_{i=1}^{5}(x_{gi} - \bar{x}_t)^2 = 432.70$$

The next step is calculation of sum of squares within groups.

$$SS_w = \sum_{g=1}^{8}\sum_{i=1}^{5}(x_{gi} - \bar{x}_g)^2 = 356.39$$

Next step is calculation of sum of squares between (SS_b) that obtained from subtraction of SS_t from SS_w:

$SS_b = SS_t - SS_w = 76.31$

Now the mean variance between (MS_b) and the mean variance within (MS_w) should be achieved by the follow formulas:

$$MS_b = \frac{SS_b}{df_b} = \frac{76.31}{7} = 10.90$$

$$MS_w = \frac{SS_w}{df_w} = \frac{356.39}{32} = 11.14$$

And finally:

$$F = \frac{MS_b}{MS_w} = \frac{10.90}{11.14} = 0.979$$

The value of the F is less than $F_{critical}$ then the difference between the values in groups are meaningless. It shows that an increment of fiber volume fraction in *NW* direction can be neglected.

3.5.4.2. Thickness effect

The other fact that should be considered is the effect of wall thickness variation alongside tangential direction. The result of segment wall thickness measuring is presented in Table 3.9 and Figure 3.47:

Table 3.9 the wall thickness of segments (mm) regarding to direction and elevation

Location	N	NE	E	SE	S	SW	W	NW
T	5.74	6.04	5.84	5.88	5.96	5.50	5.00	5.14
TM	7.26	6.42	6.04	6.18	7.42	6.90	6.84	7.12
M	10.20	10.16	10.12	10.44	10.22	10.70	10.62	10.66
BM	11.96	12.58	12.68	12.54	13.44	12.38	12.68	13.02
B	19.24	19.38	20.26	22.42	22.58	22.64	21.02	20.66

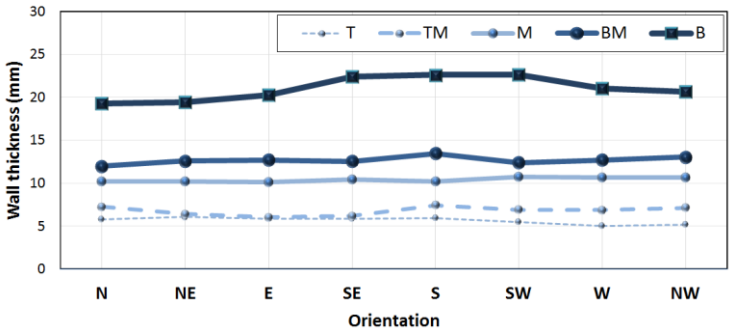

Figure 3.47 the wall thickness of segments (mm) regarding to direction and elevation

Table 3.10 Normalized wall thickness based on average thickness in each section

Location	N	NE	E	SE	S	SW	W	NW
T	1.02	1.07	1.04	1.04	1.06	0.98	0.89	0.91
TM	1.07	0.95	0.89	0.91	1.10	1.02	1.01	1.05
M	0.98	0.98	0.97	1.00	0.98	1.03	1.02	1.03
BM	0.94	0.99	1.00	0.99	1.06	0.98	1.00	1.03
B	0.92	0.92	0.96	1.07	1.07	1.08	1.00	0.98

The ANOVA is done for normalized wall thickness of segments presented in Table 3.10. As the degrees of freedom between and within are the same as before then the $F_{critical}$ remains the same.

The total mean for all normalized samples is equal to one ($\bar{x}_t = 1$). Then total and within sum of squares (SS_t and SS_w) are respectively equal to 0.1153 and 0.0983.

Then the between sum of squares (SS_b) which is subtraction of total and within sum of is equal to 0.017. The mean variance between (MS_b) and the mean variance within (MS_w) are respectively 0.0024 and 0.0031 and finally the F value

is equal to 0.79 which shows that the variation of thickness alongside the perimeter does not emphasize on a special direction.

3.5.4.3. Average Fiber Distribution (AFD) at each elevation

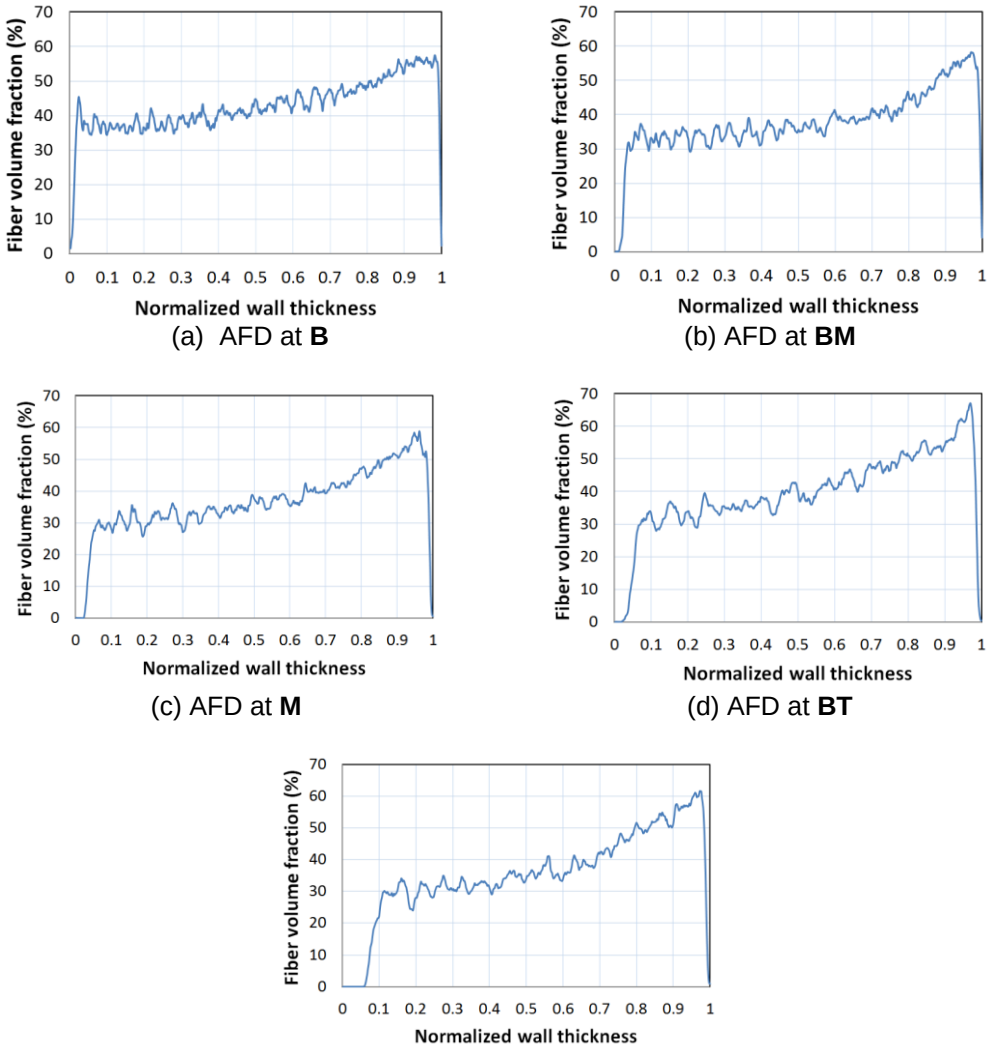

(a) AFD at **B**

(b) AFD at **BM**

(c) AFD at **M**

(d) AFD at **BT**

(e) AFD at **T**

Figure 3.48 Average fiber distribution in five different elevations

The fiber distribution for each elevation is obtained by averaging the data of all 8 segments in each section. Then from top to bottom there are five different fiber distributions. The average fiber distribution (AFD) in each elevation is presented in Figure 3.48 considering the whole normalized thickness. To eliminate the internal and external skins, 0.1 of normalized wall thickness from each external and internal side have been removed from the graphs in Figure 3.48 to achieve the useful or practical part of bamboo layer. The 2nd order polynomial

interpolation curve fitting figure and equations for practical average fiber distribution (PAFD) are presented in Figure 3.49 and Table 3.11.

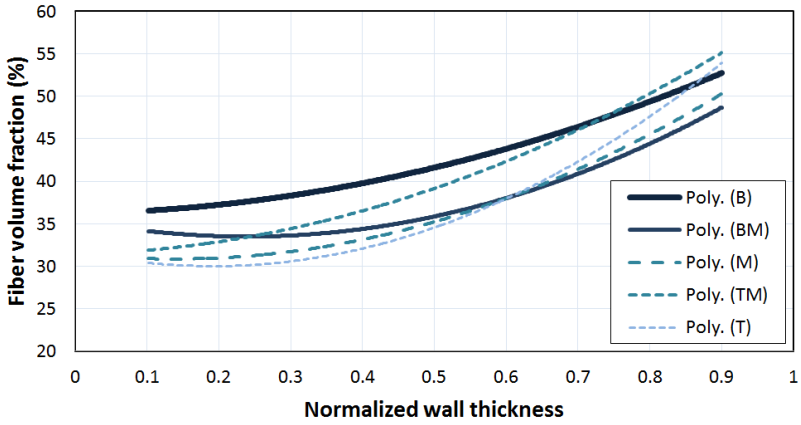

Figure 3.49 The 2nd order polynomial curves at 5 different elevations

Table 3.11 The normalized 2nd order polynomial equations for 5 different elevations

Location	Equation
B	$V_{Fn}(x) = 18.9\,x^2 + 1.3\,x + 36.2$
BM	$V_{Fn}(x) = 34.8\,x^2 - 16.7\,x + 35.5$
M	$V_{Fn}(x) = 33.6\,x^2 - 9.3\,x + 31.5$
TM	$V_{Fn}(x) = 27.2\,x^2 + 1.9\,x + 31.4$
T	$V_{Fn}(x) = 47.6\,x^2 - 18.2\,x + 31.8$

Based on the statistical analyses have been made according to data's obtained by the image process, there is not any dependency between fiber distribution alongside the tangential direction with a special direction. The same result is for the wall thickness which does not show any tendency in one special direction. The variation of fiber distribution in radial direction for all five elevations is less than 10% based on Figure 3.49. For example at the middle of section in radial direction, the fiber volume fraction is changed between 35% to 42%. Based on the Figure 3.49 for the sections more close to the base (B and BM) the fiber volume fraction difference between internal and external sides varies from 36% to 53% which means fiber volume fraction at external side is about 17% more than internal side. But from middle to the top of the culm it varies 30% to 55% which the difference is about 25%.

3.6. 3D X-ray microtomography of bamboo

The 3D X-ray microtomography (ZEISS Xradia 510 Versa) has been done for a cylindrical sample taken from middle part of a bamboo section as can be seen in Figure 3.50.

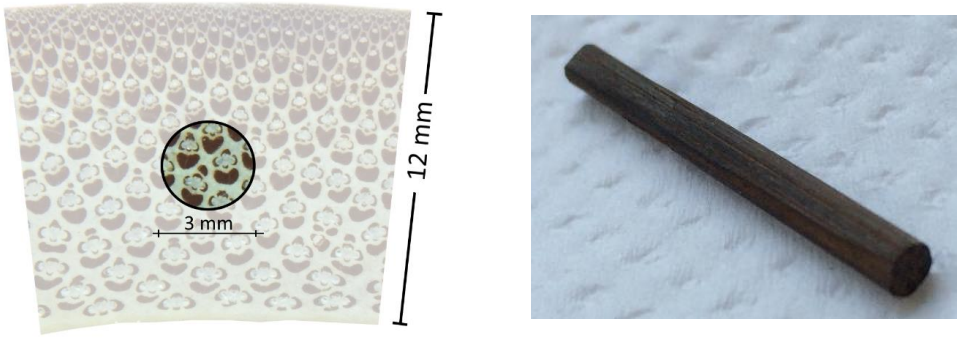

(a) The location of sampling (b) Heat treated cylindrical sample

Figure 3.50 Sample providing for Tomography test

The images prepared by stereomicroscope and X-ray microtomography presented in Figure 3.51a and b shows hollow tubes inside the sclerenchyma (fibers). At W-ray tomography images the dark areas have more density than the bright areas. After preparing the tomography image from untreated sample it placed to oven for 3 hours and then more 21 hours at 225°C and these three prepared images are compared to each other. The changes due to heat treatment for 3 hours at 225°C do not show any significant variation in bamboo texture but heat treatment for more than 21 hours creates cracks and demolish the structure of some parts as can be seen in Figure 3.52.

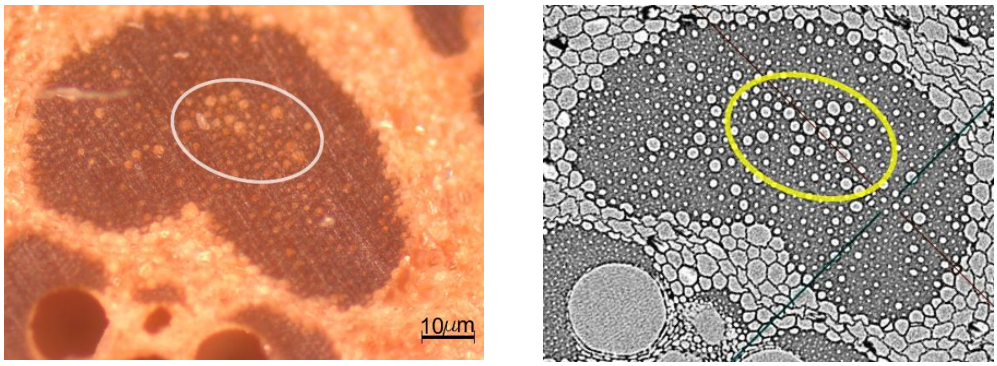

(a) stereomicroscope (b) X-ray tomography

Figure 3.51 Hollow tubes inside the sclerenchyma (fibers)

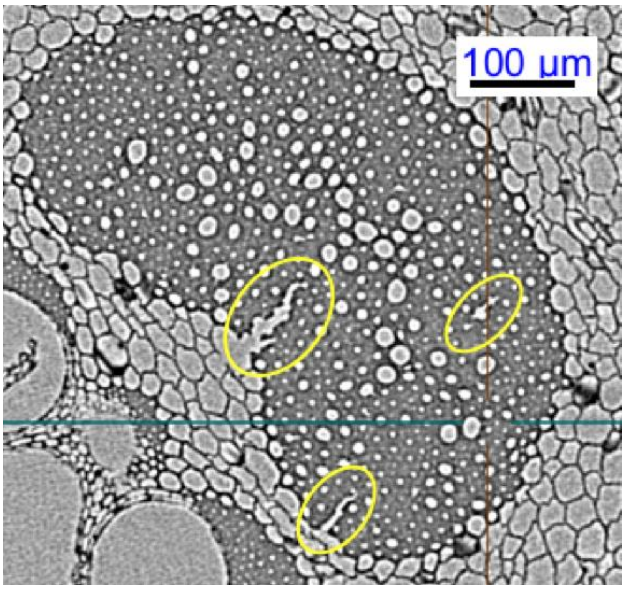

Figure 3.52 The crack in fiber group for heat treatment at 225°C for 24 hours

The bamboo section shrinks due to heat treatment as can be seen in Figure 3.53 to Figure 3.55. The initial size of the fiber is measured equal to $373.62\ \mu m$. Normalizing the values to untreated condition shows after heat treatment at 225°C for 3 hours the fiber size shrunk about 7.1% and by increasing the time exposure to 24 hours it changes remarkably and the fiber size decreases nearly 21.4%. the same evaluation for parenchyma shows nearly the same results about 6.9% shrinkage for heat treatment at 225°C during 3 hours and 19.5% for heat treatment at 225°C during 24 hours.

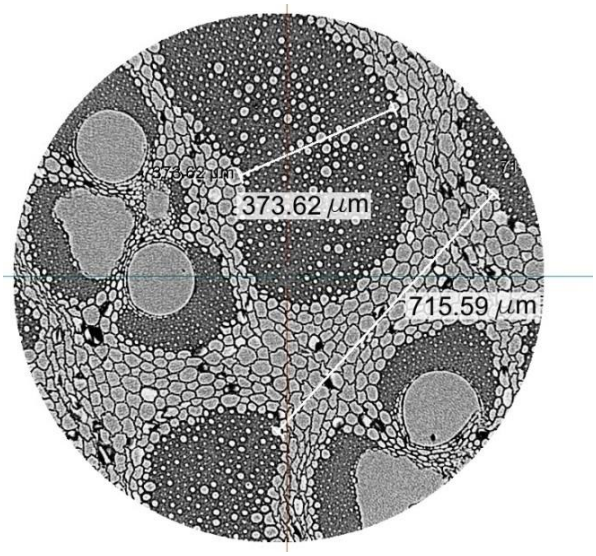

Figure 3.53 The fiber and matrix size for untreated sample

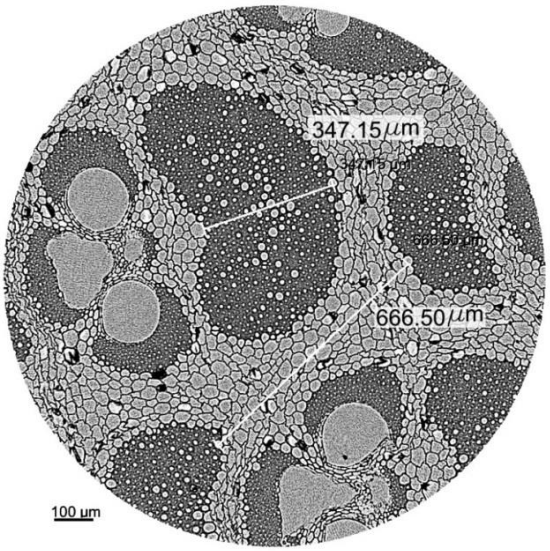

Figure 3.54 The fiber and matrix size for same sample treated at 225°C for 3 hours

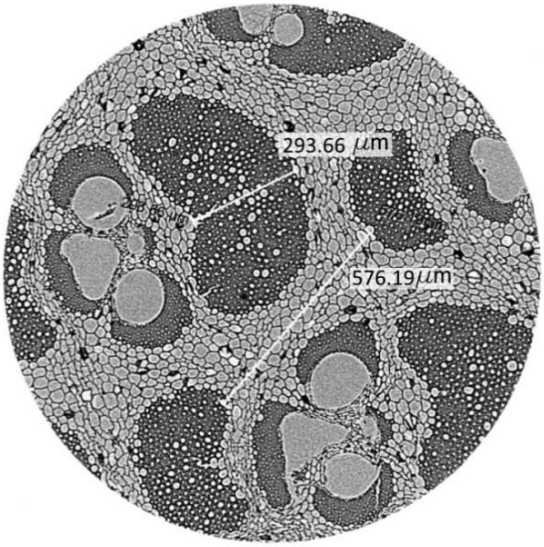

Figure 3.55 The fiber and matrix size for same sample treated at 225°C for 24 hours

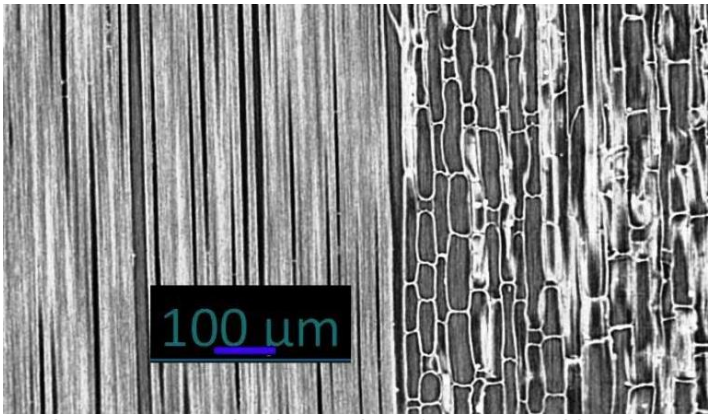

Figure 3.56 Section in XZ plane for untreated bamboo

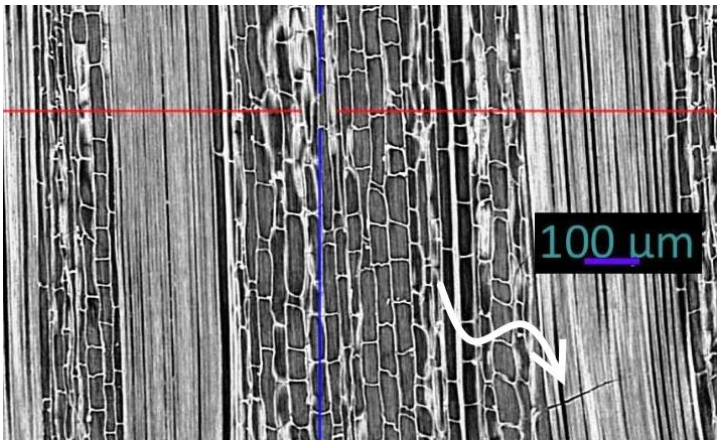

Figure 3.57 Section in XZ plane for bamboo treated at 225°C for 24 hours

In XZ plane (longitudinal section) the cell wall thickness of parenchyma reduced due to heat treatment at 225°C for 24 hours as can be seen in Figure 3.57 comparing with untreated sample shown in Figure 3.56. For samples treated at 225°C for 3 hours is not observed any cracks but for the sample treated for 24 hours the vertical and horizontal cracks can be seen in the fibers.

3.7. Scanning Electron Microscopy (SEM) images

A SEM model JSM-6510 has been used for providing the images of bamboo. After wet polishing by sandpaper no. 1200, the samples have been dried in the oven with 70^{o}C for one week and they put inside a desiccator. Then they treated in the oven to desired temperature for 3 and 24 hours. Totally 15 samples, one in ambient temperature, 7 samples treated in 100^{o}C to 225^{o}C within 3 hours and the other 7 samples at the same temperature but 24 hours have been considered to provide images.

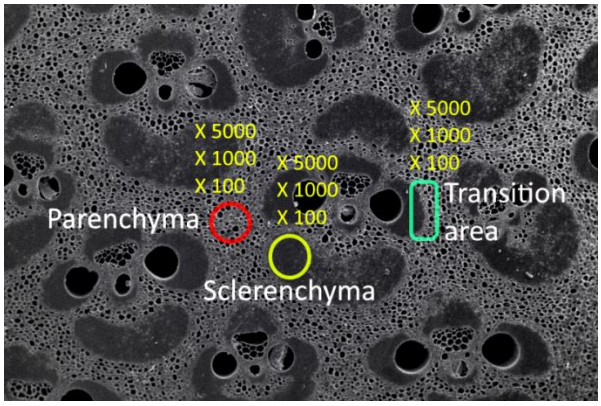

Figure 3.58 regions for providing the images

The cross section of each sample is divided to three internal, middle and external regions. Nine different images with different magnifications have been provided from each region. The regions for taking the images are Parenchyma, Sclerenchyma and Transition area between them which has been shown in Figure 3.58. The initial results of images prepared from sclerenchyma and parenchyma shows that the fiber bundles consists of groups of fibers seems dense and solid but the parenchyma has a sponge like structure with high porosity as shown in Figure 3.59.

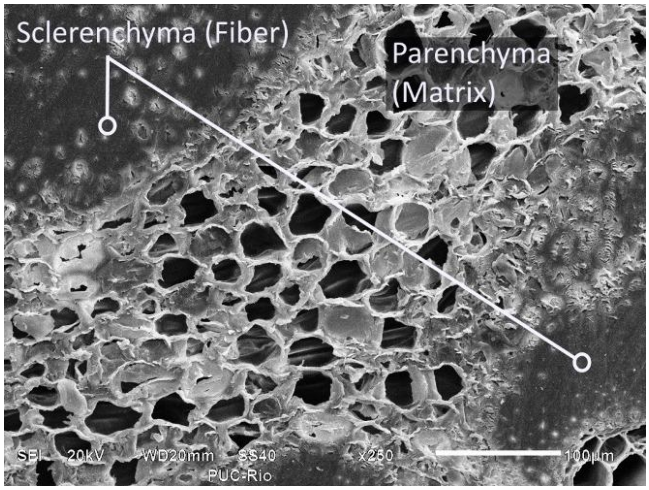

Figure 3.59 The parenchyma or matrix can be seen as a sponge area and sclerenchyma or fiber as solid and dense areas

3.7.1. The fiber appearance due to elevating the temperature

Up to 150°C is not observed any significant changes in the fiber texture but by elevating the temperature after 150°C, some radial cracks formed starting from the core of each fiber unit cell and separation between fiber units from wall cells as can be seen in Figure 3.60. At 175°C, the radial fiber cracks can be seen as bright lines obviously in Figure 3.60e,f and h.

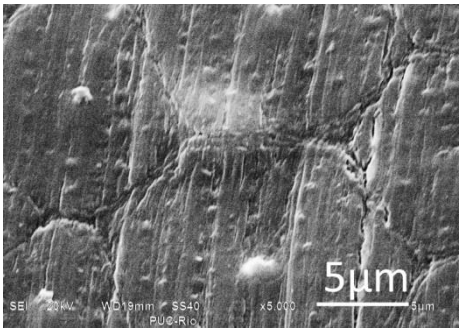

a) ambient temperature (25°C)

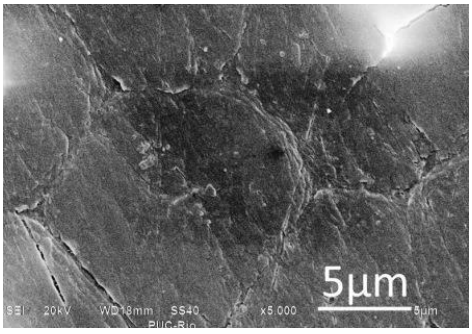

b) 100°C

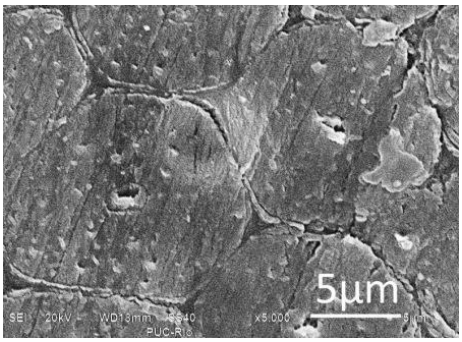

c) 125°C

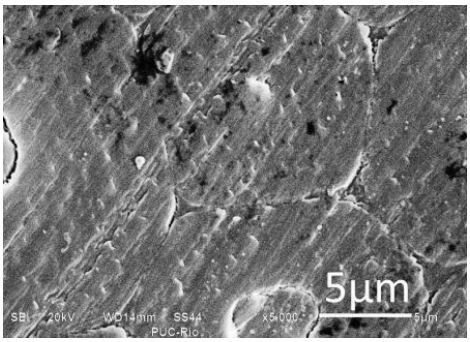

d) 150°C

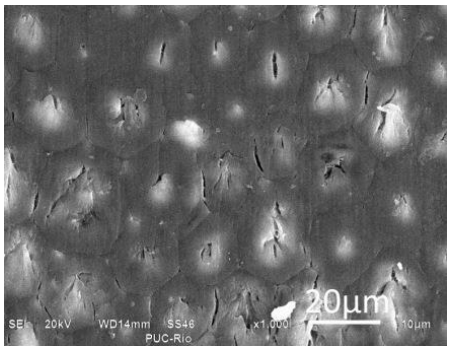

e) 175°C

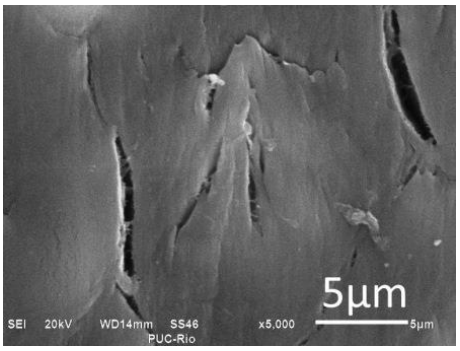

f) 175°C

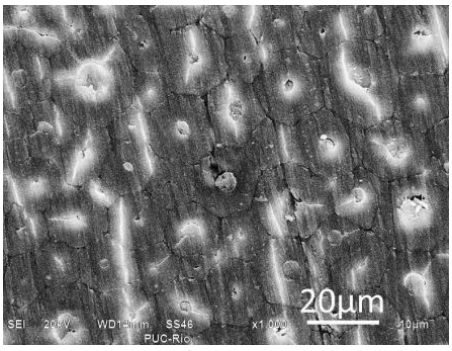

g) 200°C

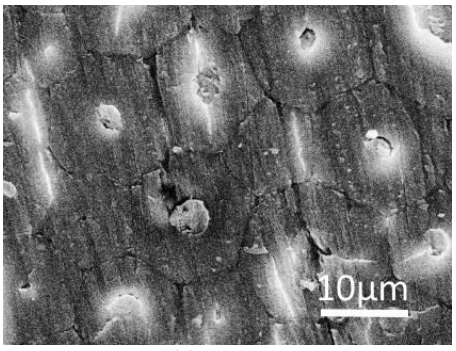

h) 200°C

Figure 3.60 The effect of heat on fiber bundles

3.7.2. The matrix appearance due to elevating the temperature

By comparing the images prepared from wall cell of parenchyma in various temperatures the thickness of wall cell is increased due to treatment in higher temperatures above 175°C as can be seen in Figure 3.61.

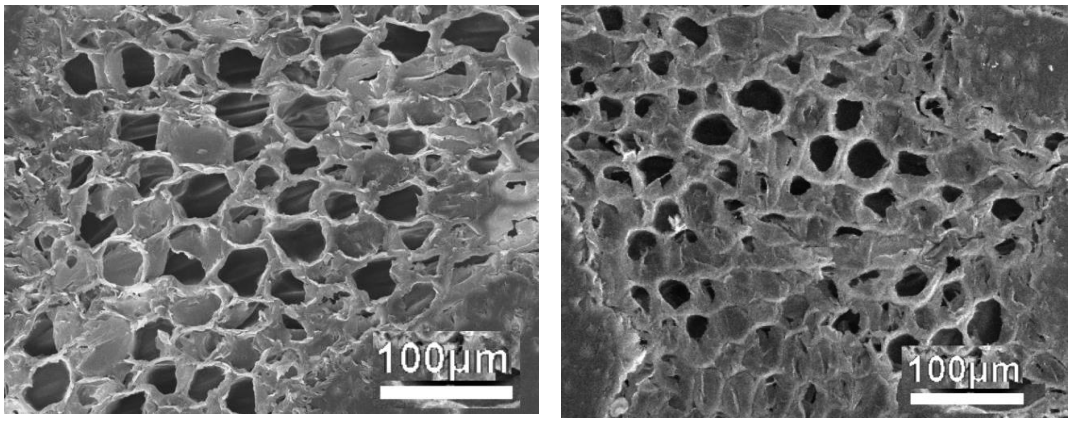

100°C 175°C

Figure 3.61 The effect of heat on matrix or parenchyma at 100°C and 175°C

3.8. Test variables

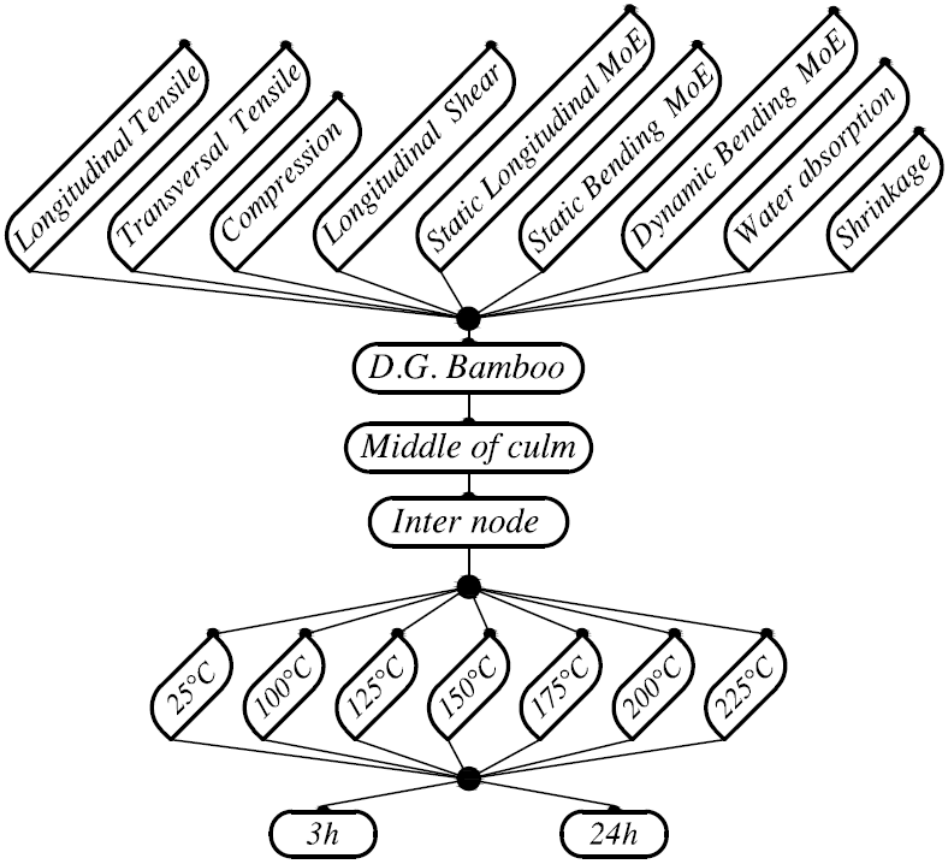

Figure 3.62 The Variables considered in present thesis

The variables for study about behavior of bamboo in high temperature selected from following parameters:

- **Location of stem**: The middle part of culm between elevations 3 *m* up to 8 *m*.
- **Temperature and time:** based on TGA analysis mentioned in section 3.43.4.4, in addition to room temperature, 6 different

temperatures from 100°C up to 225°C with the step of 25°C selected. 3h and 24h are two different times exposure.

- **Node and internode:** The internode parts are considered.
- **Bamboo type:** the bamboo type used in present thesis is *Dendrocalamus giganteus* bamboo. Figure 3.62 presents the summary of the studied variables.

3.9. Sample preparation

The samples made from the *Dendrocalamus giganteus* bamboo culms cut in Pirassununga (FZEA-USP) and PUC-Rio campus. The culms dried on the climatic conditions for one year. The tests are categorized in 8 groups:

1) Tensile test

2) Compression test

3) Longitudinal shear test

4) Transversal tensile test

5) Dynamic and static bending tests

6) General shrinkage and water absorption test

7) Uneven shrinkage and water absorption test

8) Image processing

The samples treated in 225°C for 24 hours are not used for the mechanical tests due to lack of resistance then, the group of heat treatment for 3 hours has 21 and the group of heat treatment for 24 hours has 18 samples as presented in Figure 3.62. Each group has two untreated sets one set used for dry condition and other for EMC (Equilibrium Moisture content) condition tests.

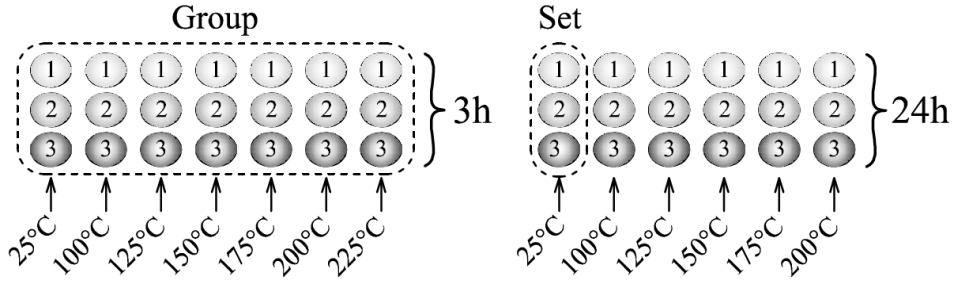

Figure 3.63 Two groups of samples each treating in 3 and 24 hours, each group has 7 sets and each set has 3 replicates

For the tensile test parallel to fibers and for the longitudinal shear test and bending test the total length of samples were 250 mm and 200 mm respectively. The initial thickness for tensile samples at splitting was about 5 mm but after using planner it is reduced to about 2 mm [90]. The width of longitudinal shear

samples is 20 mm. For the bending test samples, the cross section for both dynamic and static tests should be close to a square. The compression test samples were made the same as tensile test but 40 mm length. Water absorption samples are close to cubic and the dimension of each side is between 10 to 15mm. The sample shapes presented in Figure 3.64. The effect of accuracy in sample makings on the results and propagation of error is discussed in the Appendix 5.16. For the transversal tensile samples the thickness considered about 5mm and the length is considered about 40mm.

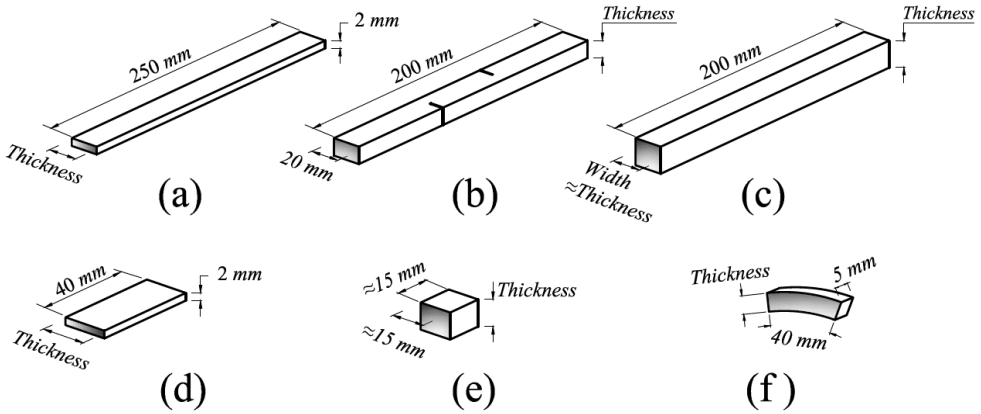

Figure 3.64 The different shapes and dimensions of the samples; a) tensile test parallel to fibers; b) longitudinal shear test; c) dynamic and static bending test; d) compression test; e) water absorption test; f) transversal tensile test

The tensile and compression test samples, prepared from the strips by splitting the culm in radial direction from an intermodal part of bamboo culm. The initial thickness in tangential direction is about 5mm as can be seen in Figure 3.65 but after passing the strips from planner, the thickness is reduced to about 2mm.

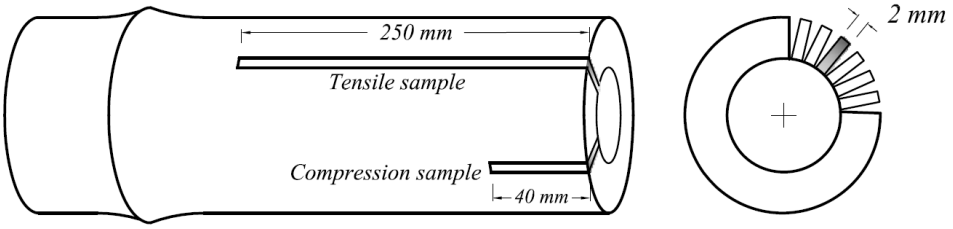

Figure 3.65 Selected cross section for the tensile and compression tests

The bending test samples, are prepared from an intermodal part of bamboo culm with 200mm length and width nearly equal to thickness.

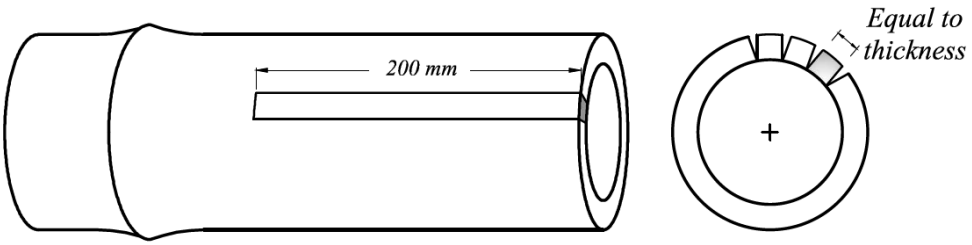

Figure 3.66 Selected cross section for the bending test

The width of the shear test bars are 20 mm and there are two types of longitudinal shearing samples; tensile and compression. The tensile samples are 200mm and the compression samples are 100mm as shown in Figure 3.67.

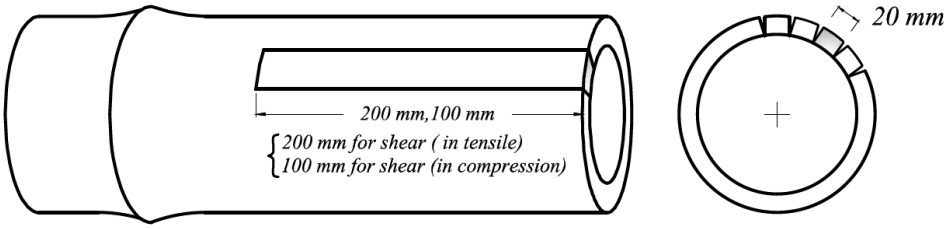

Figure 3.67 Selected cross section for the longitudinal shear test

The water absorption samples are the cubic shape with the approximate size about 15mm each side in tangential and radial direction as can be seen in Figure 3.68.

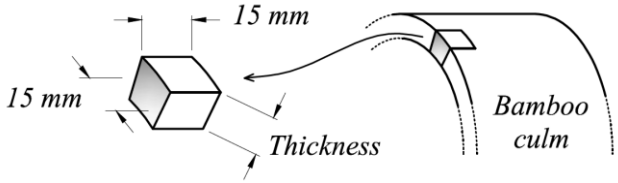

Figure 3.68 Water absorption sample

3.9.1. Sample selection for each set

Based on the results in section (3.5.4) the fiber distribution at the top, middle and bottom of a bamboo culm is different. To eliminate the effect of location and geometric variations of a bamboo has been tried to make the samples from one specific part of bamboo. This type of selection only is practical for small samples like water absorption, transversal tensile and compression test as can be seen in Figure 3.64d,e and f, but for big or long samples like tensile test, longitudinal shear test and bending test in Figure 3.64a,b and c, making numerous samples from only one intermodal part of culm is not possible. Then, each replica

of a set will be made from different parts (internodes) of a culm. To make all 42 tensile test samples, each 14 samples are made from one internode as shown in Figure 3.69. The first sample of each set always is made from the internode closer to the ground.

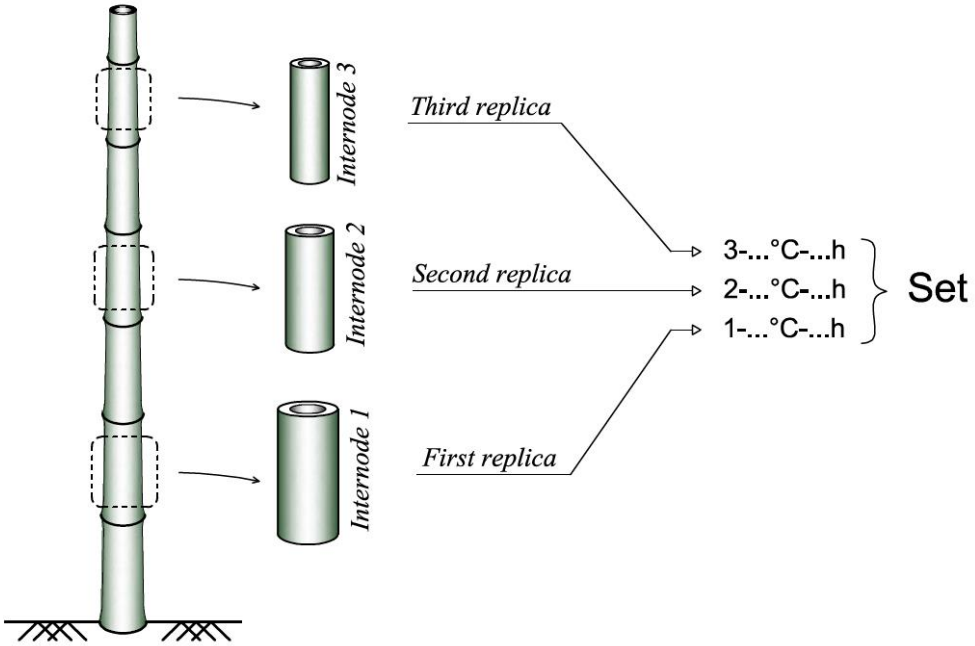

Figure 3.69 Make the samples from three different internodes

3.9.2. The code designation of specimens

The code written on the body of the specimens, states the set number, temperature and time exposure which is defined as below:

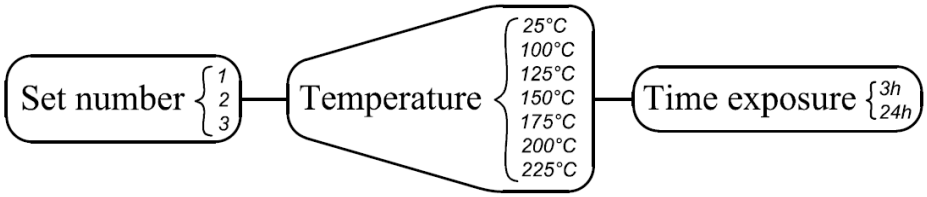

The time exposure can be 3h or 24h, temperature can varies from 25°C to 225°C (7 different thermal conditions) and the number of replicate such as 1, 2, or 3. If the sample tested at dry condition and before ambient humidity stabilization (EMC condition), a suffix "d" is added to the end right of the code. For untreated samples, the time prefix, 3h or 24h, is not used.

Body codes can be written as below:

1-225°C-3h: means sample test put in the oven for 3 hours in 225°C and tested after stabilization in room temperature and humidity (EMC condition).

1-25^{o}C-d: the code used for untreated sample in dry condition.

1-25^{o}C: means untreated sample at EMC condition.

3.10. The influence of heat on humidity absorption, water absorption and shrinkage of bamboo

This section presents the effect of heat on humidity absorption, shrinkage and water absorption of bamboo. The HST (Humidity Stabilization Time) test is carried out to establish the required time for each different geometrical shape to reach from dry condition to the 75% RH, because all the specimens which are used for mechanical tests, before doing the tests, should have been stabilized at the temperature and humidity 27°C ± 2°C and 70% ± 5% RH respectively [84]. The second study is about shrinkage, water absorption and swelling of bamboo specimens in Longitudinal, radial and tangential directions at different temperatures from 100°C up to 225°C treated in 3 hours and 24 hours. Based on the water absorption diagrams, a two components curve fitting equation is proposed to cover the rapid and slow phases of water absorption. Finally, to stablish the difference between fiber and matrix hygroscopicity, the non-uniform shrinkage and water absorption test in tangential direction for internal and external parts is carried out and the hygroscopic property of each component measured separately. The middle part of a five years old *DG* bamboo culm has been used as the material of this section. The culm dried on a covered place with the climatic conditions for one year.

3.10.1. Humidity Stabilization Time (HST)

Humidity Stabilization Time (HST) test is carried out to establish the required time for different geometrical shapes to reach from dry condition to the specific humidity which is used in this investigation. Each selected bamboo segment has six faces with different rate of water and humidity absorption. There are two cross sections (transversal faces), two radial faces, two tangential faces, one external and one internal as shown in Figure 3.70. Transversal sections contain the veins which are the surface with the highest water and moisture absorption. The longitudinal cuts which are called radial faces go through parenchyma, sclerenchyma or veins. The radial faces are not as permeable as the

transversal ones. The permeability of the internal and the external faces of bamboo are less than the radial faces. The principal directions and faces for a cubic sample of bamboo are shown in Figure 3.70.

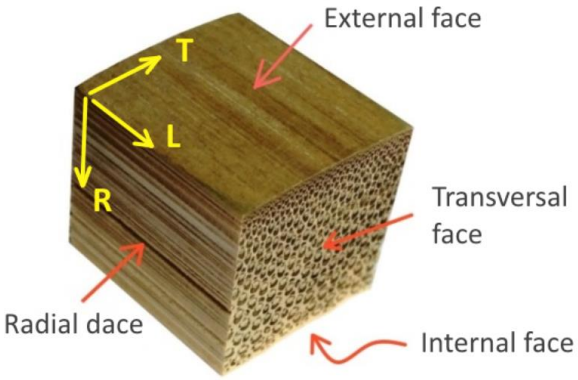

Figure 3.70 The faces in a cubic sample of bamboo

Four different geometrical shapes given in Table 3.12, selected to investigate the effect of heat and the geometrical shapes, on the moisture absorption. The approximate size of each shape resembles nearly the size of each mechanical test specimen. Tensile test specimen has a narrow width about 2 mm but longitudinal shear test and bending test specimen shapes have two equal sides and transversal tensile test specimens are transversally cut segments. Three samples from each shape placed in to the oven for three hours at different heat treatment, 100°C, 150°C and 200°C.

Table 3.12 Sample geometry and dimensions for different test types

Test type	Designation	Shape
Tensile test	T	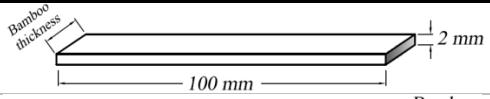
Longitudinal Shear and bending test	LS	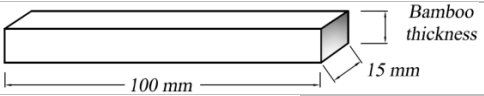
Transversal Tensile test	TT	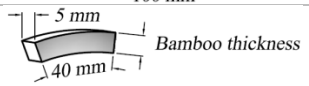
Water Absorption	WA	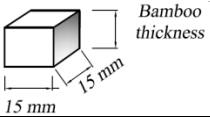

HST test needs climatic room or chamber but due to lack of these facilities, a desiccator with saturated salt water solution is used. By utilizing saturated salt water solution (by solving 357 grams of salt at 20°C in one liter of water) , the humidity can be controlled and remains constant about 75% Rh [91][92]. By

putting the heat treated and dry samples inside the desiccator as shown in Figure 3.71 and measuring the weight changes until stabilization, the HST for each shape can be achieved. The results are demonstrated in Figure 3.72 to Figure 3.75. For related tables see appendix Table 5.2.

Figure 3.71 The samples inside the desiccator with the saturated salt water solution

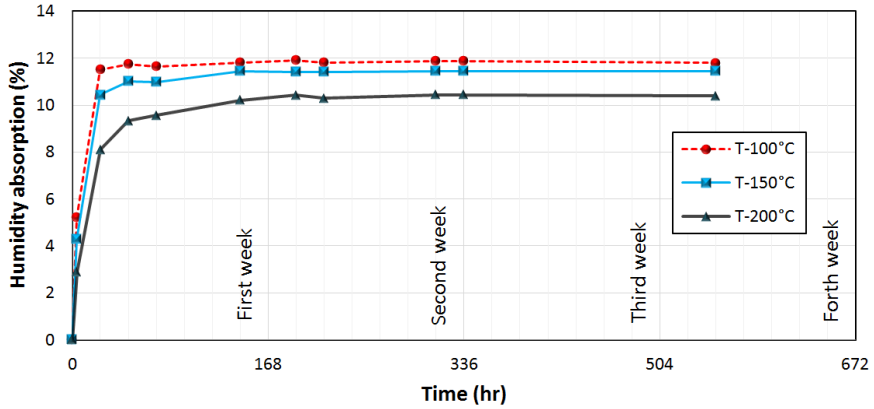

Figure 3.72 Time vs humidity absorption of tensile samples

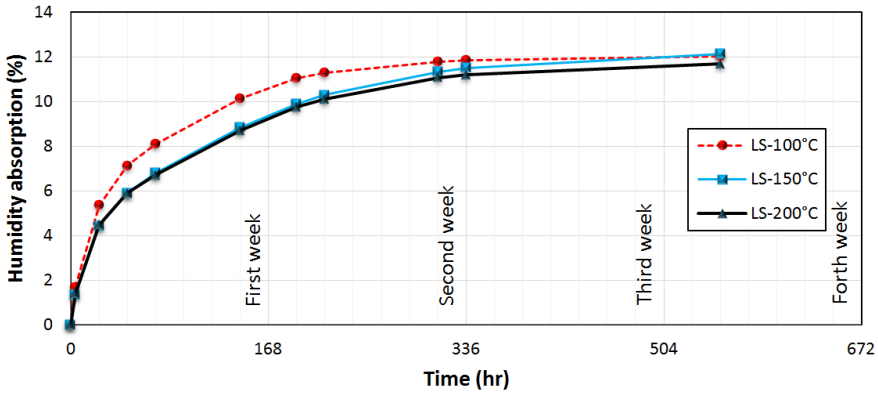

Figure 3.73 Time vs humidity absorption of shear samples

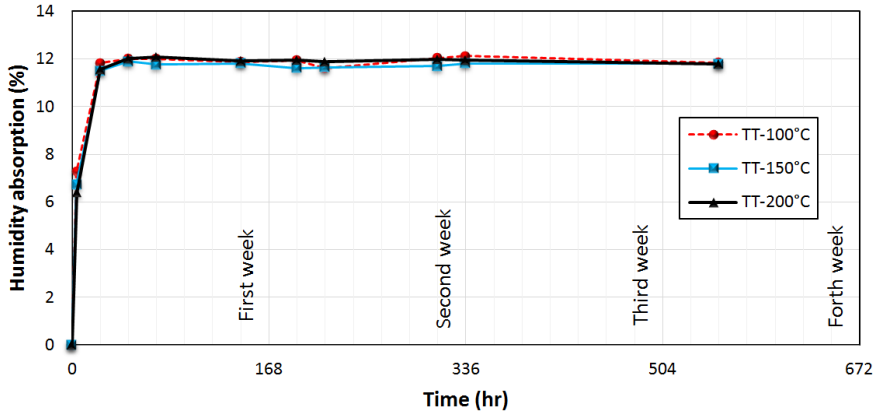

Figure 3.74 Time vs humidity absorption of transversal tensile samples

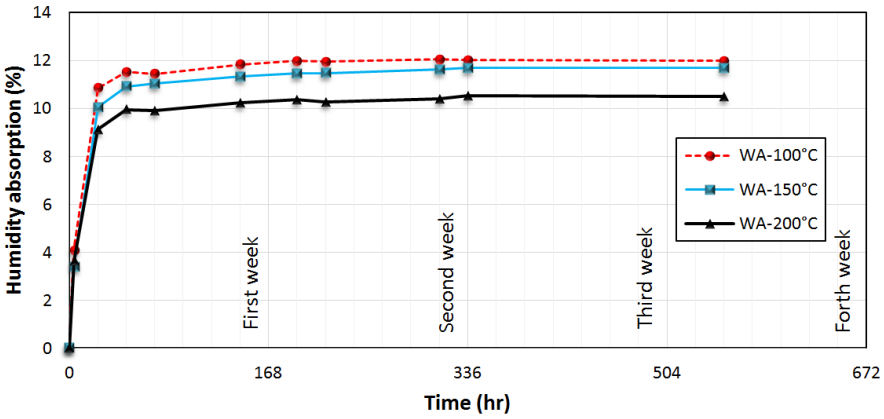

Figure 3.75 Time vs humidity absorption of water absorption samples

A general observation to the Figure 3.72 to Figure 3.75 reveals that stabilization time for transversal tensile and water absorption samples is about two days. The humidity absorption of tensile specimens for various heat treatments is different. The T-100 and T-150 specimens approach to the asymptote line of stabilization, quicker than the T-200 also approaching to the stabilization for T-100 is quicker than T-150 but both of them are equilibrated after three days as shown in Figure 3.72. Also the Figure 3.72 shows that the humidity absorption ability in heated specimen in 200°C is reduced about 20% and T-200 is equilibrated after about one week but there is an important inconsistency between transversal tensile samples with the three other shapes (WA, T and LS).

The water absorption of all three transversal tensile specimens (TT-100, TT-150, TT-200) are the same and about 12% and there are not any significant differences between them as can be seen in Figure 3.74. But in the three other groups, the specimens treated in 200°C, the hygroscopic property is decreased regarding to other samples. Proposed stabilization times for Transversal tensile

(TT), water absorption (WA), tensile (T) and longitudinal shear (LS) specimens with 3 different heat treatment temperatures, presented in Table 3.13.

Table 3.13 The humidity stabilization time of four different type of samples (HST)

sample	Treatment temp. (°C)		
	100	150	200
Tensile (T)	3 days	3 days	1 week
Transversal Tensile (TT)	2 days	2 days	2 days
Longitudinal Shear (LS)	2 weeks	2 weeks	2 weeks
Water Absorption (WA)	3 days	3 days	3 days

3.10.2. Bamboo shrinkage and water absorption

The specimens were prepared from the internodes of DG bamboo at the middle part of bamboo culm with about 15.5 cm diameter and 14 mm wall thickness as can be seen in Figure 3.76a. Two different time exposures of 3h and 24h with seven different temperatures 25°C, 100°C, and then with 25°C increment up to 225°C were considered in the test program. The time and temperature exposure of the sample matrix is shown in Figure 3.76b. This matrix consists of two groups, and each group is divided into three blocks and seven sets of samples, and each set has three specimens from three different blocks as can be seen in Figure 3.77a. This type of ordination can guarantee the same condition in terms of property, thickness and fiber distribution in each block. To make a cubic shape samples as shown in Figure 3.77b, the dimensions in tangential and longitudinal directions considered nearly equal to bamboo wall thickness (14 mm). Using a disc polishing machine and water, all the opposite faces finished almost parallel to each other.

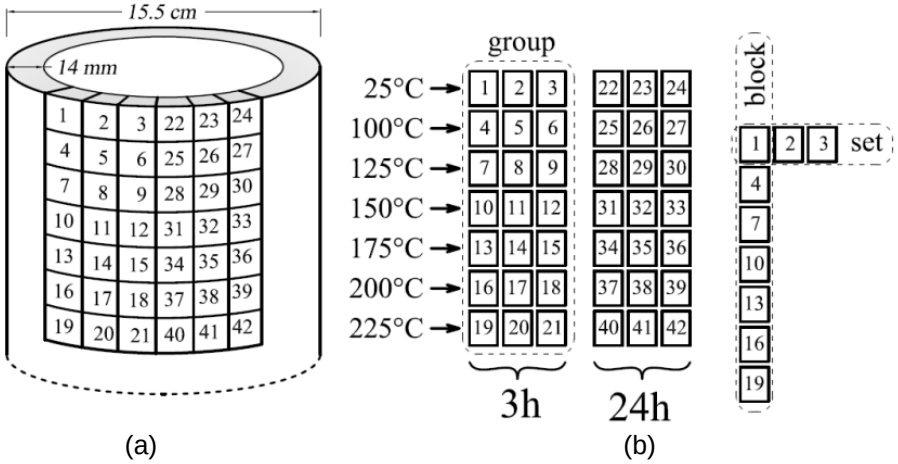

Figure 3.76 Sample selection for shrinkage and water absorption

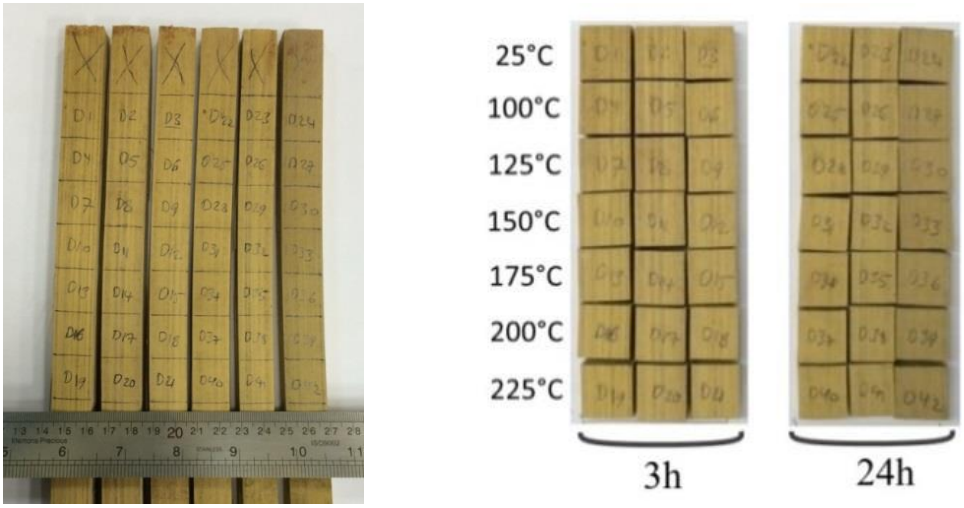

(a) sample blocks (b) prepared samples

Figure 3.77 Sample blocks and after preparation

The prepared specimens dried in the laboratory with the average temperature and humidity equal to 24°C and 60% respectively for two weeks. Then, samples kept in the oven with 70°C for one week, placed into a desiccator with humidity absorber for 3 days to absorb the residual moisture content; finally the dry weight and the dimensions of each sample were measured by a caliper rule with a precision to ±0.02 mm at the middle of the specimens and prepared for the shrinkage test. Each set of samples was placed into an oven at 6 different temperatures for 3 and 24 hours. The samples after the heating process are shown in Figure 3.78. The results are given in the Table 5.3 and Table 5.4 of appendix 5.5. No color changes for specimens heated up to 150°C for 24hrs and 175°C for 3hrs was observed. The color of the samples which heated at 225°C for 24hrs changed nearly to the color of charcoal with a visible shrinkage.

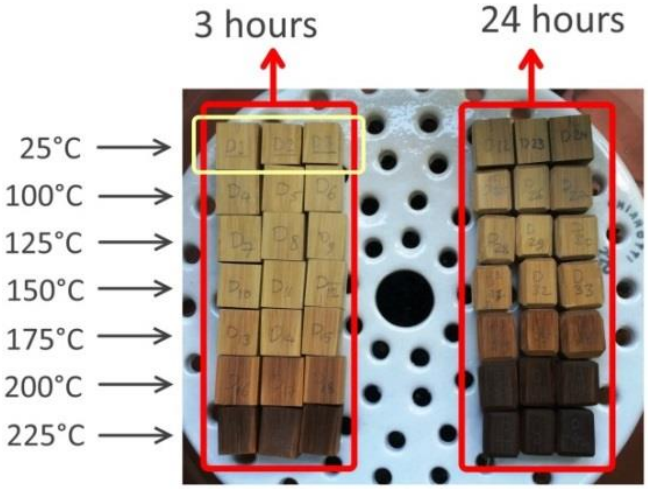

Figure 3.78 The color changes of the specimens subjected to different temperatures for 3 and 24 hours

After removing the specimens from the oven and stabilizing them in the desiccator, the weight and dimensions were registered. The weight loss percentage due to the incremental temperature for 3 hours and 24 hours is presented in Figure 3.79. The minimum and maximum of coefficient of variation (CV%) for weight loss of the samples heated in 3 hours and 24 hours are 0.7% and 9% respectively. As it can be observed, the fast rate of weight changing started from 175°C for the samples headed for 24 hours and 200°C for the samples heated for 3 hours. Also after 150°C, the weight loss of samples heated to 175°C, 200°C and 225°C for 3 hours are nearly equal to the samples heated at 150°C, 175°C and 200°C respectively but heated for 24 hours. An exponential function relates the weight loss to temperature as can be seen in Eq. 3.4. In this equation, "W" is weight loss in (%) and "T" is temperature in Celsius. A and B are two coefficients should be obtained by curve fitting. The curve fitting equations for 3 and 24 hours presented inside the related graphs. "R2" is the coefficient of determination.

$$W = Ae^{BT} \qquad 3.4$$

The dimensional changes in longitudinal, tangential and radial directions are presented in Figure 3.80 and Figure 3.81. The minimum and maximum of coefficient of variation (CV%) for shrinkage of the samples in radial and tangential directions, heated in 3 hours and 24 hours are 1.5% and 41.4%.

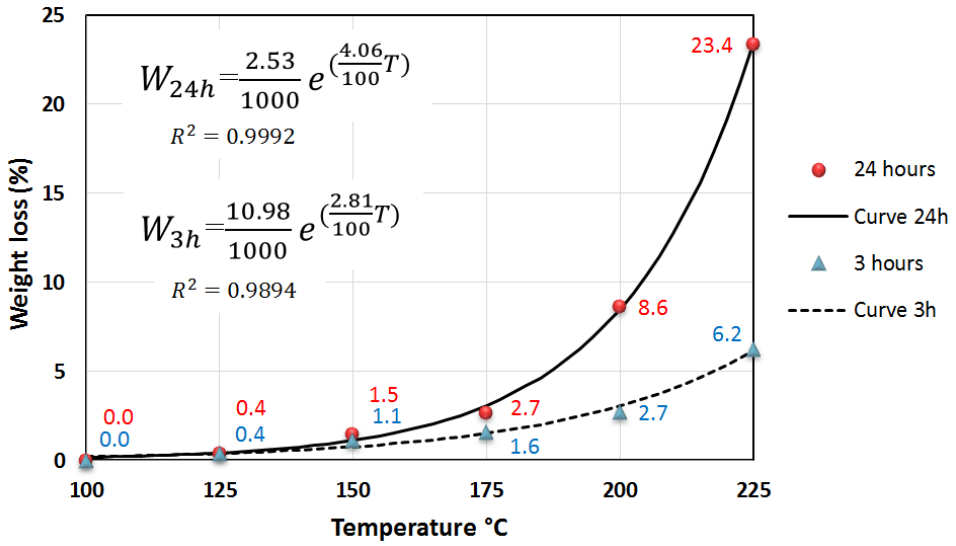

Figure 3.79 The weight loss of samples heated at six different temperatures for 3 and 24 hours

As it can be seen for temperatures higher than 200°C, the shrinkage of both specimen groups kept in the oven for 3h and 24h, increased significantly. The shrinkage for samples heated for 3 and 24 hours up to 150°C was less than one percent but the fast rate of dimension variations in radial and tangential directions started after exposure to 150°C. The longitudinal shrinkage up to 150°C heated during 3 and 24 hours was zero and up to 225°C was less than 0.3% then which is negligible compared with the dimension changes in tangential and radial directions.

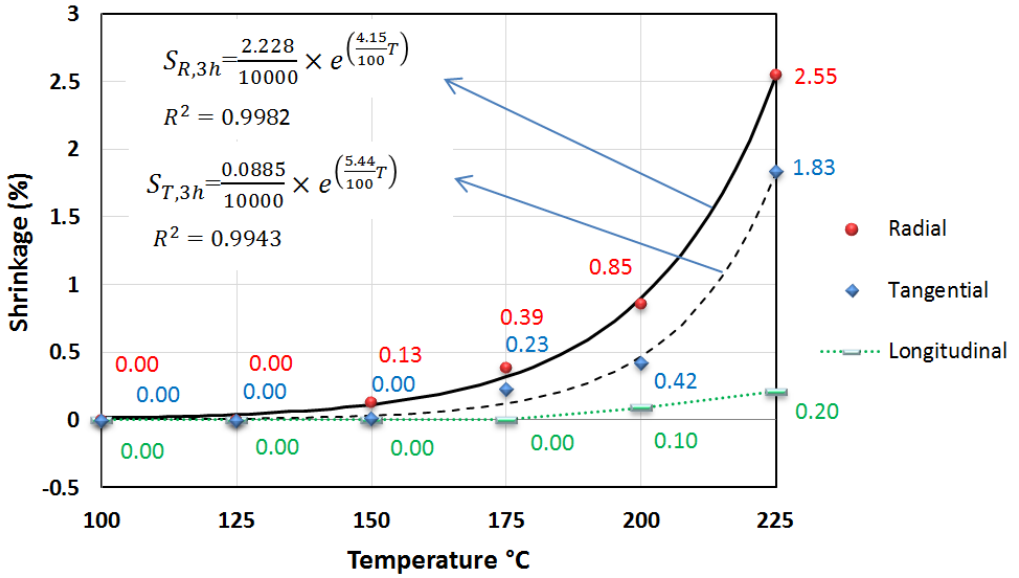

Figure 3.80 Shrinkage in radial, tangential and longitudinal directions for 3 hours heated in oven

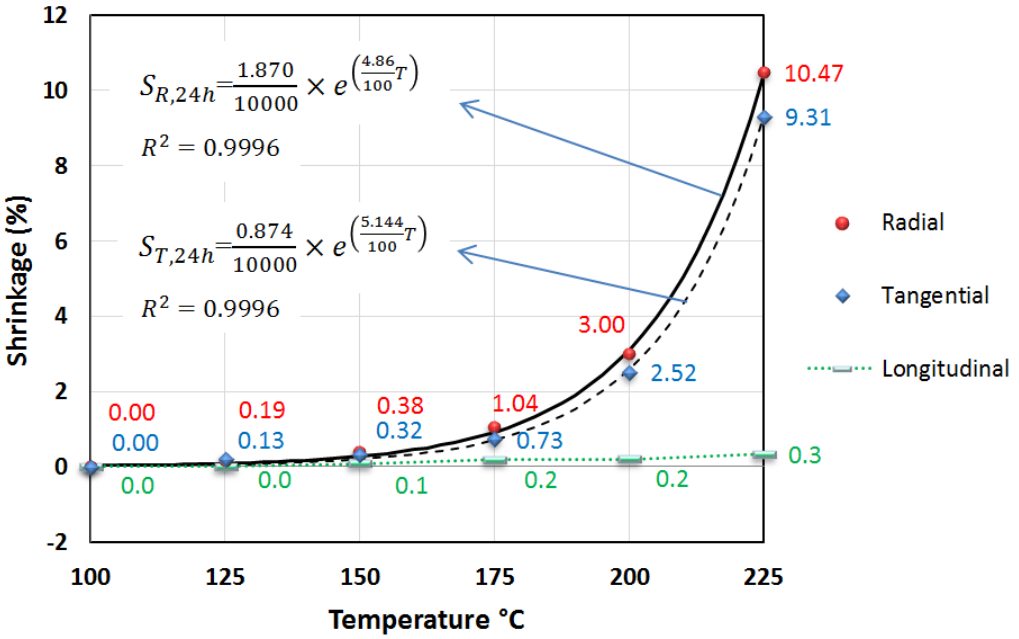

Figure 3.81 Shrinkage in radial, tangential and longitudinal directions for 24 hours heated in oven

As can be seen in Figure 3.80 and Figure 3.81, shrinkage in tangential direction is always less than radial direction. The same equation model applied for weight loss used in radial and tangential directions for 3 hours and 24 hours. “S” and “T” are the shrinkage (%) and temperature (°C) respectively in the curve fitting equations mentioned inside the graphs. The effect of time exposure can be observed comparing the Figure 3.80 and Figure 3.81. No dimension changes observed for the samples heated in 125°C for 3 hours but for the same temperature the samples heated for 24 hours shrank 0.13% and 0.19% in tangential and radial directions respectively.

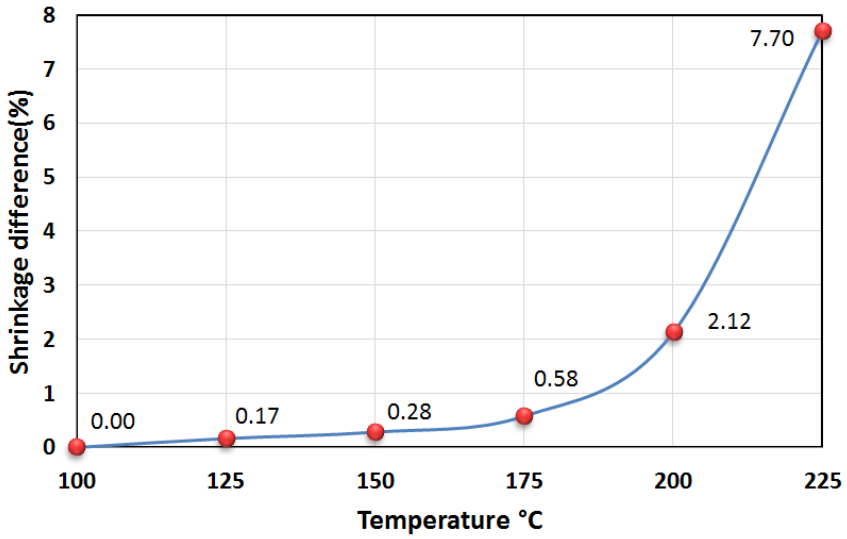

Figure 3.82 The average shrinkage difference between the samples heated for 3 and 24 hours

To establish the effect of heat exposure time, the average of shrinkages in radial and tangential directions heated for 3 hours in Figure 3.80 are compared with the same value heated for 24 hours shown in Figure 3.81. After about 175°C the effect of time exposure is significant as can be seen in Figure 3.82.

3.10.2.1. Short term and long term water absorption tests

The specimens used for the shrinkage test, were used to establish the water absorption test of bamboo. The dimension and weight of heated and dried samples before being placed into distilled water with an ambient temperature were registered. The water absorption at the start of the procedure is high [93][94], then the registration time intervals were considered short at first but increased progressively. The determined registration time intervals were 6 hours, one day,

three days, one week, two and half weeks and finally four weeks. At the first 6 hours or "*short term water absorption*" for the specimens heated for 3h and 24h, by increasing the heat exposure time and temperature, the rate of water absorption decreases as can be seen in Figure 3.83.

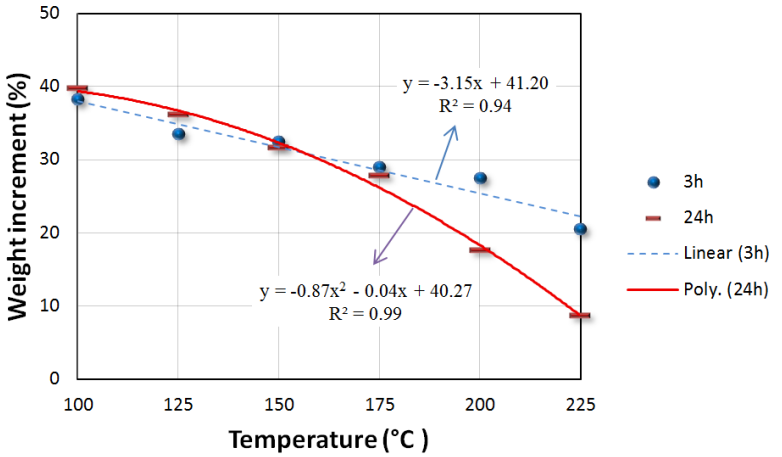

Figure 3.83 Weight increment after 6 hours water absorption for the samples heated for 3 and 24 hours

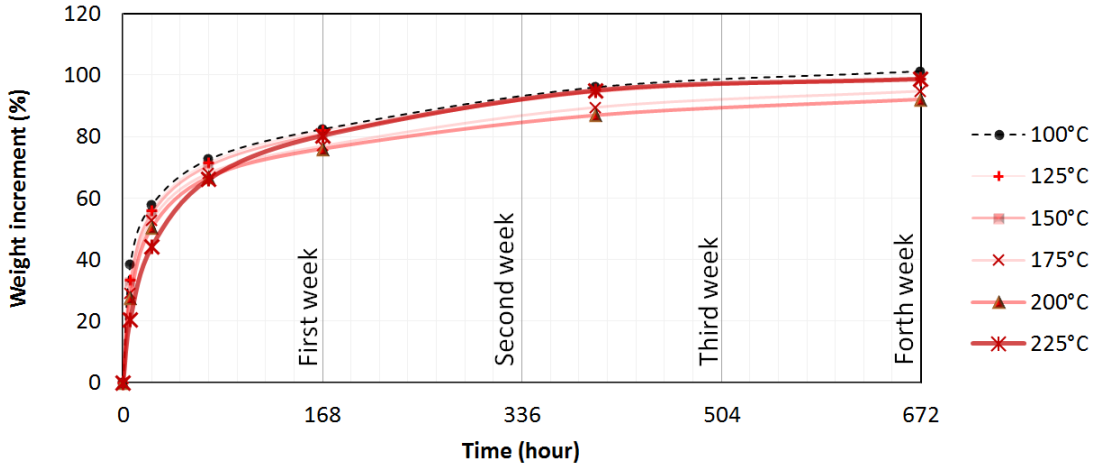

Figure 3.84 Weight increment of bamboo samples during four weeks and 3 hours subjected to heat

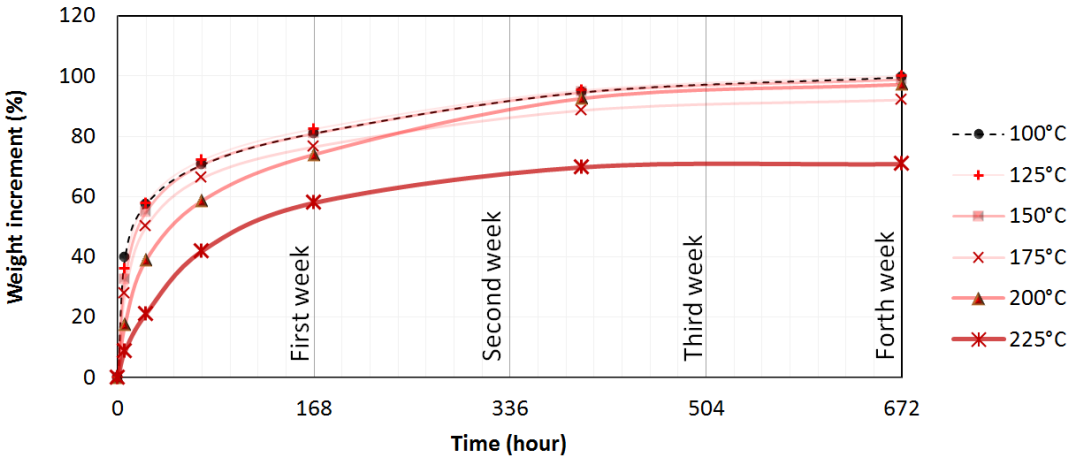

Figure 3.85 Weight increment of bamboo samples during four weeks and 24 hours subjected to heat

For the specimens heated for 3 hours the water absorption decreases by about 20% and for the specimens heated within 24 hours this value reduces from about 40% at 100°C to about 10% at 225°C. Increasing of the heat treatment temperature and time exposure can slow down the rate of water absorption. For the samples heated for 3 hours, the reduction of weight increment can be estimated by a line but for the samples heated for 24 hours; the curve fitting equation is a second order polynomial as can be seen in Figure 3.83. The effect of time exposure after 175°C is significant as can be observed in Figure 3.83. The results of the natural water absorption for the heated samples during 28 days, considered as "long term water absorption" presented in Figure 3.84 and Figure 3.85. The set of samples heated at 225°C for 24 hours are similar to charcoal and its water absorption capacity is not the same as other sets as can be seen in Figure 3.85. It means that the hygroscopic property of the samples heated at 225°C for 24 hours has been changed remarkably.

The results show that the rate of water absorption at the early hours is considerable. In average, after 24 hours the specimens absorb 50% of the total water which absorbed after four weeks. In a short term period, the rate of water absorption directly related to heat treatment temperature as can be seen in Figure 3.83. But in a long term for the sample heated during 3 hours, the water absorption capacity reduces gradually by elevating the temperature up to 200°C but for the samples heated at 225°C the water absorption capacity increases from 92.1% (heated at 200°C) to 98.7%. The same occurred for the sample heated during 24 hours. A reduction was observed up to 175°C by 92.1% but for the samples heated at 200°C the water absorption capacity increases to 97.2%. In general in the long term, all of the samples absorb about 90% to 100% of their initial dry weight. The only exception was the set of samples heated at 225°C for 24 hours which absorbed about 70% of the dry weight of the samples. It shows at the beginning of the torrefaction temperature, the hygroscopic property of bamboo changes significantly.

(a)

(b)

Figure 3.86 Removing air bubbles (forced water absorption) by vacuum and the settled samples

After four weeks, the weight and dimension of specimens were registered with regards to normal water absorption (long term water absorption in ambient pressure). Using a vacuum chamber as can be seen in Figure 3.86a (forced water absorption), the air pressure was lowered to 0.3 bar to remove any possible air bubbles trapped inside the samples. Then the samples were subjected to atmospheric pressure in order to replace the air bubbles with water. This procedure is repeated several times to stabilize the weight of the samples. The final weight and dimensions were registered after this procedure. The settled specimens on the bottom of the beaker are shown in Figure 3.86b.

The normal water absorption during four weeks and forced water absorption of the specimens subjected to heat for 3 and 24 hours are presented in Figure 3.87. Due to the excessive shrinkage and lack of hygroscopic property the specimens subjected to heat at 225°C for 24 hours are excluded from the results. In average, the capacity of water absorption for both heat treatments for 3 and 24 hours by increasing the temperature is reduced up to 15%.

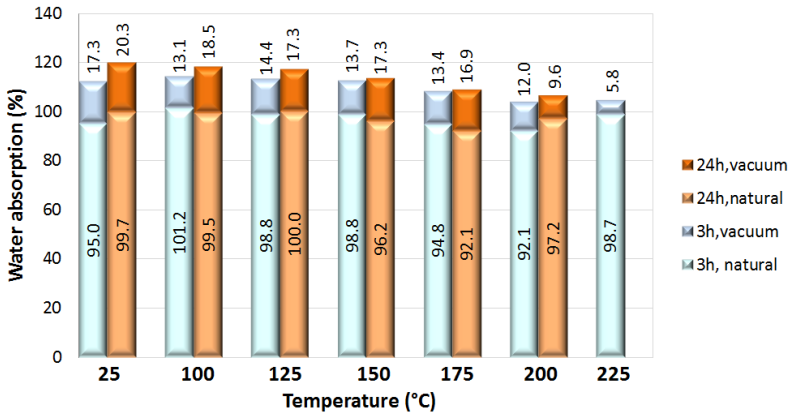

Figure 3.87 Water absorption for the specimens subjected to heat for 3 hrs and 24 hrs

3.10.2.2. Water absorption model

The test results in the previous section show that the rate of water absorption for all of the samples at the early hours is significant. After a few hours up to about one day the specimens absorb 40% to 60% of their total water absorption capacity, which is called rapid phase of water absorption, then gradually this rate is reduced and after 2 or 3 days, the samples absorb water with a slower rate up to saturation. A graph is made by averaging the results of all the samples heated in 3 hours by referring to Figure 3.84 and the result is presented in Figure 3.88. In this graph, three phases can be defined: a) rapid sorption, b) transition sorption c) slow sorption. A simple model of water absorption is a non-exponential empirical model defined by Peleg [95][96] used for one phase water absorption [97]. A two phase water absorption model defined by Mohsenin [98] does not converge to an asymptote by time increment due to having a linear component in the equation. The results in Figure 3.84 and Figure 3.85 cannot be fitted well when using the Peleg and Mohsenin models as fitting curve equations. The suggested model in this investigation presented in Eq. 3.5 has four coefficients which can be established by curve fitting.

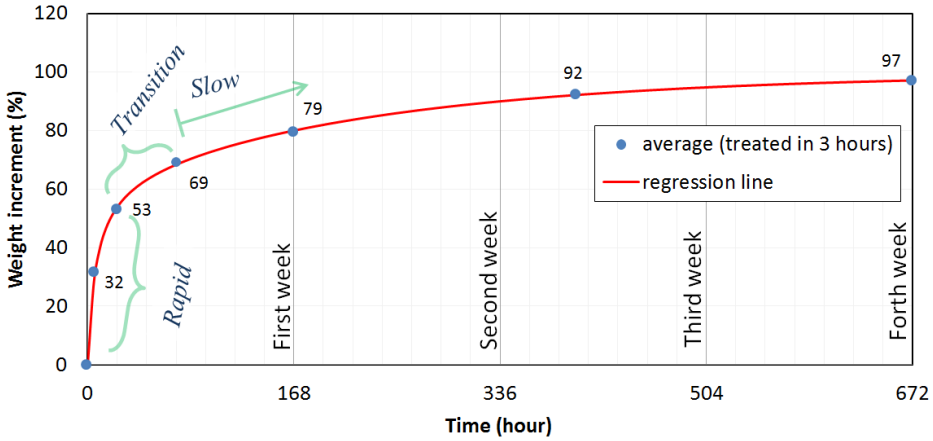

Figure 3.88 Three phases of water absorption: rapid, transition and slow sorption

$$W_a(t) = R_1\left(1 - e^{-t/R_2}\right) + S_1\left(1 - e^{-t/S_2}\right) \qquad 3.5$$

Where the $W_a(t)$ is the water absorption percentage consisting of rapid and slow water absorption components. Each component has two coefficients; R_1 and R_2 for rapid and S_1 and S_2 for slow water absorption which are presented in Table 3.14 and Table 3.15.

Table 3.14 The curve fitting equation coefficients for specimens heated for 3 hours

Coefficient	Temperature (°C)						
	25	100	125	150	175	200	225
R_1	53.50	53.44	51.60	51.18	52.46	49.48	43.80
R_2	4.801	5.250	6.433	6.693	8.385	8.528	12.30
S_1	41.92	48.01	47.35	47.92	43.07	42.40	55.31
S_2	188.7	170.6	153.6	163.0	191.0	164.14	150.6

Table 3.15 The curve fitting equation coefficients for specimens heated for 24 hours

Coefficient	Temperature (°C)						
	25	100	125	150	175	200	225
R_1	55.34	52.90	53.65	51.35	46.47	37.32	14.05
R_2	3.872	4.715	5.891	7.001	7.581	11.97	15.27
S_1	44.55	47.22	46.51	45.16	45.58	61.50	56.96
S_2	179.1	178.0	165.9	159.4	147.2	179.4	110.9

The coefficients R_2 and S_2 are related to the approximate time of the start and the end of transition period respectively. As can be seen in Table 3.14 and Table 3.15 the values of R2 are increased by elevating the heat treatment temperature. It proves that the water absorption slows down by increasing the heat treatment temperature. The summation of R_1 and S_1 shows the total capacity of water absorption. The coefficient of determination (R^2) for the samples heated for 3 and 24 hours are between 0.9982 up to 0.9992 which are close enough to one and shows the high dependency between the experiments and proposed curve fitting equation.

3.10.2.3. Dimension changes due to water absorption

The rate of dimension changes due to water absorption in L-R-T directions is different. The bamboo swelling in longitudinal direction due to water absorption is less than 0.5% but in tangential direction varies from 5% to 7% and in radial direction has the maximum swelling within 8% to 12%.

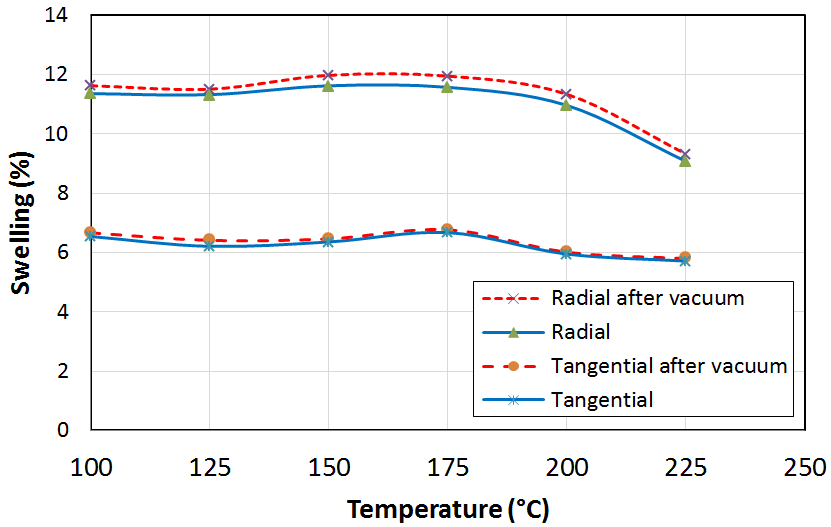

Figure 3.89 Dimensional changes due to water absorption up to saturation in radial and tangential directions for the specimens subjected to heat for 3 hours

Dimension changes for the specimens subjected to heat for 3 hours and 24 hours are shown in Figure 3.89 and Figure 3.90. By increasing the heat and time exposure, the bamboo swelling due to water absorption is reduced. For the samples heated for 3 hours, up to 175°C is not observed any remarkable changes in swelling due to water absorption. The same happens for the sample heated for 24 hours but the reduction of swelling starts from 150°C.

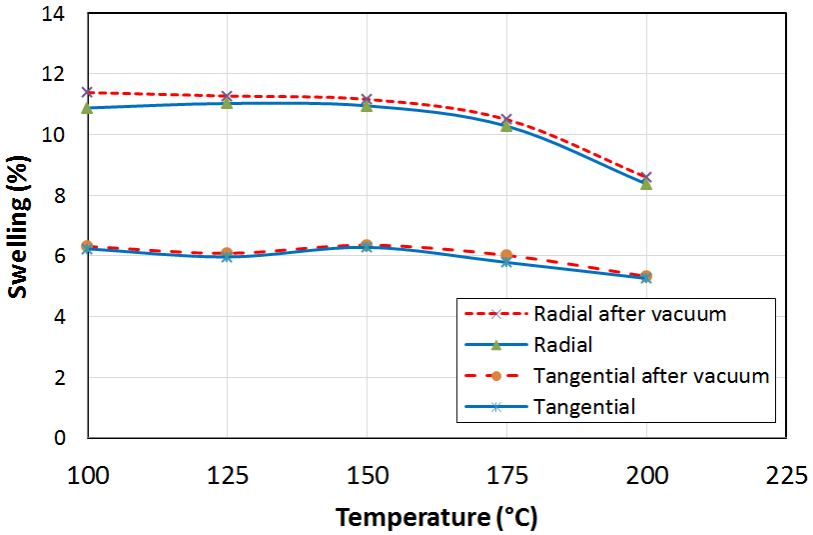

Figure 3.90 Dimensional changes due to water absorption up to saturation in radial and tangential directions for the specimens subjected to heat for 24 hours

3.10.3. Non-uniform shrinkage in tangential direction

Bamboo is a natural composite and a functionally graded material. The fiber distribution in radial direction gradually increases from the internal to external

side of bamboo as presented in Figure 2.4. Due to the different volume fraction of fibers at inner and outer parts of a bamboo transversal cross section, non-uniform shrinkage and swelling due to water absorption in tangential direction are investigated.

The specimens were placed into the oven at 70°C to dry for one week. After stabilization in the desiccator, the 6 dimensions in tangential direction (3 external and 3 internal) for each specimen are measured as shown in Figure 3.91a and Figure 3.91b. The specimens placed into the oven for 3 hours at temperatures from 100°C with the increase of 25°C up to 225°C. After stabilization in the desiccator, the same 6 dimensions in tangential direction for each specimen were measured. The result presented in Figure 3.92 shows the shrinkage in tangential direction at external and internal sides despite of different fiber volume fraction are close together. The specimen dimensions registered in the shrinkage test, are used for non-uniform water absorption tests. The specimens placed into distilled water for one month. The possible air trapped inside the samples were removed by means of a vacuum chamber. The process was repeated until full saturation of bamboo specimens and stabilization of the weight changes. Then, the swelling in tangential direction for three internal and three external points as can be seen in Figure 3.91 were registered.

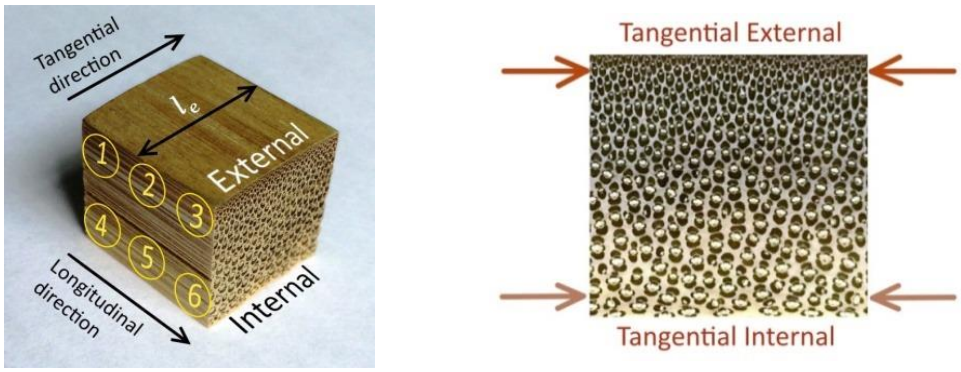

(a) (b)

Figure 3.91 Six measuring points in tangential direction from internal and external parts of a bamboo section

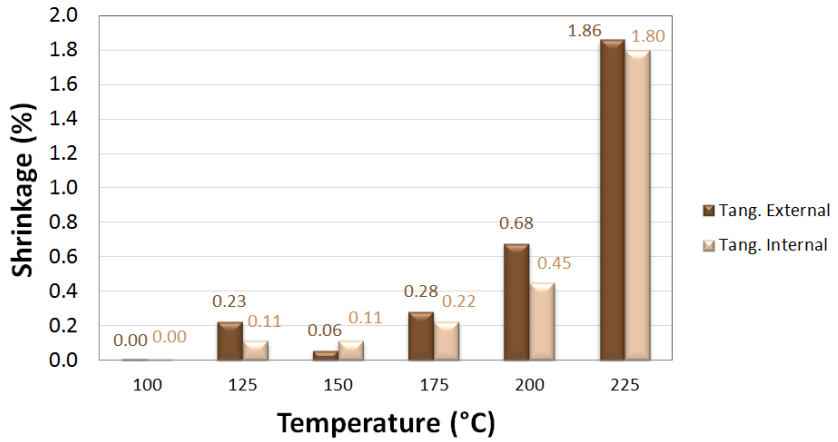

Figure 3.92 The external and internal part of bamboo shrinkage in tangential direction for the specimens subjected to heat for 3 hours

3.10.4. Non-uniform swelling in tangential direction

Based on the different fibers, matrix and veins volume fractions at internal and external sides of bamboo section as well as different swelling in tangential direction at these two sides, the contribution of fiber and matrix components, in water absorption can be measured separately.

Figure 3.93a shows a cross section of bamboo; Figure 3.93b shows the equivalent section in dry condition and Figure 3.93c the equivalent section after water saturation. Each length in tangential direction such as le is the summation of three different equivalent lengths of fiber ($l_{f,e}$), matrix ($l_{m,e}$) and vein ($l_{v,e}$). The first index shows the component such as fiber, matrix or vein and the second index indicates the internal or external part of bamboo.

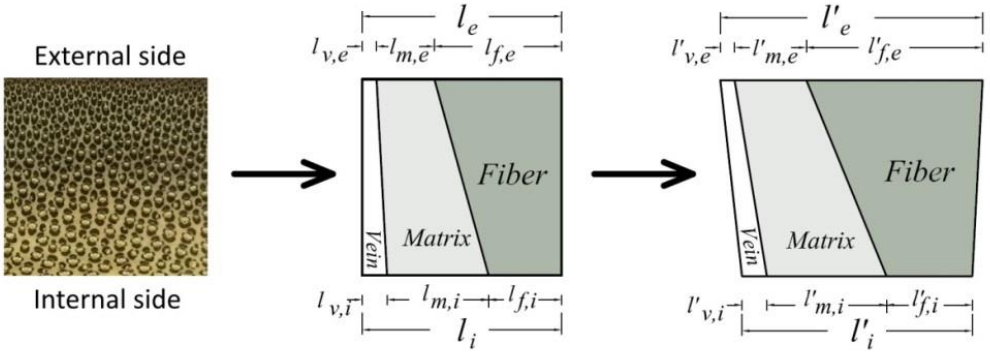

(a) Cross section (b) Dry equivalent section section (c) Saturated equivalent

Figure 3.93 Non-uniform swelling at internal and external sides

After water absorption and saturation, based on the volume fraction of each component at each side, the external and internal sides swelled at different rates.

Based on different values of fiber and matrix volume fraction at internal and external sides ($v_{f,e}$, $v_{f,i}$, $v_{m,e}$, $v_{m,i}$), two independent linear equations with two different variables k_f and k_m which respectively are the fiber and matrix water absorption coefficients will be achieved. The system of equations presented in Eq. 3.6.

$$\begin{cases} \varepsilon_e = \dfrac{l'_e - l_e}{l_e} = v_{f,e}(k_f - 1) + v_{m,e}(k_m - 1) \\ \varepsilon_i = \dfrac{l'_i - l_i}{l_i} = v_{f,i}(k_f - 1) + v_{m,i}(k_m - 1) \end{cases} \quad 3.6$$

The swelling of external and internal sides due to water absorption up to saturation in tangential direction (ε_e , ε_i), is presented in Figure 3.94. As can be seen in Figure 3.94 the swelling due to water absorption alongside the external side is always more than internal side. The results of studies carried out at image process section 3.5.3 are used for the volume fractions of fiber, matrix and vein at internal and external parts of bamboo section as presented in Table 3.16.

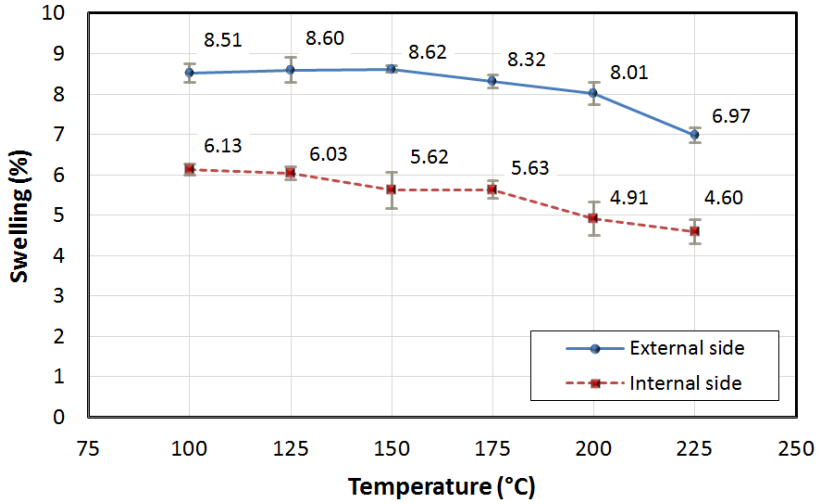

Figure 3.94 Swelling of external and internal sides in tangential direction due to water absorption

Table 3.16 Volume fraction of bamboo components at inner and outer parts of whole section

Component	External part (%)	Internal part (%)
Fiber (V_F)	56.1	30.7
Matrix (V_M)	42.2	62.9
Vein (V_V)	1.7	6.3

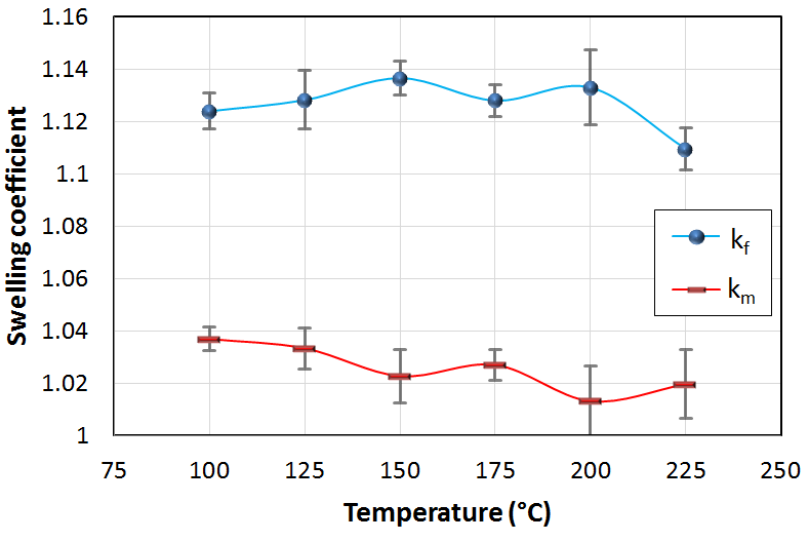

Figure 3.95 Fiber and matrix swelling coefficients

By using the system of equations mentioned in Eq. 3.6 and based on the values of external and internal sides swelling in tangential direction in Figure 3.94 and Table 3.16 for the amounts of volume fractions; the swelling coefficients for fiber and matrix at each temperature presented in Figure 3.95. Based on Figure 3.95, by water absorption up to saturation point for the sample heated at different temperatures for 3 hours, the fibers expand about 11% to 14% but the matrix expands by about 1.5% to 4%. It shows the fibers in average are about 5 times more sensible than the matrix with regards to water absorption up to the saturation point. Also the heat treatment up to 200°C has not any special effect on reducing the swelling but after 200°C up to 225°C it suddenly drops by 3%. For the matrix the changes starts gradually from 100°C and the swelling coefficient drops 2% within 100°C to 225°C and no sudden changes in the swelling coefficient can be observed.

3.11.Mechanical tests

3.11.1. Longitudinal Tensile test

Before to make decision about the sample shape for doing heat treated tensile test, the effect of sample shape and different ways to keep the sample between clamps is discussed in Appendix 5.7. Regarding to the result of the study, the samples considered the strips kept with doubled sandpapers located between the clamps and specimen.

3.11.1.1. Tensile test samples

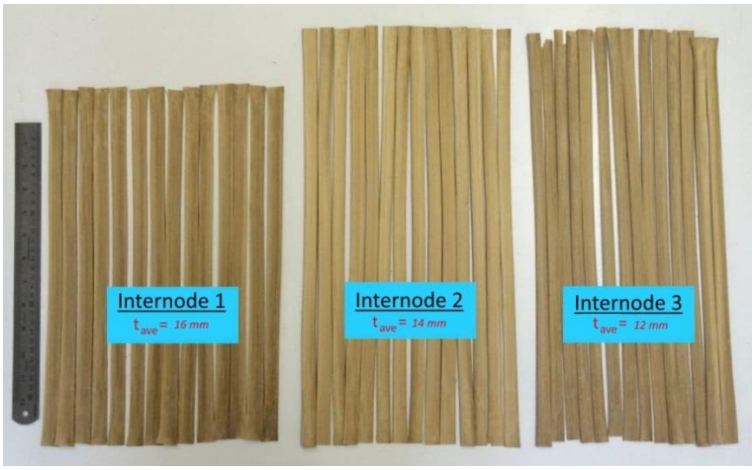

Figure 3.96 The tensile samples made from three different internodes

The tensile test samples are made from 3 different internodes as explained in Figure 3.69. Three internodes with different wall thickness are considered and from each internode 14 samples are prepared as can be seen in Figure 3.96. After cutting the end parts, all the sample lengths will be equal to 250 mm. After nomination with proper codes and before heat treatment program, they put in the oven with 70^{o}C for gradual drying.

3.11.1.2. Tensile test for non-treated bamboo samples

The result of tensile test for non-treated bamboo specimens stabilized at ambient temperature and humidity (26^{o}C and 70%RH) and MC% equal to 10.8% for three samples presented in Figure 3.97 and Table 3.17. The loading speed is

considered 0.01 mm/min [84]. All three samples are selected from one part of bamboo culm with about 13.00 mm to 13.50 mm thickness.

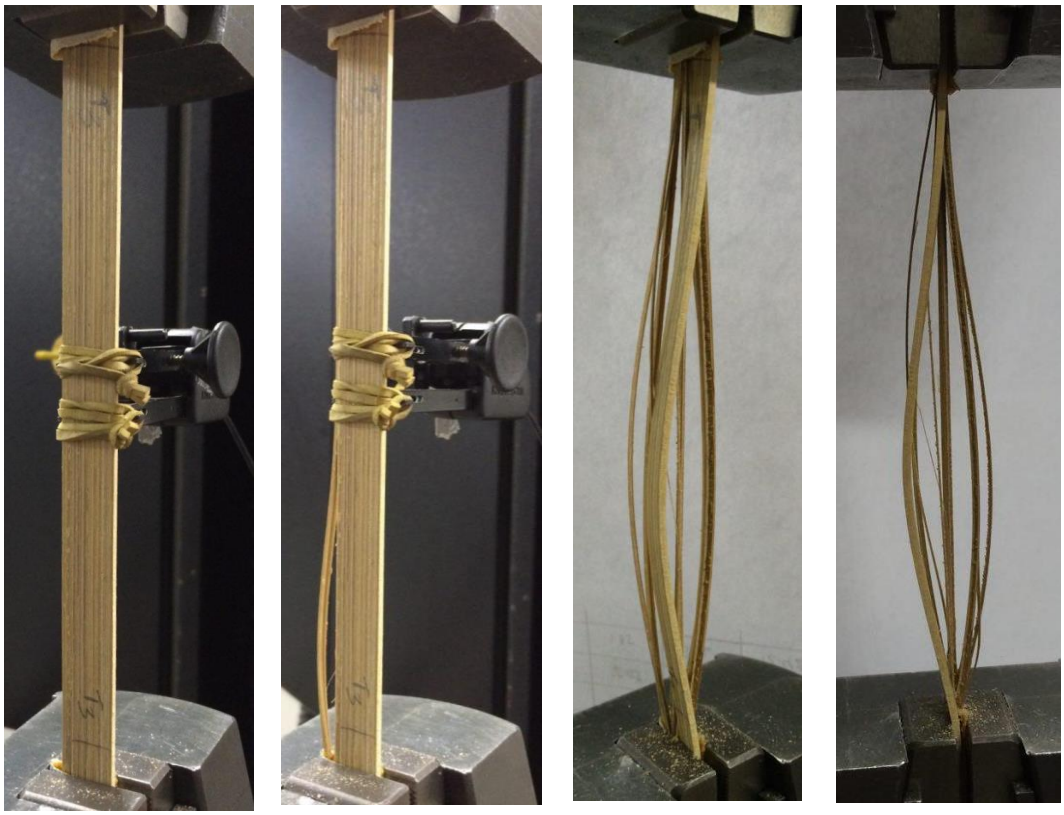

(a)before test (b) after test (c) after opening the clamps

Figure 3.97 Tensile test for not-treated sample at EMC condition

Table 3.17 The tensile test results for non-treated samples in ambient temperature.

sample	Dim (mm)	UTS (MPa)	Average (MPa)	CV (%)	E (GPa)	Average (MPa)	CV (%)
T1	250x13.50x2.48	241.7			22.42		
T2	250x13.43x2.03	230.7	243.0	5.4	21.61	21.91	2.0
T3	250x13.00x2.40	256.6			21.70		

UTS: ultimate tensile strength

The result of test shows the same pattern of failure for all three samples. At the start of failure heard the sound of the fibers pulling out inside the matrix and consequently the longitudinal cracks which occurred in the matrix. The sample after opening the clamps presented in Figure 3.97c.

3.11.1.3. Tensile test for heat treated specimens

There are two groups of samples, each of them treated inside the oven for 3 hours or 24 hours. The first group heated for 3 hours, has 7 sets of specimens started from not treated samples stabilized in ambient humidity and temperature to samples which have been heated up to 225°C. Due to rapid changes at high temperature, one more set in 200°C treated in 8 hours is tested and is presented in

Figure 3.98 with heat treated samples at 3 hours. The second group treated in 24 hours has 6 sets of specimens. Heat treatment at 225°C for 24 hours makes charcoal from bamboo set then it has been removed from the range of heat treatment as shown in Figure 3.99.

Figure 3.98 The tensile specimens heated for 3 hours in 6 different temperatures

Figure 3.99 The tensile specimens heated for 24 hours in 5 different temperatures

Figure 3.100 The untreated and heat treated samples after test, a) 25°C, b) 150°C-3h, c) 175°C-3h, d) 175°C-24h, e) 200°C-3h, f) 200°C-24h, g) 225°C-3h

Figure 3.100 shows the untreated and treated samples after tensile test. There is not any difference between failures patterns of samples treated up to 150°C-24h. Up to this temperature, the failure mode makes the sample like needles and most of fiber bundles separate in regular shapes from each other by breaking the matrix as presented in Figure 3.101a.

(a) 125°C-3h (b) 200°C-3h

Figure 3.101 Failure patterns in fiber bundles treated in two different temperatures

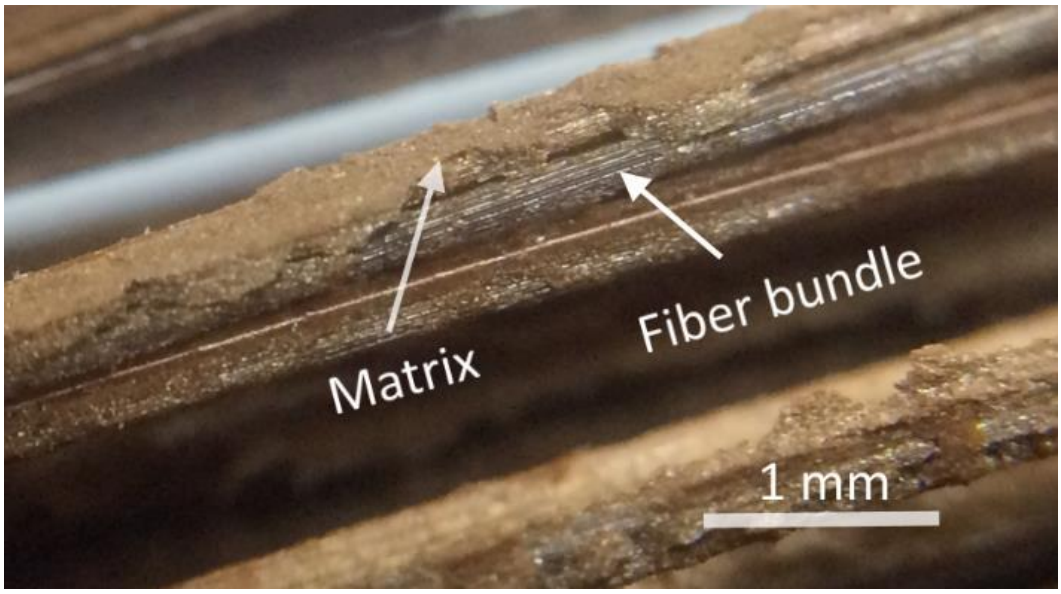

Figure 3.102 Loss of adhesion between fiber bundle and matrix

Heating more than 175°C-24h makes the matrix fragile, separate groups of fiber bundles with irregular matrix borders as can be seen in Figure 3.101b. For the samples treated at elevated temperatures the adhesion between fibers and matrix loses and makes an irregular surface as can be seen in Figure 3.102. Comparing the ultimate tensile resistance of not treated samples at dry condition and EMC conditions which are respectively equal to 250 and 248 MPa shows there are not any difference between them as can be seen in Figure 3.103. The tensile strength for the samples treated within 3 hours and 24 hours has been presented in Figure 3.104 and Figure 3.105.

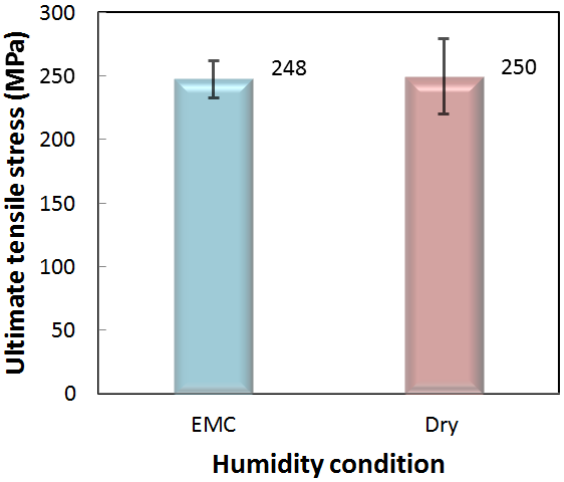

Figure 3.103 UTS for the untreated samples in EMC and dry conditions

The results presented in Figure 3.104 and Figure 3.105 shows the decrement in tensile resistance starts from 125°C for both group of samples treated in 3 and 24 hours. The two groups normalized to 100°C and presented in Figure 3.106.

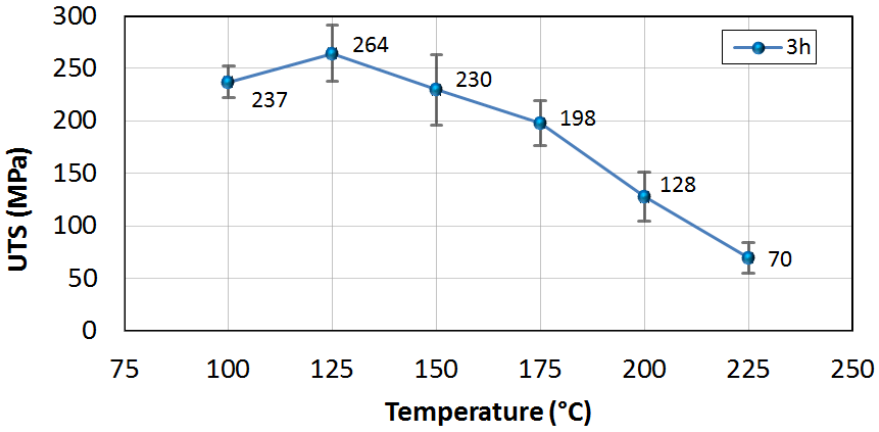

Figure 3.104 Ultimate tensile strength for the samples treated in 3 hours

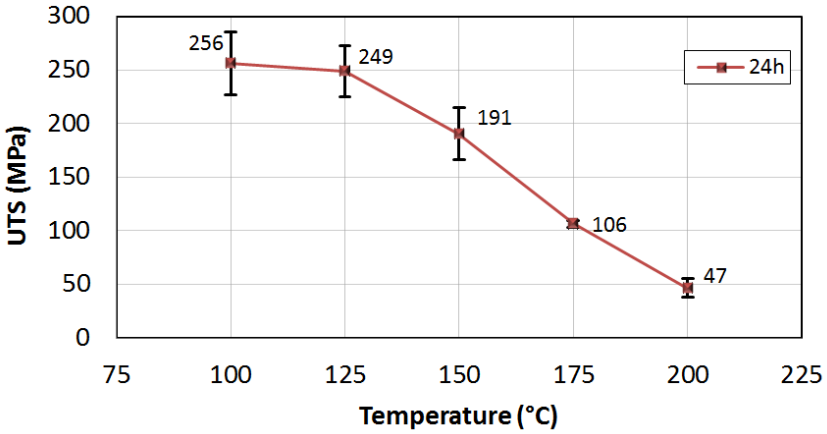

Figure 3.105 Ultimate tensile strength for the samples treated in 24 hours

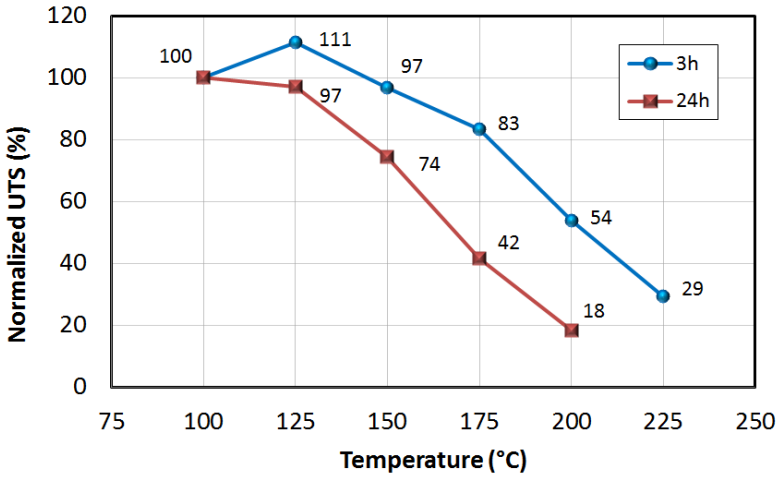

Figure 3.106 Normalized UTS changes with temperature for specimens treated for 3 and 24 hours

The effect of time exposure has been considered on three sets of samples which have been treated in 200°C for 3, 8 and 24 hours comparing with untreated samples as can be seen in Figure 3.107 and shows the effect of heat exposure at the initial hours of heat treatment is significant.

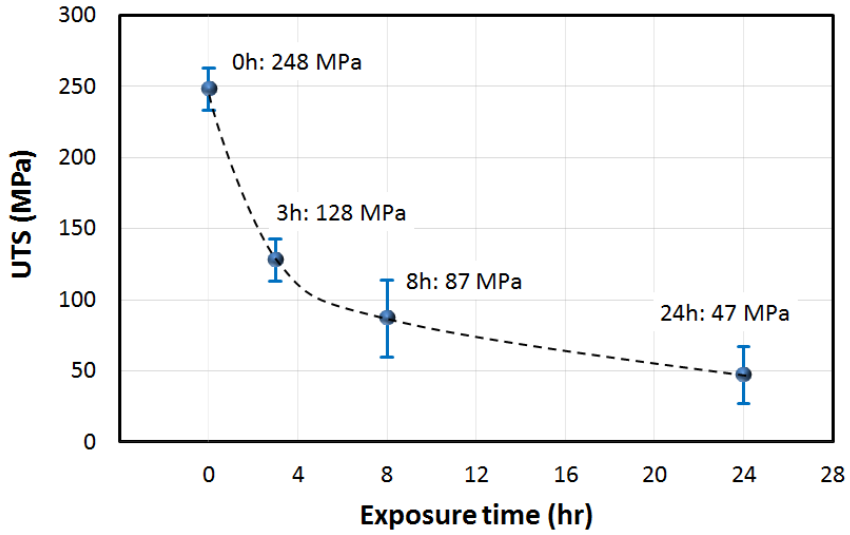

Figure 3.107 UTS for the untreated and treated samples in 200°C for 3, 8 and 24 hours

The normalized UTS presented in Figure 3.108 shows after 3 hours heat treatment, the UTS reduces about 48%. By more 5 hours heat exposure, the UTS reduces only about 17% and during the after 16 hours heat treatment, the UTS reduces nearly the same amount about 16%.

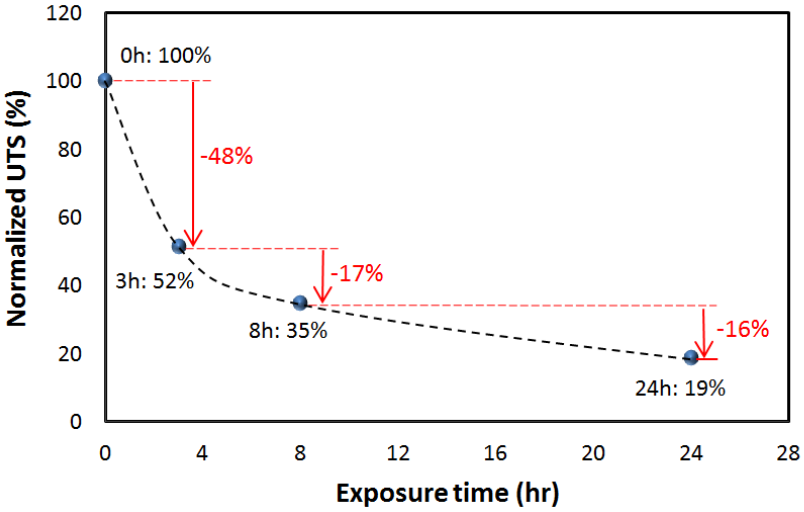

Figure 3.108 Normalized UTS for untreated and treated samples in 200°C for 3, 8 and 24 hours

The normalized UTS of three sets of samples treated in 200°C for 3, 8 and 24 hours is presented in Figure 3.109. The related graph normalized to samples treated in 200°C for 3. It shows a linear-logarithmic relation between exposure time and ultimate tensile strength.

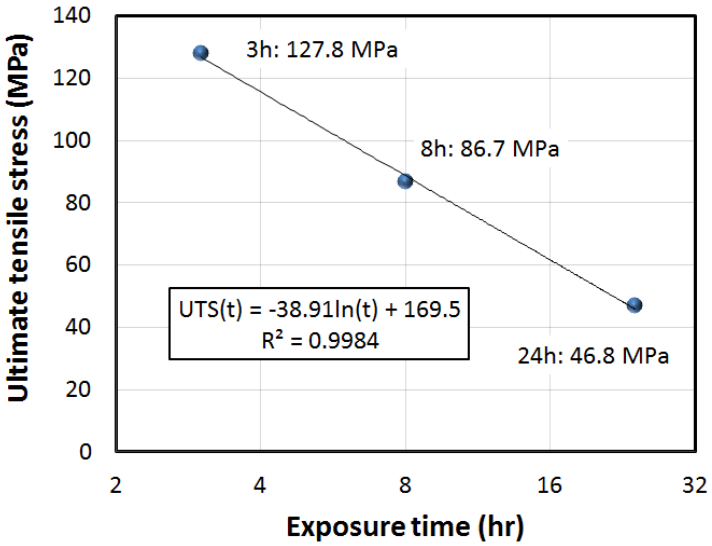

Figure 3.109 Normalized UTS for treated samples in 200°C for 3, 8 and 24 hours

By using a clip gauge for the longitudinal tensile test specimen and considering the middle range between 30% up to 70% of the stress-strain graph, the longitudinal tensile MOE for different heat treatments can be achieved. The changes in MOE for treated samples in 3 and 24 hours are presented in Figure 3.110 and Figure 3.111.

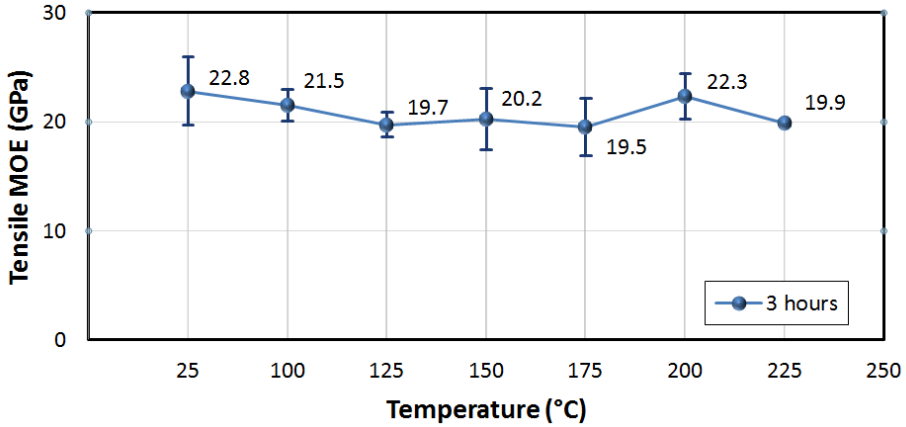

Figure 3.110 Longitudinal tensile MOE for the samples treated in different temperatures for 3 hours

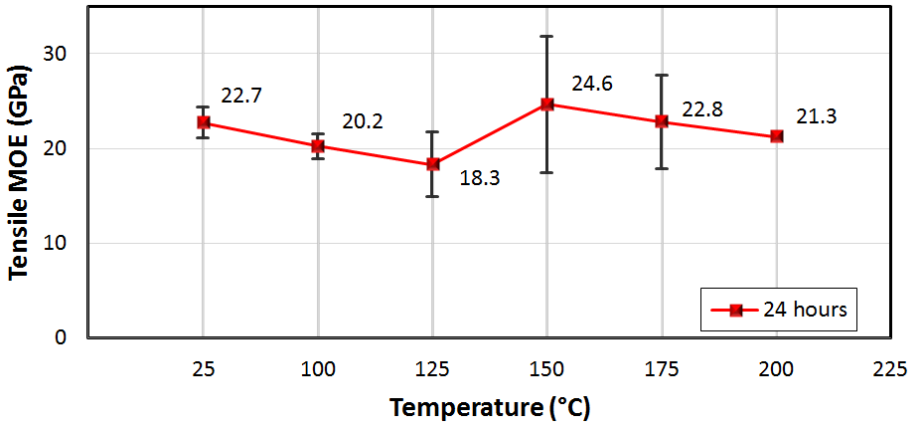

Figure 3.111 Longitudinal tensile MOE for the samples treated in different temperatures for 24 hours

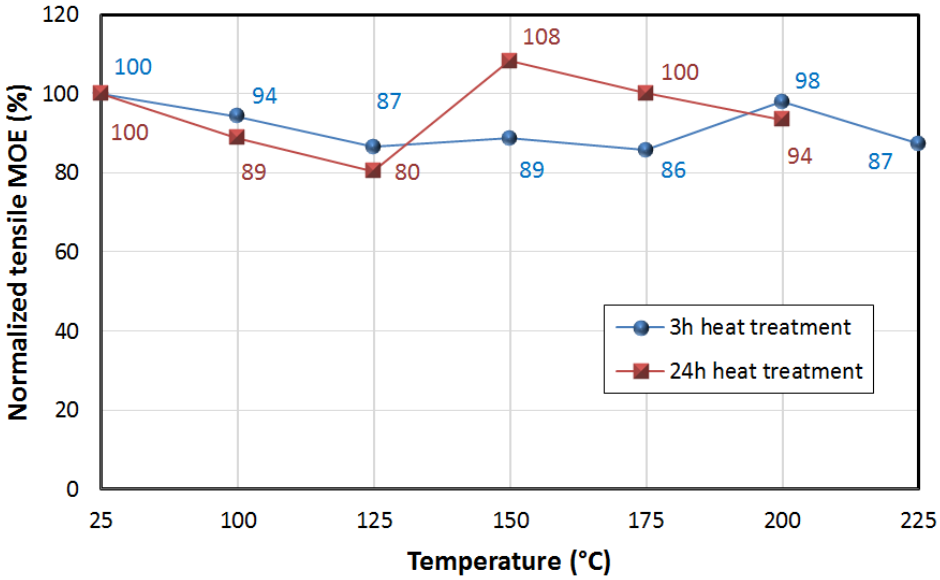

Figure 3.112 The normalized tensile MOE for the samples treated for 3 and 24 hours

The modulus of elasticity varies from 18.3 to 24.6 as can be seen in Figure 3.110 and Figure 3.111. The normalized MOE for both groups treated for 3

and 24 hours presented in Figure 3.112. It should be considered that the modulus of elasticity for each specimen is calculated at the range of its ultimate strength and it can justify the reason of relatively big values for the standard deviation at the temperatures more than 175°C for the samples treated during 24 hours. For both groups the modulus of elasticity decreases about 15% by heating up to 125°C then observed a sudden increment about 28% for the samples heated at 150°C for 24 hours after this temperature observed a decline in MOE about 14% up to 200°C. The fluctuation of the samples treated for 3 hours is less and no sudden changes is observed on successive heat treatments.

3.11.2. Transversal tensile stress test

Unlike wood, bamboo has no ray in radial or tangential directions, only the parenchyma is responsible for material tensile resistance in these directions [99][13]. In this section, the effect of heat treatment on transversal tensile stress (σ_t) of bamboo is investigated. The transversal tensile force is exerted in tangential direction as can be seen Figure 3.113. For this test, three blocks from three different internodes with different thickness will be prepared. The width of the samples is about 5 mm and from each block, 14 samples is provided as shown in Figure 3.114. Then a set will be provided by using 3 replicates from three different block. The replicate selection is the same as rule that mentioned in 3.9.1. Two Untreated set of specimens in dry and EMC condition, and treated samples heated from 100°C up to 225°C for 3h and 24h are used for the tests.

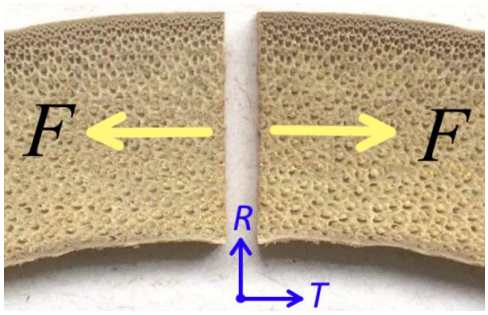

Figure 3.113 Transversal tensile forces applied in tangential direction

Due to low resistance of the samples to shear and bending forces, a special bi-functional clamp is fixed to the tensile test machine. This clamp which is suitable for small pieces of bamboo used to keep the samples (see appendix 5.2). This adjoined apparatus presented in Figure 3.115a can serve as a dual purpose

clamp and guarantees the uniform distribution of load by eliminating the shear and bending effects of the normal clamps which used in the tensile test machines. The images provided from the ruptured samples, show the fracture line passes only through parenchyma as can be seen in Figure 3.115b. This test only can measure the tensile strength of the parenchyma.

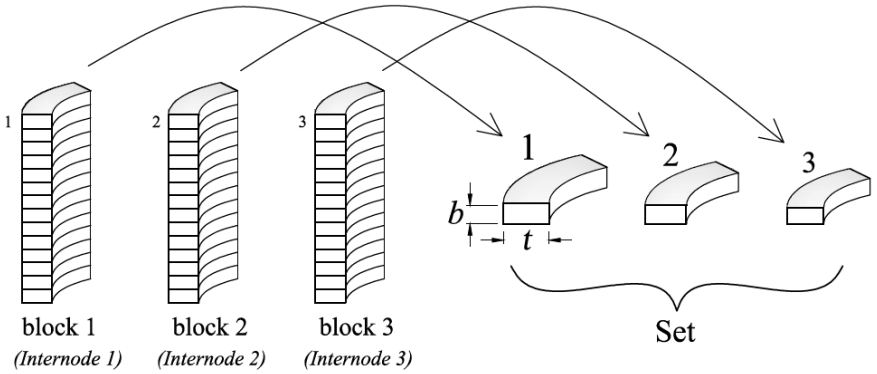

Figure 3.114 Sample selection with 3 blocks from different parts of culm

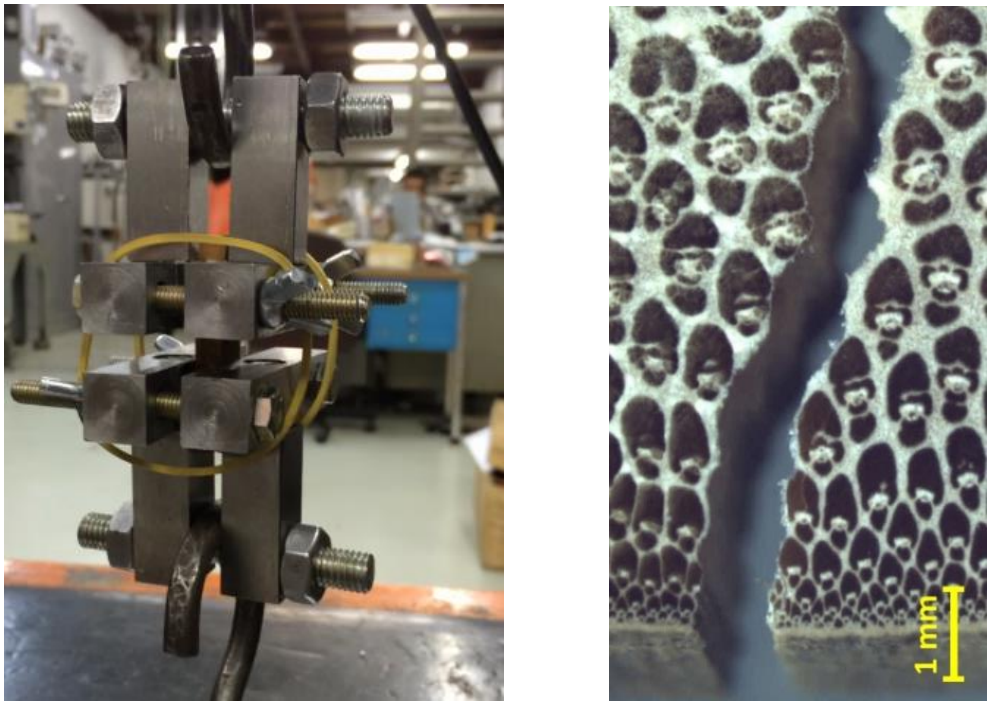

(a) Adjoined clamp (b) Fracture line after test

Figure 3.115 Adjoined clamp with ruptured test specimen

Nine samples from three different blocks with different thickness at EMC condition tested to establish the dependency between results and bamboo wall thickness. The dimensions with the ultimate transversal tensile resistance are presented in Table 5.9 in Appendix 5.9. Comparing the critical value (F_{cr}=5.14) with F value (3.67) in the ANOVA test shows there is not a meaningful difference

between the transversal tensile strength of the samples in blocks with different thickness.

3.11.2.1. Heat treated tests

The same as longitudinal tensile test there are two groups of samples, each of them treated inside the oven for 3 hours or 24 hours. Also there are two sets of non-treated bamboo at ambient temperature (25°C) one untreated set at EMC condition and the other untreated set dried for one week in 70°C. The first group heated for 3 hours, has 6 sets of specimens started from 100°C heated up to 225°C then stabilized in ambient humidity and temperature to do the test in EMC condition and the second group treated for 24 hours with 5 sets of specimens heated from 100°C up to 200°C. The transversal tensile samples with the compression samples presented in Figure 3.116.

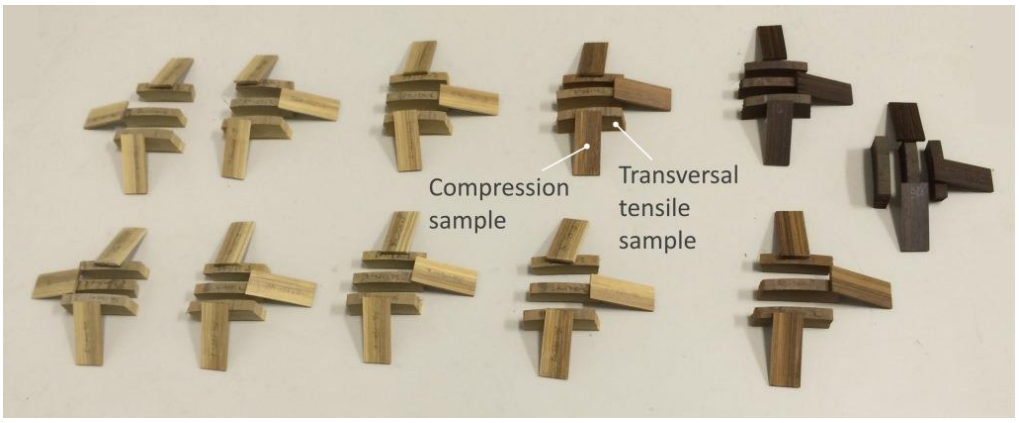

Figure 3.116 the heat treated Compression and transversal tensile samples

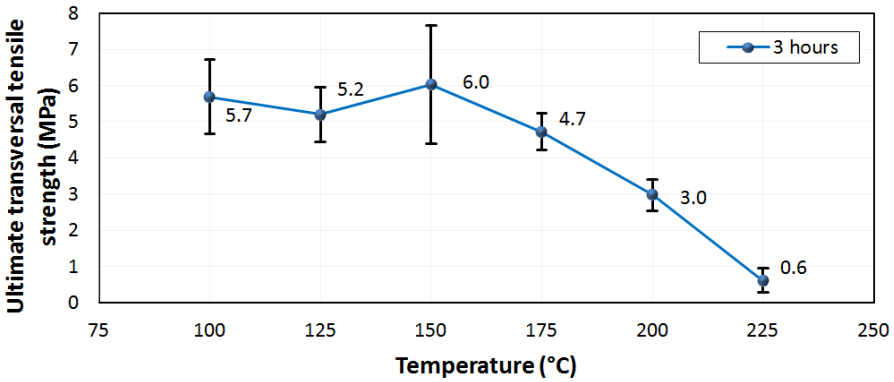

Figure 3.117 Ultimate transversal tensile strength for samples treated within 3 hours

The ultimate transversal tensile strength for samples treated for 3 and 24 hours are presented in Figure 3.117 and Figure 3.118 and shows a decrement up to about 125°C for both groups of samples. The resistance increases up to 150°C and after 150°C for both groups observes linear strength decreasing up to 200°C for

the samples treated during 24 hours, and 225°C for the samples heated for 3 hours as can be seen in Figure 3.117 and Figure 3.118.

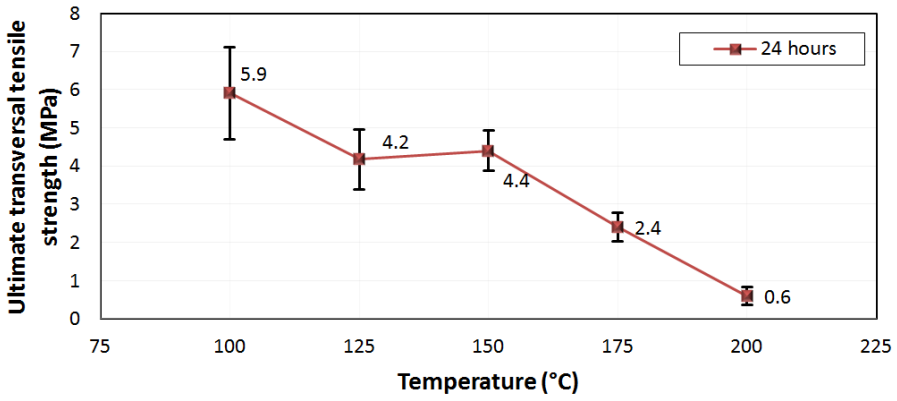

Figure 3.118 Ultimate transversal tensile strength for samples treated within 24 hours

The normalized ultimate transversal strength of the samples treated for 3 and 24 hours is presented in Figure 3.119. This graph shows that the effect of time exposure for the samples treated at different times is remarkable. The long term heat exposure during 24 hours at 125°C causes about 30% decrement in resistance but for the same temperature the samples treated for 3 hours only decrease 9%.

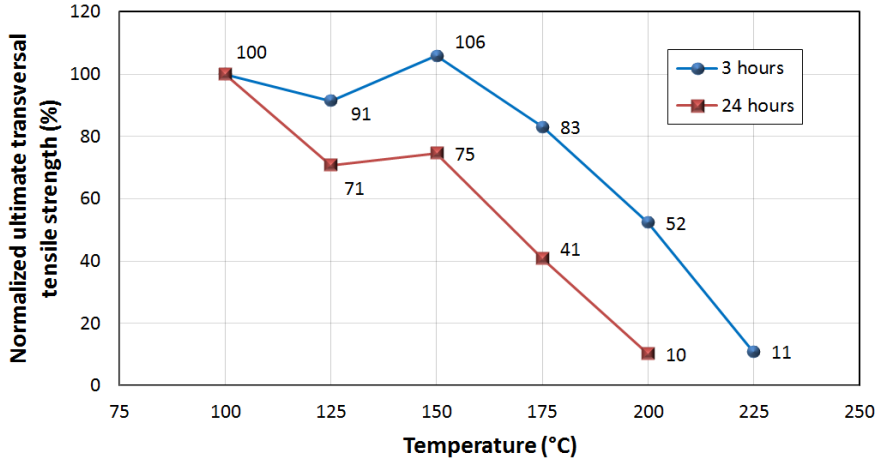

Figure 3.119 Normalized ultimate transversal tensile strength for samples treated for 3 and 24 hours

The heat exposure at 150°C can reduce the ultimate strength about 25% for samples treated for 24 hours but the samples treated within 3 hours the ultimate resistance increases about 6% with respect to samples treated in 100°C as can be observed in normalized graph in Figure 3.119. It proves that the mechanical resistance of parenchyma or matrix is more sensible to heat treatment time duration than the fibers. For detail of each test as well as average and standard deviation see appendix 5.9. Statistically, there is not meaningful difference between the transversal tensile test result for two groups of untreated samples in

dry and EMC condition presented in Figure 3.120. As can be seen in EMC condition the resistance is about 30% more than the dry condition.

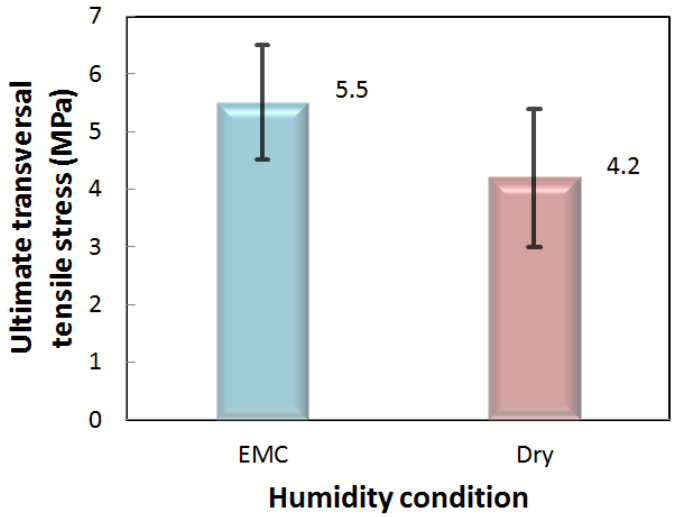

Figure 3.120 Ultimate transversal tensile strength for the untreated samples in EMC and dry conditions

3.11.3.Compression test

The fixture for the compression test according to ASTM D3410 [100] presented in Figure 3.121. But instead, a part of bi-functional apparatus which has been explained in detail at 5.2 can serve for this purpose. By removing the tensile pads the remained part is used for keeping the sample. The sample dimension and the location of the sample fixed by the clamps between the plates of Instron machine is shown in Figure 3.122. The length of specimen is equal to 4 cm and the thickness of specimen in tangential direction is equal to 2mm.

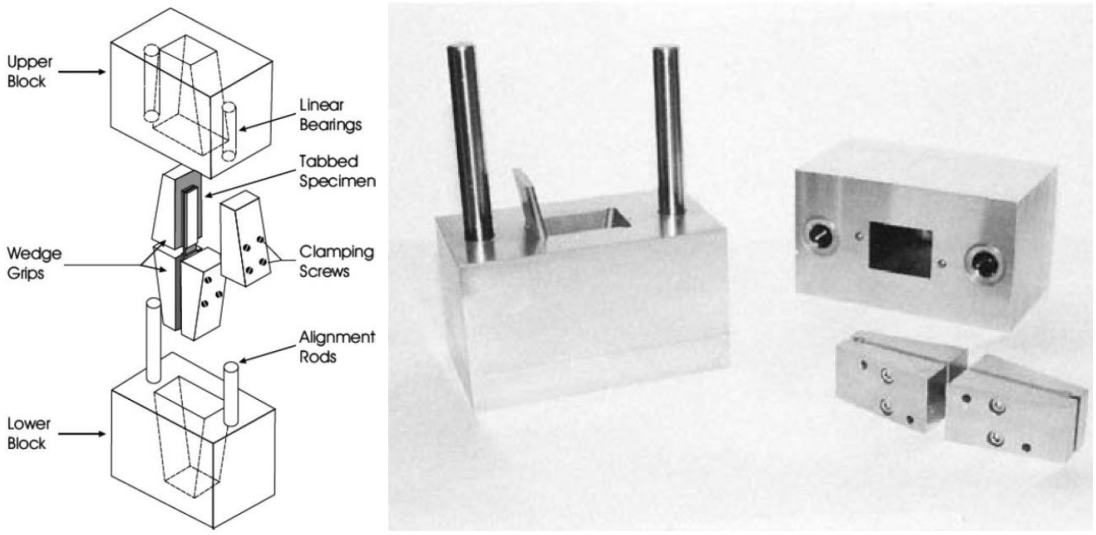

Figure 3.121 Compression Test Fixture [100][101]

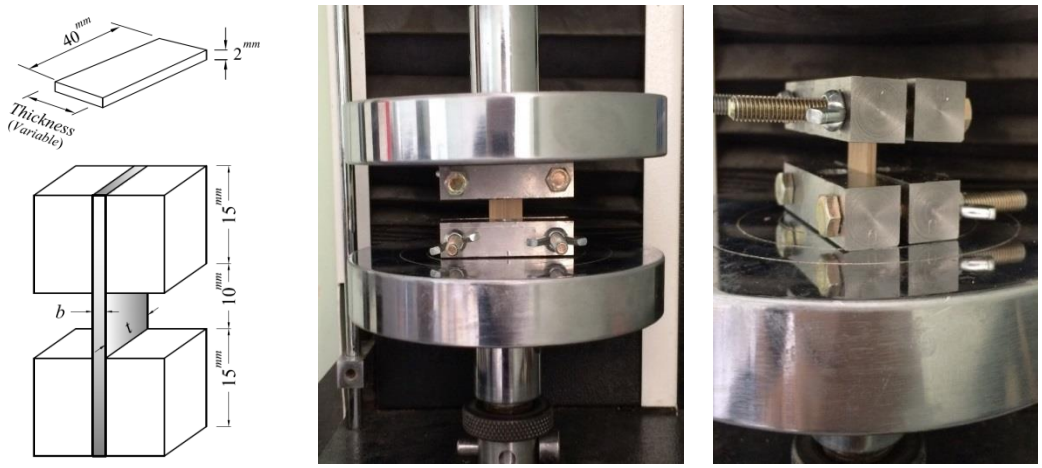

Figure 3.122 compression test sample

3.11.3.1. Sample preparation

Due to the small length of sample (40 mm), the compression test samples can be prepared from only one internode. The laminates are made the same as tensile test samples as can be seen in Figure 3.123 and after they cut to small pieces with 40 mm length. Before testing the treated samples, the preliminary tests were implemented in order to get knowledge about the behavior of the apparatus. The dried samples in the normal ambient temperature have been tested in EMC condition. Before starting the compression tests with different test machines, buckling analysis and different failure modes of samples in compression will be discussed.

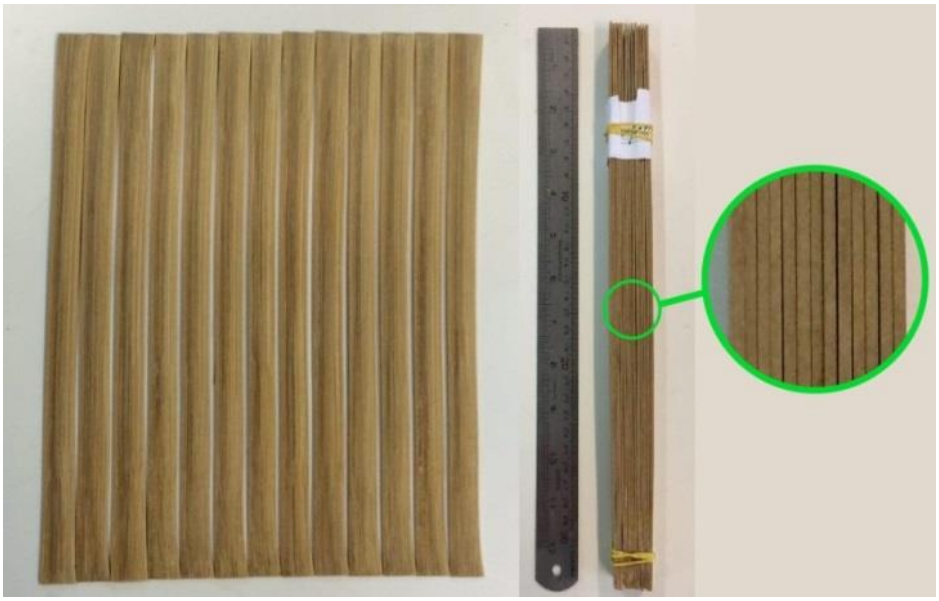

Figure 3.123 prepared compression laminates before cutting to samples

3.11.3.2. Buckling analysis

By using the results obtained by Krause [102] the modulus of elasticity in compression for the base, middle and top part of a *DG* bamboo are respectively 2.19, 3.73 and 4.43 GPa. Based on the minimum value of modulus of elasticity and using 2 mm thickness as minimum thickness (r = 0.58 mm) and considering 10 mm as effective length, the critical stress can be obtained by the equation 3.7.

$$\sigma_{cr} = \frac{E.\pi^2}{(kL/r)^2} = \frac{2.19 \times 10^3 \times \pi^2}{(1 \times 10/0.58)^2} = 73\ MPa \qquad 3.7$$

The value of k is considered one as the worst case due to the probable movement of the support clamps [103]. This result comparing with the preliminary compression tests shows that the rupture for all samples in both groups happens before reaching to the critical stress value or before buckling.

3.11.3.3. Different modes of failure

ASTM D143 defines 6 different types of failure for the wooden samples; crushing, wedge split, shearing, splitting, compression and shearing parallel to grains, and end-rolling. For the bamboo laminates parallel to fibers based on the implemented test there are two modes of failure presented in Figure 3.124. For the first mode (a) shown in Figure 3.124, the supports able to have horizontal movements relative to each other, makes two maximum bending points close to the supports.

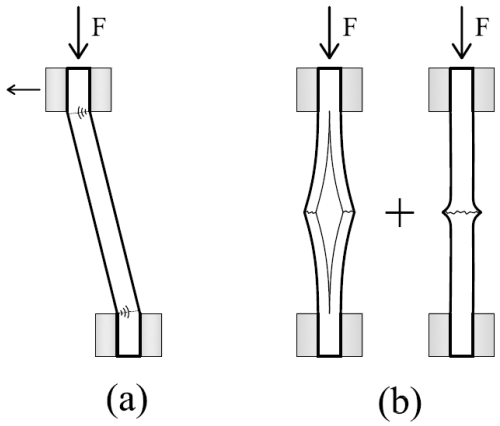

Figure 3.124 different modes of bamboo failure in compression test, a) bending failure; b) local buckling failure

(a) Bending failure (b) Ruptured sample

Figure 3.125 The first mode of failure in MTS machine

(a) Local buckling failure (b) Ruptured sample

Figure 3.126 The second mode of failure in MTS machine

The failure starts in these two points at different sides of sample, close to the clamps as shown in Figure 3.125. This type of rupture is named bending failure. The second mode (b) presented in Figure 3.124 will happen when the clamps are not free to move in horizontal direction. Figure 3.126 shows the local buckling of fibers inside the matrix which sometimes it comes with longitudinal tearing in parenchyma. The local buckling of fibers inside the matrix can occur anywhere along the column between lower to upper clamp. The effect of test machine on the compression results is discussed in Appendix 5.10.

Figure 3.127 different shapes of fiber buckling for not treated samples

Some different shapes of local buckling for not treated samples presented in Figure 3.127. The buckling of fibers can occur in the radial or tangential plane.

3.11.3.4. Compression test for heat treated specimens

There is significant difference between the compression test result for two groups of untreated samples in dry and EMC condition presented in Figure 3.128. As can be seen in dry condition the compression is about 2.5 times more than EMC condition. This enormous difference can be justified due to buckling of the fibers inside the matrix.

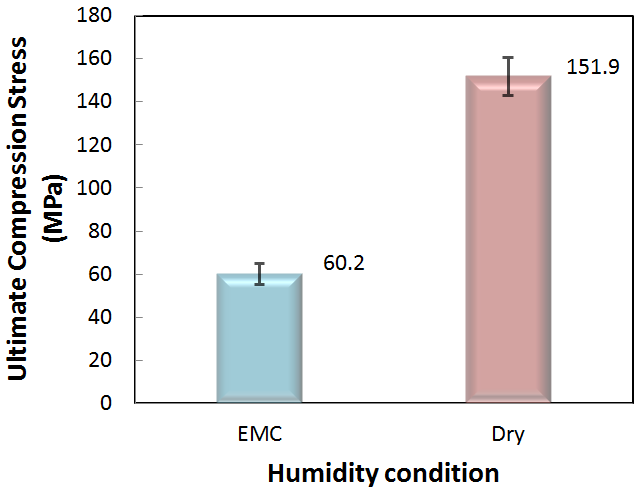

Figure 3.128 Ultimate compression strength for the untreated samples in EMC and dry conditions

The fiber represents the limiting case of the beam on an elastic foundation for $EI \rightarrow 0$ [103]. In this situation, the critical compression load is directly related to the MOE of matrix. The Rosen model for compressive buckling [104] of microfibers proposes two equations [105] for shear and extensional modes presented in Figure 3.129.

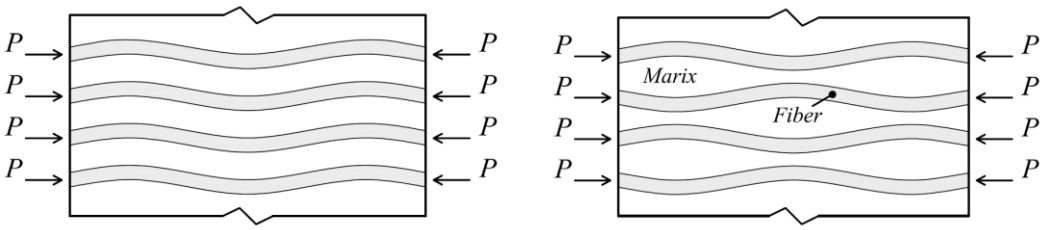

(a) shear mode (b) Extensional mode

Figure 3.129 The buckling modes of fibers in compressive load [105]

$$\sigma_{cr} = \frac{G_m}{1 - V_f} \qquad (For\ shear\ mode) \tag{3.8}$$

$$\sigma_{cr} = 2V_f \sqrt{\left[\frac{V_f E_m E_f}{3(1 - V_f)}\right]} \qquad (For\ extensional\ mode) \tag{3.9}$$

In both equations 3.8 and 3.9, it can be observed that the critical stress is related directly to MOE and shear modulus of matrix. Then, the effect of humidity can change the MOE and shear modulus of matrix. This analysis should be investigated in a separate research.

The result of heat treatments on ultimate compression strength is presented in Figure 3.130 and Figure 3.131. The result of heat treatment for 3 hours shows a decrement about 12% in 125°C and increment after 175°C up to 225°C as can be seen in Figure 3.132. But for the samples treated for 24 hours, a linear increment in resistance up to 175°C is observed. The ultimate compression resistance in 175°C is about 36% more than the samples treated at 100°C. For the compressive samples, the time duration of heat treatment has an important effect on increasing the compressive resistance.

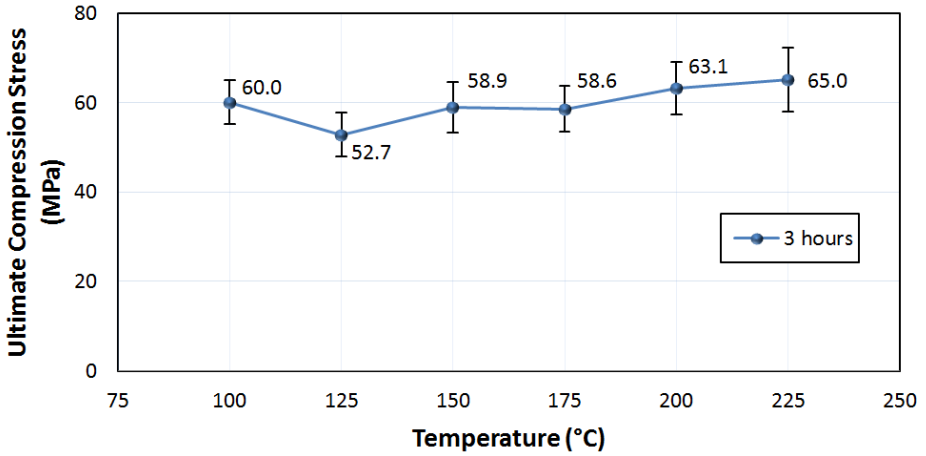

Figure 3.130 Ultimate compression strength for the samples treated in 3 hours

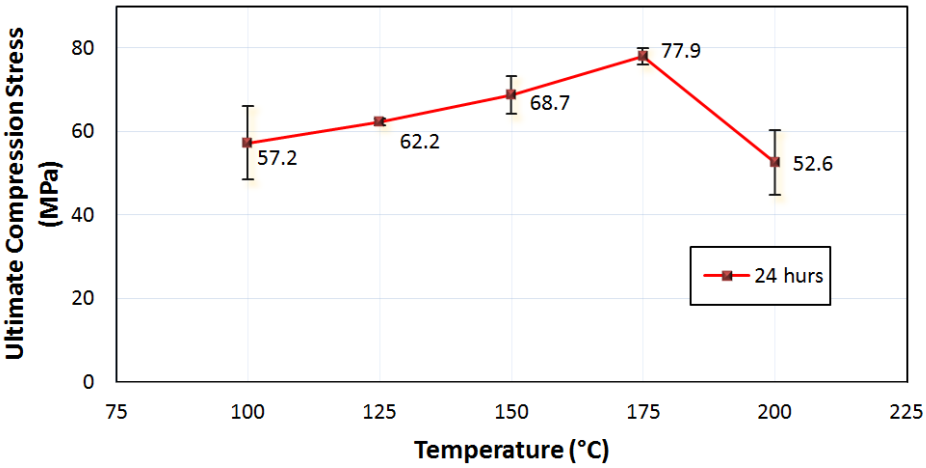

Figure 3.131 Ultimate compression strength for the samples treated in 24 hours

For the tensile test specimens, the results of heat treated samples shows a decrement in ultimate tensile strength for both groups heated for 3 and 24 hours

after 150°C which is related to fiber resistance decrement. For the compression test, the increment of MOE of matrix by heat treatment can justify the increment of critical buckling compression of the fibers.

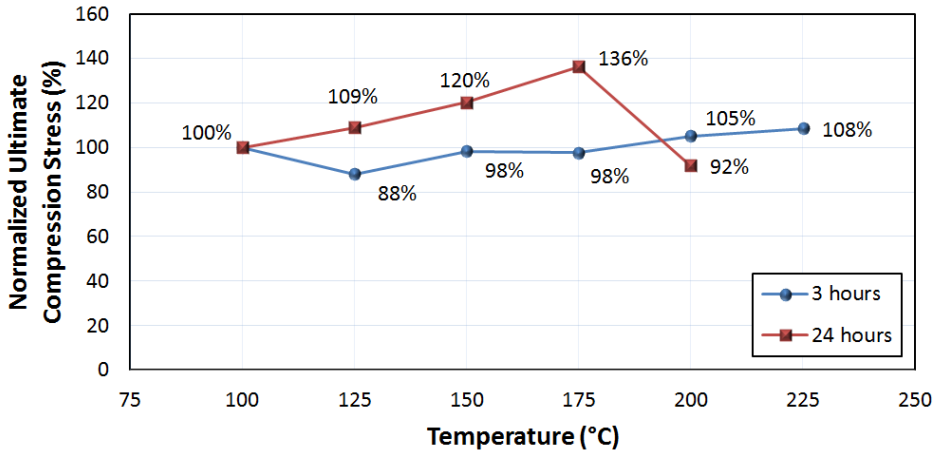

Figure 3.132 Normalized Ultimate compression strength for specimens treated for 3 and 24 hours

For the samples treated up to 150°C-24h or 175°C-3h, the soft buckling occurs which means the groups of fibers bend and buckle inside the matrix without breaking. The soft buckling occurs for the samples treated at 100°C-3h as can be seen in Figure 3.133a. The fragile buckling happens for higher treatment temperatures more than 150°C-24h or 175°C-3h and the fibers break before buckling under the compression loading. An example of fragile buckling for a sample treated at 175°C-24h is presented in Figure 3.133b. The broken fibers due to fragile buckling for the samples treated at 225°C-3h illustrated at Figure 3.133c.

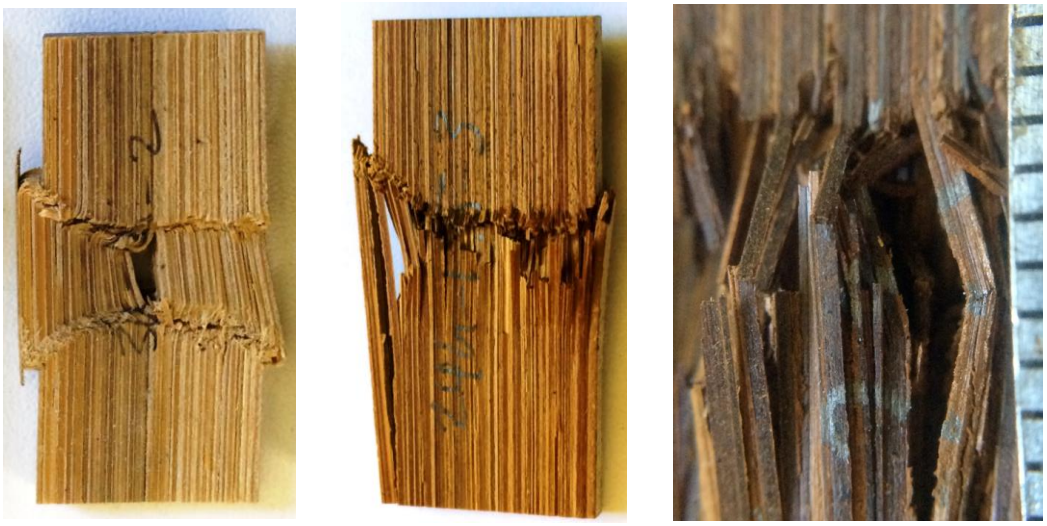

(a) Treated at 100°C-3h (b) Treated at 175°C-24h (c) Treated at 225°C-3h

Figure 3.133 The soft and fragile buckling of the samples treated in different temperatures

Figure 3.134a shows the soft buckling and as can be seen the fibers buckle inside the matrix close to the lower support and a single buckled fiber in Figure 3.134a shows the flexibility of the sclerenchyma. Figure 3.134b shows fragile buckling of specimens during the compression loading. The broken fibers can be observed in Figure 3.134c.

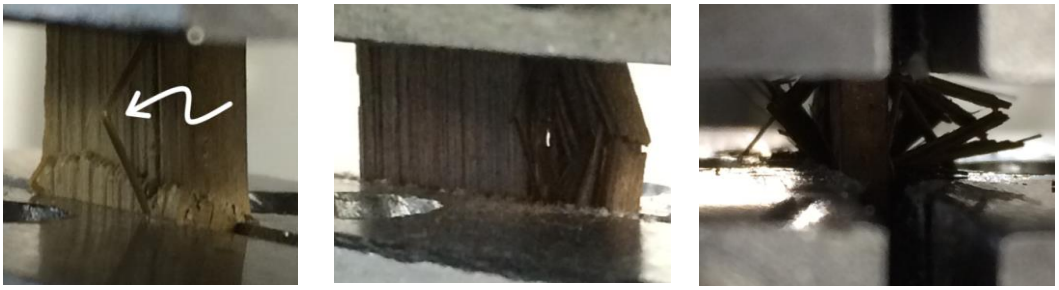

(a) soft buckling failure (b) fragile buckling failure

Figure 3.134 Specimen after different types of buckling

3.11.4. Shear test

There are different methods for testing the shear resistance of a material alongside the grain or fibers. The method proposed by ASTM D143 [106] is a direct shear test with two opposite eccentrically loads which are exerted at the top and bottom of sample as can be seen in Figure 3.135a and b. The thickness and diameter of bamboo is not appropriate to make the standard specimens with the dimensions presented in Figure 3.135c.

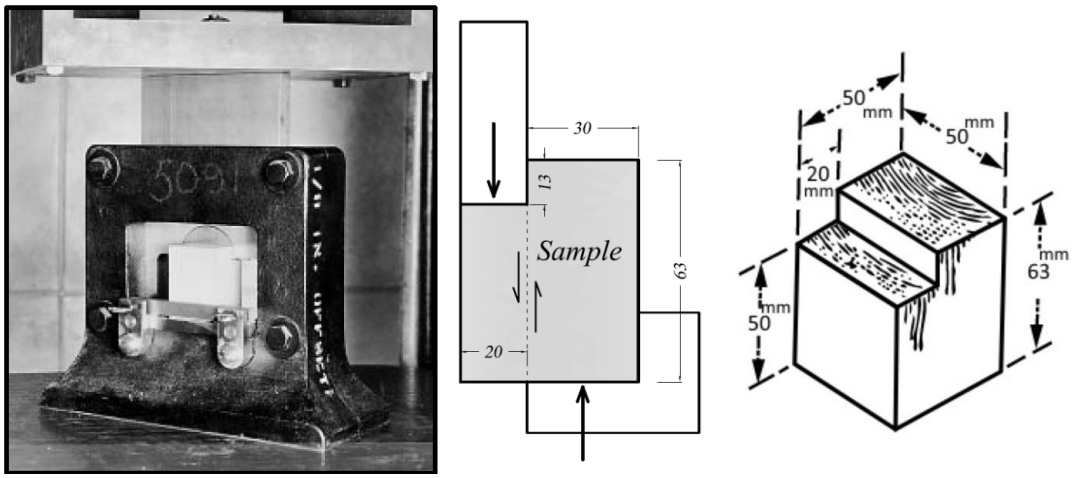

(a) Apparatus (b) shear test diagram (c) sample dimensions

Figure 3.135 The shear fixture and diagram used for ASTM D143 [106]

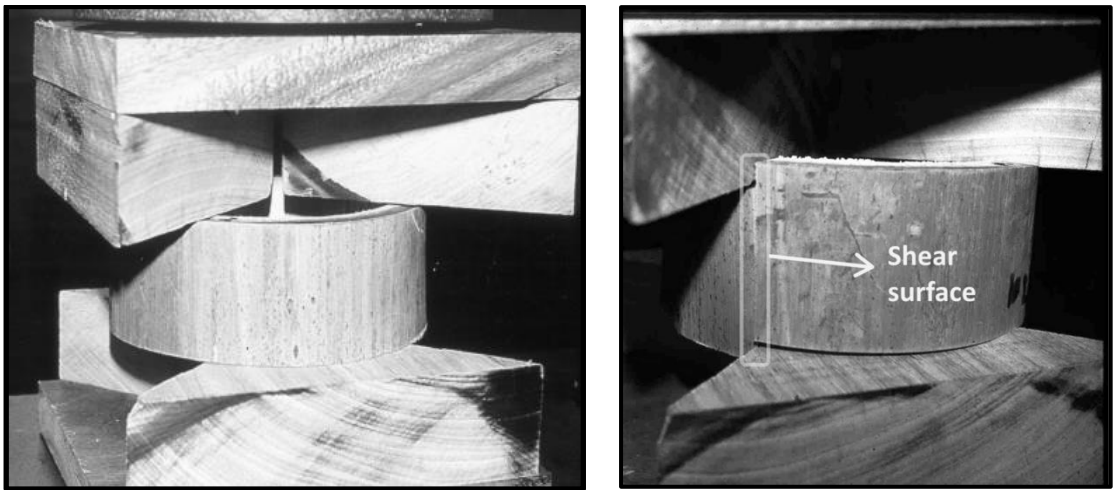

Figure 3.136 The method for shear test based on ISO 22157 before and after test [84]

The proposed equipment for shear fixture in ISO 22157-1 [84] can be used only for cylindrical pieces of bamboo culm. Two supports in opposite direction at top and bottom create four shear surfaces and the same as ASTM D143 the loads are exerted in both sides of the sample as can be seen in Figure 3.136. The two cut faces of the annular shape sample prepared for this method should be finished parallel. This method is not practical for the bamboo with big diameter such as *DG* bamboo.

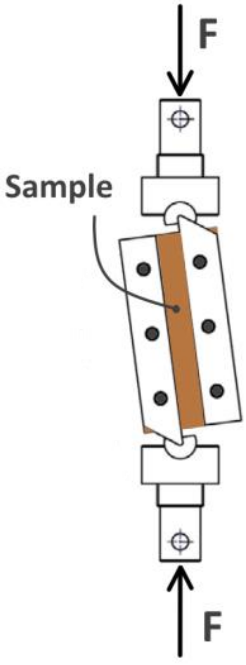

Figure 3.137 The method for shear test based on ASTM D4255 [107]

The method proposed by ASTM D4255 [107] needs a special clamps for distribution two opposite eccentrically loads alongside the shear surface as can be seen in Figure 3.137. This method can be applied for composites or woods to

measure the shear parallel to fibers or grains. The limitation of this method for applying to bamboo is making the proper shape and size of samples. The plate shape samples are more appropriate to use for this method.

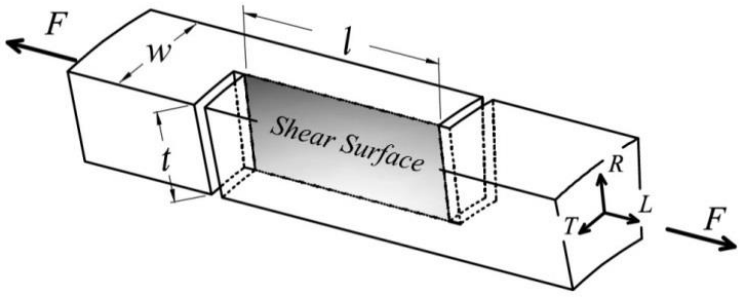

Figure 3.138 3D presenting the shear surface perpendicular to tangential direction

A simple practical method to measure the shear alongside the fibers is proposed by Ghavami [108]. The samples are the bamboo strips with two notches up to half way of thickness in two opposite sides. As the notches cut the sample in tangential directions, the shear surface is perpendicular to the tangential normal vector as shown in Figure 3.138. The average ultimate shear strength of bamboo is calculated theoretically by a simple formula which is presented in Eq. 3.10.

$$\bar{\tau}_{ult} = \frac{F}{l \times t} \qquad 3.10$$

The parameters of Eq. 3.10 are shown in Figure 3.138. The distance between two notches (l) is a determinative parameter and has been discussed in present thesis as preliminary test. Also the effect of tensile and compression loading on ultimate shear strength has been investigated. The relation between internal and external forces and tensions in the rigid body of longitudinal shear test specimen has been discussed in Appendix 5.11

3.11.4.1. Longitudinal Shear with Tensile load (LST test)

In this case, the effect of applying a tensile force on ultimate shear strength and crack initiation and propagation is investigated. Practically, as the sample is not a rigid body, exerting the tensile force creates deformation in sample which can be seen in Figure 3.139a. The clamps of the equipment are not fix, then by exerting the load they align and dislocate themselves with the deformation of the sample as can be seen in Figure 3.139b. The top clamp in Figure 3.139b can rotate and moved in horizontal plane around the hinge support.

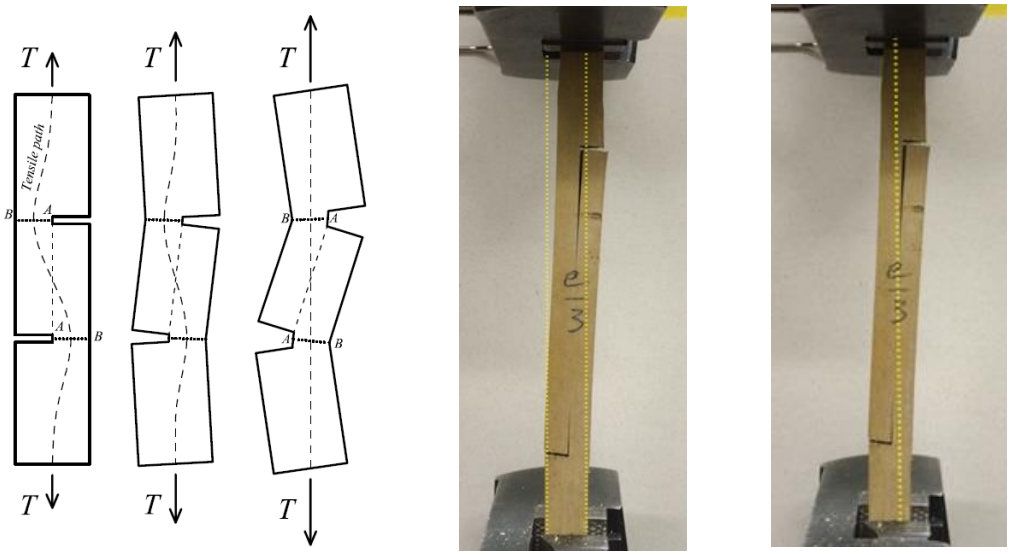

(a) (b)

Figure 3.139 a) gradual sample deformation; b) top clamp dislocation due to sample deformation

The moment in face AB with a tensile stress in vertical direction at point A together can create a longitudinal crack at the point A [109]. Creation this crack from point A and developing alongside the shear surface changes the failure mechanism by reducing the shear surface area as can be seen in Figure 3.140.

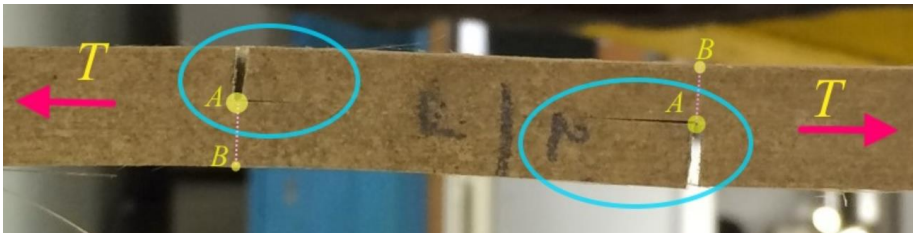

Figure 3.140 longitudinal crack initiation and propagation

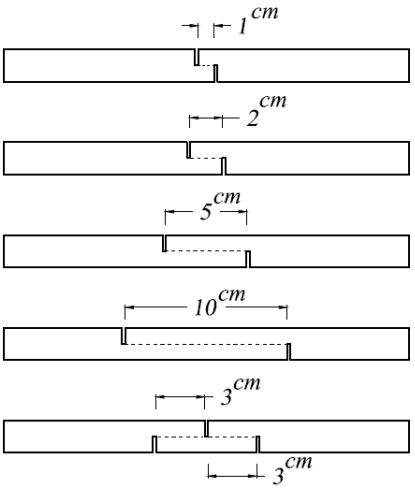

Figure 3.141 five different longitudinal shear samples

To establish the influence of the notch distance 15 test with different distances from 1 cm to 10 cm. For comparison one set of test with three notches is

used as shown in Figure 3.141. The longitudinal shear samples after failure by applying tensile force can be seen in Figure 3.142.

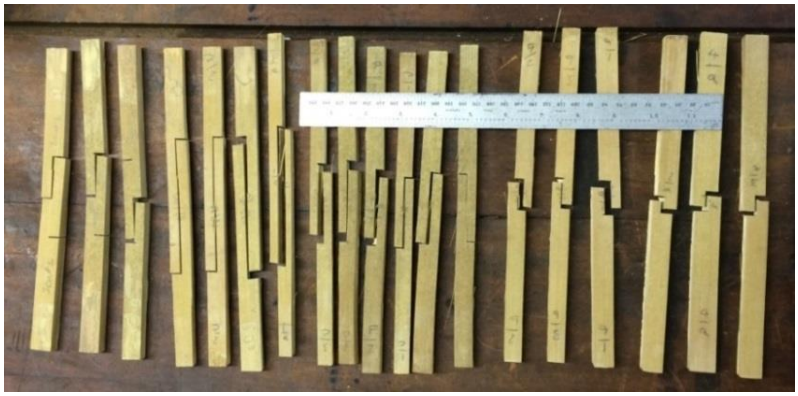

Figure 3.142 the longitudinal shear samples after failure by applying tensile force

By increasing distance between the notches, the ultimate shear resistance is reduced as shown in the Figure 3.143 (for test details see Appendix 5.11.3). The result for samples with only two notches is shown in Figure 3.144.

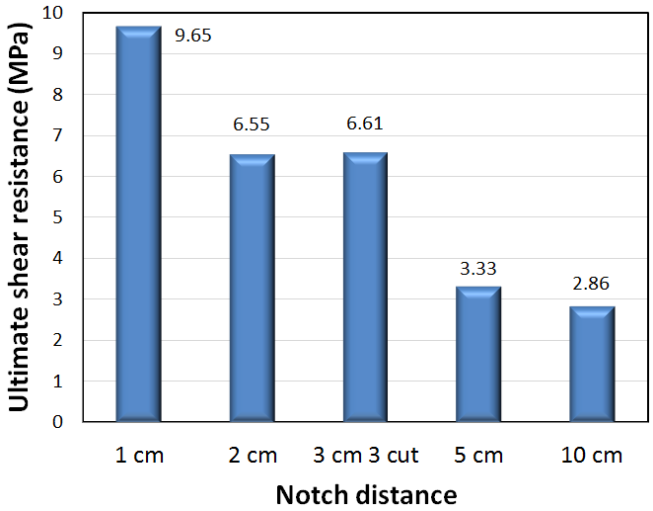

Figure 3.143 Ultimate shear resistance by applying tensile force for 5 group of samples with different vertical cut distances

Figure 3.144 shows the bigger notch distance results lower ultimate shear tension. It means the distribution of shear tension at the shear surface is not uniform and the effect of length between two notches is determinative. The effect of applying compression force on ultimate shear stress of 12 samples with 4 different distances between notches has been discussed in Appendix 5.11.2.

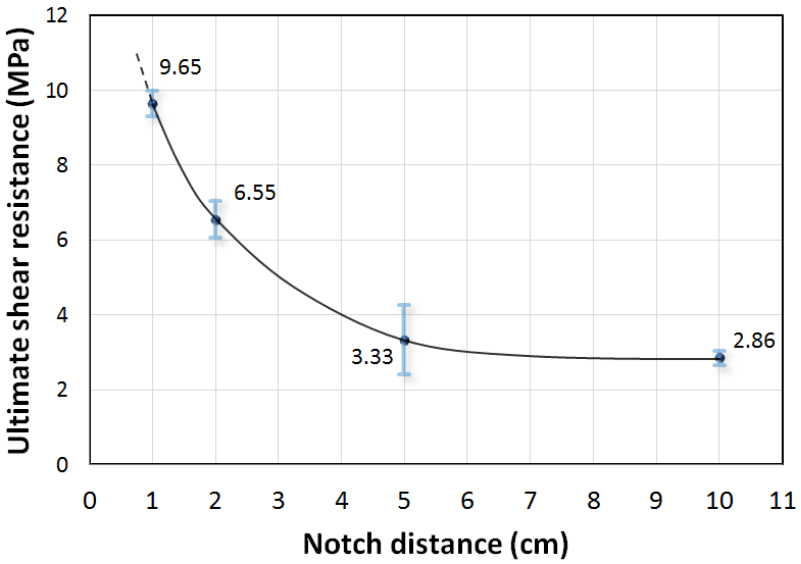

Figure 3.144 reducing the ultimate longitudinal shear resistances by increasing the notch distance for four groups of samples with two notches

3.11.4.2. ANSYS Model to find the optimum notch distance

A comprehensive finite element model of bamboo as a unidirectional and functionally graded material with different compression, tensile and bending modulus of elasticity and different Poisson ratio at each direction which can meet all of requirements and different loading conditions should be studied in a separate investigation. A simple theoretical model based on a rigid body only mentioned in Appendix 5.11, could give a general idea about the forces and tensions but cannot be used for the stress concentration around the notches. In this case due to asymmetric deformation of sample in LT plane and stress concentration at the edge of the notches the results obtained through the tests, shows the values that are underestimating from expected longitudinal shear strength.

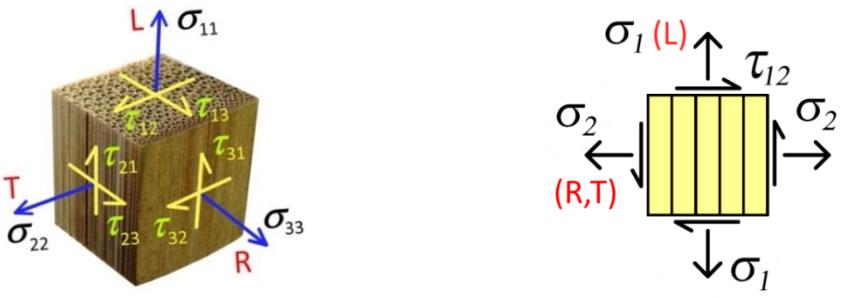

(a) 3D (b) 2D

Figure 3.145 Bamboo modeling in 3D and 2D

For an orthotropic and three dimensional model in principal coordinate shown in Figure 3.145a, the relation between stresses and strains is defined as can be seen in Figure 3.146 [110]. For this case there are 12 non-zero with 9 independent coefficients for the compliance matrix.

$$\begin{Bmatrix} \epsilon_1 \\ \epsilon_2 \\ \epsilon_3 \\ \gamma_{23} \\ \gamma_{31} \\ \gamma_{12} \end{Bmatrix} = \begin{bmatrix} 1/E_1 & -\nu_{21}/E_2 & -\nu_{31}/E_3 & 0 & 0 & 0 \\ -\nu_{12}/E_1 & 1/E_2 & -\nu_{32}/E_3 & 0 & 0 & 0 \\ -\nu_{13}/E_1 & -\nu_{23}/E_2 & 1/E_3 & 0 & 0 & 0 \\ 0 & 0 & 0 & 1/G_{23} & 0 & 0 \\ 0 & 0 & 0 & 0 & 1/G_{31} & 0 \\ 0 & 0 & 0 & 0 & 0 & 1/G_{12} \end{bmatrix} \begin{Bmatrix} \sigma_1 \\ \sigma_2 \\ \sigma_3 \\ \tau_{23} \\ \tau_{31} \\ \tau_{12} \end{Bmatrix}$$

Figure 3.146 The compliance matrix of three dimensional orthotropic model in principal coordinate

Bamboo is not a transversely isotropic material and in the radial direction is a functionally graded material (FGM) but as a simplifying assumption, bamboo is considered as a unidirectional lamina and transversely isotropic material in tangential and radial directions. It means the properties in radial and tangential directions which don't have fibers are considered the same. For bamboo the value of the compression modulus of elasticity in one direction is different form the tensile modulus of elasticity at the same direction. The other assumption is the value of tensile and compression modulus of elasticity in each direction considered to be the same. After these assumptions, it remains only four independent compliances. To simplify the modeling, the bamboo is considered as an orthotropic plane stress lamina [111] as can be seen in Figure 3.145b. The relation between stresses and strains for this specially orthotropic lamina is defined by a compliance matrix and the constants are defined in Eq. 3.11

$$\begin{Bmatrix} \epsilon_1 \\ \epsilon_2 \\ \gamma_{12} \end{Bmatrix} = \begin{bmatrix} S_{11} & S_{12} & 0 \\ S_{21} & S_{22} & 0 \\ 0 & 0 & S_{66} \end{bmatrix} \begin{Bmatrix} \sigma_1 \\ \sigma_2 \\ \tau_{12} \end{Bmatrix}$$

Figure 3.147 The relation between stresses and strains by a compliance matrix

$$S_{11} = \frac{1}{E_1} \; S_{22} = \frac{1}{E_2} \, , S_{12} = S_{21} = -\frac{\nu_{21}}{E_2} = -\frac{\nu_{12}}{E_1} \, , S_{66} = \frac{1}{G_{12}} \qquad 3.11$$

The values of modulus of elasticity in transversal and longitudinal directions, Poisson ratio and shear modulus for the bamboo should be determined. Correal *et al.* (2010) [112] investigated about the effect of age on modulus of

elasticity and shear modulus of bamboo *Guadua angustifolia* with about 12 cm diameter in green condition with about 65% MC. The average compression and shear MOE of 2 years up to 5 years old bamboo samples from middle part of a culm reported E_1=16.8 GPa and G_{12}=7.8 GPa respectively. Ahmed and Kamke (2005) [75] reported the MOE obtained by tensile test without mentioning the age with about 11% MC for *Calcutta* bamboo (*Dendrocalamus strictus*) with about 3.3cm diameter parallel to fibers equal to E_1=15.76 GPa. The experiments to determine the anisotropic elastic constants of bamboo has been carried out by Jaime *et al.* (2012) [113] reported some constants for 3 to 5 years *Guadua angustifolia* bamboo with average diameter and thickness about 107 mm and 11 mm respectively. In this research the Poisson ratio (ν_{12}), circumferential Young's modulus (E_2) and (G_{23}) reported 0.22, 0.36 GPa and 0.59 GPa respectively. The compressive MOE for longitudinal and transversal directions for a three years *Moso* bamboo [38] at the middle section reported equal to 4.43 GPa and 0.456 GPa which shows about ten times difference between E_1 and E_2. A research has been done by Zou *et al.* (2009) [114] by using nanoindentation, the MOE of fibers and matrix of a six years old *Phyllostachys edulis* is measured 10.4 and 3.4 GPa respectively. Then by using the relation between fiber and matrix in composite and the related volume fractions, the MOE in longitudinal direction is reported equal to 6.2 GPa. In this investigation the volume fraction of fiber and matrix is 40% and 60% respectively. The MOE and the shear modulus values which can be used for the numerical analysis is presented in Table 3.18.

Table 3.18 Different bamboo constants

Constant	Value
E1 (GPa)	15.76* [75], 16.8** [112], 4.43** [38], 6.2 [114], (2.19, 3.73, 4.43)**[102]
E2 (GPa)	0.36** [113] , 0.456** [38]
ν_{12}	0.22 [113]
G12 (GPa)	7.8 [112]
G23 (GPa)	0.59 [113]

* Tensile test
** Compression test

As can be seen in Table 3.18 the variation of the MOE values for tensile and compression investigated by different researchers is significant. For modeling by ANSYS in present research the values of MOE in longitudinal and tangential direction, shear modulus (G12) and Poisson ratio are considered, 10 GPa, 1 GPa,

4 GPa and 0.22 respectively. One end of the sample considered to be fixed and a 100 N load is applied to other end. The total length of the sample is 200 mm and the width is 20 mm. The thickness of the sample varies and is equal to bamboo wall thickness. The result of ANSYS analysis for sample with 20 mm distance between notches presented in Figure 3.148 shows the maximum shear is concentrated at the edges of the notches. The shear distribution alongside the shear surface is not uniform and close to the notches the value is remarkably more than the middle Section as can be seen in Figure 3.149.

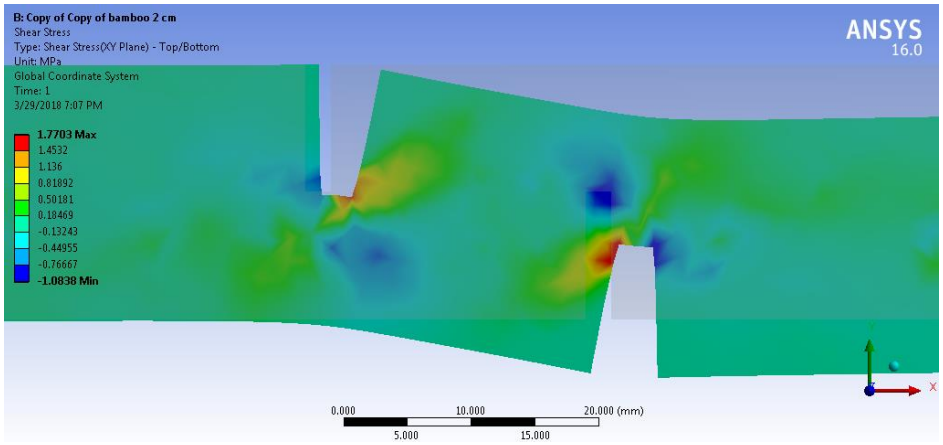

Figure 3.148 The shear stress for a sample with 20mm notch distance

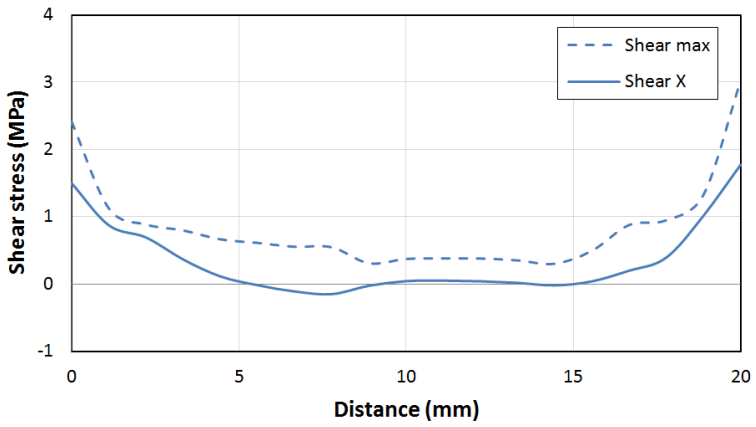

Figure 3.149 The shear stress distribution alongside the shear surface for the sample with 20 mm distance between two notches

By reducing the distance between notches to 4 mm presented in Figure 3.150, the shear distribution alongside the shear surface become more uniform as presented in Figure 3.151. Practically, the maximum shear stress is always concentrated close to the notches then by increasing the notch distance; the ultimate shear resistance is reduced.

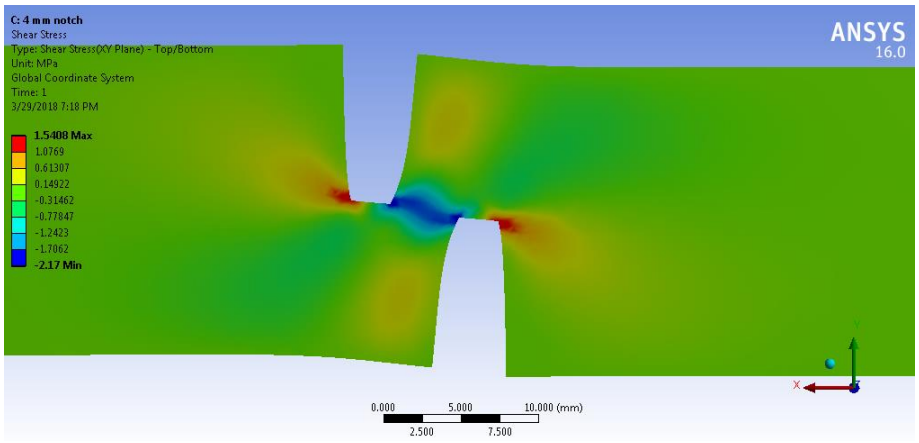

Figure 3.150 The shear concentration at the edges for a sample with 4 mm notch distance

Also by reducing the notch distance less than 20 mm, the shear area become very small and susceptive to break at the time of installation the sample to the clamps of tensile machine. The practical notch distance for this investigation is considered to be 20 mm. Preliminary tests and modeling show that the proportion of notch length and width of the sample is important factor to uniform distribution of shear alongside the shear surface.

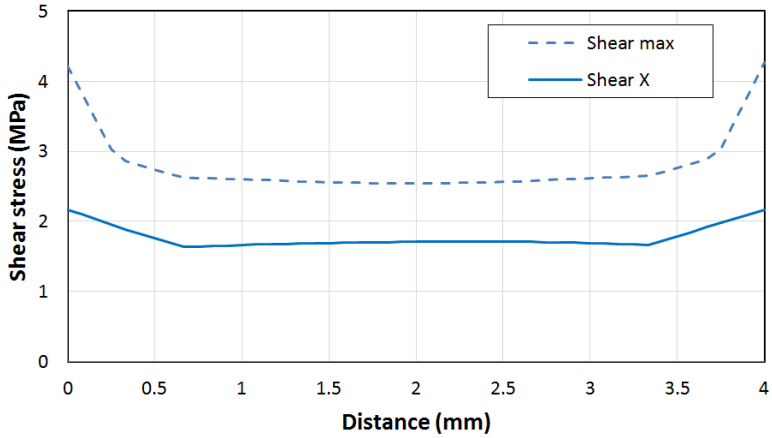

Figure 3.151 The shear stress distribution alongside the shear surface for the sample with 4mm distance between two notches

3.11.4.3. The shear test results of heat treated samples

For the shear tests based on results achieved in chapter 3.10.1, the samples placed in humid chamber or desiccator for at least 4 weeks. Comparison between two groups of untreated samples - one stabilized in humidity and one group dried in oven without stabilizing - shows there is no significant difference between their longitudinal shear tests as can be seen in Figure 3.154 based on one way ANOVA analysis. The effect of heat treatment for 3 and 24 hours on ultimate shear strength of bamboo presented in Figure 3.155 and Figure 3.156. In order to compare the

effect of heat treatment for 3 and 24 hours, Figure 3.155 and Figure 3.156 are normalized to 100°C and presented in Figure 3.157. An improve to ultimate shear resistance about 11% for the heat treated samples at 125°C and 150°C for 3 hours and 125°C for 24 hours is observed as can be seen in Figure 3.157. The effect of heat treatment for 24 hours on ultimate shear resistance is nearly equal to heat treatment for 3 hours but in 25°C higher. For test detail see appendix 5.11.3.

Figure 3.152 Heat treated Shear samples before test

Figure 3.153 Heat treated Shear samples after test

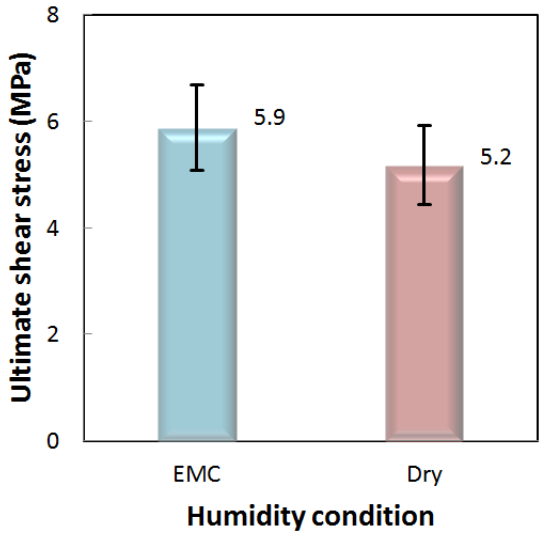

Figure 3.154 Ultimate shear stress for the untreated samples in EMC and dry conditions

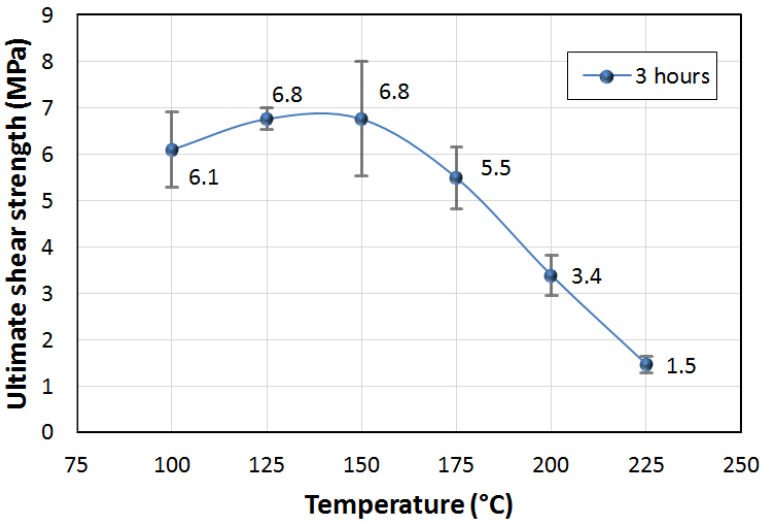

Figure 3.155 The effect of heat treatment for 3 hours on ultimate shear strength of bamboo

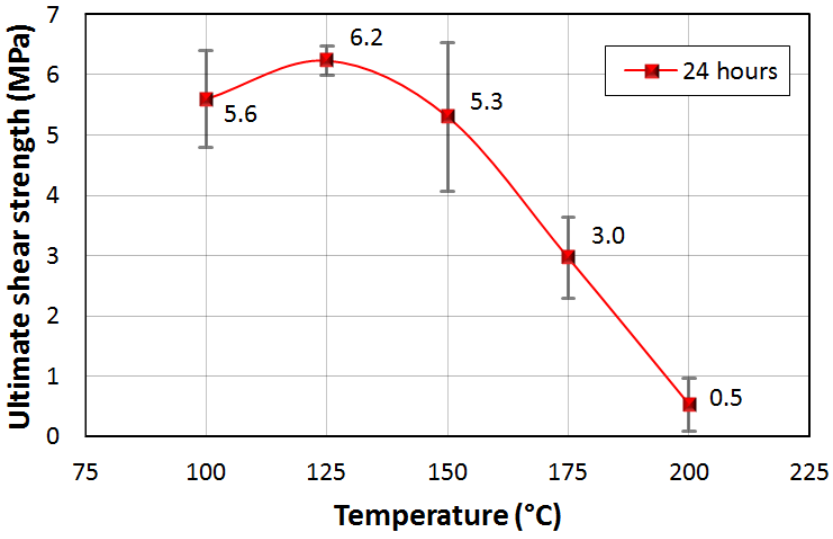

Figure 3.156 The effect of heat treatment for 24 hours on ultimate shear strength of bamboo

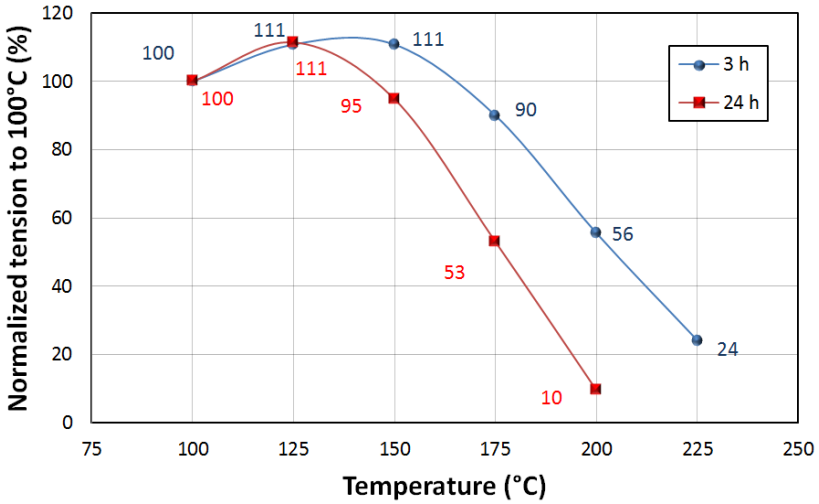

Figure 3.157 The normalized ultimate shear strength for the samples treated for 3 and 24 hours

3.11.5. Flexural behavior of heat treated bamboo

There are two different static and dynamic methods to measure the bending modulus elasticity of bamboo. In the static method by using a four point loading beam and create a pure bending region at the middle of the beam, the flexural properties is studied. This test is destructive and the same sample cannot be used again. The dynamic method selected in this study to measure the modulus of elasticity is a non-destructive method which utilizes the natural vibration frequency of a material. In this research dynamic method is used for the heated samples in 100°C, 125°C, 150°C, 175°C and 200°C during 3h and 24h for obtaining the DBMOE (Dynamic Bending Modulus of Elasticity). SBMOE (Static Bending Modulus of Elasticity) is done only for not treated samples to get knowledge about behavior of the bamboo beams as a functionally graded material and the difference between upward and downward positions. At the preliminary static bending tests, the failure modes of bamboo are investigated and by putting the strain gauges at the top and bottom of the bamboo beams, the difference between strains at top and bottom fibers is calculated and compared with the results obtained from the part of bamboo section moment of inertia.

For the static bending tests, the samples can be located in three upward, downward and lateral position as can be seen in Figure 3.158a, b and c. For the dynamic tests there is no difference between upward and downward position. These two terms (upward and downward) have been replaced by upright position. Then, there are only two different positions for putting the sample on the supports

of the dynamic test equipment, upright and lateral as presented in Figure 3.159a and Figure 3.159b.

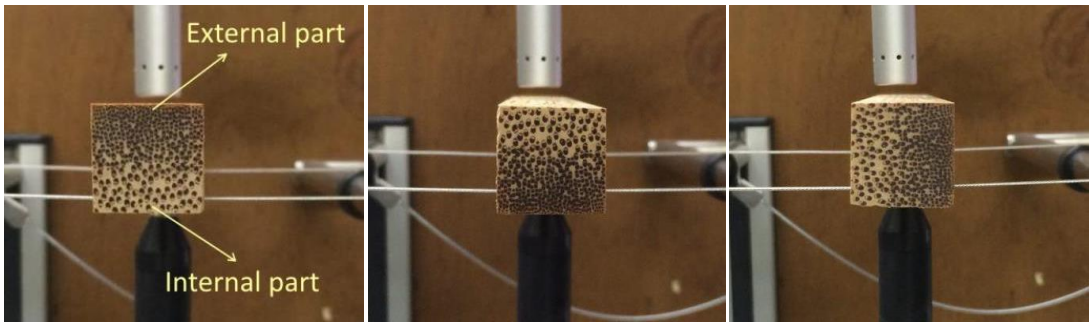

(a) upward position (b) downward position (c) lateral position

Figure 3.158 three types of bamboo position on supports

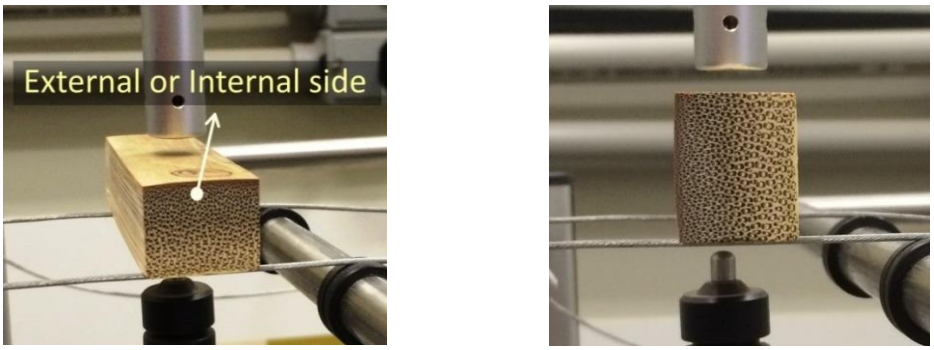

(a) upright position (b) lateral position

Figure 3.159 The two different positioning of the sample for measure the DBMOE

3.11.5.1. Failure modes of static bending tests

Three samples without any treatment at EMC condition are used to observe the quality, load and shape of rupture. The size of samples are mentioned in Table 3.19.

Table 3.19 dimension of initial bending samples

sample	dimension (mm)				Maximum load (N)
	l_e	b	t	l_e/t	
1		17	14.3	14	2325
2	200	11.3	13.1	15.3	1459
3		12.2	11.5	17.4	1164

These simply supported four point loaded beams located in upward position as presented in Figure 3.160. Two shear failure and one bending failure modes observed in bamboo beams. For bigger thickness relation to the length of the beam, the longitudinal or laminar shear failure usually happens as can be seen in Figure 3.161b and Figure 3.163, sample 1and 2. For bamboo beams (sample 3)

with smaller thickness regarding to length the bending failure is govern as shown in Figure 3.162 and Figure 3.163.

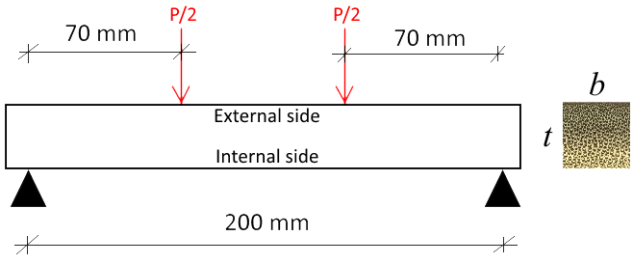

Figure 3.160 Flexural beam for static bending test at upward position

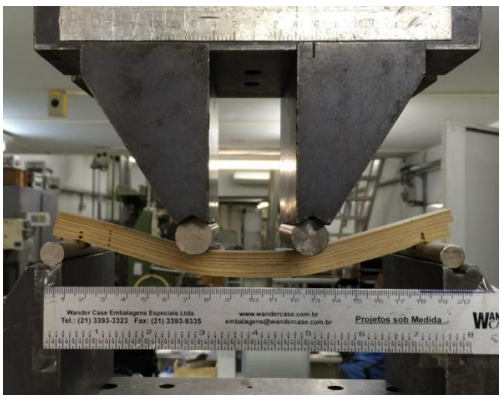

(a) Excessive deflection

(b) shear failure

Figure 3.161 The deflection and shear failure of sample at support

(a) bending failure

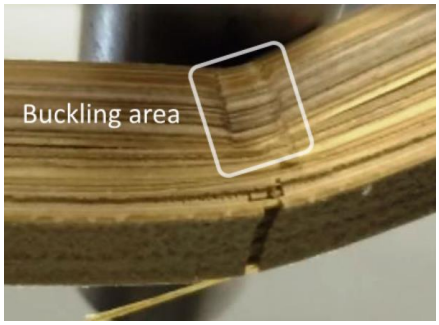

(b) fiber buckling at compression region

Figure 3.162 the failure of sample due to bending failure mechanism

The maximum shear for the samples 1 and 2 with shear failure shows the average shear resistance about 7.3 MPa. It can be considered as an indirect way to calculate the shear strength of the bamboo but it passes from a surface perpendicular to the radial direction. The effect of lower MOE of bamboo in compression regarding to tensile can be seen in Figure 3.162b. The vertical size of fiber buckling at the compression part of beam shows the difference between MOE of bamboo in tensile and compression. The neutral axis has been moved significantly close to the bottom face of the beam.

Figure 3.163 The failure shapes of samples

3.11.5.2. Top and bottom strain of a bamboo beam

By using two strain gauges at the middle of the section on top and bottom of the bamboo beam with free span equal to 180 mm and a LVDT as can be seen in Figure 3.164 the difference between strains in upward and downward positions is investigated.

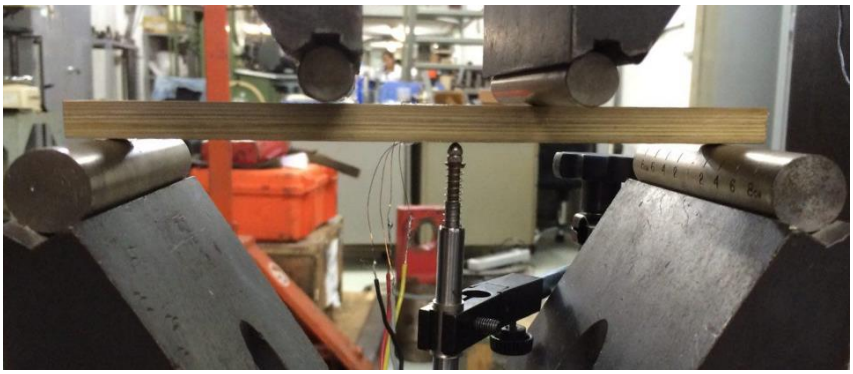

Figure 3.164 Static bamboo beam test with top and bottom strain gauges and LVDT

Figure 3.165 testing at upward position

Loading starts with the rate of 1mm per minute. To avoid failure, based on results achieved in Appendix 5.12 the maximum deflection is considered about 1mm.

In the upright positioning the high fiber density region is on the top and under compression. Based on the test the relation between strains in low fiber density (ε_{LF}) to high fiber density (ε_{HF}) region is about 1.292 as can be seen in Figure 3.166a. In the downward positioning like the situation demonstrated in Figure 3.166b the ratio of strain in low fiber to high fiber region will change to 1.261.

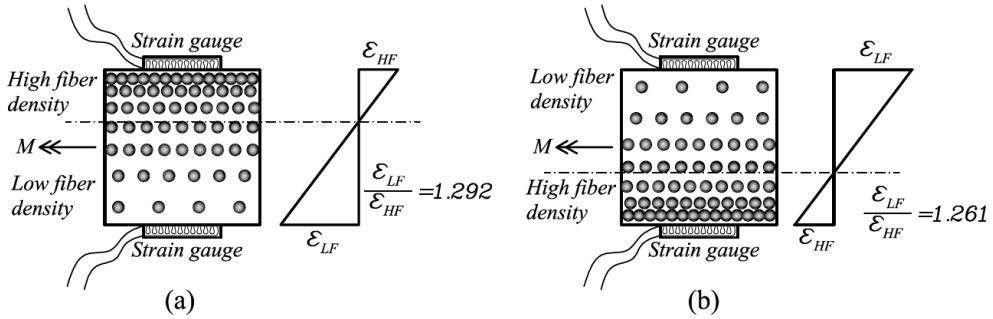

Figure 3.166 Up and down ward positioning

For the upward and downward situation the strain ratio is presented in Table 3.20.

Table 3.20 Strain of High and low fiber density areas in up and downward positions

Position	section (mm)		P (N)	$\boldsymbol{\delta}$ (mm)	$\boldsymbol{\varepsilon_{HF}}$ μm/m	$\boldsymbol{\varepsilon_{LF}}$ μm/m	Ratio ($-\frac{\boldsymbol{\varepsilon_{LF}}}{\boldsymbol{\varepsilon_{HF}}}$)
	w	t					
Upward	10.84	11.78	105.43	0.5	-298.1	385.2	1.292
Downward	10.84	11.78	92.90	0.5	280.2	-353.4	1.261

By using the ratios mentioned in Table 3.20, the distance of neuter axis are 0.564t and 0.558t for the ratio equal to1.292 and 1.261 respectively. Based on the thickness of bamboo which is equal to 11.78mm and using the average polynomial for middle and bottom middle of a *DG* bamboo section mentioned in section 3.5.4.3 and using the formulas 5.7 and 5.9 the neuter axis is calculated as presented in Eq. 3.13.

$$V_F\,(x) \;=\; 34.2\,x^2 \;-\; 13x \;+\; 33.5 \qquad 3.12$$

$$\bar{x}_F = \frac{\int_0^t x V_F(x)\,dx}{\int_0^t V_F(x)\,dx} = 0.546 \qquad 3.13$$

The maximum difference between the neuter axes is about 3% which can show the concordance between the results in Table 3.20 in bending test with the same values resulted by image process. The calculated modulus of elasticity by considering two equal MOE for tensile and compression at the top and bottom of

the beam and the cross section considered to be isotropic; for upward and downward positions are equal to 14.8 GPa and 13.0 GPa respectively.

3.11.5.3. Dynamic bending modulus of elasticity (DBMOE)

Impulse excitation technique (IET) is a non-destructive method which used mainly to measure the dynamic modulus of elasticity and some other dynamic mechanical property of a material. This method which is based on natural vibration frequency can measure young's modulus, Shear modulus, Poisson's Ratio and damping ratio. When a sample is subjected to an impulse (light mechanical impact), emits a characteristic sound according to dimension, geometrical shape, mass and elastic properties. By recording the emitted sound then FFT analyzing (Fast Fourier Transmission) and selecting the first harmonic component as fundamental resonant frequency of the sample, the modulus of elasticity is obtained. Depend on the boundary conditions (supports) and the location of mechanical impact the mention parameters is achieved. In this research, the bar of bamboo with almost square cross section is considered to measure the modulus of elasticity in radial and tangential direction with different temperature heat treatments. Also the effect of humidity in modulus of elasticity variations is investigated.

3.11.5.3.1. Theory

General differential equation for transverse vibration of a thin beam (thin: to decrease the effect of shear resistance) is presented in Eq. 3.14 [115] . The characteristic equation in specific boundary condition which the beam ends are free, presented in Eq.3.15.

$$\frac{\partial^4 w}{\partial x^4} + \left(\frac{\rho A}{EI}\right)\frac{\partial^2 w}{\partial t^2} = 0 \qquad 3.14$$

By using non-trivial solution for vibration in the first mode of a free-free boundary condition and obtaining the value of $\beta_{n=1}$ in Eq. 3.15 the modulus of elasticity is calculated and presented in Eq. 3.16. The additional part (T_c) is a correction factor for fundamental flexural mode and for different conditions mentioned in ASTM E1876-09 [116].

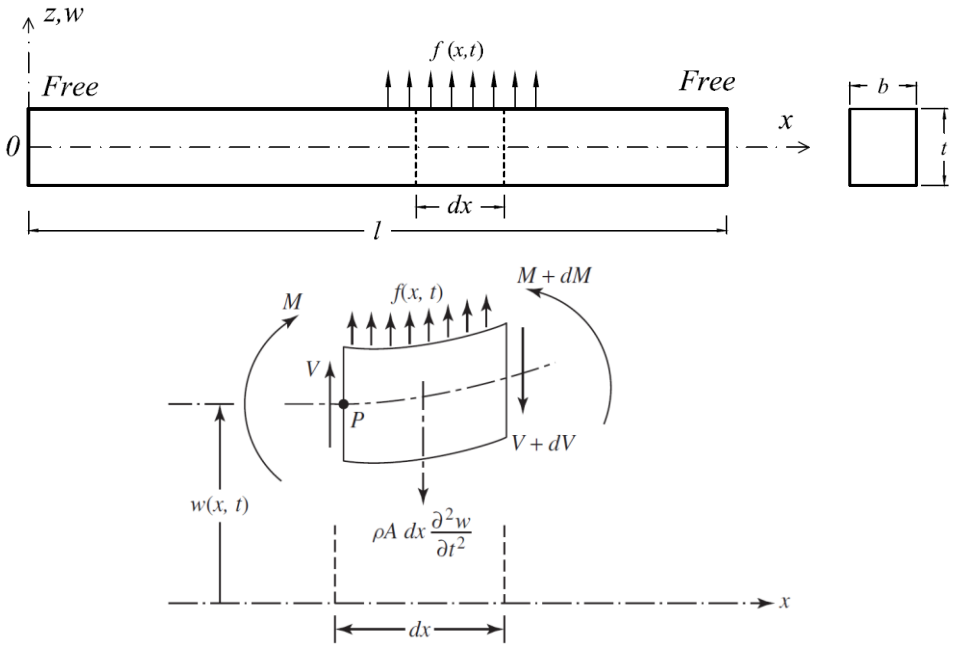

Figure 3.167 Transverse vibration of a thin beam [117]

$$\omega_n = (\beta_n l)^2 \sqrt{\left(\frac{EI}{\rho A l^4}\right)}, \qquad \left(\omega_n = \frac{f_n}{2\pi}\right) \tag{3.15}$$

$$E = 0.9465\left(m\frac{f_1^2}{b}\right)\left(\frac{l}{t}\right)^3 T_c \tag{3.16}$$

Eq. 3.16 is used for an isotropic material. For the bamboo as a FGM material instead of the beam dimensions (*b* and *t*), the modulus of inertia will be used as can be seen in Eq.3.17.

$$E = .07887 f_1^2 \left(\frac{ml^3}{I}\right) T_c \tag{3.17}$$

For an isotropic material with square cross section the moment of inertia about *x* and *y* axis are equal. For a bamboo beam with square cross section the second moment of Inertia in radial direction (upright position) due to uneven distribution of fibers is different from the lateral position as can be seen in Figure 3.168. A real bamboo fiber distribution model is presented in Figure 5.24b. By expanding the fibers at tangential direction, a uniform distributed fiber section is established which can represent the real second moment of Inertia as can be seen in Figure 5.24c. The difference between moment of inertia in upright and lateral positions discussed in Appendix 5.15.

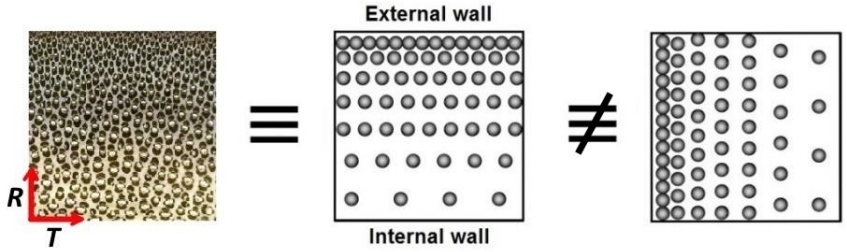

(a) Bamboo section (b) Upright position (c) Lateral position

Figure 3.168 Difference between upright and lateral moment of inertia for a bamboo section

3.11.5.3.2. SONELASTIC equipment

SONELASTIC is a set of equipment containing a microphone, frame with adjustable sample supports (based on the mode of vibration) and a pulse producer for hitting a light strike to the sample. The sound induced by this impact processed by the related software and the result is a series of natural frequencies. The other parameters like dimensions (*b*,*t* and *l*) and mass (*m*) of the cubical sample should be entered manually [118].

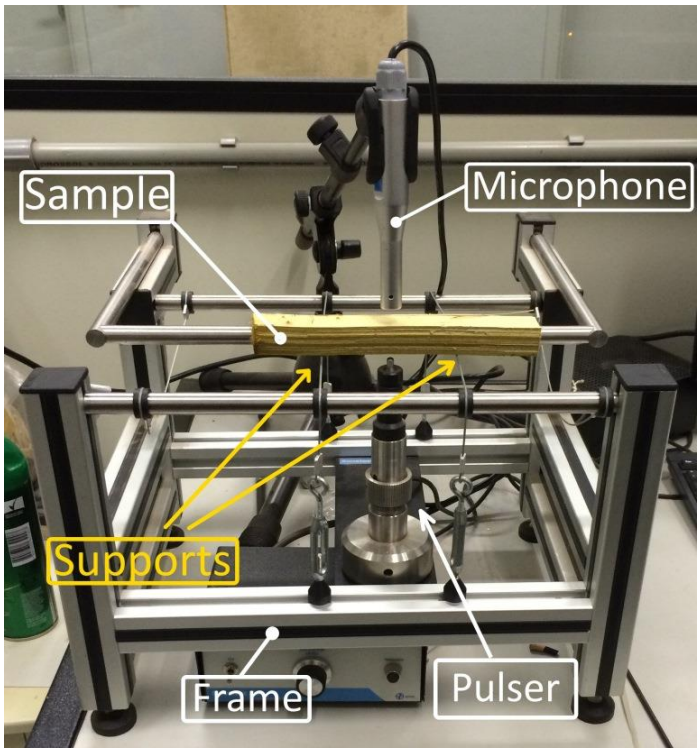

Figure 3.169 SONELASTIC Frame with supports, pulser and microphone

3.11.5.3.3. Test procedure

Each set of test has 3 replicates with different wall thicknesses and the modulus of elasticity is measured in both lateral and upright positions, and the average of them is used to present the DBMOE of the sample. The samples prepared by removing the internal and external curve parts to make an almost

square cross section. Due to some imperfections in diameter and wall thickness and warping of bamboo culms, removing the internal and external skin to make a perfect square section creates the variation of modulus of elasticity for each specimen then it cannot represent the real DBMOE of section. The privilege of impulse excitation technique test is using the same sample for heat treatment to eliminate the effect of different FVF and size effects. All the values are normalized based on the untreated sample at EMC condition.

For each heat treatment, dry and EMC conditions considered for the test. After removing from oven, the samples are in dry condition. By putting them in ambient humidity and temperature, they absorb humidity and changed to EMC condition. The measured relative humidity and temperature in SONELASTIC Lab in PUC-Rio shows this room is always in the range of the standard condition mentioned in ISO 22157-1 [84]. The measured humidity of the laboratory varies between 60% up to 80%.

To understand about the difference between the DBMOE of humid and dry samples, a test carried out by using untreated specimens. The DBMOE is normalized based on the untreated samples at EMC condition as can be seen in Figure 3.170, point 1. Drying for one week in 70°C increases the DBMOE about 2.7% as can be seen in Point 2 of Figure 3.170 and after leaving the samples in ambient by humidity absorption for two days, a reduction about 3.5% in DBMOE is observed at point 3. This reduction can be justified due to the humidity absorption from surface of the sample. Based on the relation between frequency, mass and dimensions of the sample mentioned before in Eq. 3.16, not only the surface humidifying can soften the fibers and matrix, but also there is not enough time to penetrate the humidity in the core of the sample to increase the mass of the sample, then it shows less modulus of elasticity than the reality. By placing the samples in the oven and drying at 100°C for 24 hours, the DBMOE increases about 2.5% as can be seen in point 4 and after one month leaving the samples in ambient humidity and temperature the DBMOE goes back to the same value at the start of the test as can be seen in point 5. It shows that the heating up to 100°C does not change permanently the DBMOE.

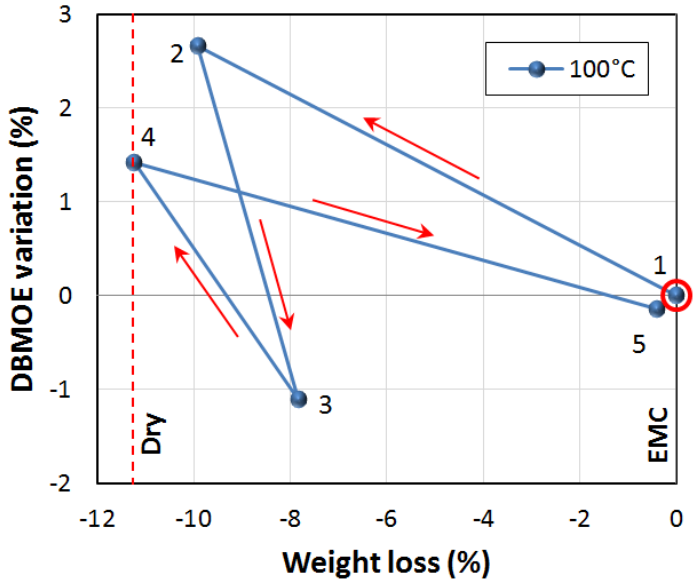

Figure 3.170 The effect of two cycles of drying and humidity absorption

3.11.5.3.4. Heat treated sample tests

15 samples in 5 sets (each set of tests has 3 replicates) are considered for the test. The procedure of the test is presented in 6 steps.

1- The weight and DBMOE of non-treated at EMC condition are measured.
2- The samples put in the oven at 70°C for one week to dry. The dried weight and DBMOE of the samples are registered.
3- Each set of samples put in the oven in 5 different temperatures 125°C, 150°C, 175°C, 200°C and 225°C for 3 hours. After removing from oven in dry condition the weight and MOE are registered.
4- By putting the samples inside the wet desiccator (75% Rh) after four weeks they reach to the stabilized moisture content or EMC condition. The weight and MOE of the samples is registered.
5- The samples put in the oven for more 21 hours to accomplish the cycle of 24 hours treatment. After removing from oven and in dry condition the DBMOE and weight are registered.
6- By putting the samples inside the wet desiccator (75% Rh) after four weeks they reach to the stabilized moisture content or EMC condition. The weight and MOE of the samples is registered.

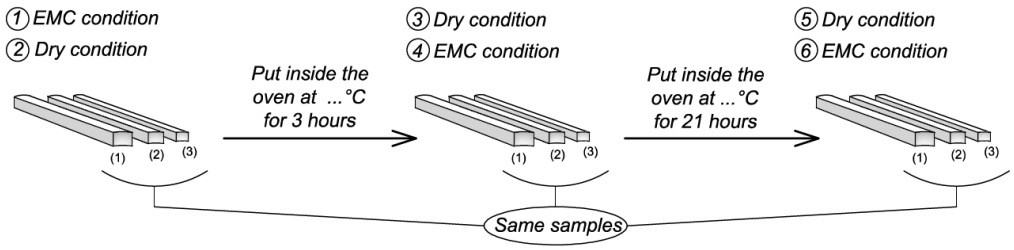

Figure 3.171 the process of weighing and measuring the dynamic MOE test

The mentioned process briefly demonstrated in Figure 3.171 and the related tables are in the Appendix 5.13. The dimension changes due to heat treatment have been considered in the DBMOE measurements. The heat treated samples presented in Figure 3.172.

Figure 3.172 DBMOE Heat treated samples

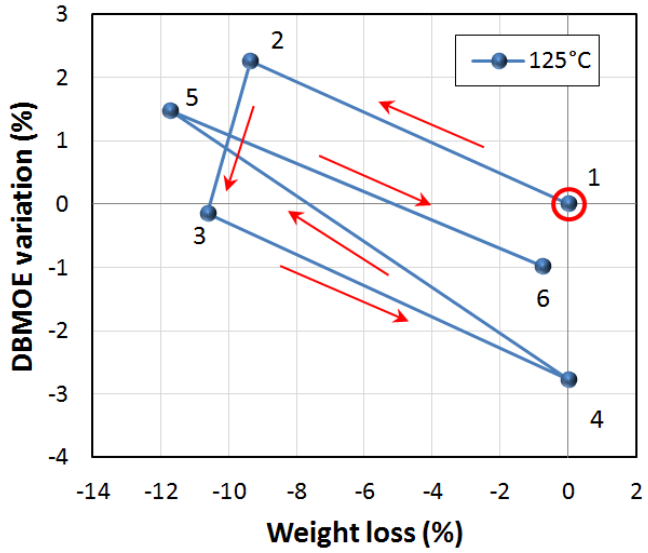

Figure 3.173 DBMOE changes vs heat treatment in 125°C

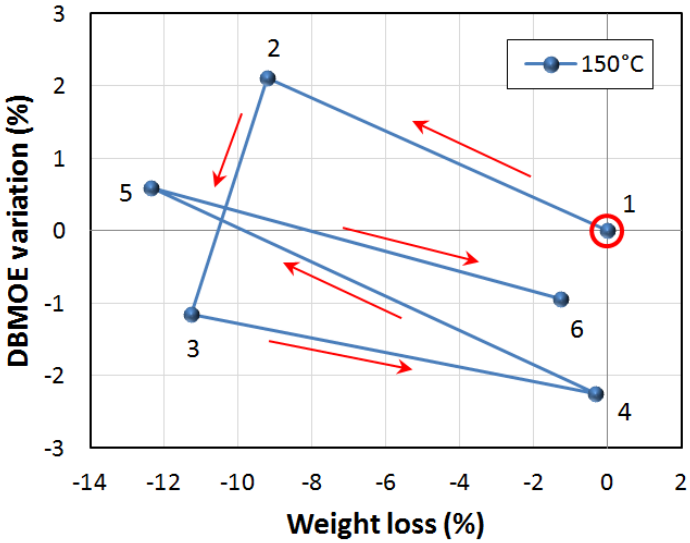

Figure 3.174 DBMOE changes vs heat treatment in 150°C

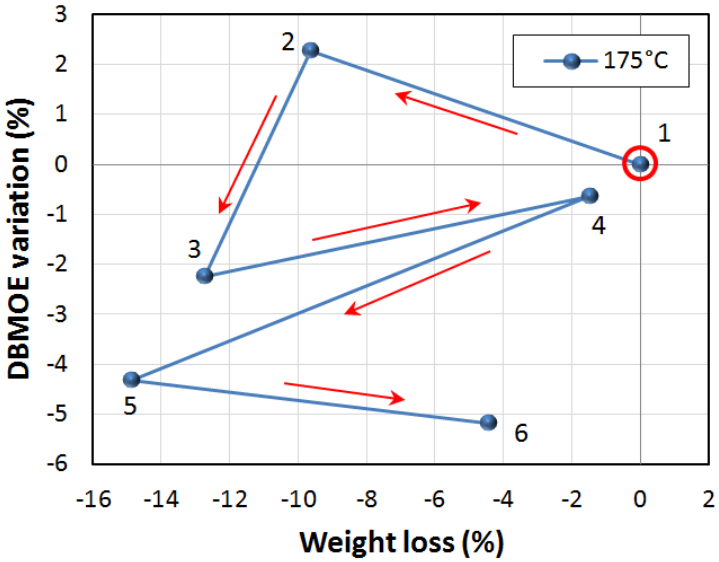

Figure 3.175 DBMOE changes vs heat treatment in 175°C

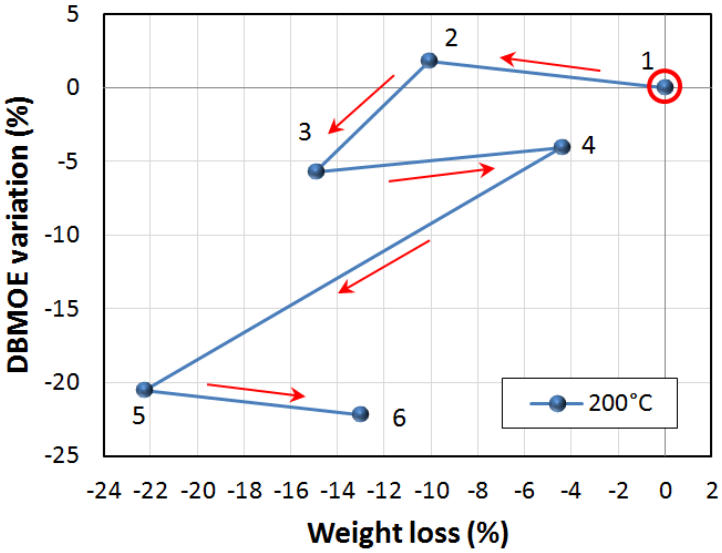

Figure 3.176 DBMOE changes vs heat treatment in 200°C

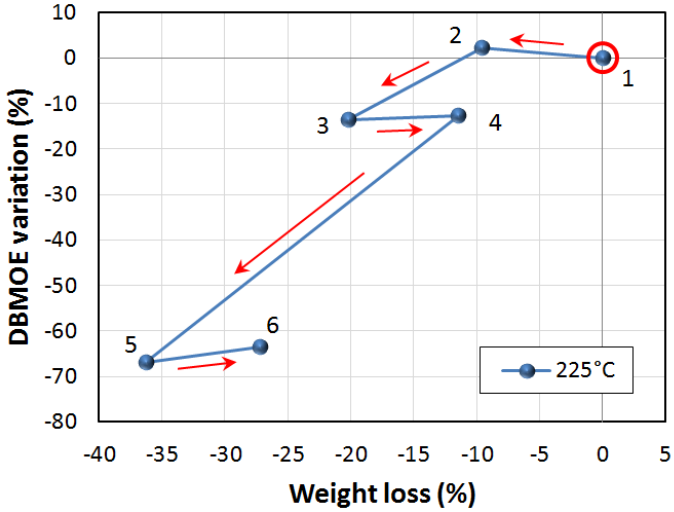

Figure 3.177 DBMOE changes vs heat treatment in 225°C

The DBMOE changes due to heat treatment procedure in Figure 3.171, presented in Figure 3.173 to Figure 3.177. The summary table of normalized DBMOE changes at each step for different heat treatment temperatures and durations at dry and EMC conditions is presented in Table 3.21.

Table 3.21 DBMOE variations (%) in dry and EMC conditions due to heat treatment comparing with untreated samples at EMC condition

Temperature	Step 1 (Un*,EMC)	Step 2 (Un,Dry)	Step 3 (3h,Dry)	Step 4 (3h,EMC)	Step 5 (24h,Dry)	Step 6 (24h,EMC)
100°C	0.0	2.7	-	-	1.4	-0.1
125°C	0.0	2.3	-0.1	-2.8	1.5	-1.0
150°C	0.0	2.1	-1.1	-2.2	0.6	-0.9
175°C	0.0	2.3	-2.2	-0.6	-4.3	-5.2
200°C	0.0	1.8	-5.7	-4.1	-20.6	-22.2
225°C	0.0	2.2	-13.7	-12.6	-66.9	-63.5

*Un: Untreated sample

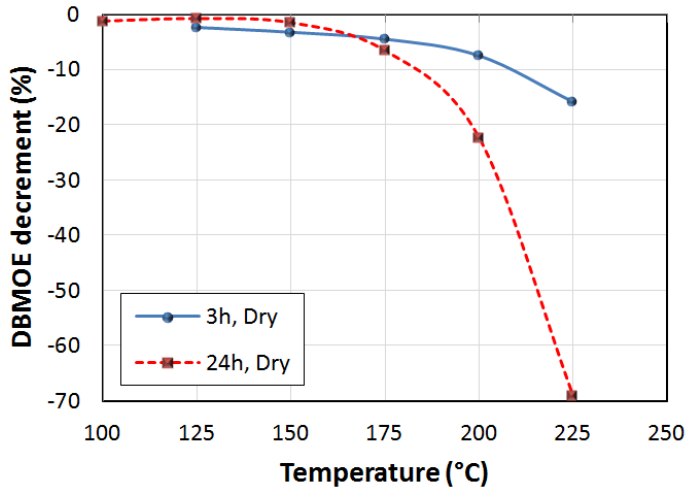

Figure 3.178 DBMOE decrement for samples treated in different temperatures for 3h and 24 h at dry condition comparing with untreated samples at dry condition

DBMOE decrement for samples treated in different temperatures for 3h and 24h at dry condition comparing with untreated dried samples is presented in Figure 3.178. The comparison between heat treated samples at EMC condition (comparing step 4 and step 6 with step 1) also can be seen in Figure 3.179. Based on the results presented in these two figures, heat treatment always reduces the DBMOE at all temperatures but up to 150°C the changes is less than 5%. The significant change is started from 175°C during 24h.

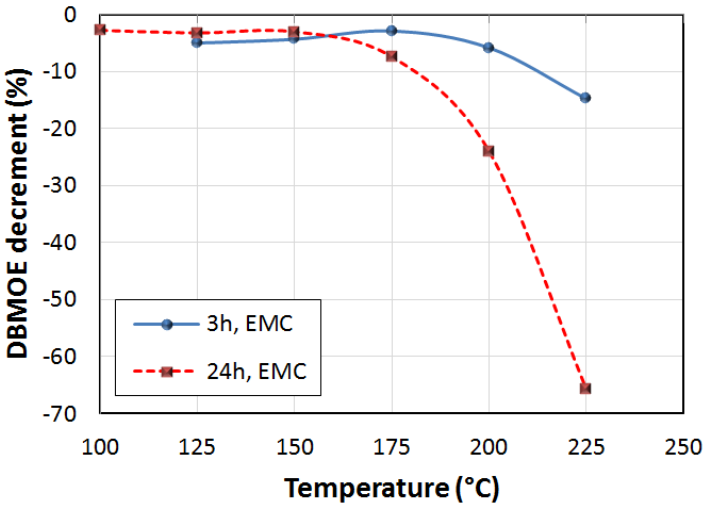

Figure 3.179 DBMOE decrement for samples treated in different temperatures for 3h and 24 h at EMC condition comparing with untreated samples at EMC condition

3.11.6. Comparison the mechanical tests

The results of longitudinal tensile, transversal tensile, compression, shear and DBMOE tests are normalized based on the 100°C treated for 3 hours and 24 hours presented in Figure 3.180 and Figure 3.181. After 150°C for heat treatment during 3 hours the tensile, shear and transversal tensile ultimate strength decreased but for the compression samples increment in ultimate tensile is observed up to 225°C. For heat treatment during 24 hours the mentioned trend is the same as 3 hours but after 175°C the compression ultimate strength decreased. The decrement of DBMOE shows that it is between the results of tensile and compression test with more tendency to compression values.

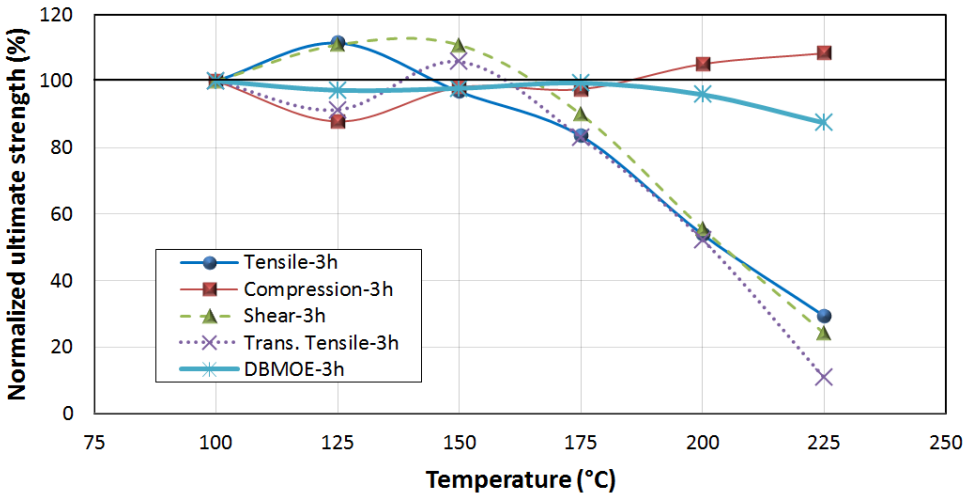

Figure 3.180 Comparing the tensile, compression, shear and transversal tensile normalized ultimate strength of heat treated samples for 3 hours

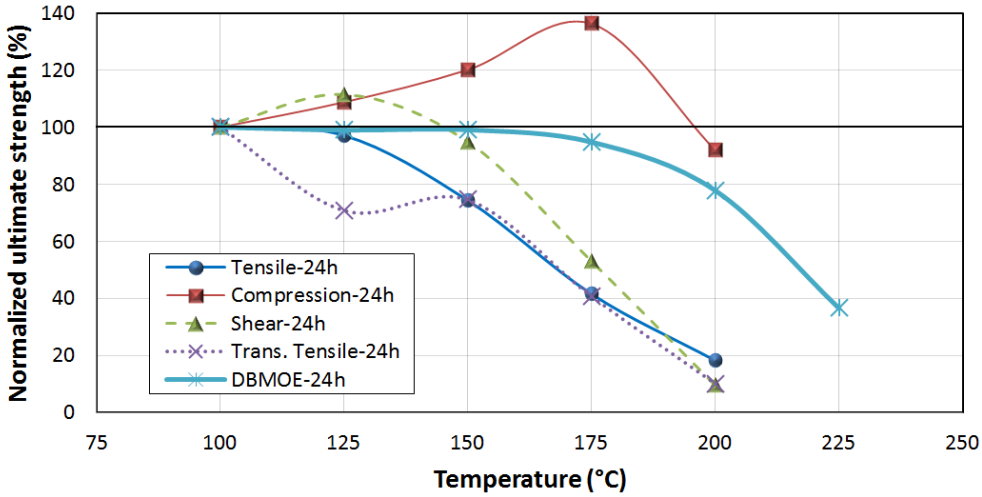

Figure 3.181 Comparing the tensile, compression, shear and transversal tensile normalized ultimate strength of heat treated samples for 24 hours

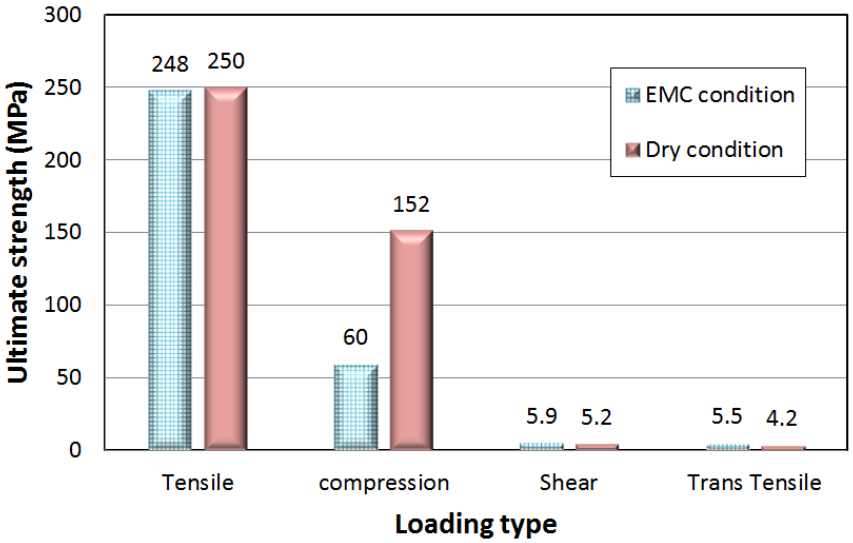

Figure 3.182 Comparing the tensile, compression, shear and transversal tensile ultimate strength for EMC and dry conditions

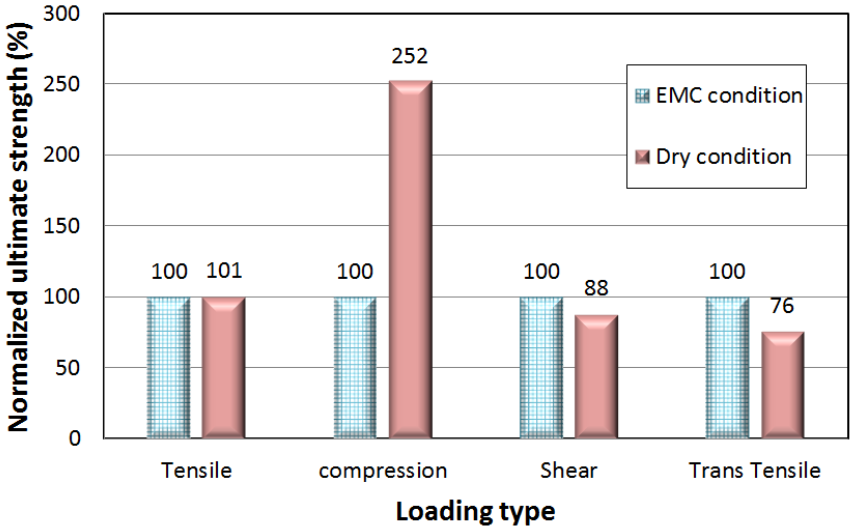

Figure 3.183 Comparing the normalized tensile, compression, shear and transversal tensile ultimate strength normalized based on EMC condition

The sample resistance for shear and transversal tensile test are close together as presented in Figure 3.182. For these tests, only the matrix resistance is important then they can represent the tensile and shear matrix resistance.

3.12. Suggestions

All the mechanical tests can be implemented in ambient temperature or inside a heat chamber. The tests in ambient temperature are useful when the heat treatment is considered to be the objective of the research. The second type of tests is done inside the heat chamber which can simulate the effect of in-situ heat (fire) which is not accomplished at the present investigation. The effect of chemical product used as fire retardant or wood and bamboo treatment against pests on mechanical properties of bamboo in short and long term can be investigated in separate investigation. One of the well-known products for bamboo treatment against pests is borax and acid boric [121][122].

The bamboo shear test needs more investigation and FEM modeling to standard the size of specimen. A coefficient should be defined to compromise the size effect of bamboo specimen.

The result of bamboo compression test shows that it needs more study about the fiber buckling at internal and external area. The test should be implemented for external and internal wall thickness of bamboo with more and less fiber volume fraction respectively.

Comparing the compression test results for specimens at dry and EMC condition shows the effect of MC% is remarkable. This effect should be investigated in separated research to find the reasons. The compression test should be applied for different types of bamboo such as *Moso* bamboo and *Guadua*.

4. Result discussion and conclusion

The result of chemical analysis shows the internal part of DG bamboo has more extractive and lignin than the external part. Comparing the results of this study with the chemical components presented in literature review shows the chemical components of Iranian (Persian) bamboo (IR) is close to phyllostachys pubescens. The average values of the chemical component for internal and external parts of DG bamboo in this study is between the values of the Dendrocalamus giganteus munro and the Dendrocalamus asper mentioned in literature review.

The TGA obtained in this investigation verifies the results of other researchers about the effect of heating rate with the optimum of 10oC/min. The TGA results for both DG bamboo and Moso bamboo shows for the external part with more fiber volume fraction. At about 380oC, maximum speed of losing weight happens and at the part with less fibers volume fraction it is about 320oC. Comparing the TGA results of internal and external part of DG bamboo does not show significant difference between these two parts.

The result of image processing for Moso bamboo and DG bamboo shows the remarkable difference between the fiber distributions alongside the radial direction. The fiber volume fraction at internal part of Moso bamboo wall thickness is about 20% less than DG bamboo, but at the external part, the FVF for both are close the each other. The ANOVA analysis shows that there is not any dependency between fiber distributions alongside the tangential direction. The same result is for the wall thickness which does not show any tendency in one special direction. The variation of fiber distribution in radial direction for all five sections from different elevations is less than 10%. The 3D X-ray microtomography on morphology of a cylindrical sample from the middle part of a bamboo section for not treated, treated at 225°C for 3 hours and treated at 225°C for 24 hours shows the remarkable changes on bamboo structure occurs for 225°C-24h. At this heat treatment point the vertical and horizontal cracks in the fibers can be observed. The result from SEM shows the cracks between fiber cell walls as well as radial crack for each fiber cell.

In general, heat treatment of bamboo slows down the rate of water absorption. The rate of water absorption reduces from 7.5% per hour for normal specimens, soaked in water during 6h, to 3% per hour for specimens, subjected to 200°C for 24 hours. The weight increment due water soaking for all of the specimens heated in different temperatures are around 100%. To absorb the additional water up to complete saturation for normally saturated specimens the vacuum chamber used. The natural (not heated) samples absorb water up to 20% and the samples heated up to 225°C, the water sorption in vacuum is 6%.

Heating up to 225°C for 3hrs or 200°C for 24hrs can reduce the bamboo water absorption capacity up to 15% as compared with the natural samples. The water absorption after heating at 175°C for 24 hours and at 200°C for 3 hours are the same. In both cases reduced significantly the swelling in radial and tangential directions due to water absorption. Water absorption during four weeks shows the rapid, transition and slow phases of water absorption for all the 15 mm cub samples, heated for 3 hours and 24 hours.

There is no significant difference between shrinkage at external and internal parts of a bamboo section. The swelling of external part due to water absorption in average is about 40% more than the internal part of bamboo. The fiber swelling is nearly five times more than the matrix due to water absorption up to saturation point. The fiber swelling coefficient does not change up to 200°C but after this temperature up to 225°C a drop of more than 2% occurs. The matrix swelling coefficient is about 4% for heat exposure at 100°C and gradually decreases to 2% for heat exposure at 225°C.

There is not any difference in tensile strength failure patterns of samples treated up to 150°C during 24h. A significant difference observed at 175°C-24h which makes the matrix fragile. At higher temperatures the adhesion between fibers and matrix loses creating an irregular surface between fiber bundles and matrix. There is no difference between ultimate tensile resistance of natural samples at dry and EMC conditions. Heat treatment from 100°C up to 225°C reduces the ultimate tensile strength of bamboo but not its modulus of elasticity.

In radial and tangential directions the transversal tensile test shows only the matrix resistance. The ultimate transversal tensile strength decreases subjected to temperature up to125°C, but after this temperature an increment of resistance for

3 and 24 hours exposure up to 150°C, occurred. A linear decrement after 150°C for both heat exposures during 3 and 24 hours observed.

The compression strength of the bamboo is mainly related to MOE and shear modulus of matrix. The increase of these two parameters of matrix by heat treatment is related to the increase of critical buckling compression of the fibers. Heat exposure makes the fibers more rigid and changes the flexible to fragile buckling. Increasing the temperature up to 175°C-24h the compression ultimate resistance increases 36%. Heat exposure for 3 hours up to 225°C does not change the compression strength of bamboo. There is significant difference between the compression test result for natural samples in dry and EMC condition. The ultimate compression strength in dry condition is 2.5 times more than the EMS condition.

The ultimate longitudinal shear resistance increases by decreasing the notch distance. Comparing the experimental test results with finite element model in ANSYS shows by lowering the distance between notches the shear is distributed more uniform alongside the shear surface area. Reducing excessively the notch distance makes the specimen susceptive to break then the optimized notch distance is considered to be 20 mm. There is not significant difference between the longitudinal shear test result for natural samples in dry and EMC condition. Heat exposure at 150°C for 3 hours or 125°C for 24 hours increases the ultimate shear resistance about 11%. Proximity of the ultimate transversal tensile strength with ultimate longitudinal shear strength shows the rupture mechanism is depends on matrix property.

Static flexural test carried out to measure the static bending modulus of elasticity shows different values for upward and downward positions. Using two strain gauges at the top and bottom in the mid. span shows different values due to non-uniform distribution of fibers alongside the radial direction comparing with an isotropic cross section. Dynamic flexural test carried out to measure the dynamic bending modulus of elasticity shows there is not any difference between upward and downward position. The significant change in dynamic bending modulus of elasticity starts at 175°C and the effect of heat exposure time by increasing the temperature is remarkable.

Comparing the mechanical test results shows the tensile, transversal tensile and shear resistance of bamboo is related mainly to the matrix behaviour. Heat

exposure at 200°C for 3 hours reduces the ultimate tensile, transversal tensile and shear strength nearly 45% while the compression strength increases by heat exposure at this temperature.

5. APPENDIX

5.1.Bamboo cutting

There are two different ways for dividing a whole column of bamboo. The first is when both nodes and internodes are necessary for doing the test. The second is when only the internode parts are needed for doing the tests. For the first purpose the proper dividing points are one in the middle of internode the other in node and repeated the same for the entire column as shown in Figure 5.1. When only the internodes are needed, all the nodes with 50mm width will be removed from internodes as can be seen in Figure 5.2.

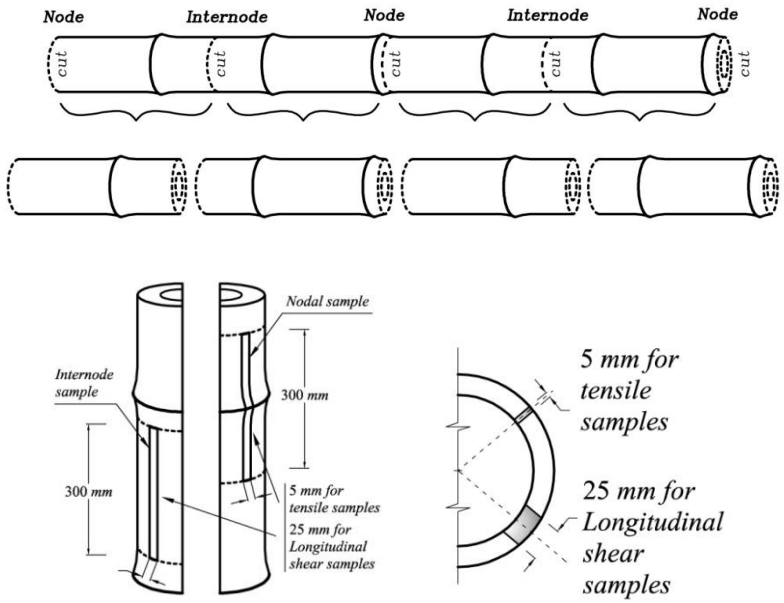

Figure 5.1 Column of Bamboo with node and internode samples

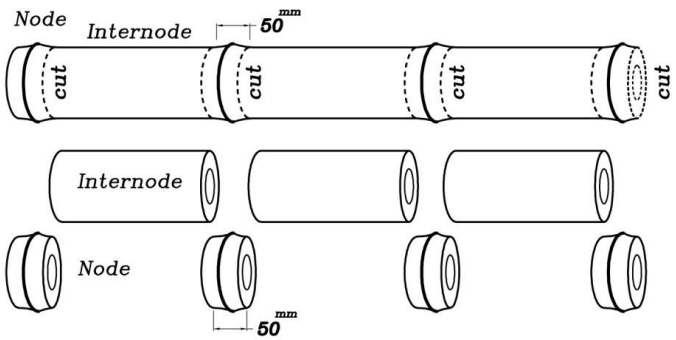

Figure 5.2 Column of bamboo for making the internode samples

5.2. Apparatus for transversal tensile and compression tests

This equipment is a bi-functional apparatus made by author in mechanical workshop of Tehran University and works with half assembly and full assembly. At half assembly it can be used as a guide for the compression samples and fix the sample ends like a clamp support. After fixing the sample by clamps, it is located between the compression plates of the Instron machine for doing the compression test as shown in Figure 3.122. At full assembly it serves as an adjunct tensile apparatus and eliminates the shear and bending forces exerted by clamps. In this situation it is used for transversal tensile test as can be seen in Figure 3.115a.

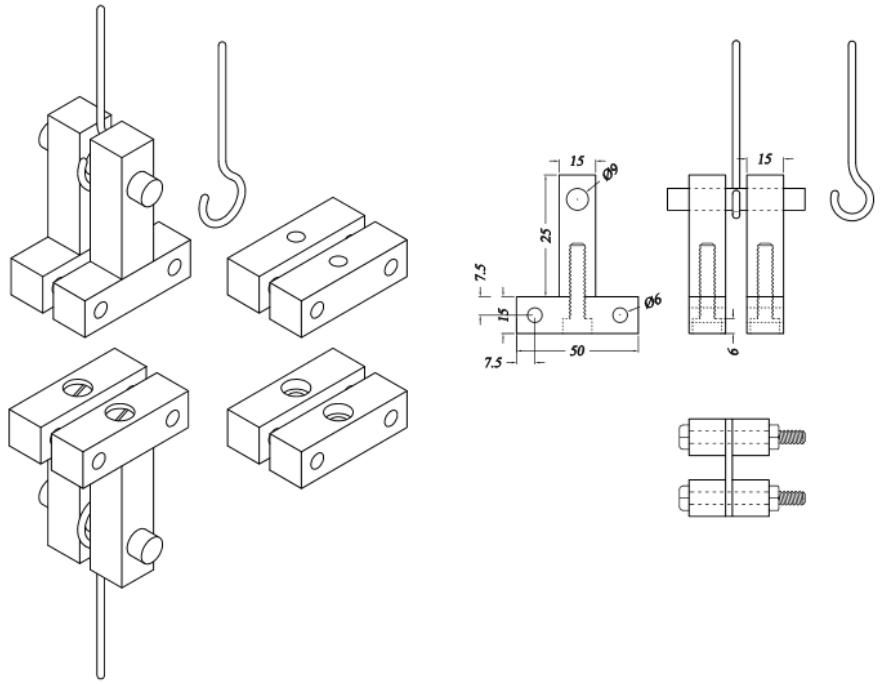

Figure 5.3 Detail of bi-functional apparatus

5.3. Uneven water absorption table

Table 5.1 the results of length measurement in tangential direction

Item	No.	Dry		Saturated	
		W (gr)	dim. (mm)	W (gr)	dim. (mm)
B1 (100)	1	2.7444	16.48	5.7368	17.92
	2		16.59		17.81
	3		16.58		17.61
	4		16.45		17.47
	5		16.26		17.23
	6		16.10		17.44
	7		16.19		17.53
	8		16.34		17.73
B2 (125)	1	2.6243	16.26	5.9071	17.71
	2		16.43		17.59
	3		16.48		17.46
	4		16.56		17.59
	5		16.52		17.50
	6		16.53		17.67
	7		16.37		17.73
	8		16.34		17.74
B3 (150)	1	1.9375	12.76	4.271	13.87
	2		12.85		13.69
	3		12.54		13.31
	4		12.88		13.58
	5		13.00		13.69
	6		13.04		13.81
	7		12.88		13.99
	8		12.88		13.98

Item	No.	Dry		Saturated	
		W (gr)	dim. (mm)	W (gr)	dim. (mm)
B4 (175)	1	2.2041	14.82	4.8145	16.03
	2		14.87		15.84
	3		14.78		15.63
	4		14.75		15.60
	5		14.52		15.30
	6		14.64		15.57
	7		14.62		15.86
	8		14.79		16.02
B5 (200)	1	2.127	14.01	0.8558	15.12
	2		14.09		15.02
	3		14.25		15.01
	4		14.32		15.02
	5		14.19		14.83
	6		14.04		14.85
	7		13.98		15.07
	8		14.06		15.23
B6 (225)	1	2.4358	16.56	5.426	17.68
	2		16.50		17.44
	3		16.45		17.15
	4		16.65		17.45
	5		16.68		17.47
	6		16.72		17.59
	7		16.76		17.95
	8		16.73		17.91

5.4.Bamboo humidity stabilization table

Table 5.2 bamboo humidity stabilization table

Sample	Weight (gr)											
	0h	4h	24h	48h	72h	144h	192h	216h	312h	336h	552h	744h
T-100	1.9457	2.0470	2.1699	2.1745	2.1724	2.1757	2.1775	2.1758	2.1768	2.1768	2.1752	2.1851
T-150	1.9898	2.0748	2.1975	2.2090	2.2085	2.2174	2.2171	2.2168	2.2176	2.2176	2.2174	2.2260
T-200	2.1762	2.2394	2.3525	2.3795	2.3846	2.3985	2.4030	2.4004	2.4034	2.4034	2.4026	2.4124
LS-100	11.2068	11.3935	11.8067	12.0067	12.1143	12.3421	12.4466	12.4729	12.5290	12.5371	12.5547	12.5985
LS-150	11.6882	11.8440	12.2054	12.3787	12.4839	12.7217	12.8455	12.8917	13.0133	13.0341	13.1062	13.1668
LS-200	10.5531	10.7010	11.0253	11.1763	11.2607	11.4729	11.5833	11.6206	11.7223	11.7347	11.7881	11.8263
TT-100	2.2308	2.3932	2.4946	2.4988	2.4989	2.4960	2.4970	2.4901	2.4993	2.5013	2.4952	2.5064
TT-150	2.2361	2.3867	2.4934	2.5020	2.4992	2.5001	2.4958	2.4966	2.4977	2.5004	2.4998	2.5087
TT-200	2.3161	2.4640	2.5838	2.5946	2.5962	2.5924	2.5928	2.5916	2.5938	2.5927	2.5889	2.6007
WA-100	2.0330	2.1161	2.2538	2.2673	2.2657	2.2737	2.2765	2.2760	2.2780	2.2773	2.2765	2.2807
WA-150	2.2517	2.3279	2.4779	2.4977	2.5002	2.5067	2.5097	2.5101	2.5133	2.5150	2.5148	2.5195
WA-200	1.7256	1.7885	1.8830	1.8975	1.8968	1.9025	1.9043	1.9026	1.9049	1.9075	1.9070	1.9112

5.5.Sample shrinkage tables

Table 5.3 weight and dimensions changes by putting in the oven for 3 hours

Sample number	ID code	After drying and before putting in the oven				After removing from oven			
		Weight (gr)	Size (mm)			Weight (gr)	Size (mm)		
			L	R	T		L	R	T
1	D-W-3h-25c-1	2.6634	19.52	12.75	16.9	-	-	-	-
2	D-W-3h-25c-2	1.9741	16.95	12.20	16.00	-	-	-	-
3	D-W-3h-25c-3	1.8328	17.45	12.35	14.75	-	-	-	-
4	D-W-3h-100c-1	2.3260	17.05	12.25	17.30	2.2787	17.05	12.20	17.20
5	D-W-3h-100c-2	2.4366	18.85	13.00	16.60	2.3871	18.85	12.90	16.50
6	D-W-3h-100c-3	1.9738	18.85	11.75	15.05	1.9349	18.85	11.65	15.00
7	D-W-3-125c-1	2.6335	18.95	12.55	17.30	2.5695	18.95	12.50	17.20
8	D-W-3h-125c-2	2.4666	19.25	12.70	16.65	2.4069	19.25	12.60	16.55
9	D-W-3h-125c-3	2.0897	19.20	12.10	15.10	2.0396	19.20	12.00	15.00
10	D-W-3-150c-1	2.4613	17.95	12.70	17.20	2.3838	17.95	12.60	17.15
11	D-W-3h-150c-2	2.4708	19.10	12.45	16.85	2.3935	19.10	12.35	16.75
12	D-W-3h-150c-3	2.0829	18.84	12.05	15.20	2.0188	18.85	11.95	15.10
13	D-W-3h-175c-1	2.3750	18.30	12.50	16.45	2.2917	18.30	12.35	16.35
14	D-W-3h-175c-2	2.4444	18.75	12.85	16.50	2.3557	18.75	12.70	16.35
15	D-W-3h-175c-3	2.0728	19.25	12.20	14.70	1.9989	19.25	12.10	14.60
16	D-W-3h-200c-1	2.7233	19.10	12.95	17.05	2.5942	19.10	12.72	16.90
17	D-W-3h-200c-2	2.5825	19.40	12.75	16.85	2.464	19.40	12.60	16.70
18	D-W-3h-200c-3	2.1050	18.80	12.25	15.00	2.0024	18.75	12.05	14.85
19	D-W-3h-225c-1	2.3629	18.90	12.82	15.35	2.1763	18.88	12.45	15.02
20	D-W-3h-225c-2	2.5248	19.36	13.02	16.60	2.3202	19.32	12.60	16.20
21	D-W-3h-225c-3	2.0770	19.39	12.10	14.65	1.8962	19.33	11.67	14.29

Table 5.4 weight and dimensions changes by putting in the oven for 24 hours

Sample number	ID code	After drying and before putting in the oven				After removing from oven			
		weight (gr)	size (mm)			weight (gr)	size (mm)		
			L	R	T		L	R	T
22	D-W-24h-25-1	2.0678	18.60	12.20	15.45	-	-	-	-
23	D-W-24h-25-2	1.5354	17.72	11.20	13.75	-	-	-	-
24	D-W-24h-25-3	2.1302	17.95	12.30	16.75	-	-	-	-
25	D-W-24h-100-1	1.7752	18.20	11.65	15.65	1.7375	18.20	11.60	15.60
26	D-W-24h-100-2	1.7768	19.75	12.60	14.00	1.7390	19.75	12.50	13.95
27	D-W-24h-100-3	1.9801	18.80	12.80	17.10	1.9387	18.85	11.75	17.00
28	D-W-24h-125c-1	1.9465	19.95	12.25	15.00	1.8849	19.95	12.15	14.85
29	D-W-24h-125c-2	1.6543	18.10	12.35	14.70	1.6028	18.10	12.25	14.65
30	D-W-24h-125c-3	2.0873	17.85	12.80	17.10	2.0235	17.80	12.70	16.95
31	D-W-24h-150c-1	1.9905	19.15	12.30	15.45	1.9215	19.15	12.20	15.30
32	D-W-24h-150c-2	1.8956	19.65	12.55	14.75	1.8268	19.60	12.45	14.65
33	D-W-24h-150c-3	2.3660	19.45	12.95	17.25	2.2816	19.45	12.80	17.15
34	D-W-24h-175c-1	2.0686	19.30	12.55	15.60	1.9714	19.30	12.35	15.40
35	D-W-24h-175c-2	1.8368	18.80	12.60	14.75	1.7489	18.75	12.40	14.60
36	D-W-24h-175c-3	2.3036	19.05	12.90	17.30	2.1911	19.00	12.70	17.10
37	D-W-24h-200c-1	2.0176	18.85	12.55	15.65	1.7843	18.80	12.05	15.10
38	D-W-24h-200c-2	1.8603	19.50	12.65	14.65	1.6714	19.40	12.23	14.30
39	D-W-24h-200c-3	2.1703	18.25	12.70	17.20	1.9426	18.25	12.28	16.70
40	D-W-24h-225c-1	1.9272	18.70	12.49	15.49	1.4577	18.56	11.16	14.00
41	D-W-24h-225c-2	1.8092	18.35	12.90	14.41	1.3480	18.37	11.47	13.08
42	D-W-24h-225c-3	2.2565	18.79	13.01	16.55	1.6564	18.72	11.54	14.84

5.6. Water absorption tables

Table 5.5 The 3h heat treated samples, weight and dimension changes

Sample number	ID code	initial condition after drying				4 weeks (672h)				4 weeks + vacuum (768h)			
		weight (gr)	size (mm)			weight (gr)	size (mm)			weight (gr)	size (mm)		
			L	R	T		L	R	T		L	R	T
1	D-W-3h-25c-1	2.6634	19.52	12.75	16.90	5.0600	19.52	14.10	18.02	5.5106	19.54	14.15	18.04
2	D-W-3h-25c-2	1.9741	16.95	12.20	16.00	3.8821	16.98	13.46	17.04	4.2237	17.05	13.51	17.04
3	D-W-3h-25c-3	1.8316	17.45	12.35	14.75	3.6715	17.42	13.64	15.65	3.9991	17.42	13.75	15.70
4	D-W-3h-100c-1	2.3260	17.10	12.20	17.20	4.6317	17.04	13.56	18.40	4.9010	17.06	13.60	18.44
5	D-W-3h-100c-2	2.4366	18.90	12.90	16.50	4.9362	18.87	14.32	17.62	5.2657	18.88	14.37	17.62
6	D-W-3h-100c-3	1.9738	18.90	11.65	15.00	3.9870	18.90	13.04	15.88	4.2709	18.95	13.05	15.90
7	D-W-3-125c-1	2.6335	18.95	12.50	17.20	5.1533	19.00	13.90	18.30	5.5069	19.06	13.94	18.35
8	D-W-3h-125c-2	2.4666	19.25	12.60	16.55	4.9204	19.27	14.01	17.56	5.2817	19.33	14.03	17.59
9	D-W-3h-125c-3	2.0897	19.20	12.00	15.00	4.2176	19.24	13.39	15.92	4.5380	19.30	13.40	15.94
10	D-W-3-150c-1	2.4613	17.95	12.60	17.15	4.8493	17.94	14.06	18.28	5.1578	17.94	14.10	18.32
11	D-W-3h-150c-2	2.4708	19.10	12.35	16.75	4.9571	19.07	13.80	17.80	5.2808	19.16	13.83	17.79
12	D-W-3h-150c-3	2.0829	18.85	11.95	15.10	4.1390	18.90	13.33	16.04	4.4650	18.93	13.39	16.06
13	D-W-3h-175c-1	2.3750	18.30	12.35	16.35	4.6323	18.30	13.86	17.45	4.9224	18.38	13.88	17.50
14	D-W-3h-175c-2	2.4444	18.75	12.70	16.35	4.7294	18.84	14.14	17.46	5.0693	18.87	14.19	17.48
15	D-W-3h-175c-3	2.0728	19.25	12.10	14.60	4.0629	19.24	13.45	15.55	4.3533	19.31	13.52	15.53
16	D-W-3h-200c-1	2.7233	19.10	12.72	16.90	5.0826	19.14	14.17	17.96	5.4211	19.15	14.22	17.96
17	D-W-3h-200c-2	2.5825	19.40	12.60	16.70	5.0110	19.40	13.96	17.69	5.3151	19.52	14.00	17.71
18	D-W-3h-200c-3	2.1050	18.80	12.05	14.85	4.1436	18.80	13.34	15.69	4.3940	18.86	13.39	15.70
19	D-W-3h-225c-1	2.3629	18.88	12.45	15.02	4.6070	18.86	13.64	15.98	4.7500	18.88	13.67	15.99
20	D-W-3h-225c-2	2.5248	19.32	12.60	16.20	5.0530	19.30	13.78	17.08	5.2048	19.30	13.79	17.10
21	D-W-3h-225c-3	2.0770	19.33	11.67	14.29	4.1789	19.33	12.64	15.05	4.2914	19.38	12.69	15.06

Table 5.6 The 24h heat treated samples, weight and dimension changes

Sample number	ID code	initial condition after drying				4 weeks (672h)				4 weeks + vacuum (768h)			
		weight	size (mm)			weight	size (mm)			weight	size (mm)		
		(gr)	L	R	T	(gr)	L	R	T	(gr)	L	R	T
22	D-W-24h-25-1	2.0637	18.60	12.20	15.45	4.13	18.62	13.53	16.46	4.5245	18.64	13.57	16.43
23	D-W-24h-25-2	1.5321	17.72	11.20	13.75	3.1785	17.78	12.46	14.58	3.4827	17.80	12.47	14.61
24	D-W-24h-25-3	2.1256	17.95	12.30	16.75	4.1186	17.88	13.53	17.79	4.5811	17.90	13.57	17.81
25	D-W-24h-100-1	1.7752	18.25	11.60	15.60	3.6028	18.32	12.88	16.6	3.8650	18.35	12.98	16.60
26	D-W-24h-100-2	1.7768	19.80	12.50	13.95	3.609	19.75	13.85	14.78	3.9653	19.73	13.88	14.78
27	D-W-24h-100-3	1.9801	18.85	11.75	17.00	3.826	18.78	13.02	18.08	4.2334	18.78	13.07	18.12
28	D-W-24h-125c-1	1.9465	19.90	12.15	14.85	3.8743	19.91	13.54	15.75	4.1948	19.88	13.57	15.75
29	D-W-24h-125c-2	1.6543	18.00	12.25	14.65	3.4068	18.02	13.6	13.46	3.6980	17.99	13.65	15.47
30	D-W-24h-125c-3	2.0873	17.80	12.70	16.95	4.0927	17.87	14.05	18.02	4.4629	17.90	14.06	18.07
31	D-W-24h-150c-1	1.9905	19.15	12.20	15.30	3.8623	19.14	13.55	16.36	4.2101	19.21	13.73	16.32
32	D-W-24h-150c-2	1.8956	19.60	12.45	14.65	3.8202	19.72	13.82	15.5	4.1628	19.64	13.85	15.53
33	D-W-24h-150c-3	2.366	19.45	12.80	17.15	4.5858	19.49	14.18	18.2	4.9799	19.51	14.20	18.18
34	D-W-24h-175c-1	2.0686	19.30	12.35	15.40	3.924	19.32	13.62	16.33	4.2700	19.36	13.66	16.38
35	D-W-24h-175c-2	1.8368	18.75	12.40	14.60	3.6264	18.62	13.7	15.39	3.9431	18.76	13.73	15.42
36	D-W-24h-175c-3	2.3036	19.00	12.70	17.10	4.3756	19.04	13.98	18.11	4.7599	19.05	13.99	18.14
37	D-W-24h-200c-1	2.0176	18.85	12.05	15.10	3.8929	18.92	13.08	15.92	4.0879	18.86	13.10	15.94
38	D-W-24h-200c-2	1.8603	19.50	12.23	14.30	3.8193	19.47	13.27	15	3.9809	19.50	13.30	15.01
39	D-W-24h-200c-3	2.1703	18.25	12.28	16.70	4.2141	18.28	13.27	17.61	4.4372	18.28	13.30	17.61
40	D-W-24h-225c-1	1.9272	18.56	11.16	14.00	3.2759	18.58	11.28	15.1				
41	D-W-24h-225c-2	1.8092	18.37	11.47	13.08	3.1419	18.46	11.58	13.94				
42	D-W-24h-225c-3	2.2565	18.72	11.54	14.84	3.8162	18.74	12	15.88				

5.7. The effect of the sample shape and ways to keep the sample between clamps

Three different types of specimens are considered to observe the behavior of the samples in tensile test. The first type, a bone shape sample, was prepared based on ISO 22157 [84]. For this type, the longitudinal cracks start to propagation from the narrow part of specimen toward the clamps. Followed by each crack observed a decrease in tensile strength but the hardening is continued to ultimate strength by tensile failure mechanism as can be seen in Figure 5.4. Bone shape sample is not proper for short lengths due to crack initiation from the connection between thick and thin parts as can be seen in Figure 5.4.

Figure 5.4 Longitudinal cracks initiation and propagation in tensile samples from left to right

For the second type, based on ASTM D3039 [28] a strip of bamboo with thickness about 2 mm and width equal to wall thickness of bamboo is used to compare with the bone shape. Also two different ways to keep the specimens with clamp is considered, one by aluminum plates glued to the ends of the specimens; the other by innovative use of doubled sandpaper between the clamp and specimen as shown in Figure 5.6. The tensile tests realized by using doubled sandpaper as can be seen in Figure 5.7 shows higher resistance comparing with the samples used aluminum plate. For the heat subjected specimens only the sandpaper will be used as the spacer between specimen and clamp.

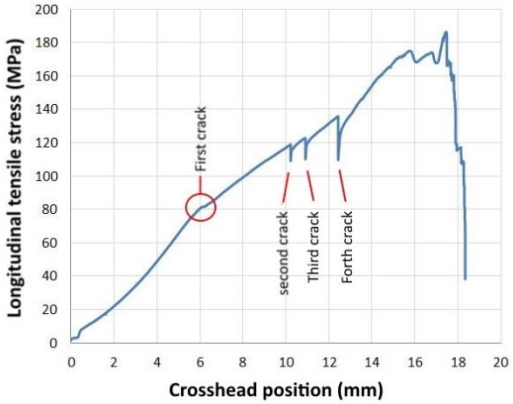

Figure 5.5 Longitudinal cracks initiation and propagation in tensile

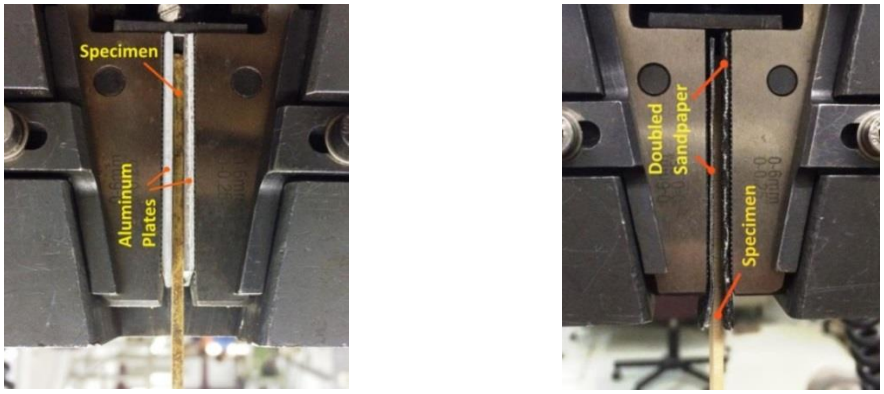

(a) aluminum plate (b) sandpaper

Figure 5.6 Using two different spacers between specimen and clamp

Figure 5.7 Bamboo strip sample with clip gauge at the middle of samples

The bone shape sample shows more deflection comparing to the strip samples by using the sandpapers as spacer but the ultimate resistance of both are close with difference about 10%. Hence, in present thesis, the strips of bamboo will be used as can be seen in Figure 5.7.

5.8.The tensile test results

Table 5.7 The results of the tensile test samples treated in 3 hours

number	ID code	b (mm)	t (mm)	W_0 (gr)	W_d (gr)	δW (gr)	σ_s	σ_{ave}	SD	E_s	E_{ave}	SD
1	T-25-1	16.32	2.3				237.7			19.3		
2	T-25-2	14.5	2.44	18.078	16.328	10.7	240.4	247.6	14.8	25.9	22.8	3.3
3	T-25-3	12.96	2.32				264.6			23.2		
4	T-100-3h-1	15.2	2.22				254.1			22.5		
5	T-100-3h-2	13.8	2.26	15.201	13.920	9.2	206.2	237.3	26.9	18.0	21.5	3.1
6	T-100-3h-3	12.78	2.1				251.5			24.0		
7	T-125-3h-1	16.32	2.18				269.3			18.8		
8	T-125-3h-2	14.5	2.4	16.891	15.476	9.1	228.9	264.4	33.3	21.4	19.7	1.5
9	T-125-3h-3	12.84	2.06				294.9			19.0		
10	T-150-3h-1	15.28	2.22				243.1			20.4		
11	T-150-3h-2	13.78	2.26	15.845	14.125	12.2	241.1	229.6	21.7	21.3	20.2	1.2
12	T-150-3h-3	13.92	2.26				204.6			19.0		

Continue of Table 5.7

number	ID code	b (mm)	t (mm)	W_0 (gr)	W_d (gr)	δW (gr)	σ_s	σ_{ave}	SD	E_s	E_{ave}	SD
13	T-175-3h-1	15.78	2.26	6.150	15.704	10.8	171.3	198.0	23.2	16.3	19.5	2.9
14	T-175-3h-2	15.02	2.32	6.420			213.5			21.7		
15	T-175-3h-3	12.8	2.16	4.837			209.2			20.6		
16	T-200-3h-1	15.96	2.1	5.940	16.485	10.1	111.0	127.8	14.7	19.8	22.3	2.6
17	T-200-3h-2	15.2	2.36	6.737			134.0			25.0		
18	T-200-3h-3	13.3	2.2	5.465			138.3			22.1		
19	T-200-8h-1	14.82	2.1	5.275	14.230	9.0	59.5	86.7	26.8	20.5	23.6	5.9
20	T-200-8h-2	13.16	2.24	5.353			87.7			30.4		
21	T-200-8h-3	12.82	2.08	4.884			113.0			19.9		
22	T-225-3h-1	14.7	2.02	4.887	14.912	-2.4	51.9	69.6	15.5	17.5	19.9	2.1
23	T-225-3h-2	13.84	2.24	5.369			76.4			21.0		
24	T-225-3h-3	12.1	2.08	4.298			80.5			21.2		

Table 5.8 The results of the tensile test samples treated in 24 hours

Sample number	ID code	b (mm)	t (mm)	W_0 (gr)	W_d (gr)	δW (%)	σ_s	σ_{ave}	SD	E_s	E_{ave}	SD
1	T-25-d-1	14.96	2.12				237.8			21.7		
2	T-25-d-2	13.20	2.30		15.047		228.4	249.9	29.4	23.1	22.7	0.9
3	T-25-d-3	12.06	2.00				283.4			23.4		
4	T-100-24h-1	16.06	2.14	5.875			259.5			18.4		
5	T-100-24h-2	14.28	2.32	5.363	14.602	10.8	231.4	256.3	23.5	21.5	20.2	1.6
6	T-100-24h-3	13.26	2.10	4.940			278.1			20.9		
7	T-125-24h-1	15.70	2.12	5.727			258.0			18.3		
8	T-125-24h-2	13.56	2.32	4.919	14.327	10.6	221.1	248.9	24.6	16.9	18.3	1.4
9	T-125-24h-3	13.04	2.16	5.195			267.6			19.7		
10	T-150-24h-1	15.48	2.30	6.170			193.5			25.2		
11	T-150-24h-2	14.50	2.30	5.792	15.329	10.0	186.6	190.6	3.5	27.8	24.6	3.4
12	T-150-24h-3	13.42	2.08	4.904			191.5			21.0		
13	T-175-24h-1	15.40	2.16	5.991			106.5			20.4		
14	T-175-24h-2	14.52	2.32	5.436	14.436	9.7	97.7	106.5	8.7	17.0	22.8	7.2
15	T-175-24h-3	12.56	2.04	4.410			115.2			30.8		
16	T-200-24h-1	15.14	2.02				31.8			16.4		
17	T-200-24h-2	13.44	2.22				39.0	46.8	20.0	26.3	21.3	4.9
18	T-200-24h-3	12.26	2.08				69.5			21.2		

5.9. Transversal tensile tables

Table 5.9 Test results for three groups of transversal tensile test with different average thickness

group	sample	t (mm)	b (mm)	F (N)	σ_{uTT} (Mpa)	$\bar{\sigma}_{uTT}$ (Mpa)	S.D. (Mpa)
one	TT1	18.55	3.54	461.1	6.98	6.35	0.67
	TT2	18.82	5.34	569.9	5.64		
	TT3	18.70	4.01	484.8	6.42		
two	TT4	16.00	3.28	221.3	4.16	5.14	1.03
	TT5	15.80	3.18	315.3	6.22		
	TT6	16.40	3.08	258.1	5.05		
three	TT7	14.12	6.15	549.2	6.32	6.78	0.49
	TT8	14.00	4.90	460.8	6.72		
	TT9	14.00	5.00	510.2	7.29		
average	-	-	-	-	6.09		

Table 5.10 Heat treated transversal tensile samples in 3 hours

Sample ID	t (mm)	b (mm)	F (N)	σ_{max} (Mpa)	σ_{ave} (Mpa)	S.D. (Mpa)
TT-25-1	17.04	7.26	725	5.9	5.5	1.0
TT-25-2	14.04	7.04	624	6.3		
TT-25-3	12.9	7.24	407	4.4		
TT-100-3h-1	16.76	7.22	706	5.8	5.7	0.7
TT-100-3h-2	13.84	6.9	607	6.4		
TT-100-3h-3	13.2	7.08	456	4.9		
TT-125-3h-1	16.34	7.1	740	6.4	5.2	1.6
TT-125-3h-2	13.82	7.2	585	5.9		
TT-125-3h-3	12.84	7.08	302	3.3		
TT-150-3h-1	16.2	7.42	728	6.1	6.0	0.5
TT-150-3h-2	13.82	7.28	654	6.5		
TT-150-3h-3	12.96	6.34	452	5.5		
TT-175-3h-1	16	6.98	477	4.3	4.7	0.4
TT-175-3h-2	13.52	6.9	480	5.1		
TT-175-3h-3	13	7.12	439	4.7		
TT-200-3h-1	15.66	7.18	316	2.8	3.0	0.3
TT-200-3h-2	13.4	7.06	260	2.8		
TT-200-3h-3	12.26	6.8	280	3.4		
TT-225-3h-1	15.74	7.1	51	0.5	0.6	0.3
TT-225-3h-2	12.7	6.96	38	0.4		
TT-225-3h-3	11.7	6.64	74	0.9		

Table 5.11 Heat treated transversal tensile samples in 24 hours

Sample ID	t (mm)	b (mm)	F (N)	σ_{max} (Mpa)	σ_{ave} (Mpa)	S.D. (Mpa)
TT-100-24h-1	16.98	7.62	850	6.6	5.9	0.8
TT-100-24h-2	13.96	6.80	580	6.1		
TT-100-24h-3	13.30	7.08	475	5.0		
TT-125-24h-1	15.80	7.16	537	4.8	4.2	0.5
TT-125-24h-2	14.55	7.00	381	3.7		
TT-125-24h-3	13.50	6.86	375	4.0		
TT-150-24h-1	16.50	7.16	470	4.0	4.4	0.4
TT-150-24h-2	14.40	7.08	468	4.6		
TT-150-24h-3	12.52	6.80	395	4.6		
TT-175-24h-1	16.50	7.00	250	2.2	2.4	0.2
TT-175-24h-2	14.14	6.88	235	2.4		
TT-175-24h-3	12.48	6.84	225	2.6		
TT-200-24h-1	15.38	7.06	57	0.5	0.6	0.1
TT-200-24h-2	13.38	7.04	66	0.7		
TT-200-24h-3	11.74	6.66	45	0.6		

5.10. The effect of test machine on the compression tests

There are two different test machines which can be used for the compression test. The first group of the tests with 5 specimens has been implemented by the compression test machine with a 500 kN MTS actuator which mounted on a rigid handmade frame in structure laboratory as can be seen in Figure 5.8. Due to the long neck of the movable compression part and lacking a proper support to prevent the lateral movements, 4 of 5 samples ruptured due to horizontal movement of upper clamp. The result of the tests presented in Figure 5.9. The C-5 is the only sample that rupture happened without movement of upper clamp but for the four others happened in the mode (a) presented in Figure 3.124 [123].

Figure 5.8 Compression test machine with 500 kN MTS actuator

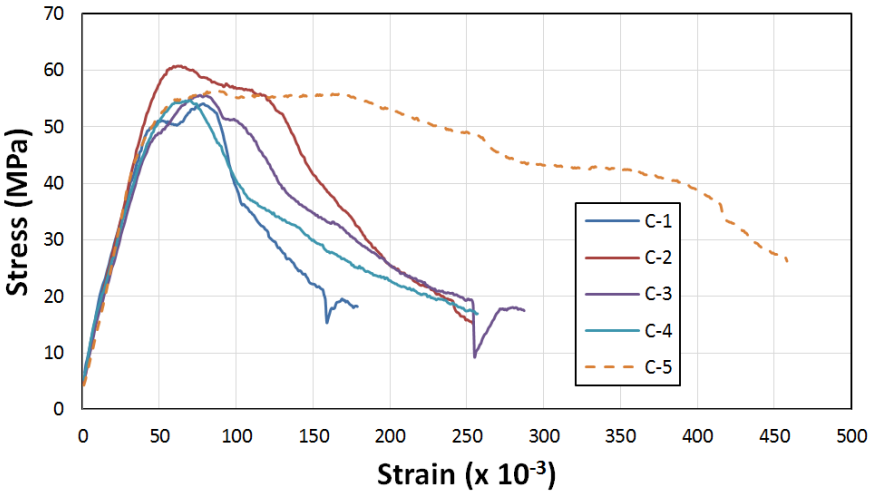

Figure 5.9 The stress-strain curves for initial compression tests has been done by MTS machine

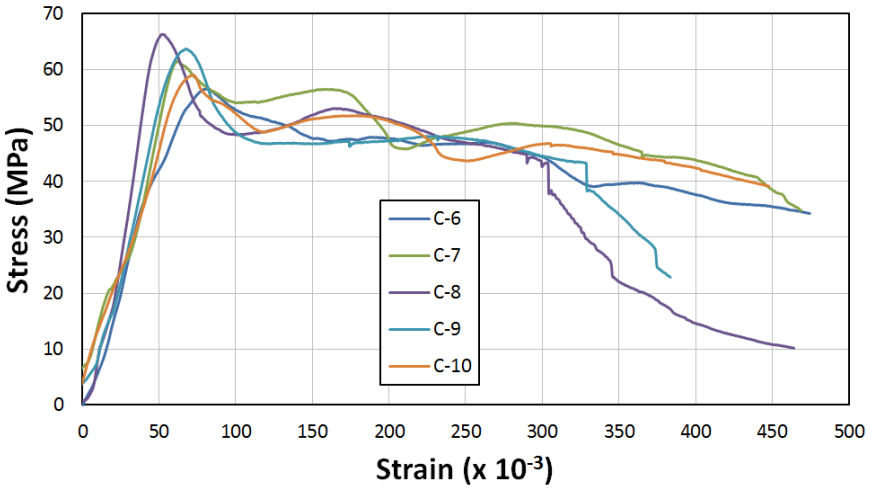

Figure 5.10 The stress-strain curves for initial compression tests has been done by INSTRON machine model 5500R in the structure laboratory of PUC-Rio

The same tests have been done in ITUC, by the INSTRON machine model 5500R to compare the results with the samples C-1 to C-5 accomplished by MTS. The 5 similar samples have been used for this purpose. The geometrical properties of the samples have been mentioned in Table 5.12 and Table 5.13. The result of the tests has been demonstrated in Figure 5.10.

Table 5.12 Geometrical property of the initial compression tests for MTS machine

Sample	L (mm)	L_e (mm)	t (mm)	b (mm)	A (mm^2)	r (mm)	$\lambda = \frac{k.L_e}{r}$
C-1			15.0	2.1	31.5	0.61	16.5
C-2			15.1	2.8	42.3	0.81	12.4
C-3	40	10	14.8	2.8	41.4	0.81	12.4
C-4			15.1	2.7	40.8	0.78	12.8
C-5			14.9	3.1	46.2	0.89	11.2

Table 5.13 Geometrical property of the initial compression tests for INSTRON machine

Sample	L (mm)	L_e (mm)	B (mm)	T (mm)	A (mm^2)	r (mm)	$\lambda = \frac{k.L_e}{r}$
C-6			13.34	2.58	34.42	0.74	6.7
C-7			13.70	2.28	44.94	0.95	5.3
C-8	40	10	13.46	2.70	36.34	0.78	6.4
C-9			13.25	2.36	31.27	0.68	7.3
C-10			13.20	2.70	35.64	0.78	6.4

The results of test with MTS and INSTRON presented in Table 5.14 shows higher resistance for the samples tested by INSTRON. A single factor ANOVA shows that there is a meaningful relevancy between the test results and machines. It means that the results of the MTS machine (which are about 8% less than the

INSTRON) are not acceptable. The test for both MTS and INSTRON samples carried out in EMC condition.

Table 5.14 Ultimate Compressive Strength (UCS) of two groups of samples tested by MTS and INSTRON machines

Group	Sample	UCS (MPa)	Average (MPa)	S.D. (MPa)	Max (MPa)	Min (MPa)	Machine
one	CP-1	54.09	56.31	6.99	60.77	54.09	MTS
	CP-2	60.77					
	CP-3	55.58					
	CP-4	54.70					
	CP-5	56.39					
two	CP-6	56.56	61.41	14.62	66.31	56.56	INSTRON
	CP-7	61.46					
	CP-8	66.31					
	CP-9	63.70					
	CP-10	59.02					

5.10.1.Compression tests of heat treated samples

Table 5.15 Compression test for heat treated samples during 3 hours

Sample number	ID code	b (mm)	t (mm)	W_0 (gr)	W_d (gr)	δW (%)	σ_{max}	σ_{ave}	SD
1	C-25-1	17.22	2.28	-	-	-	62.96	60.2	4.9
2	C-25-2	18.06	2.19				63.02		
3	C-25-3	18.09	2.36				54.49		
4	C-100-3h-1	18.34	2.6	3.274	2.952	10.9	54.94	60.0	4.9
5	C-100-3h-2	17.72	2.44				64.73		
6	C-100-3h-3	17.88	2.22				60.48		
7	C-125-3h-1	18.18	2.36	3.031	2.734	10.9	48.35	52.7	5.7
8	C-125-3h-2	17.82	2.34				50.69		
9	C-125-3h-3	17.7	2.22				59.19		
10	C-150-3h-1	18.17	2.3	3.286	2.971	10.6	53.17	58.9	5.1
11	C-150-3h-2	18.35	2.42				60.66		
12	C-150-3h-3	18	2.2				62.96		
13	C-175-3h-1	16.6	2.24	2.902	2.632	10.3	62.18	58.6	5.9
14	C-175-3h-2	17.62	2.06				51.78		
15	C-175-3h-3	17.7	2.24				61.74		
16	C-200-3h-1	17	2.24	2.950	2.685	9.9	67.43	63.1	7.2
17	C-200-3h-2	16.73	2.14				54.82		
18	C-200-3h-3	16.66	2.2				67.06		
19	C-225-3h-1	15.65	2.12	2.656	2.431	9.3	71.13	65.0	7.4
20	C-225-3h-2	16.95	2.03				56.79		
21	C-225-3h-3	15.65	2.02				67.23		

Table 5.16 Compression test for heat treated samples during 24 hours

Sample number	ID code	b (mm)	t (mm)	W_0 (gr)	W_d (gr)	δW (%)	σ_{max}	σ_{ave}	SD
1	C-25-d-1	16.78	2.14	3.271	2.951	10.8	151.0	151.9	8.8
2	C-25-d-2	17.10	2.18				143.6		
3	C-25-d-3	16.64	2.10				161.1		
4	C-100-24h-1	17.30	2.40	3.051	2.754	10.8	56.2	57.2	0.9
5	C-100-24h-2	17.30	2.38				57.6		
6	C-100-24h-3	18.10	2.33				57.9		
7	C-125-24h-1	17.30	2.02	2.913	2.648	10.0	61.3	62.2	4.5
8	C-125-24h-2	18.34	2.28				67.2		
9	C-125-24h-3	17.02	2.16				58.3		
10	C-150-24h-1	16.70	2.33	3.378	3.076	9.8	67.2	68.7	2.0
11	C-150-24h-2	18.04	2.30				71.0		
12	C-150-24h-3	17.54	2.35				67.9		
13	C-175-24h-1	17.60	2.00	3.241	2.951	9.8	71.5	77.9	7.8
14	C-175-24h-2	17.91	2.25				86.6		
15	C-175-24h-3	17.52	2.26				75.7		
16	C-200-24h-1	15.88	2.14	-	-	-	58.4	52.6	5.9
17	C-200-24h-2	16.15	2.04				46.7		
18	C-200-24h-3	16.00	2.14				52.6		

5.11.Shear tests

5.11.1. Rigid body analysis of longitudinal shear test

Figure 5.11a shows a free body diagram of a longitudinal shear specimen with tensile load. Theoretically, when the load exerted at the mid-section of a rigid body only produces pure shear at the shear surface. At the face AB in Figure 5.11b in addition to the tensile force there is a moment equal to $M = \frac{T.w}{4}$. The result of super positioning the bending and tensile stresses shows that the point B is in compression and point A in tensile stress as can be seen in Figure 5.11c.

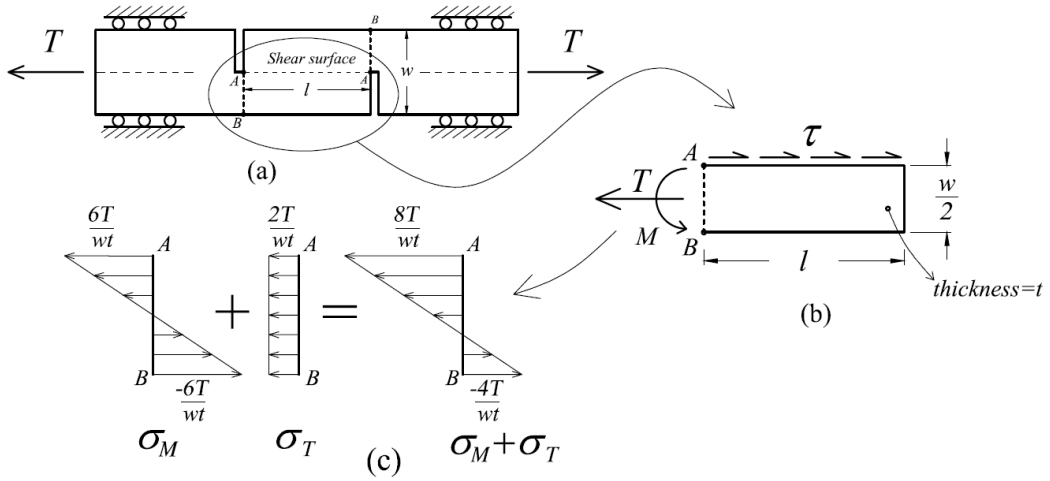

Figure 5.11 a) rigid sample within slide supports with pure shear at the shear surface; b) equilibrium between force, bending at shear surface area; c) The bending and stress in face AB

When the two end cut points of notches finished at the middle of the section there is not any overlapping distance as can be seen Figure 5.12a but when the opposite notches pass from mid-line, makes an overlapping distance as can be seen in Figure 5.12b. It creates an additional moment at the shear surface which can add a splitting tension component consequently. This type of failure cannot represent the real longitudinal shear strength and the obtained results are less than the expected values.

Figure 5.13 shows deformation of the sample and crack initiation. The notches of the sample presented in

Figure 5.13 have been beveled for better observation.

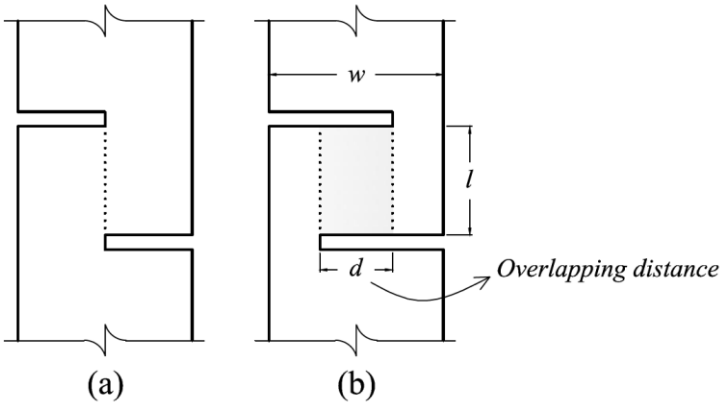

Figure 5.12 a) without overlapping distance; b) with overlapping distance

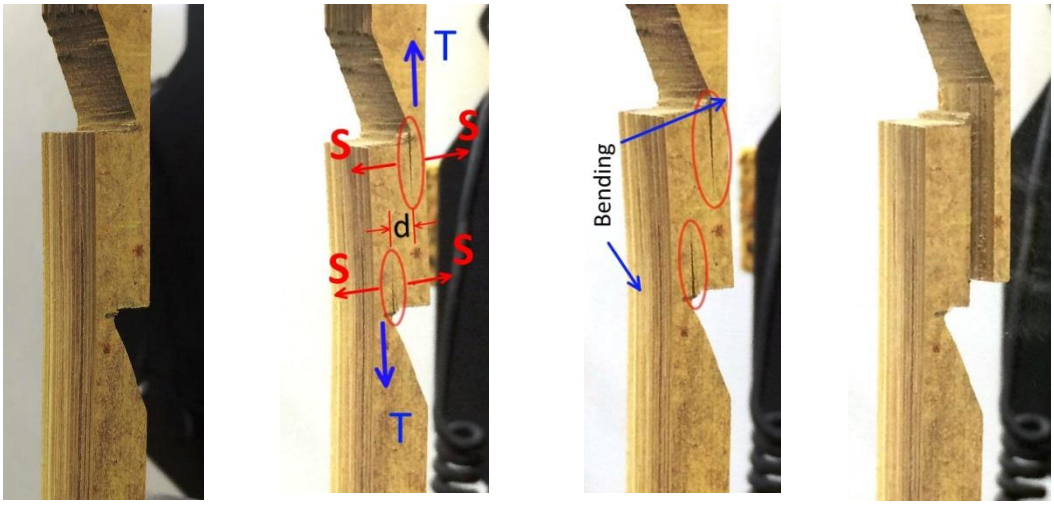

(a) start of loading (b) cracks initiation (c) crack propagation (d) failure

Figure 5.13 The shear test steps up to failure due to combination of a transversal tensile stress and longitudinal shear stress

By considering the shear zone as a rigid body shown in Figure 5.14, the values of $\bar{\tau}_V$, M_H, M_V, σ_T, σ_H, σ_V based on geometry and value of the tensile force (T) are obtained and demonstrated in Table 5.17.

When (d=0) the values of σ_V and M_V are zero (σ_V can be called the splitting tension) then by removing the distance (d) the effect of additional moment (M_V) is eliminated. The value of M_H in Figure 5.14 can be converted to tension which shows a vertical tensile stress at point A equal to $\sigma_T + \sigma_H = \frac{8T}{w-d}$ which increases by increasing the (d). This moment (M_H) as mentioned before can be the cause of crack initiation and splitting at point A due to bending at face *AB*

Figure 5.13c [109].

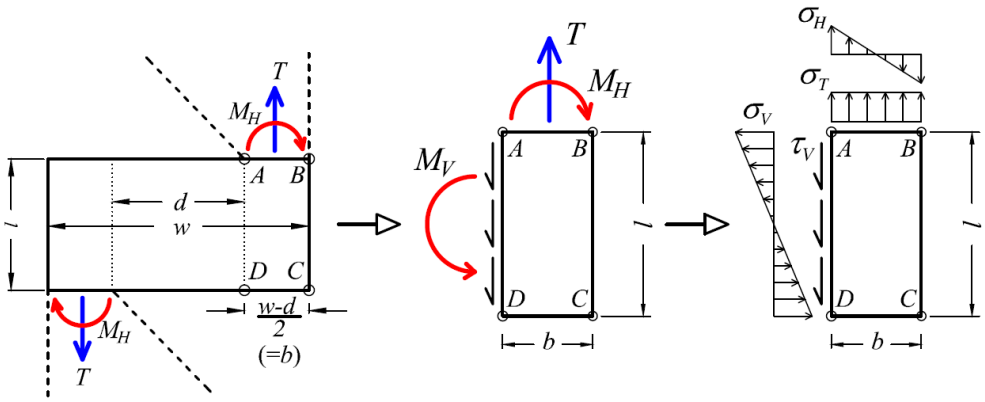

Figure 5.14 Free diagram of force and tension at the shear area by applying tensile load (thickness is considered unit)

By increasing the value of (l) or the distance between notches, the tensile force will be increased and this effect will be intensified. It means by increasing the notch distance in the tests the ultimate shear strength will be reduced. The other parameter is the width of the sample. By increasing this value the value of σ_H will be reduced and this effect can increase the ultimate shear strength.

Table 5.17 the values of tension and moments

Load and stress	$\boldsymbol{d \neq 0}$	$\boldsymbol{d = 0}$
$\bar{\tau}_V$	$\frac{T}{l}$	$\frac{T}{l}$
σ_T	$\frac{2T}{(w-d)}$	$\frac{2T}{w}$
M_H	$T\frac{(w+d)}{4}$	$T\frac{w}{4}$
σ_H	$\frac{6T}{(w-d)}$	$\frac{6T}{w}$
M_V	$T\frac{d}{2}$	0
σ_V	$\frac{3Td}{l^2}$	0

5.11.2. Longitudinal shear test (LSC) by applying Compression load

This test carried out for 12 samples. By applying compression instead of tensile force, the vertical tensile stress will be changed to vertical compression stress, which can prevent to initiate the crack in point A and the results of ultimate shear strength will be higher than the tensile samples with same conditions. In this case the length of the samples is considered as 10 cm with four different notch lengths, 1, 2, 3 and 4 cm.

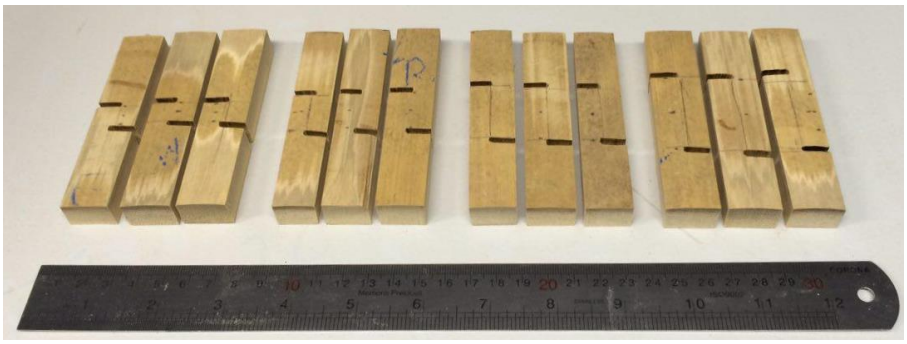

Figure 5.15 The longitudinal shear test samples prepared to apply compression before test

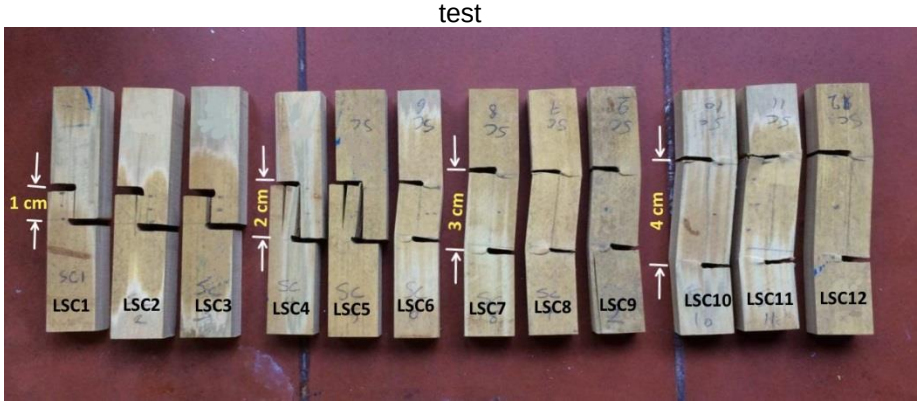

Figure 5.16 The longitudinal shear test samples by applying compression after test

As observed in Figure 5.16 the samples with notch length $d = 1\ cm$ only has one mode of failure which is shear failure. For the samples with $d = 2\ cm$ has two different mode which one is shear and the other is bending and for samples with $d \geq 3\ cm$ only the bending failure mode is happened. The average value of ultimate shear resistance for three samples with notch length $d = 1\ cm$ is 11.2 MPa and the coefficient of variation (CV%) is equal to 2.7% which the related graph has been represented in Figure 5.17.

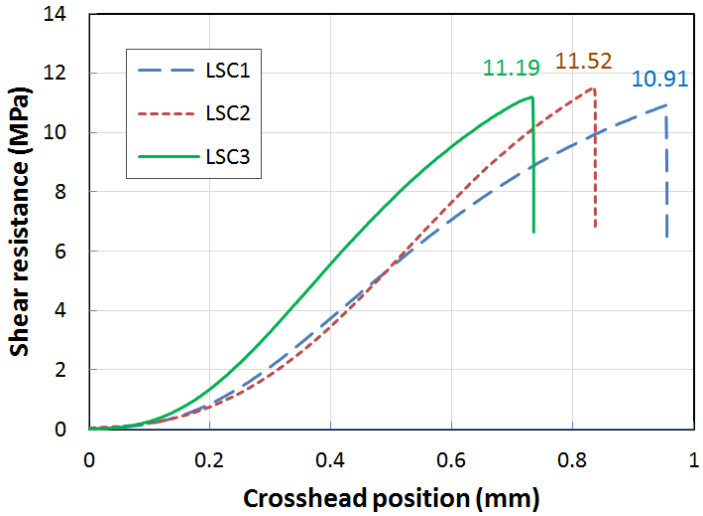

Figure 5.17 Shear resistance for the samples with notch length equal to 1 cm

For the LSC4 to LSC6 which are the samples with 2 cm distance between notches the results shows two different rupture modes. LSC4 is equal to samples LSC1 to LSC3 and its failure is the shear rupture mode with less resistance regarding to LSC1 to LSC3 about 10.62 MPa. LSC5 shows a mix failure mode of bending and longitudinal shear but finally is ruptured by shear. LSC6 is a sample with bending failure mode.

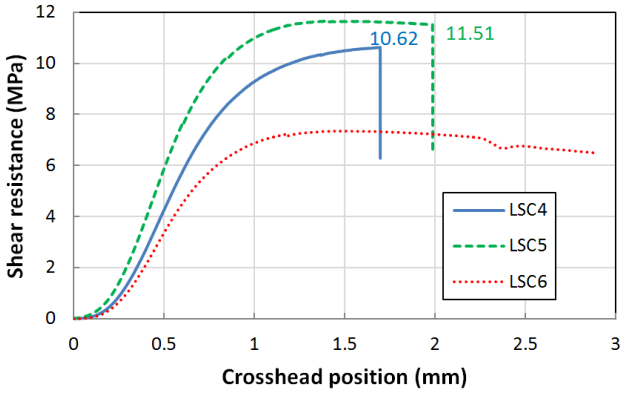

Figure 5.18 Shear resistance for the samples with notch length equal to 2 cm

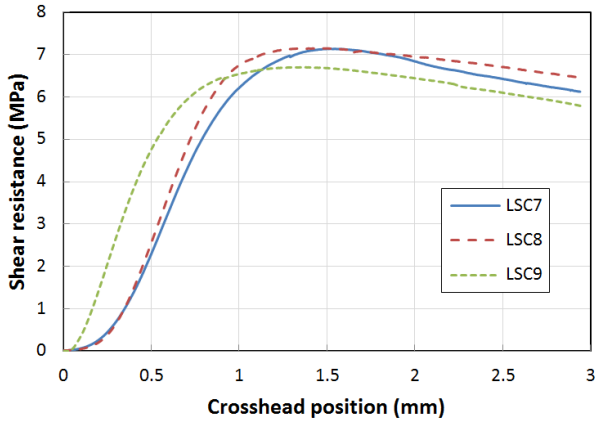

Figure 5.19 Shear resistance for the samples with notch length equal to 3 cm

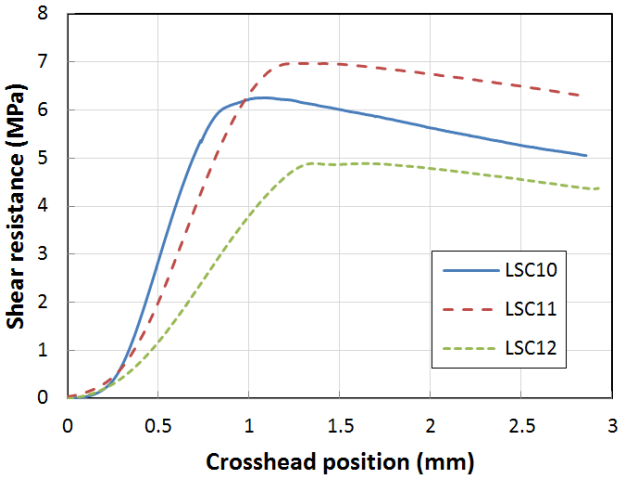

Figure 5.20 Shear resistance for the samples with notch length equal to 4 cm

For the other 6 remained samples from LSC7 to LSC12 with 3 and 4 cm notch distance, the bending failure mode is dominated and none of them fail due to shear rupture as shown in Figure 5.19 and Figure 5.20. Comparing the results obtained by longitudinal shear tensile and compression shows for the same notch length, the results of longitudinal shear with compression are more than longitudinal shear tensile. It happens due to the flexure at the face AB which prevents crack at the shear surface area.

Practically, the less notch distance due to creating less moment at the face (AB) as can be seen in Figure 5.11b give the results which is more close to shear behavior of the specimen due to preventing the excessive deformation. Reducing too much the length of shear surface makes the sample very sensitive to break during the fixing the sample between clamps. The optimum suggested distance between notches which can meet the requirements such as installation the sample and the behavior more close to reality is considered to be 2cm.

5.11.3.Bamboo shear tests tables

Table 5.18 The effect of distance between notchs to tensile shear stress

cut length	Sample code	Max load (N)	l (mm)	t (mm)	Shear stress (Mpa)	SD (Mpa)	Average (Mpa)
1 cm	a1	1058	10.3	10.30	9.97	0.34	9.65
	a2	1131	10.6	11.00	9.70		
	a3	1065	10.2	11.24	9.29		
2 cm	b1	1202	18.4	10.88	6.00	0.50	6.55
	b2	1499	20.2	10.64	6.97		
	b3	1308	18.2	10.78	6.67		
3 cm 3 cut	3cut1	2098	30.4	11.10	6.22	0.93	6.61
	3cut2	2658	30.1	11.52	7.67		
	3cut3	2043	30.3	11.35	5.94		
5 cm	c1	1796	50.16	10.20	3.51	0.19	3.33
	c2	1808	52.64	10.24	3.35		
	c3	1680	52.52	10.22	3.13		
10 cm	d1	3198	101	11.02	2.87	0.02	2.86
	d2	2924	99.2	10.30	2.86		
	d3	3170	100.4	11.12	2.84		

Table 5.19 The tensile shear stress test for heat treated samples within 3 hours

Sample	b (mm)	t (mm)	F (N)	sigma (Mpa)	ave (Mpa)	SD (Mpa)	cv (%)
25°C -EMC-1	20.4	14.7	1874	6.2	5.9	0.8	13.7
25°C -EMC-2	19.6	12.2	1534	6.4			
25°C -EMC-3	19.7	11.1	1082	4.9			
100°C-3h -1	19.6	13.5	1612	6.1	6.1	0.2	3.9
100°C-3h -2	19.9	13.15	1658	6.3			
100°C-3h -3	20.4	11	1315	5.9			
125°C-3h -1	20.2	14	1705	6.0	6.8	1.2	18.2
125°C-3h -2	20.3	13.1	1613	6.1			
125°C-3h -3	20.5	13.5	2264	8.2			
150°C-3h -1	19.7	13.2	1767	6.8	6.8	0.7	10.0
150°C-3h -2	19.7	14.5	2116	7.4			
150°C -3h-3	20.3	12.25	1508	6.1			
175°C -3h-1	20.25	13.4	1541	5.7	5.5	0.4	8.0
175°C -3h-2	19.7	14	1375	5.0			
175°C -3h-3	20.5	12	1425	5.8			
200°C -3h-1	19.8	14.1	952	3.4	3.4	0.2	5.3
200°C -3h-2	20.4	14.35	1040	3.6			
200°C -3h-3	20.2	13	840	3.2			
225°C -3h-1	19.8	12.3	243	1.0	1.5	0.4	29.6
225°C -3h-2	20.1	14	522	1.9			
225°C -3h-3	20.4	11	350	1.6			

Table 5.20 The tensile shear stress test for heat treated samples within 24 hours

Sample	b (mm)	t (mm)	F (N)	sigma (Mpa)	ave (Mpa)	SD (Mpa)	cv (%)
25°C -Dry-1	20.5	13.7	1233	4.39	5.2	0.7	14.4
25°C -Dry-2	19.9	11.95	1250	5.26			
25°C -Dry-3	19.7	10	1157	5.87			
100°C-24h -1	19	13.75	1449	5.55	5.6	1.1	20.5
100°C-24h -2	19.8	12.9	1142	4.47			
100°C-24h -3	20.3	11.6	1592	6.76			
125°C-24h -1	20	13	1597	6.14	6.2	0.1	2.3
125°C-24h -2	19.9	13.2	1618	6.16			
125°C-24h -3	19.4	12.25	1521	6.40			
150°C-24h -1	19.8	12.9	1100	4.31	5.3	0.9	16.7
150°C-24h -2	20	13.4	1500	5.60			
150°C -24h-3	20.1	13	1570	6.01			
175°C -24h-1	20	13.2	632	2.39	3.0	0.6	18.7
175°C -24h-2	19.9	13.5	940	3.50			
175°C -24h-3	20.4	13.2	807	3.00			
200°C -24h-1	20.5	13.5	164	0.59	0.5	0.3	48.0
200°C -24h-2	20.3	13	199	0.75			
200°C -24h-3	20.8	11.8	62	0.25			

5.12.Sonelastic tables

5.12.1. Initial tests

Table 5.21 The DBMOE for *DG* specimens in EMC and dry condition at upward and lateral position

SAMPLE	size			EMC wt. (gr)	Upward MOE (Mpa)	Lateral MOE (Mpa)	Dry wt. (gr)	Upward MOE (Mpa)	Lateral MOE (Mpa)	Humidity (%)	Upward MOE div (%)	Lateral MOE div(%)
	L (mm)	w_{ave} (mm)	t_{ave} (mm)									
B-1	199.50	20.12	18.25	49.334	18.21	18.28	44.477	18.24	18.39	10.92	0.2	0.6
B-2	200.20	19.43	17.62	45.171	18.23	17.95	40.710	18.29	18.08	10.96	0.3	0.7
B-3	202.00	19.71	18.77	47.601	16.23	17.28	42.480	16.53	17.48	12.06	1.8	1.1
M-1	199.80	17.52	15.31	38.099	19.59	20.39	33.790	19.84	20.38	12.75	1.3	0.0
M-2	200.40	16.76	15.37	36.770	19.99	20.78	32.640	20.14	20.85	12.65	0.7	0.3
M-3	197.90	16.74	15.29	35.858	19.73	20.41	31.820	19.94	20.51	12.69	1.1	0.5
T-1	200.10	11.77	11.04	17.710	19.92	20.56	15.727	19.74	20.27	12.61	-0.9	-1.4
T-2	201.20	11.31	11.36	17.729	20.22	21.52	15.817	20.06	21.16	12.09	-0.8	-1.7
T-3	201.50	11.76	10.92	17.704	20	20.93	15.793	19.78	20.63	12.10	-1.1	-1.5

5.13.DBMOE tables for heat treated samples

Table 5.22 DBMOE of untreated samples at EMC and dry condition

SAMPLE	size			Step 1, Untreated at EMC condition			Step 2, Untreated at Dry condition		
	L (mm)	w (mm)	t (mm)	wt. (gr)	Upward MOE (Mpa)	Lateral MOE (Mpa)	wt. (gr)	Upward MOE (Mpa)	Lateral MOE (Mpa)
125C-1	201.7	19.73	18.82	47.428	15.96	16.87	43.177	16.62	17.57
125C-2	201	17.91	17.49	39.182	15.95	16.65	35.505	16.51	17.25
125C-3	202	9.97	10.69	14.285	19.43	20.37	12.773	19.35	20.3
150C-1	200	20.21	18.32	49.507	17.8	17.8	45.156	18.44	18.5
150C-2	200.2	16.63	15.42	36.52	19.91	20.87	33.173	20.38	21.5
150C-3	200.4	11.39	10.81	16.637	20.17	20.07	14.885	20.16	20.1
175C-1	200.5	19.55	19.65	48.22	14.35	16.5	43.702	14.9	17.12
175C-2	200	15.15	15.38	32.252	17.78	20.22	28.937	18.23	20.66
175C-3	201.6	11.68	11.00	17.605	19.65	20.94	15.984	19.81	21.2
200C-1	200.8	19.30	18.69	45.921	15.66	16.47	41.239	16.37	16.4
200C-2	203	16.69	14.81	33.996	18.48	18.58	30.459	18.92	19.11
200C-3	200.5	11.28	11.41	17.627	19.75	21.12	16.006	19.92	21.29
225C-1	198.5	19.05	16.72	40.509	17.21	17.02	36.655	17.74	17.72
225C-2	199.5	17.62	15.42	37.853	19.06	19.38	34.375	19.58	20.09
225C-3	200	11.18	10.95	16.004	18.65	20.01	14.288	18.64	20.02

Table 5.23 DBMOE of treated samples during 3 hours at EMC and dry condition

SAMPLE	size			Step 3, treated for 3h at Dry condition			Step 4, treated for 3h at EMC condition		
	L (mm)	w (mm)	t (mm)	wt. (gr)	Upward MOE (Mpa)	Lateral MOE (Mpa)	wt. (gr)	Upward MOE (Mpa)	Lateral MOE (Mpa)
125C-1	201.7	19.73	18.82	42.59	16.14	17.13	47.572	15.9	16.75
125C-2	201	17.91	17.49	35.01	16.15	16.9	39.194	15.93	16.52
125C-3	202	9.97	10.69	12.59	18.89	19.87	14.154	19.27	17.88
150C-1	200	20.21	18.30	44.14	17.82	17.87	49.475	17.78	15.76
150C-2	200.2	16.63	15.40	32.41	19.77	20.82	36.458	19.92	20.71
150C-3	200.4	11.39	10.79	14.56	19.55	19.45	16.414	20.06	19.75
175C-1	200.5	19.51	19.58	42.15	14.16	16.31	47.57	14.32	16.33
175C-2	200	15.11	15.32	27.91	17.48	19.77	31.62	17.85	20.02
175C-3	201.6	11.66	10.96	15.53	18.98	20.29	17.42	19.53	20.66
200C-1	200.6	19.22	18.53	38.97	15.09	14.76	43.9	15.17	15.34
200C-2	202.8	16.62	14.68	28.82	17.77	17.82	32.475	18.08	17.88
200C-3	200.3	11.23	11.31	15.18	18.53	19.76	16.858	18.97	20.12
225C-1	198.1	18.70	16.29	32.16	14.75	14.62	35.747	14.96	14.67
225C-2	199.1	17.30	15.02	30.43	16.67	17.03	33.826	16.89	17.09
225C-3	199.6	10.98	10.67	12.68	15.97	17.08	13.999	16.36	17.36

Table 5.24 DBMOE of treated samples during 24 hours at EMC and dry condition

SAMPLE	size			Step 5, treated for 24h at Dry condition			Step 6, treated for 24h at EMC condition		
	L (mm)	w (mm)	t (mm)	wt. (gr)	Upward MOE (Mpa)	Lateral MOE (Mpa)	wt. (gr)	Upward MOE (Mpa)	Lateral MOE (Mpa)
125C-1	201.7	19.71	18.78	42.051	16.48	17.01	47.247	16.3	16.79
125C-2	201	17.89	17.45	34.538	16.86	16.91	38.84	16.68	16.68
125C-3	202	9.96	10.67	12.481	19.57	19.91	14.06	19.88	20.16
150C-1	199.8	20.14	18.25	43.57	18.17	17.81	49.03	18.18	17.74
150C-2	200	16.58	15.36	32.02	20.48	20.81	36.11	20.59	20.82
150C-3	200.2	11.35	10.77	14.42	20.4	19.62	16.25	20.74	19.86
175C-1	200.1	19.41	19.45	41.11	13.84	15.6	46.084	14	15.71
175C-2	199.6	15.04	15.22	27.282	17.69	19.29	30.76	17.97	19.55
175C-3	201.2	11.60	10.89	15.094	18.69	19.53	16.864	19.05	19.75
200C-1	200.4	18.81	18.13	35.52	12.31	12.38	39.869	12.43	10.15
200C-2	202.6	16.27	14.36	26.55	15.56	15.31	29.765	15.46	15.32
200C-3	200.1	11.00	11.07	13.75	15.3	16.55	15.215	15.5	16.7
225C-1	197.9	17.28	14.97	25.57	5.76	5.59	29.353	6.64	6.32
225C-2	198.9	15.98	13.80	24.98	8.08	8.08	28.562	8.63	8.71
225C-3	199.4	10.14	9.80	9.56	3.31	6.06	10.751	3.76	6.64

5.14. Static bending of a bamboo beam

5.14.1. Criteria for maximum load and deformation of four point bending test of a bamboo beam

Two criteria should be considered for four point bending test. The first one is maximum allowable bending resistance of the beam and the second one is the maximum allowable deformation of strain gauges. Then to measure the modulus of elasticity of the bamboo beams these two criteria should be taken to account.

Maximum deflection and strain criterion

A four point loaded beam has been shown in Figure 5.21a. The value of maximum deflection of this beam in Figure 5.21b is calculated in 5.1. The relation between strain in the top and bottom fibers, section and material property and moment is presented in 5.2. By substituting the moment from one equation to the other, the relation between strain and deflection will be obtained and presented in 5.3.

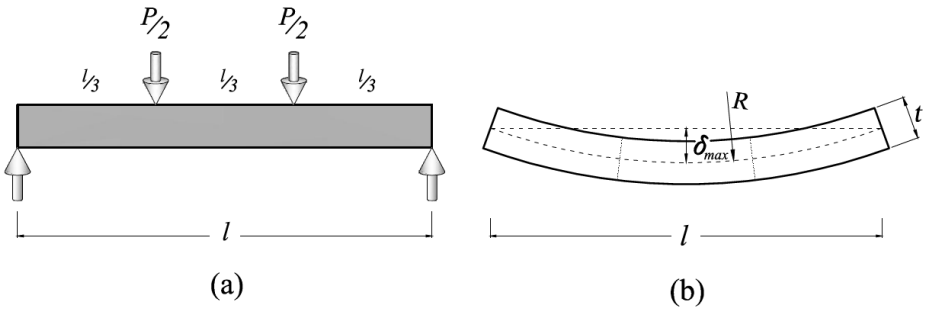

Figure 5.21 a) A four point loaded beam b) beam deflection

$$\delta_{max} = \frac{23Pl^3}{1296EI} = \frac{23Ml^2}{216EI} \quad 5.1$$

$$\sigma = \frac{My}{I} \rightarrow \varepsilon = \frac{My}{EI} \quad 5.2$$

$$\varepsilon_u = \varepsilon_d = \frac{216\delta_{max}y}{23l^2} \rightarrow \delta_{max} = \frac{23l^2\varepsilon}{216y} \quad 5.3$$

The strains in top and bottom sides of different geometrical isotropic cross sections are presented in Figure 5.22. For a rectangular cross section the neutral axis is located in the middle of the section and the two top and bottom strains are equal as presented in Figure 5.22a and 5.3. For the sections like a trapezoid, the strain in one side is less than to the other side as presented in Figure 5.22b. For a functionally graded material such as bamboo due to concentration of fibers in one side (here on the top) the strain in the bottom fibers will be more than the top of the beam as presented in Figure 5.22c.

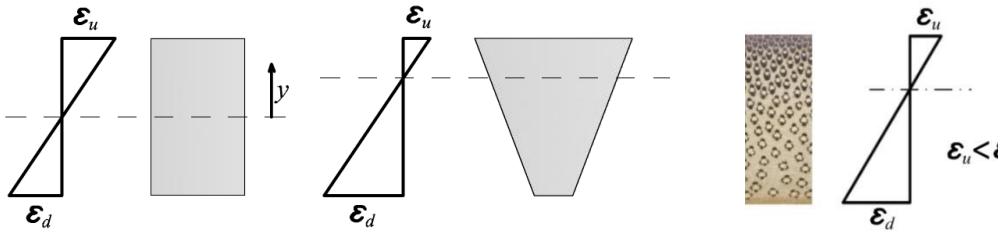

Figure 5.22 The strains in top and bottom sides of; a) rectangle; b) trapezoid and c) bamboo cross sections

The length of the test beam is 200 mm (with 180 mm free span) and thickness is about 15*mm* and the maximum allowable capacity of strain gauge is 2% then maximum allowable deflection based on 5.3 for a rectangular and isotropic section would be about 9.4 mm. In the worst case, which the top side has remarkable rigidity regarding to the bottom side, the maximum strain value

become close to $2\varepsilon_d$ mentioned in 5.3 and the maximum deflection should be limited to half of 9.4mm. Then the maximum deflection considered for the beams with about 15 mm thickness is limited to about 4.7 mm.

Maximum load criteria

Due to the difference between tensile and compression resistance of bamboo the behavior of a bamboo beam is different when is located in upward or downward position for the four point bending test. The worst case happens when the bamboo beam is located in downward position. The region with low fiber density positioned on the top and compression. The tensile and compression resistance of bamboo for different types of bamboo is different. For *DG* bamboo the tensile and compression ultimate resistance test results are considered about 164 MPa and 64 MPa respectively [108], also the modulus of elasticity for tensile and compression tests are 19.11 *GPa* and 15.29 *GPa* respectively.

The maximum deflection under the middle of the beam with four points loading presented in 5.1. By using 5.1 and 5.2 the relation between tension and deformation is presented in 5.4.

$$\delta_{max} = \frac{23l^2\sigma_c}{216E_c y_c} \qquad 5.4$$

By considering $\sigma_c = 64\,MPa$, $E_c = 15.29\,GPa$, $y_c = 7.5\,mm$ and $l = 180\,mm$ the deformation will be equal to 2 mm. which is less than to maximum value of deflection and strain criterion. This value is considered as maximum allowable deflection for the static flexural tests.

5.15. Second moment of Inertia for a bamboo section in radial and tangential directions

Due to uneven distribution of fibers in bamboo section, the second moment of inertia could be different from an isotropic section. The distribution of fibers is not uniform and the volume fraction of fibers at the external part is more than the internal part. The gradual increment of fibers in radial direction from internal to external part of bamboo wall thickness can be estimated by a second order polynomial equation. The results of the tensile tests along the fibers for different species of bamboo shows that the external part of the bamboo with more fiber volume fraction, has higher tensile resistance and MOE, compared with the

internal part [124][125][126]. The MOE reported for sclerenchyma and parenchyma of a *Moso bamboo* are 48 GPa and 0.26 GPa respectively [127][128][129]. It shows that the MOE of fibers is about 185 times more than the matrix. Based on these values and the remarkable difference between the modulus of elasticity's, the effect of the matrix in compression and tensile is negligible and only works as glue to fasten the fiber bundles together.

The second moment of inertia of bamboo calculated using conventional method considering geometrical sizes of the cross section presented as b and t as shown in Figure 5.23. The second moment of Inertia I for a rectangular section at upright position is shown in Eq. 5.5.

(a) Conventional directions (b) conventional dimensions

Figure 5.23 Conventional direction and dimensions

$$I = \frac{1}{12} bt^3 \qquad 5.5$$

The Eq. 5.5 of moment of inertia has been developed for a homogenous materials or composites with uniform distribution of fibers perpendicular to xy plane. For a functionally graded material composite, the section should be transformed to an equivalent geometrical shape with uniform distribution of fibers across the section. The effective cross section depends on the arrangement of fibers in the section. Figure 5.24a shows a bamboo cross section. The fiber volume fraction at external wall is higher than the internal wall as can be seen in Figure 5.24b. the cross section presented in Figure 5.24c is the effective cross section only made by uniform distributed fibers. The right side follows a second order equation as shown in the Figure 5.24c based on the fiber volume fraction equation.

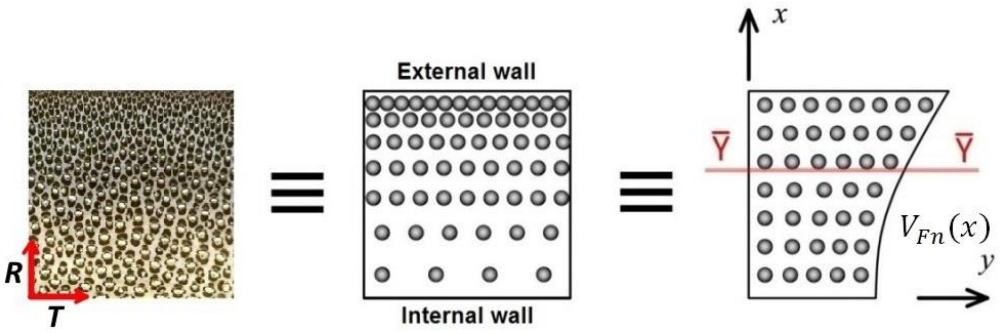

(a) bamboo section (b) fiber real distribution (c) even distribution of fibers

Figure 5.24 Uneven fiber distribution in radial direction

Eq.5.6 presents a normalized second order equation for volume fraction of bamboo. The normalized second order equations for *DG* bamboo at different levels have been presented in Table 3.11. By considering the thickness (*t*) in radial direction and width of section (*b*), the normalized fiber distribution equation transformed to fiber distribution equation as shown in Eq.5.7.

$$V_{Fn}(x) = mx^2 + nx + p \tag{5.6}$$

$$V_F(x) = b\left[m\left(\frac{x}{t}\right)^2 + n\left(\frac{x}{t}\right) + p\right] \tag{5.7}$$

Section property about $\boldsymbol{y}$ axis (upright position)

The section area for a rectangular cross section of bamboo is $b \times h$ but the effective area is the summation of fibers area. The total fiber area presented in Eq. 5.8 is the integration of volume fraction equation with respect to x presented in Eq.5.7 over to interval [0,t]. The centroidal axis for a bamboo section shown in Figure 5.25 is calculated by Eq.5.9 [130]. Finally, the fiber moment of inertia about y centroidal axis is obtained by Eq.5.10.

$$A_F = \int_0^t V_F(x)\,dx = bt\left(\frac{m}{3} + \frac{n}{2} + p\right) \tag{5.8}$$

$$\bar{x}_F = \frac{\int_0^t xV_F(x)\,dx}{A_F} \tag{5.9}$$

$$I_{Fy} = \int_0^t x^2V_F(x)\,dx - A_F\bar{x}^2 \tag{5.10}$$

Section property about **x** axis (lateral position)

For the section property about x axis, the fiber area remains the same and the centroidal axis is located in the middle of section ($\bar{y} = 0.5b$) as shown in Figure 5.26. The fiber moment of inertia is presented in eq. 5.11.

$$I_{Fx} = \frac{b^2}{12} A_F \quad 5.11$$

The relation between the conventional moment of inertia in both x and y directions is defined as λ and shown in Eq.5.12. The relation between the fiber moment of inertia in both x and y directions is defined by λ_F and shown in Eq.5.13. Finally, the deviation factor (φ) is defined as the ratio between λ_F and λ and is presented in Eq. 5.12.

$$\lambda = \frac{I_y}{I_x} = \left(\frac{t}{b}\right)^2 \quad 5.12$$

$$\lambda_F = \frac{I_{Fy}}{I_{Fx}} \quad 5.13$$

$$\varphi = \frac{\lambda_F}{\lambda} \quad 5.14$$

The deviation factor is equal to one means the section considered as a rectangular section. For explanation the conditions with smaller and bigger values of φ, two different types of bamboo (*DG* and *Moso bamboo)* are considered as examples and the values are compared together. The procedure is explained by a second order normalized equation of *DG bamboo* for basal part of a culm based on Table 3.11 which has been shown by Eq.5.15. Consequently, the actual fiber distribution equation is presented by Eq.5.16.

$$V_{Fn}(x) = 18.9x^2 + 1.3x + 36.2 \quad 5.15$$

$$V_F(x) = b\left[18.9\left(\frac{x}{t}\right)^2 + 1.3\left(\frac{x}{t}\right) + 36.2\right] \quad 5.16$$

The fiber distribution based on Eq.5.16, is shown in Figure 5.25. The volume fraction percentage of fibers starts with $0.362b$ at $x = 0$ up to $0.565b$ at $x = t$. The total fiber area (A_F), the centroidal axis ($\bar{x}_F$) and the effective moment of inertia for the equivalent fiber area (I_{Fy}) based on Eq.5.8, 5.9 and 5.10 [130] are presented and compared with a conventional section in Table 5.25. For the section properties about x axis, the distribution of the fibers is considered as a rectangle and shown in Figure 5.26. The section property in Figure 5.26 is presented in Table 5.26.

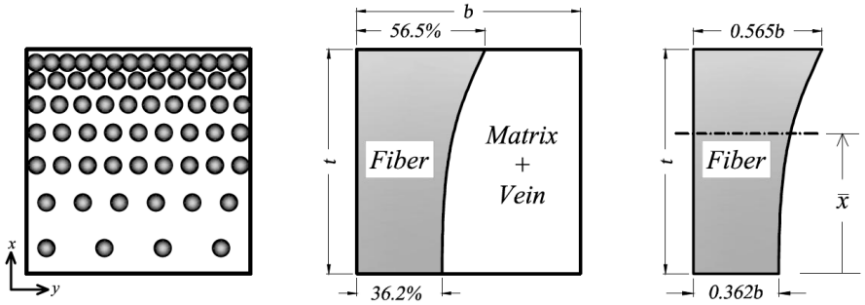

Figure 5.25 The schematic shape of fiber distribution along the radial direction for basal part of *DG* bamboo culm for the section property about y axis

Table 5.25 The section properties of conventional and effective area about y axis for *DG bamboo*

section	A	$\bar{x}, \bar{x}_F$	I_y, I_{Fy}	S_y	
				max	min
Conventional area	bt	$0.5\ t$	$\frac{1}{12}bt^3$	$\frac{1}{6}bt^2$	$\frac{1}{6}bt^2$
Effective area	$0.432\ bt$	$0.539\ t$	$\frac{1}{27.49}bt^3$	$\frac{1}{12.67}bt^2$	$\frac{1}{14.82}bt^2$

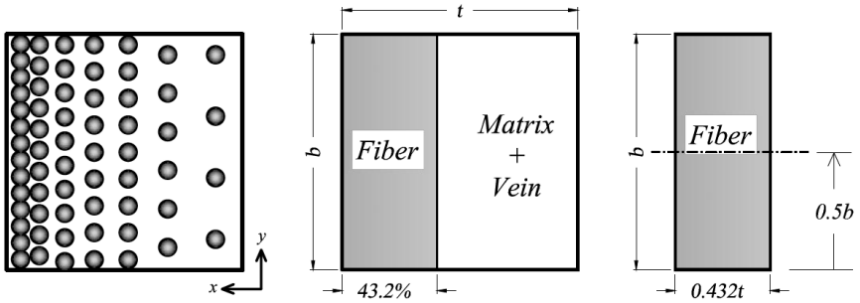

Figure 5.26 The schematic shape of fiber distribution along the tangential direction for basal part of *DG* bamboo culm for the section property about x axis

Table 5.26 The section properties of conventional and effective area about x axis for *DG bamboo*

section	A	$\bar{y}, \bar{y}_F$	I_x, I_{Fx}	S_x
Conventional area	bt	$0.5\ b$	$\frac{1}{12}tb^3$	$\frac{1}{6}tb^2$
Effective area	$0.432\ bt$	$0.5\ b$	$\frac{1}{27.78}tb^3$	$\frac{1}{13.89}tb^2$

The property of the fiber sections about x and y axis are compared together in Table 5.27. The difference is calculated based on Eq.5.17.

$$\text{Difference} = \frac{\text{value}(y) - \text{value}(x)}{\text{value}(x)} \times 100 \qquad 5.17$$

Table 5.27 Effective section properties about x and y axis for *DG bamboo*

section	A	$\bar{x}$, $\bar{y}$	$I_{Fx,Fy}$	$S_{Fx,Fy}$	
				max	min
x axis	$0.432\ bt$	$0.5\ b$	$\frac{1}{27.78}tb^3$	$\frac{1}{13.89}tb^2$	$\frac{1}{13.89}tb^2$
y axis	$0.432\ bt$	$0.539\ t$	$\frac{1}{27.49}bt^3$	$\frac{1}{12.65}bt^2$	$\frac{1}{14.84}bt^2$
Difference	0	+8%	+1.05%	+9.8%	-6.4%

There is +1% difference between moment of inertia about x and y directions and the positive sign imply the moment of Inertia about y is higher. The deviation factor (φ) is 1.0105. For Moso bamboo, the second order normalized equation which has been developed by Ghavami *et al.* [16] is used as shown in Eq. 5.18. The results for *Moso bamboo* in x and y directions are presented in Table 5.28.

$$V_{Fn}(x) = 49.46x^2 + 0.66x + 11.72 \quad 5.18$$

Table 5.28 Effective section properties about x and y axis for *Moso bamboo*

section	A	$\bar{x}$, $\bar{y}$	$I_{Fx,Fy}$	$S_{Fx,Fy}$	
				max	min
x axis	$0.285\ bt$	$0.5\ t$	$\frac{1}{42.05}tb^3$	$\frac{1}{21.03}tb^2$	$\frac{1}{21.03}tb^2$
y axis	$0.285\ bt$	$0.646\ t$	$\frac{1}{48.98}bt^3$	$\frac{1}{17.32}bt^2$	$\frac{1}{31.66}bt^2$
Difference	0	+29.2%	-14.15%	+21.42%	-33.58%

In Table 5.28 the difference between section properties about x and y axes for *Moso bamboo* are significantly higher than the same values for *DG* bamboo. Based on Table 5.27 and Table 5.28, the difference of the moment of inertia about x and y axes for a *DG* bamboo is about 1%, but for a *Moso* bamboo is more than 14% which is considerable. Also it should be considered that in some cases like *DG* bamboo at basal part of culm, the effective moment of inertia about x axis could be smaller than the same parameter about y axis. But in the cases like *Moso* bamboo which the difference between the fiber distribution amount at internal and external is remarkable, the effective moment of inertia about x axis is bigger. But

in both situations, the critical section modulus about y axis is always smaller than the same parameter about x axis.

Table 5.29 The MOE in upward and lateral positions

SAMPLE	size		Upward MOE (Mpa)	Lateral MOE (Mpa)	Upward to lateral ratio	Upward to lateral average ratio	CV%
	w_{ave} (mm)	t_{ave} (mm)					
B-1	20.12	18.25	18.21	18.28	0.996	0.984	4.0
B-2	19.43	17.62	18.23	17.95	1.016		
B-3	19.71	18.77	16.23	17.28	0.939		
M-1	17.52	15.31	19.59	20.39	0.961	0.963	0.3
M-2	16.76	15.37	19.99	20.78	0.962		
M-3	16.74	15.29	19.73	20.41	0.967		
T-1	11.77	11.04	19.92	20.56	0.969	0.955	1.5
T-2	11.31	11.36	20.22	21.52	0.940		
T-3	11.76	10.92	20.00	20.93	0.956		

The results of DBMOE about *x* and *y* axis for three groups base, middle and top shows the difference between upright and lateral MOE for the *DG* bamboo samples prepared from location more close to base is more than the group of samples prepared from top. ANOVA shows a meaningful and significant difference between the results as can be seen in Table 5.29.

5.16.Accuracy of results and propagation of error

The measurement accuracy and precision of the initial variables will effect on the final result. It means the error or uncertainty of each parameter propagates through the relation between them and the target function, to the final result. If F is a function of $x, y, \ldots$ written as $f(x, y, \ldots)$, then the uncertainty in F is obtained by taking the partial derivatives of F with repsect to each variable, multiplication with the uncertainty of that variable. By addition of these individual terms in quadrature as mentioned in Eq. 5.20 [131] the final uncertainty is achieved.

$$F = f(x, y, \ldots) \tag{5.19}$$

$$\varepsilon_F = \sqrt{\left(\frac{\partial F}{\partial x}\varepsilon_x\right)^2 + \left(\frac{\partial F}{\partial y}\varepsilon_y\right)^2 + \cdots} \tag{5.20}$$

The dimension of the samples in present research has been done by a vernier caliper with accuracy equal to $\pm 0.05mm$. The sample weighing has been done by a digital balance with accuracy equal to $\pm 0.001gr$. Also the accuracy of the load cells based on the Lab documents is $\pm 0.2\%$ of load cell capacity.

5.16.1. Accuracy in compression, tensile and shear tests

One formula is used to measure the tensile, compression and shear tests which can be seen in Eq. 5.21.

$$P = f(F, b, t) = \frac{F}{b.t} \tag{5.21}$$

$$\frac{\partial P}{\partial F} = \frac{1}{b.t} \tag{5.22}$$

$$\frac{\partial P}{\partial b} = \frac{-F}{b^2.t} \tag{5.23}$$

$$\frac{\partial P}{\partial t} = \frac{-F}{b.t^2} \tag{5.24}$$

$$\varepsilon_P = \sqrt{\left(\frac{\partial P}{\partial F}\varepsilon_F\right)^2 + \left(\frac{\partial P}{\partial b}\varepsilon_b\right)^2 + \left(\frac{\partial P}{\partial t}\varepsilon_t\right)^2} \tag{5.25}$$

For tensile samples with approximate tensile force about 10 kN and $b \times t = 2mm \times 20mm$ the accuracy of measuring the "*P*" is calculated by Eq. 5.26.

$$\frac{\varepsilon_P}{P} = \sqrt{\left(\frac{\varepsilon_F}{F}\right)^2 + \left(-\frac{\varepsilon_b}{b}\right)^2 + \left(-\frac{\varepsilon_t}{t}\right)^2} = \pm 4.33\% \tag{5.26}$$

5.16.2. Accuracy for bending tests

As an example a four point loaded beam considered for calculation of error. The modulus of elasticity is achieved by a cantilever beam equation:

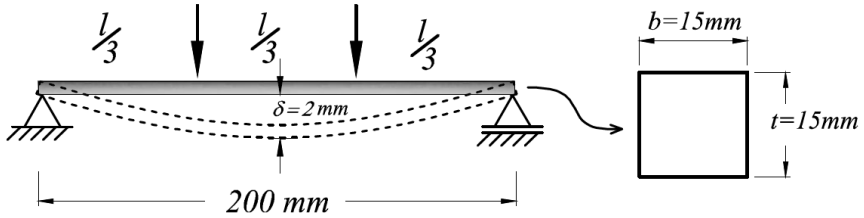

Figure 5.27 Four point loaded beam dimension, load and deflection

$$E = f(P, l, b, t, \delta) = \frac{23Pl^3}{1296\delta I} = \frac{23Pl^3}{108bt^3\delta} \tag{5.27}$$

The partial derivatives of E with respect to each variable are presented in Eq. 5.28 to Eq. 5.32.

$$\frac{\partial E}{\partial P} = \frac{23l^3}{108bt^3\delta} \quad 5.28$$

$$\frac{\partial E}{\partial l} = \frac{69Pl^2}{108bt^3\delta} \quad 5.29$$

$$\frac{\partial E}{\partial b} = \frac{-23Pl^3}{108b^2t^3\delta} \quad 5.30$$

$$\frac{\partial E}{\partial \delta} = \frac{-23Pl^3}{108t^3\delta^2} \quad 5.31$$

$$\frac{\partial E}{\partial t} = \frac{-69Pl^3}{108bt^4\delta} \quad 5.32$$

$$\varepsilon_E = \sqrt{\left(\frac{\partial E}{\partial P}\varepsilon_P\right)^2 + \left(\frac{\partial E}{\partial l}\varepsilon_l\right)^2 + \left(\frac{\partial E}{\partial b}\varepsilon_b\right)^2 + \left(\frac{\partial E}{\partial t}\varepsilon_t\right)^2 + \left(\frac{\partial E}{\partial \delta}\varepsilon_\delta\right)^2} \quad 5.33$$

After replacing values in Eq. 5.33 the result would be:

$$\varepsilon_E = \left(\frac{23Pl^3}{108bt^3\delta}\right)\sqrt{\left(\frac{\varepsilon_P}{P}\right)^2 + \left(3\frac{\varepsilon_l}{l}\right)^2 + \left(-\frac{\varepsilon_b}{b}\right)^2 + \left(-3\frac{\varepsilon_t}{t}\right)^2 + \left(-\frac{\varepsilon_\delta}{\delta}\right)^2} \quad 5.34$$

The measured errors for length, width, thickness, load and deflection are respectively $\varepsilon_l = \pm 0.1mm$, $\varepsilon_b = \pm 0.05mm$, $\varepsilon_t = \pm 0.05mm$, $\varepsilon_P = \pm 0.1\,N$, $\varepsilon_\delta = \pm 0.01mm$. By using these values in 5.34 the measurement error for modulus of elasticity is obtained. The relative error (Δ_E) is calculated via the 5.35.

$$\frac{\varepsilon_E}{E} = \sqrt{\left(\frac{\varepsilon_P}{P}\right)^2 + \left(3\frac{\varepsilon_l}{l}\right)^2 + \left(-\frac{\varepsilon_b}{b}\right)^2 + \left(-3\frac{\varepsilon_t}{t}\right)^2 + \left(-\frac{\varepsilon_\delta}{\delta}\right)^2} = \pm 1.67\% \quad 5.35$$

5.17.Air moisture capacity

Table 5.30 presents the maximum moisture content in a cubic meter of air at various temperatures. At sea level and at 15°C air has a density of approximately **1.225 kg/m^3**. The amount of moisture in air at different temperature and relative humidity presented at Figure 5.28.

Table 5.30 Relation between temperature and Max. water content [132]

Temperature (°C)	Max. Water Content (gr/m3)
-25	0.64
-20	1.05
-15	1.58
-10	2.31
-5	3.37
0	4.89
5	6.82
10	9.39
15	12.8
20	17.3
30	30.4
40	51.1
50	83
60	130

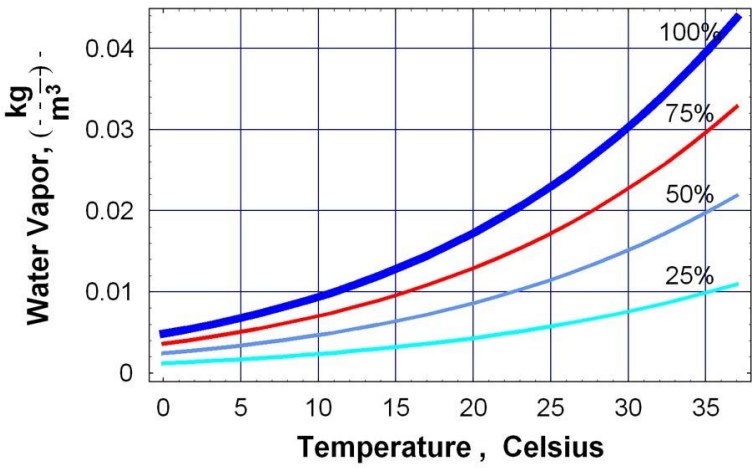

Figure 5.28 Amount of moisture in air at different temperature and relative humidity [133]

The relation between relative humidity with wet and dry bulb is presented in Figure 5.29. The relation between dry and wet bulb temperature to dew point can be seen in Figure 5.30.

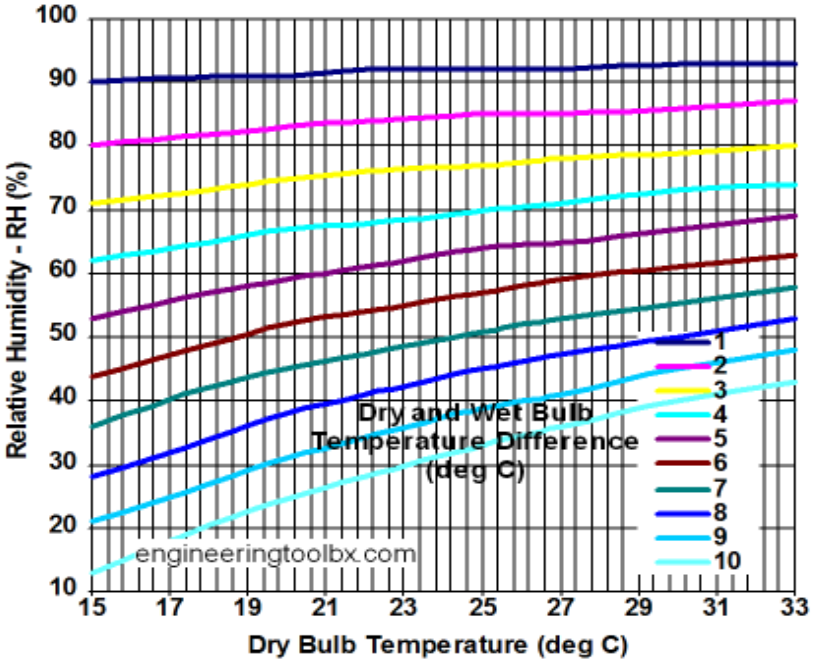

Figure 5.29 relation between RH(%) with dry and wet bulb [134]

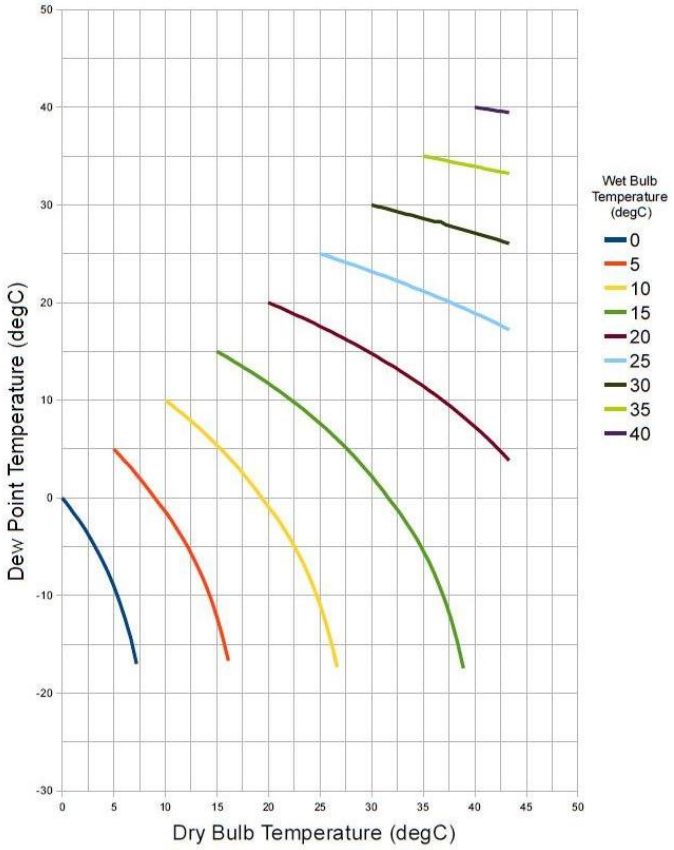

Figure 5.30 Dew point temperature from dry and wet bulb temperatures [135]

6 References

[1] K. Ghavami, "Introduction to nonconventional materials and an historic retrospective of the field," in *Nonconventional and Vernacular Construction Materials: Characterisation, Properties and Applications*, Woodhead Publishing, 2016, pp. 37–61.

[2] J. M. O. Scurlock, D. C. Dayton, and B. Hames, "Bamboo: An overlooked biomass resource?," *Biomass and bioenergy*, vol. 19, no. 4, pp. 229–244, 2000.

[3] J. J. A. Janssen, *Designing and building with bamboo*. International Network for Bamboo and Rattan China, 2000.

[4] D. J. A. Trujillo, "Axially loaded connections in Guadua bamboo," in *Proceedings of the Non-conventional Materials and Technologies*, 2009.

[5] K. Ghavami and I. G. Solorzano, "Comparison between microstructure of bamboo culm and wood," in Acta Microscopia 3rd Inter-American Conference on Electron Microscopy and XV Meeting of the Brazilian Society for Electron Microscopy, 1995.

[6] K. Ghavami, "Bamboo as reinforcement in structural concrete elements," *Cem. Concr. Compos.*, vol. 27(6), pp. 637–649, 2005.

[7] A. Azadeh and H. H. Kazemi, "New Approaches to Bond between Bamboo and Concrete," *Key Eng. Mater.*, vol. 600, pp. 69–77, 2014.

[8] S. A. A. Jayaweera and E. Robensa, "Some aspects on the history of thermal analysis," *Ann. UMCS Chem.*, vol. 67, no. 1–2, pp. 1–29, 2012.

[9] B. Kieback, A. Neubrand, and H. Riedel, "Processing techniques for functionally graded materials," *Mater. Sci. Eng. A*, vol. 362, no. 1, pp. 81–106, 2003.

[10] "Dendrocalamus giganteus — Guadua Bamboo." [Online]. Available: http://www.guaduabamboo.com/species/dendrocalamus-giganteus. [Accessed: 29-Aug-2016].

[11] C. Ratti, "Hot air and freeze-drying of high-value foods: a review," *J. Food Eng.*, vol. 49, no. 4, pp. 311–319, 2001.

[12] T. K. H. Tang, J. Welling, T. D. Ho, and W. Liese, "Investigation on optimisation of kiln drying for the bamboo species Bambusa stenostachya,

Dendrocalamus asper and Thyrsostachys siamensis.," *Bamboo Sci. Cult.*, vol. 25, no. 1, 2012.

[13] W. Liese, "The anatomy of bamboo culms. International Network for Bamboo and Rattan (INBAR)," 1998.

[14] W. Liese, "Anatomy and properties of bamboo," in *Proceedings of the International Bamboo Workshop*, 1985, pp. 196–208.

[15] W. Liese, "The structure of bamboo in relation to its properties and utilization," in Zhu, S., Li, W., Zhang, X. Wang, Z. ed., Bamboo and its use. Proceedings of the International symposium on Industrial Use of Bamboo, Beijing, China, 1992, pp. 7–11.

[16] K. Ghavami, C. de S. Rodrigues, and S. Paciornik, "Bamboo: functionally graded composite material," *Asian J. Civ. Eng*, vol. 4, no. 1, pp. 1–10, 2003.

[17] a. K. Ray, S. Mondal, S. K. Das, and P. Ramachandrarao, "Bamboo—A functionally graded composite-correlation between microstructure and mechanical strength," *J. Mater. Sci.*, vol. 40, no. 19, pp. 5249–5253, 2005.

[18] G. Udupa, S. S. Rao, and K. V Gangadharan, "Functionally graded composite materials: an overview," *Procedia Mater. Sci.*, vol. 5, pp. 1291–1299, 2014.

[19] I. Bharti, N. Gupta, and K. M. Gupta, "Novel applications of functionally graded nano, optoelectronic and thermoelectric materials," *Int. J. Mater. Mech. Manuf.*, vol. 1, no. 3, pp. 221–224, 2013.

[20] S. V Vassilev, D. Baxter, L. K. Andersen, and C. G. Vassileva, "An overview of the chemical composition of biomass," *Fuel*, vol. 89, no. 5, pp. 913–933, 2010.

[21] H. Rabemanolontsoa and S. Saka, "Holocellulose determination in biomass," in *Zero-Carbon Energy Kyoto 2011*, Springer, 2012, pp. 135–140.

[22] L. J. Gibson, "The hierarchical structure and mechanics of plant materials," *J. R. Soc. Interface*, vol. 9, no. 76, pp. 2749–2766, 2012.

[23] M. A. Millett and A. J. Stamm, "Molecular properties of hemicellulose fractions.," *J. Phys. Chem.*, vol. 51, no. 1, pp. 134–148, 1947.

[24] W. J. Cousins, "Young's modulus of hemicellulose as related to moisture content," *Wood Sci. Technol.*, vol. 12, no. 3, pp. 161–167, 1978.

[25] A. Ebringerová, "Structural diversity and application potential of hemicelluloses," in *Macromolecular Symposia*, 2005, vol. 232, no. 1, pp. 1–12.

[26] J. G. Speight, *The Biofuels Handbook*. Royal Society of Chemistry, 2015.

[27] L. J. Gibson, M. F. Ashby, and B. A. Harley, *Cellular materials in nature and medicine*. Cambridge University Press, 2010.

[28] K. Freudenberg, "Lignin: its constitution and formation from p-hydroxycinnamyl alcohols," *Science (80-.).*, vol. 148, no. 3670, pp. 595–600, 1965.

[29] A. Pandey, *Handbook of plant-based biofuels*. CRC Press, 2008.

[30] W.-H. Chen, S.-H. Liu, T.-T. Juang, C.-M. Tsai, and Y.-Q. Zhuang, "Characterization of solid and liquid products from bamboo torrefaction," *Appl. Energy*, vol. 160, pp. 829–835, Dec. 2015.

[31] L. E. Hernandez-Mena, A. A. B. Pécoraa, and A. L. Beraldob, "Slow pyrolysis of bamboo biomass: Analysis of biochar properties," *Chem. Eng.*, vol. 37, 2014.

[32] D. Fengel and X. Shao, "A chemical and ultrastructural study of the Bamboo species Phyllostachys makinoi Hay," *Wood Sci. Technol.*, vol. 18, no. 2, pp. 103–112.

[33] F. Meng, Y. Yu, Y. Zhang, W. Yu, and J. Gao, "Surface chemical composition analysis of heat-treated bamboo," *Appl. Surf. Sci.*, vol. 371, pp. 383–390, May 2016.

[34] S. Kamthai, Alkaline sulfite pulping and ECF-bleaching of sweet bamboo (Dendrocalamus asper Backer). Kasetsart University, 2003.

[35] T. Higuchi, "Biochemical studies of lignin formation. III," *Physiol. Plant.*, vol. 10, no. 4, pp. 633–648, 1957.

[36] X. B. Li, T. F. Shupe, G. F. Peter, C. Y. Hse, and T. L. Eberhardt, "Chemical changes with maturation of the bamboo species Phyllostachys pubescens," *J. Trop. For. Sci.*, pp. 6–12, 2007.

[37] P. Chaowana, "Bamboo: An alternative raw material for wood and wood-based composites," *J. Mater. Sci. Res.*, vol. 2, no. 2, p. 90, 2013.

[38] X. Li, "Physical , Chemical , and Mechanical Properties of Bamboo and Its Utilization Potential for Fiberboard Manufacturing," Doctoral dissertation, Beijing Forestry University, 2004.

[39] C.-M. Popescu, G. Singurel, M.-C. Popescu, C. Vasile, D. S. Argyropoulos, and S. Willför, "Vibrational spectroscopy and X-ray diffraction methods to

establish the differences between hardwood and softwood," *Carbohydr. Polym.*, vol. 77, no. 4, pp. 851–857, 2009.

[40] H. P. S. Abdul Khalil, I. U. H. Bhat, M. Jawaid, A. Zaidon, D. Hermawan, and Y. S. Hadi, "Bamboo fibre reinforced biocomposites: A review," *Mater. Des.*, vol. 42, pp. 353–368, Dec. 2012.

[41] W. Yueping, W. Ge, C. Haitao, T. Genlin, L. Zheng, X. Q. Feng, Z. Xiangqi, H. Xiaojun, and G. Xushan, "Structures of bamboo fiber for textiles," *Text. Res. J.*, vol. 80, no. 4, pp. 334–343, 2010.

[42] S. Amada, T. Munekata, Y. Nagase, Y. Ichikawa, A. Kirigai, and Y. Zhifei, "The Mechanical Structures of Bamboos in Viewpoint of Functionally Gradient and Composite Materials," *J. Compos. Mater.*, vol. 30, no. 7, pp. 800–819, May 1996.

[43] A. W. Coats and J. P. Redfern, "Thermogravimetric analysis. A review," *Analyst*, vol. 88, no. 1053, pp. 906–924, 1963.

[44] W. Jin, K. Singh, and J. Zondlo, "Pyrolysis Kinetics of Physical Components of Wood and Wood-Polymers Using Isoconversion Method," *Agriculture*, vol. 3, no. 1, pp. 12–32, 2013.

[45] Z. Song-lin, G. Shang-yu, Y. Xi-gen, and X. Bo-sen, "Carbonization mechanism of bamboo (phyllostachys) by means of Fourier Transform Infrared and elemental analysis," *J. For. Res.*, vol. 14, no. 1, pp. 75–79, Mar. 2003.

[46] H. Sixta, "Pulp properties and applications," *Handb. pulp*, pp. 1009–1067, 2006.

[47] L. Gašparovič, Z. Koreňová, and Ľ. Jelemenský, "Kinetic study of wood chips decomposition by TGA," *Chem. Pap.*, vol. 64, no. 2, pp. 174–181, Jan. 2010.

[48] W.-H. Chen and P.-C. Kuo, "A study on torrefaction of various biomass materials and its impact on lignocellulosic structure simulated by a thermogravimetry," *Energy*, vol. 35, no. 6, pp. 2580–2586, Jun. 2010.

[49] G. Dorez, A. Taguet, L. Ferry, and J. M. M. Lopez-Cuesta, "Thermal and fire behavior of natural fibers/PBS biocomposites," *Polym. Degrad. Stab.*, vol. 98, no. 1, pp. 87–95, Jan. 2013.

[50] D. Chen, J. Zhou, and Q. Zhang, “Effects of heating rate on slow pyrolysis behavior, kinetic parameters and products properties of moso bamboo,” *Bioresour. Technol.*, vol. 169, pp. 313–319, 2014.

[51] A. Skreiberg, Ø. Skreiberg, J. Sandquist, and L. Sørum, “TGA and macro-TGA characterisation of biomass fuels and fuel mixtures,” *Fuel*, vol. 90, no. 6, pp. 2182–2197, 2011.

[52] Y. Li, L. Du, C. Kai, R. Huang, and Q. Wu, “Bamboo and high density polyethylene composite with heat-treated bamboo fiber: Thermal decomposition properties,” *BioResources*, vol. 8, no. 1, pp. 900–912, 2013.

[53] R. M. Rowell and R. L. Youngs, “Dimensional Stabilization of Wood in Use.,” DTIC Document, 1981.

[54] B. M. Esteves and H. M. Pereira, “Wood modification by heat treatment: A review,” *BioResources*, vol. 4, no. 1, pp. 370–404, 2009.

[55] W. Shangguan, Y. Gong, R. Zhao, and H. Ren, “Effects of heat treatment on the properties of bamboo scrimber,” *J. Wood Sci.*, vol. 62, no. 5, pp. 383–391, 2016.

[56] P. Bekhta and P. Niemz, “Effect of high temperature on the change in color, dimensional stability and mechanical properties of spruce wood,” *Holzforschung*, vol. 57, no. 5, pp. 539–546, 2003.

[57] O. Unsal, S. Korkut, and C. Atik, “The effect of heat treatment on some properties and colour in eucalyptus (Eucalyptus camaldulensis Dehn.) wood,” *Maderas. Cienc. y Tecnol.*, vol. 5, no. 2, pp. 145–152, 2003.

[58] D. S. Korkut and S. Hiziroglu, “Experimental test of heat treatment effect on physical properties of red oak (Quercus falcate Michx.) and southern pine (Pinus taeda L.),” *Materials (Basel).*, vol. 7, no. 11, pp. 7314–7323, 2014.

[59] S. Metsä-Kortelainen, T. Antikainen, and P. Viitaniemi, “The water absorption of sapwood and heartwood of Scots pine and Norway spruce heat-treated at 170 C, 190 C, 210 C and 230 C,” *Eur. J. Wood Wood Prod.*, vol. 64, no. 3, pp. 192–197, 2006.

[60] W. Scheiding, M. Direske, and M. Zauer, “Water absorption of untreated and thermally modified sapwood and heartwood of Pinus sylvestris,” *Eur. J. Wood Wood Prod.*, vol. 74, no. 4, pp. 585–589, 2016.

[61] C. Eng, J. E. Waning, and Y. T. Mekonnen, “An Experimental Investigation of the Effects of Moisture Content on the Mechanical Properties of Bamboo

and Cane," *Cyber Journals Multidiscip. Journals Sci. Technol. J. Sel. Areas Bioeng.*, no. November Edition, pp. 8–14, 2011.

[62] S. Yildiz, E. D. Gezer, and U. C. Yildiz, "Mechanical and chemical behavior of spruce wood modified by heat," *Build. Environ.*, vol. 41, no. 12, pp. 1762–1766, 2006.

[63] Y. M. Zhang, Y. L. Yu, and W. J. Yu, "Effect of thermal treatment on the physical and mechanical properties of Phyllostachys pubescen bamboo," *Eur. J. Wood Wood Prod.*, vol. 71, no. 1, pp. 61–67, 2013.

[64] K.-T. Wu, "The effect of high-temperature drying on the antisplitting properties of makino bamboo culm (Phyllostachys makinoi Hay.)," *Wood Sci. Technol.*, vol. 26, no. 4, pp. 271–277, 1992.

[65] T.-H. Yang, C.-H. Lee, C.-J. Lee, and Y.-W. Cheng, "Effects of different thermal modification media on physical and mechanical properties of moso bamboo," *Constr. Build. Mater.*, vol. 119, pp. 251–259, 2016.

[66] A. Hailwood and S. Horrobin, "Absorption of water by polymers: analysis in terms of a simple model," *Trans. Faraday Soc.*, 1946.

[67] Y. S. Wang and J. L. Tang, "Studies on the structure of introduced bamboos," *For. Prod. Ind.*, vol. 7, no. 1, pp. 53–63, 1988.

[68] S. OCHI, H. TAKAGI, and R. NIKI, "Mechanical properties of heat-treated natural fibers," *Zairyo*, vol. 51, no. 10. Society of Materials Science, pp. 1164–1168.

[69] S. Ochi, "Tensile Properties of Bamboo Fiber Reinforced Biodegradable Plastics," *International Journal of Composite Materials*, vol. 2, no. 1. Scientific & Academic Publishing, pp. 1–4, 2012.

[70] ISO 13061-3, "Physical and mechanical properties of wood — Test methods for small clear wood specimens." 2014.

[71] C. C. Gerhards, "Effect of moisture content and temperature on the mechanical properties of wood: an analysis of immediate effects," *Wood Fiber Sci.*, vol. 14, no. 1, pp. 4–36, 2007.

[72] J. A. Gome Neto, "Painel modular intertravado de matriz cimentícia com reforço estrutural de Bambusa vulgaris," Dissiertação Mestrado. Prorgrama de Pós-graduação em Engeneharia Civil e Ambiental. Universidade Federal da Paraíba, João Pessoa, Brasil, 2017.

[73] E. H. Achá Navarro, “Bamboo, High Tech material for Concrete reinforcement,” Pontifícia Universidade Católica do Rio de Janeiro, 2011.

[74] H. Wang, H. Wang, W. Li, D. Ren, and Y. Yu, “Effects of moisture content on the mechanical properties of moso bamboo at the macroscopic and cellular levels,” *BioResources*, vol. 8, no. 4, pp. 5475–5484, 2013.

[75] M. Ahmad and F. A. Kamke, “Analysis of Calcutta bamboo for structural composite materials: physical and mechanical properties,” *Wood Sci. Technol.*, vol. 39, no. 6, pp. 448–459, 2005.

[76] G. Gündüz, P. Niemz, and D. Aydemir, “Changes in specific gravity and equilibrium moisture content in heat-treated fir (Abies nordmanniana subsp. bornmülleriana Mattf.) wood,” *Dry. Technol.*, vol. 26, no. 9, pp. 1135–1139, 2008.

[77] J. Mena, S. Vera, J. F. Correal, and M. Lopez, “Assessment of fire reaction and fire resistance of Guadua angustifolia kunth bamboo,” *Constr. Build. Mater.*, vol. 27, no. 1, pp. 60–65, 2012.

[78] P. Stollard and J. Abrahams, Fire from First Principles: A Design Guide to Building Fire Safety. Taylor & Francis, 1999.

[79] D. Drysdale, *An Introduction to Fire Dynamics*. John Wiley & Sons, 2011.

[80] V. Babrauskas, “Ignition of Wood: A Review of the State of the Art,” *J. Fire Prot. Eng.*, vol. 12, no. 3, pp. 163–189, Aug. 2002.

[81] N. K. Sharma, V. M. Chariar, and R. Prasad, “Impact of fire on Dendrocalamus strictus - a natural green composite building material,” *Indoor Built Environ.*, vol. 24, no. 6, pp. 740–745, May 2014.

[82] N. G. McCrum, C. P. Buckley, and C. B. Bucknall, *Principles of Polymer Engineering*. Oxford University Press, 1997.

[83] A. C. ICBO, “162: Acceptance criteria for structural bamboo,” *ICBO Eval. Serv. Ltd., California, USA*, 2000.

[84] “ISO 22157-1:2004 - Bamboo -- Determination of physical and mechanical properties -- Part 1: Requirements.” [Online]. Available: http://www.iso.org/iso/iso_catalogue/catalogue_tc/catalogue_detail.htm?csnumber=36150. [Accessed: 03-Mar-2016].

[85] “International Standards Organization (ISO) (2004b) ‘22157-2 Bamboo -- Determination of physical and mechanical properties -- Part 2: Laboratory manual’ 17 pp. ISO, Geneva Switzerland.” .

[86] “ASTM D4442 - 15 Standard Test Methods for Direct Moisture Content Measurement of Wood and Wood-Based Materials.” [Online]. Available: http://www.astm.org/Standards/D4442.htm. [Accessed: 03-Mar-2016].

[87] G. Sridhar, D. Subbukrishna, S. D. HSridhar, P. Paul, and H. Mukunda, “Torrefaction of bamboo,” in *15th European Biomass Conference and Exhibition. Berlin, Germany*, 2007.

[88] W.-H. Chen and P.-C. Kuo, “Isothermal torrefaction kinetics of hemicellulose, cellulose, lignin and xylan using thermogravimetric analysis,” *Energy*, vol. 36, no. 11, pp. 6451–6460, 2011.

[89] W.-H. Chen, J. Peng, and X. T. Bi, “A state-of-the-art review of biomass torrefaction, densification and applications,” *Renew. Sustain. Energy Rev.*, vol. 44, pp. 847–866, 2015.

[90] “ASTM D3039 / D3039M - 14 Standard Test Method for Tensile Properties of Polymer Matrix Composite Materials.” [Online]. Available: http://www.astm.org/Standards/D3039. [Accessed: 02-Mar-2016].

[91] D. E. Goldberg, *Fundamentals of chemistry*. McGraw-Hill, 2006.

[92] M. J. Wheeler, S. Russi, M. G. Bowler, and M. W. Bowler, “Measurement of the equilibrium relative humidity for common precipitant concentrations: facilitating controlled dehydration experiments,” *Acta Crystallogr. Sect. F Struct. Biol. Cryst. Commun.*, vol. 68, no. 1, pp. 111–114, 2012.

[93] A. Espert, F. Vilaplana, and S. Karlsson, “Comparison of water absorption in natural cellulosic fibres from wood and one-year crops in polypropylene composites and its influence on their mechanical properties,” *Compos. Part A Appl. Sci. Manuf.*, vol. 35, no. 11, pp. 1267–1276, 2004.

[94] I. Ghasemi and B. Kord, “Long-term water absorption behaviour of polypropylene/wood flour/organoclay hybrid nanocomposite,” *Iran. Polym. J.*, vol. 18, no. 9, pp. 683–691, 2009.

[95] J. Khazaei, “Water absorption characteristics of three wood varieties,” *Cercet. Agron. în Mold.*, vol. 41(2), p. 134, 2008.

[96] M. PELEG, “An empirical model for the description of moisture sorption curves,” *J. Food Sci.*, vol. 53, no. 4, pp. 1216–1217, 1988.

[97] N. Abu-Ghannam and B. McKenna, “The application of Peleg’s equation to model water absorption during the soaking of red kidney beans (Phaseolus vulgaris L.),” *J. Food Eng.*, vol. 32, no. 4, pp. 391–401, 1997.

[98] N. N. Mohsenin, “Physical properties of plant and animial materials. Vol. 1. Structure, physical characterisitics and mechanical properties.,” *Phys. Prop. plant animial Mater. Vol. 1. Struct. Phys. characterisitics Mech. Prop.*, vol. 1, 1970.

[99] S. Carlquist, Comparative wood anatomy: systematic, ecological, and evolutionary aspects of dicotyledon wood. Springer Science & Business Media, 2013.

[100] “ASTM D3410 / D3410M-16, Standard Test Method for Compressive Properties of Polymer Matrix Composite Materials with Unsupported Gage Section by Shear Loading, ASTM International, West Conshohocken, PA,” 2016.

[101] L. A. Carlsson, D. F. Adams, and R. B. Pipes, “Basic experimental characterization of polymer matrix composite materials,” *Polym. Rev.*, vol. 53, no. 2, pp. 277–302, 2013.

[102] J. Q. Krause, “Estruturais, Micro e macromecânica de lâminas de bambu Dendrocalamus giganteus para aplicações Applications, Micro and macromechanics of Dendrocalamus giganteus bamboo laminae for structural,” 2015.

[103] Z. P. Bažant and L. Cedolin, Stability of structures: elastic, inelastic, fracture and damage theories. World Scientific, 2010.

[104] B. W. Rosen, “Fiber composite materials,” *Am. Soc. Met. Met. Park. Ohio*, vol. 37, 1965.

[105] A. M. Waas, C. D. Babcock, and W. G. Knauss, “A mechanical model for elastic fiber microbuckling,” *J. Appl. Mech.*, vol. 57, no. 1, pp. 138–149, 1990.

[106] D. ASTM, “143-94 (2000),” Stand. Test Methods Small Clear Specimens Timber, 2000.

[107] “ASTM D4255 / D4255M - 15a Standard Test Method for In-Plane Shear Properties of Polymer Matrix Composite Materials by the Rail Shear Method.” [Online]. Available: http://www.astm.org/Standards/D4255.htm. [Accessed: 03-Mar-2016].

[108] K. GHAVAMI and A. B. MARINHO, “Determinacão das propriedades dos bambus das espécies: Mosó, Matake, Guadua angustifolia, Guadua tagoara e

Dendrocalamus giganteus para utilizacão na engenharia," *Publicação–RMNC BAMBU Janeiro de*, 2001.

[109] T. Tan, N. Rahbar, S. M. Allameh, S. Kwofie, D. Dissmore, K. Ghavami, and W. O. Soboyejo, "Mechanical properties of functionally graded hierarchical bamboo structures," *Acta Biomater.*, vol. 7, no. 10, pp. 3796–3803, 2011.

[110] M. H. Sadd, *Elasticity : theory, applications, and numerics*, Third edit. Academic Press, 2014.

[111] R. F. Gibson, Principles of composite material mechanics. CRC press, 2016.

[112] D. Correal, J. Francisco, and C. Arbeláez, "Influence of age and height position on Colombian Guadua angustifolia bamboo mechanical properties," *Maderas. Cienc. y Tecnol.*, vol. 12, no. 2, pp. 105–113, 2010.

[113] J. J. García, C. Rangel, and K. Ghavami, "Experiments with rings to determine the anisotropic elastic constants of bamboo," *Constr. Build. Mater.*, vol. 31, pp. 52–57, 2012.

[114] L. Zou, H. Jin, W.-Y. Lu, and X. Li, "Nanoscale structural and mechanical characterization of the cell wall of bamboo fibers," *Mater. Sci. Eng. C*, vol. 29, no. 4, pp. 1375–1379, 2009.

[115] D. J. Mead, "Structural Vibration: Analysis and Damping, CF Beards, Arnold, Hodder Headline Group, 338 Euston Road, London NW1 3BH. 1996. 276pp. Illustrated.£ 24.99.," *Aeronaut. J.*, vol. 100, no. 999, p. 406, 1996.

[116] A. Standard, "'ASTM E1876 - Standard test method for dynamic Young's modulus, shear modulus, and Poisson's ratio by impulse excitation of vibration,' ASTM International, West Conshohocken, PA, 2003." .

[117] S. S. Rao, "Vibration of Continuous Systems (2007)," *John Wileys. ISBN-13*, pp. 71–351.

[118] "ATCP, Physical Engineering." [Online]. Available: http://www.atcp.com.br/. [Accessed: 01-Feb-2017].

[119] S. Sutnaun, S. Srisuwan, P. Jindasai, B. Cherdchim, N. Matan, and B. Kyokong, "Macroscopic and microscopic gradient structures of bamboo culms," *Walailak J. Sci. Technol.*, vol. 2, no. 1, pp. 81–97, 2011.

[120] "TAPPI Test Methods." [Online]. Available: https://www.tappi.org/standards-and-methods/test-methods/. [Accessed: 11-Jun-2016].

[121] "BAMBOO PRESERVATlON TECHNlQUES: A REVIEW." [Online]. Available: http://www.inbar.int/wp-content/uploads/downloads/2012/09/inbar_technical_report_no03.pdf. [Accessed: 27-Nov-2015].

[122] "Protection of bamboo structures." [Online]. Available: http://www.inbar.int/publication/pdf/INBAR_Technical_Report_No19.pdf. [Accessed: 05-Dec-2015].

[123] C. H. Yoo and S. Lee, Stability of structures: principles and applications. Elsevier, 2011.

[124] P. G. Dixon, P. Ahvenainen, A. N. Aijazi, S. H. Chen, S. Lin, P. K. Augusciak, M. Borrega, K. Svedström, and L. J. Gibson, "Comparison of the structure and flexural properties of Moso, Guadua and Tre Gai bamboo," *Constr. Build. Mater.*, vol. 90, pp. 11–17, 2015.

[125] Z.-P. Shao, C.-H. Fang, S.-X. Huang, and G.-L. Tian, "Tensile properties of Moso bamboo (Phyllostachys pubescens) and its components with respect to its fiber-reinforced composite structure," *Wood Sci. Technol.*, vol. 44, no. 4, pp. 655–666, 2010.

[126] H. Yu, Z. Jiang, C. Hse, and T. Shupe, "Selected physical and mechanical properties of moso bamboo (Phyllostachys pubescens)," *J. Trop. For. Sci.*, pp. 258–263, 2008.

[127] E. Obataya, P. Kitin, and H. Yamauchi, "Bending characteristics of bamboo (Phyllostachys pubescens) with respect to its fiber–foam composite structure," *Wood Sci. Technol.*, vol. 41, no. 5, pp. 385–400, 2007.

[128] S. Chuma, M. Hirohashi, T. Ohgama, and Y. Kasahara, "Composite structure and tensile properties of Mousou bamboo," *Zairyou*, vol. 39, pp. 847–851, 1990.

[129] S. Amada and S. Untao, "Fracture properties of bamboo," *Compos. Part B Eng.*, vol. 32, no. 5, pp. 451–459, 2001.

[130] F. P. Beer and E. R. Johnston, "Statics and Dynamics." McGraw-Hill, New York, 1962.

[131] G. B. M. Heuvelink, Error propagation in environmental modelling with GIS. CRC Press, 1998.

[132] “Maximum Moisture Carrying Capacity of Air.” [Online]. Available: http://www.engineeringtoolbox.com/maximum-moisture-content-air-d_1403.html. [Accessed: 23-Dec-2016].

[133] “Dew, Frost, Condensation, and Radiation.” [Online]. Available: http://windowoutdoors.com/WindowOutdoors/Dew Frost Condensation and Radiation.htm. [Accessed: 03-Jan-2017].

[134] “Relative Humidity.” [Online]. Available: https://www.engineeringtoolbox.com/humidity-measurement-d_561.html. [Accessed: 15-Feb-2018].

[135] “Dew point temperature.” [Online]. Available: https://www.engineeringtoolbox.com/dry-wet-bulb-dew-point-air-d_682.html. [Accessed: 15-Feb-2018].